Monitoring drought and salinity stress in agriculture by remote sensing for a sustainable future

Wen, W.

Monitoring Drought and Salinity Stress in Agriculture by Remote Sensing for a Sustainable Future

Wen Wen

文 雯

Wen Wen (2023). Monitoring Drought and Salinity Stress in Agriculture by Remote Sensing for a Sustainable Future

PhD thesis at Leiden University, The Netherlands

The research described in this thesis was conducted at the Institute of Environmental Sciences (CML), Leiden University, The Netherlands.

ISBN: 978-90-5191-255-5

Cover Photograph & Design: Wen Wen

Layout: Wen Wen

Printing: printsupport4u

Monitoring Drought and Salinity Stress in Agriculture

by Remote Sensing for a Sustainable Future

Proefschrift

ter verkrijging van

de graad van doctor aan de Universiteit Leiden,

op gezag van rector magnificus prof.dr.ir. H. Bijl,

volgens besluit van het college voor promoties

te verdedigen op dinsdag 30 Januari 2024

klokke 11:15 uur

door

Wen Wen

geboren te Sichuan province, China

in 1993

PROMOTORES:

Prof. dr. P. M. van Bodegom

Dr. ir. J. Timmermans

PROMOTIECOMMISSIE:

Prof. dr. ing. J.W. Erisman

Prof. dr. ing. M.G. Vijver

Dr. ir. M.D. Visser

Prof. dr.ir. L. Kooistra (Wageningen University)

Dr.ir. A.A. Verhagen (Delft University of Technology)

Contents

Chapter 1

General introduction

Food security is defined as a “situation that exists when all people, at all times, have physical, social, and economic access to sufficient, safe, and nutritious food that meets their dietary needs and food preferences for an active and healthy life” by the Food and Agriculture Organization (FAO 2002). Food security is highly related to economic growth, human rights, poverty, society security and stability, and human health. As such, to ensure a secure and sustainable future for everyone, the United Nations (UN) has formulated sustainable development goals (SDGs) for 2030 highlighting sustainable agriculture and food security (in SDG 2) to be crucial pillars (UN 2015). However, in 2021, according to the FAO, 11.7% of the world's population experienced extreme food insecurity, and around 2.3 billion people were either moderately or severely food insecure (FAO 2022b; UN 2022). Despite the progress made from multiple perspectives towards SDG 2 (to ‘End hunger’), food insecurity, hunger, and malnutrition are still increasing in the world at the current state (FAO 2022b).

To feed 9.1 billion people in 2050, global food production needs to increase by 70% by 2050, and specifically that of developing counties to increase with 100% (FAO 2009; Tilman et al. 2011). Meanwhile, 670 million people are projected to face hunger in 2030 (FAO 2022b). The overall food demand is projected to rise by 35% to 56% by 2050 compared to the 2010 base year while simultaneously climate change is estimated to increase the challenges for food production even further (van Dijk et al. 2021). We therefore need to increase the productivity (in particular those of small-scale food producers, SDG 2.2), while ensuring “Sustainable food production and resilient agricultural practices (SDG 2.4), by “implementing resilient agricultural practices that increase productivity and production, that help maintain ecosystems, that strengthen capacity for adaptation to pending disasters (e.g., climate change, drought, flooding, and others), and that progressively improve land and soil quality”.

1.1 Threats to food production

Agricultural crops are frequently subjected to a variety of environmental stresses, which limit agricultural productivity and decrease food production. These stresses fall into two categories, namely biotic stress (i.e. disease pathogens infection, herbivores attacks, etc.) and abiotic stress (i.e., water scarcity, metal toxicities, extreme temperature, etc.) (Oshunsanya et al. 2019; Summy et al. 2020). Abiotic stress such as drought, frost, heat waves, and salinity negatively impact crop growth, crop development as well as crop quality (Audil et al. 2019). Abiotic stress was observed to be the dominant factor impacting crop productivity worldwide and is estimated to cause annually 51% - 82% of crop yield loss worldwide (Arun-Chinnappa et al. 2017; Mantri et al. 2012). Furthermore, climate change is expected to result in higher temperatures, altered rainfall patterns, and frequent

extreme weather (Wheeler and von Braun 2013). These patterns were projected to increase the risk of abiotic stress (including but not limited to flood, drought, heat, etc.) regionally and globally, thus posing major constraints on food availability, access, utilization as well as stability (Lorenz and Kunstmann 2012; Rosenzweig et al. 2014; Wheeler and von Braun 2013). Therefore, it is crucial to recognize and estimate the impact of abiotic stress on food production to ensure food security.

As one of the major abiotic stresses, drought inhibits crop yield and distribution, causing substantial reductions in food production at a global scale (Eckardt et al. 2022; Madadgar et al. 2017). Over 40% of the global land area is affected by drought (Dunn et al. 2020) and it was estimated to cause $124 billion economic loss annually worldwide (Tsegai et al. 2022). More than 2.3 billion people have experienced water stress in 2022, and approximately 160 million children have encountered severe and protracted droughts (Tsegai et al. 2022). Drought impacts three components of food security, namely availability (e.g. crop production), access (e.g. food price), and stability (sufficient access to food) both in direct and indirect ways (He et al. 2019). Over the previous four decades, droughts led to a loss in cereals production (i.e. maize, rice, and wheat) of 1820 million Mg globally (Lesk et al. 2016). Climate change is predicted to exacerbate drought frequency and severity, particularly in semi-arid regions already under severe water stress (Dai 2011, 2013). Meanwhile, there will be 700 million people in danger of being displaced by drought by 2030 (Tsegai et al. 2022). Thus, food security will be further threatened by frequent droughts in the future. Given this, there is a need to understand and evaluate drought effects on crops aiming to maintain food production.

Aside from drought, soil salinity is another major stress that negatively impacts agricultural production, particularly in the dry and semi-arid regions (El hasini et al. 2019). There are 954 million hectares (Mha) of salt-affected soil in 120 countries worldwide, leading to approximately 7% - 8% agriculture productivity loss (Meena et al. 2019; Yadav 2003). Soil salinity affects approximately 20% of the total cultivated land and 33% of the irrigated agricultural areas globally (Jamil et al. 2011; Metternicht and Zinck 2003) while the salt-affected area is predicted to expand at a rate of 1.0 - 2.0 Mha per year (ITPS and FAO 2015). With climate change in terms of changing rainfall patterns and increased temperature, water scarcity is expected to accelerate soil salinity in the near future (Eswar et al. 2021). Meanwhile, soil and groundwater salinity in arid regions and coastal regions can be exacerbated due to seawater intrusion caused by mean sea-level rise and excessive groundwater extraction (Dasgupta et al. 2015; Mukhopadhyay et al. 2021). Therefore, soil salinity urgently needs to be tackled to enable food security and a sustainable agriculture system to balance soil degradation and population expansion.

Although the impacts of drought and salinity stress on food production have been evaluated individually for a variety of crops, under natural conditions, crops normally face a combination of abiotic stresses in natural and agricultural ecosystems, such as drought and salinity, which result in greater yield loss than either stress alone (Mittler 2006). Drought and salinity interact to produce a combined effect when soil water evaporates and salt concentrations increase in the soil solution (Munns 2002). Salinity has been observed to considerably rise in rivers during hydrological droughts because of reduced river levels (Jones and van Vliet 2018; Mosley 2015). Moreover, salinity stress is expected to frequently accompany drought on cultivated land, especially in coastal, arid, and semi-arid regions (Angon et al. 2022; Corwin 2020). Thus, more frequent and severe droughts will therefore intensify the accumulation of salinization, a combination that leads to adverse impacts on food production and sustainable agricultural development.

1.2 Impact pathways of drought and salinity

Drought-induced water stress decreases crop yield by delaying crop maturation and slowing root growth, which results in less available food, especially in areas (like sub-Saharan Africa) that are heavily reliant on rain-fed agriculture (He et al. 2019). Moreover, drought directly impacts plant transpiration processes, leading to the short to long-term closure of the stomata, hampering photosynthesis and thus crop productivity (Farooq et al. 2009). In response to drought stress, plants are observed to reduce leaf area and leaf chlorophyll content, increase leaf thickness, and decrease the activities of photosynthetic enzymes (Yang et al. 2021). Due to altered plant-water interactions, CO_2 assimilation, cell membrane damage, oxidative stress, and enzyme inhibition, drought stress decreases plant growth and productivity (Kousik et al. 2022).

Salinity-induced stress negatively affects crop growth in two growth responses, namely osmotic stress and ion toxicity (Munns and Tester 2008; Shrivastava and Kumar 2015). The presence of high salt concentration in the soil solution can adversely impact the water acquisition capacity of crops. Moreover, salinity stress inhibits plant growth due to specific-ion toxicities (in particular induced by high concentrations of Na^+) and the subsequent nutritional imbalances of other cations (such as K^+ and Ca^{2+}). The co-occurrence of reduced water uptake, ion toxicity, and nutrient imbalances results in a reduction in crop yields (Shrivastava and Kumar 2015).

The combination of salinity and drought exerts an even more detrimental effect on plant growth, photosynthesis, oxidative balance, and ionic balance compared to the individual stresses alone (Angon et al. 2022). Both drought and salinity impacts on crops are highly dependent on e.g. growth stage and cultivar (Hopmans et al. 2021;

Xu et al. 2019). Indeed, numerous studies indicate the detrimental effects of combined drought and salt stress on crops (Hussain et al. 2020; Ors and Suarez 2017). However, these studies are limited to a few crop varieties and large regional uncertainties and do not consider real-life agriculture settings. Consequently, there is still a major gap in our knowledge regarding the comprehensive evaluation of the individual and collective impacts of co-occurring stresses (e.g., salinity and drought) on divergent crop varieties in real-life scenarios, especially on a large-scale.

1.3 Large-scale monitoring of food production

To improve food security, agricultural productivity around the world (and in particular of small-scale food producers) needs to double (SDG 2.3). In order to track progress along this target, it requires detailed estimations of crop yield and production. Traditionally, crop yield and production are estimated on the basis of in-season variables from field surveys in combination with crop simulation models, statistical regression models, and historical data (Basso and Liu 2019; Calvao and Pessoa 2015). However, considering their time-consuming and substantial running cost, these methods are inefficient for large-scale applications (Calvao and Pessoa 2015). Moreover, field estimates of soil salinity impacts on crops are limited by the small-scale nature of many experiments (Corwin and Scudiero 2019; Eswar et al. 2021).

There is a wide range of crop simulation models available, including DSSAT (Jones et al. 2003), EPIC (Williams et al. 1989), and WOFOST (Diepen et al. 1989). These models couple descriptions of eco-physiological processes (such as nutrient uptake, water uptake, and photosynthesis) to large-scale climate variables and management variables to estimate crop growth and crop yields. Most of these models include the impacts of water shortage on crop growth as one of their key elements. However, they are mostly unable to deliver accurate projections of the impacts of local climate variables as well as of extreme events (e.g. drought and storms) (Rauff and Bello 2015). Moreover, there exist only a few attempts to evaluate crop yield under salinity stress based on modified crop simulation models, such as CROPGRO, ORYZA v3, and APSIM-Oryza (Radanielson et al. 2018; Webber et al. 2010). Consequently, crop simulation models so far have been constrained by the simplification of the scenarios and uncertainties/availability of input parameters (Wang et al. 2013a). Finally, statistical regression models are likely unable to capture the interaction of the climate-soil-plant-management continuum in light of the increased number of extreme events with climate change, leading to inaccurate yield outcomes (Basso and Liu 2019). Hence, for large-scale applications, alternative methods are essential. Remote sensing poses a promising

tool to aid in the global food security, by providing reliable information on both the extent of arable land as well as the food production on those lands.

1.3.1 Remote sensing estimation of arable land area extent

Remote sensing already is used extensively to characterize the extent and reduction of agricultural areas under productive and sustainable agriculture, using land cover maps, such as Global Land Cover (GLC) 2000, CORINE Land Cover, GlobCover 2009, GlobeLand30, etc (Radwan et al. 2021). Likewise, several more agricultural-dedicated products have been produced, including the Global irrigated area map (GIAM) at 1km resolution (Thenkabail et al. 2009), Global Rain-fed, Irrigated, and Paddy Croplands (GRIPC) map at 500m resolution in 2005 (Salmon et al. 2015), and the European Space Agency's Climate Change Initiative-Land Cover (ESA-CCI) at 300 m resolution in 2000, 2005, and 2011 (Bontemps et al. 2013), to map irrigated area and non-irrigated area at global scale (Karthikeyan et al. 2020). In addition, remote sensing can not only be used to detect agricultural areas but it can also be applied to identify different crop types. The Cropland Data Layer (CDL) products covering the Continental United States were developed each year from 2008 to 2022 at 30m resolution by integrating multiple satellite imageries including Landsat 8, Landsat 9 OLI/TIRS, the ISRO ResourceSat-2 LISS-3, and Sentinel-2 during crop growing season (Boryan et al. 2011). While such remote sensing land cover maps provide an ideal manner to monitor the extent and change of suitable arable land, they do not provide information regarding the suitability of the land for agricultural production.

In response, remote sensing has also been extensively used to estimate soil properties that affect crop growth and food production. Specifically remote soil properties, including soil minerals (e.g. clay minerals, carbonate minerals, silicate minerals), soil organic matter, soil surface roughness, and soil moisture, have been retrieved from different satellite platforms (e.g. ASTER (Nawar et al. 2015)) with high confidence (Wang et al. 2023a). This has allowed the production of various datasets (e.g. FAO soils portal, Global Soil Information System (GloSIS), Global Earth Observation System of Systems (GEOSS) portal) that provide maps of various soil properties at the regional scale to global scale (ISRIC 2023). In addition to monitoring the previous and current state of soil properties, remote sensing shows a high potential to predict soil property changes in future scenarios. Hassani et al. (2021) predicted soil salinity (ECe) under four different future scenarios in the 2050s and 2100s based on remote sensing data using Machine Learning (ML) algorithms. Hence, remote sensing does not only contribute to evaluating current food production at a large scale but also remote sensing can also be used to project future food production.

1.3.2 Remote sensing estimation of crop growth

Remote sensing also poses a promising way to monitor agricultural production on arable lands with timely, synoptic, and reliable information covering multiple spatial and temporal scales (Calvao and Pessoa 2015; Karthikeyan et al. 2020). By characterizing crop growth on these lands, satellite remote sensing (e.g. Landsat, MODIS, SPOT-Vegetation, etc.) has been used to monitor crop productivity at medium- to high- resolutions (Basso and Liu 2019). Meanwhile, with the development of cloud-computing platforms (e.g., Amazon, Microsoft AI, and Google Earth Engine (GEE)), the capabilities of crop monitoring frameworks to access and process such satellite data have also been improved (Wu et al. 2023). Crop monitoring primarily focuses on providing qualitative information on crop conditions at the desired temporal-spatial scale, which is essential for policy-making and supporting early warning systems for food security (López-Lozano and Baruth 2019). Crop biophysical characteristics are viewed as proxies for crop conditions. To monitor the growth status of crops, multispectral vegetation indices (VIs) have been established, which provide a simplified view on the morphological, physiological, and biophysical traits of crops (Wu et al. 2023).

Normalized Difference Vegetation Index (NDVI) (Tucker 1979) is the most popular VI for assessing the dynamics and health of vegetation. NDVI has been used for evaluating crop growing conditions and predicting crop yield and can be retrieved from different satellites (Basso and Liu 2019). In addition to NDVI, other VIs such as Enhanced Vegetation Index (EVI) (Liu and Huete 1995), the Perpendicular Vegetation Index (PVI) (Rondeaux et al. 1996), the Soil Adjusted Vegetation Index (SAVI) (Huete 1988), and the Green-Red Vegetation Index (GRVI) (Motohka et al. 2010), are proposed to monitor crop growth and production. However, these VIs are usually affected by uncertainties due to differences in background (e.g. soil color), crop type, crop phenology, and crop rotation. For instance, NDVI is often affected by inherent nonlinear interactions with biophysical parameters and the background's optical properties and saturates when it comes to high biomass levels (Calvao and Pessoa 2015; López-Lozano and Baruth 2019; Wu et al. 2023).

In addition, drought (impact) indicators have been developed, e.g. the Vegetation Health Index (VHI) (Kogan 1997), the Vegetation Condition Index (VCI) (Kogan 1995b), and the Normalized Difference Water Index (NDWI) anomalies (Gao 1996). However, these drought indicators have their own distinct drawbacks that restrict their utility as drought early warning signals (Liu et al. 2016). Typically, there is a lag time between the onset of a drought and the subsequent response in vegetation. This lag time poses a challenge in accurately assessing the impact of drought on vegetation (Ji and Peters 2003; Zhang et al. 2016). Likewise, vegetation

indices, that are employed for monitoring crop salinity stress, are also subject to limitations in relation to background noise, the presence of halophytes, and spatial resolution (Allbed and Kumar 2013; Metternicht and Zinck 2003). As a consequence, the results obtained from different indices vary, and most applications utilizing these indicators focus on local scales and specific crop types. Thus, a method that can directly evaluate crop condition and health based on directly measured crop parameters under stress conditions is required to effectively monitor crop growth under stressed conditions using remote sensing.

1.4 Remote sensing monitoring food security under stress based on plant traits

Plant functional traits are identified as physiological, structural, biochemical, or phenological characteristics that impact plant species fitness by indirectly affecting growth, reproduction, resource use, survival, etc. (Cornelissen et al. 2003; Violle et al. 2007). Plant functional traits have been used to quantify species-specific responses and stress strategies to environmental stress (Kramp et al. 2022; Lavorel and Garnier 2002). Plant functional traits have been proposed to address plant responses to drought and salinity stress for a variety of plants. In particular, leaf water and economic traits are considered to demonstrate coordination in drought and saline environments (Anderegg et al. 2019; Kramp et al. 2022). However, most studies concentrated on the individual roles of a given trait functioning on a specific stress (Caruso et al. 2019). Given stress is frequently coupled and plant functional traits can express the tolerance of plants to various stresses (Sack and Buckley 2020), an approach that can simultaneously analyze multiple traits and multiple vegetation or crop types is required to evaluate the responses of plants to combined stresses at a large scale.

Plant traits can be estimated qualitatively or quantitatively from remote sensing data. Qualitative methods involve the utilization of classification techniques that employ a predefined set of decision rules to assign image pixels with comparable spectral properties to distinct thematic vegetation classes. Qualitative approaches employed for the interpretation of optical remote sensing data can be classified into two groups: empirical methods (e.g. VI) and physical methods (e.g. radiative transfer models (RTMs)), or a combination of both (Homolova et al. 2013). In particular, hyperspectral data has been demonstrated to have a significant ability to identify biophysical and biochemical characteristics (Serbin et al. 2015; Serbin et al. 2016). Plant traits such as leaf chlorophyll content (Cab), leaf water content (Cw), leaf area index (LAI), the fraction of absorbed photosynthetically active radiation (FAPAR), and the fraction of vegetation cover (FVC) have been assessed with high accuracy and fidelity from remote sensing (Colombo et al. 2008; Myneni et al. 2002; Zarco-Tejada et al. 2004). Hence, remote sensing traits associated with

different functioning aspects provides a foundation for a comprehensive understanding of crop conditions at a large scale.

Plant traits that can be assessed by remote sensing also show a tremendous potential for characterizing vegetative stress in different species (Gerhards et al. 2019; Vereecken et al. 2012). Berger et al. (2022) reviewed the response of plants to drought stress with optimal sensing domains for different traits. The study indicated that the responses of crops to stress with different durations can be detected by remote sensing. LAI, Cab, Cw, FVC, and FAPAR retrieved from multiply satellites (e.g., MODIS, Sentinel-2, SPOT-VGT1/2, and PROBA-V) are identified as key variables in drought or salinity impact monitoring due to their sensitivity of vegetation stress (Berger et al. 2022; Jiao et al. 2021; Richter et al. 2008; Zhang et al. 2015). Moreover, FAPAR anomalies serve as a crucial component in calculating comprehensive drought indicators: the Combined Drought Indicator (CDI) in the European Drought Observatory and the Risk of Drought Impact for Agriculture (RDrI-Agri) indicator in the Global Drought Observatory (Cammalleri et al. 2019). Although there are several studies evaluating crop response to drought and salinity stress based on remote sensing traits, these studies are limited to specific traits, crop types, and singular stress. Thus, there is still a challenge to simultaneously assess the co-occurrence stress impact on divergent crops based on traits assessed by remote sensing at a large scale.

1.5 Research aims and questions

This research aims to evaluate the impact of drought and salinity stress on agriculture and sustainable development goals using remote sensing technology. In this Ph.D. thesis, the following research questions have been addressed:

- Which remote sensing features are available to monitor crops under drought and salinity stress and what are the shortcomings of the various features? (Chapter 2)
- How can the impacts of drought and salinity stress on crop traits be evaluated simultaneously using remote sensing observations (Sentinel-2) in a quantitative way? (Chapter 3 & Chapter 4)
- How to evaluate the tolerance of diverse crops to drought and salinity stress in real-life agriculture settings by remote sensing (Sentinel-2)? (Chapter 4)
- How to utilize the salt-affected area by cultivating salt-tolerant potato to enhance global food production and secure SDG 2.4? (Chapter 5)

1.6 Thesis outline

First, I illustrated an overview of food security and its associated threats, emphasizing the potential of remotely sensed plant functional traits to monitor crop responses under drought and salinity stress at large scale (Chapter 1). A systematic review was conducted to evaluate the current capacity of remote sensing to detect the impact of drought and salinity stress on crops based on vegetation indices (VIs) and plant traits (Chapter 2). Based on multiple plant traits retrieved from remote sensing observations, I developed a novel approach to estimate the impacts of drought, salinity, and their combination on crop growth in the Netherlands (Chapter 3). Next, I upscaled this approach to assess the tolerance of eight crops to drought, salinity, and their combination based on five functional traits across the entire U.S. continent throughout the crop growing season from remote sensing (Chapter 4). Then, I quantified the viability and potential of enhancing food production and achieving SDG 2 by planting salt-tolerant potato in salt-affected areas in present and future scenarios (Chapter 5). Finally, the challenges and implications of remote sensing in agricultural applications for a sustainable future were discussed based on the principal findings of this thesis (Chapter 6). Figure 1.1 shows the conceptual scheme of this thesis.

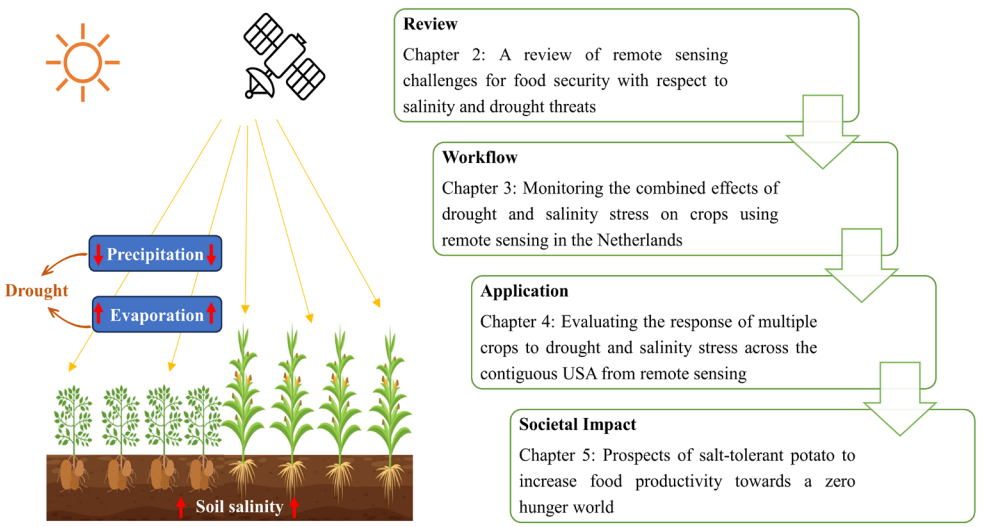

Figure 1.1 Conceptual scheme of the topics of Chapters 2, 3, 4, and 5.

Chapter 1: General introduction

This chapter provides a general introduction on food security and threats (particularly due to abiotic stress) for food security. Then, the chapter illustrates the high potential of remote sensing technologies in monitoring food production at a

large scale by their capacity to map land cover, detect soil properties, and monitor vegetation properties both in the present and the future. In addition, this chapter highlights the significance of remotely sensed plant functional traits to monitor crop responses under drought and salinity stress in real-life scenarios for large-scale applications. The research aims, questions, and individual chapters of this thesis are outlined.

Chapter 2: A review of remote sensing challenges for food security with respect to salinity and drought threats

This chapter presents a systematic review on the current ability of remote sensing to identify and assess the impacts of drought and salinity stress on agricultural crops through vegetation indices and plant traits. We found that there are still several challenges remaining for using remote sensing to monitor drought and salinity stress impacts on crop growth. VIs do not provide consistently accurate estimation of these impacts while plant traits are promising to directly link to the biochemical/biophysical pathway of crop growth, thereby reflecting the stress response mechanisms.

Chapter 3: Monitoring the combined effects of drought and salinity stress on crops using remote sensing in the Netherlands

In this chapter, a novel approach is presented to evaluate the impacts of drought, salinity, and their combination on five crop traits, including leaf area index (LAI), leaf chlorophyll content (Cab), leaf water content (Cw), the fraction of absorbed photosynthetically active radiation (FAPAR) and the fraction of vegetation cover (FVC) using remote sensing in the Netherlands. The separate and combined effects of drought and salinity stress on five traits were quantitatively assessed. The results indicate that the exacerbating effects of co-occurring drought and salinity stress highly depended on the moment in the growing season. Moreover, LAI, FAPAR, and FVC impact most under severe drought conditions for maize and potato while Cab and Cw are generally more inhibited by combined drought and salinity stress. As a result, the proposed approach provides a way to simultaneously assess the impact of drought and salinity stress on crops from remote sensing with possible large-scale applications.

Chapter 4: Evaluating crop-specific responses to drought and salinity stress from remote sensing

Food security is facing a significant challenge by co-occurring stresses (e.g., salinity and drought) under global climate change. Extreme weather events are projected to become more frequent, impacting crop performance and reducing crop yields under these adverse conditions. Complementary to existing field trials of controlled small-scale experiments, this chapter assesses the responses of various

crops to the occurrence of drought and salinity stress, alone and collectively across the entire U.S. continent in real-life agricultural conditions, using five traits representative of different plant functions by remote sensing. The results show the differential responses of crops to these stresses. Stress impacts were highly time-dependent, and crops were more susceptible to combined drought and salinity than to individual stresses, although stress impacts varied significantly between species and over time. Prior to decreasing their water or chlorophyll levels, most crops initially decreased primary production capability by decreasing LAI. This chapter creates a quantitative foundation to inform sustainable food production, aiding in monitoring food security upon global climate change.

Chapter 5: Prospects of salt-tolerant potato to increase food productivity towards a zero hunger world

Food security and sustainable agriculture are crucial elements of achieving the SDGs, but global climate change is threatening them increasingly. This chapter estimates the local suitability and the regional suitability areas for salt-tolerant potato cultivation in salt-affected soils to allow for achieving SDGs in current and future scenarios. The results reveal that Oceania (particularly Australia) has the greatest potential for enhancing food production through salt-tolerant potato cultivation in salt-affected soils. In addition, Kazakhstan, the Russian Federation, and Australia can address food shortage challenges and achieve sustainable development goals in the current state as well as in future scenarios. In this chapter, salt-tolerant potatoes are evaluated as a proxy for saline farming, allowing for increased food production in salt-affected areas and laying the groundwork for promoting saline farming practices to enhance agricultural resilience and ensure food security.

Chapter 6: General discussion

This chapter synthesizes the principal findings with a discussion on the limitations and prospects of this thesis. It emphasizes the potential and feasibility of monitoring food security by trait-based evaluation although there are still a few challenges remaining in agricultural applications from remote sensing. In addition, this chapter elaborates on the implications of remote sensing for securing sustainable goals at a global scale, both in the current state as well as in the future.

Chapter 2

A review of remote sensing challenges for food security with respect to salinity and drought threats

Wen Wen, Joris Timmermans, Qi Chen, Peter M. van Bodegom

Remote Sensing, 2021, 13(1): 1-14.

https://doi.org/10.3390/rs13010006

Abstract

Drought and salinity stress are considered to be the two main factors limiting crop productivity. With climate change, these stresses are projected to increase, further exacerbating the risks to global food security. Consequently, to tackle this problem, better agricultural management is required on the basis of improved drought and salinity stress monitoring capabilities. Remote sensing makes it possible to monitor crop health at various spatiotemporal scales and extents. However, remote sensing has not yet been used to monitor both drought and salinity stresses simultaneously. The aim of this paper is to review the current ability of remote sensing to detect the impact of these stresses on vegetation indices (VIs) and crop trait responses. We found that VIs are insufficiently accurate ($0.02 \leq R^2 \leq 0.80$) to characterize crop health under drought and salinity stress. In contrast, we found that plant functional traits have a high potential to monitor the impacts of such stresses on crop health, as they are more in line with the vegetation processes. However, we also found that further investigations are needed to achieve this potential. Specifically, we found that the spectral signals concerning drought and salinity stress were inconsistent for the various crop traits. This inconsistency was present (a) between studies utilizing similar crops and (b) between investigations studying different crops. Moreover, the response signals for joint drought and salinity stress overlapped spectrally, thereby significantly limiting the application of remote sensing to monitor these separately. Therefore, to consistently monitor crop responses to drought and salinity, we need to resolve the current indeterminacy of the relationships between crop traits and spectrum and evaluate multiple traits simultaneously. Using radiative transfer models (RTMs) and multi-sensor frameworks allows monitoring multiple crop traits and may constitute a way forward toward evaluating drought and salinity impacts.

2.1 Introduction

Food security is a serious problem around the world with a significantly large number of food production systems currently at risk (FAO 2011). It is predicted that by 2030, the population suffering from food insecurity will rise to more than 840 million. Meanwhile, it is projected that the ongoing COVID-19 could further worsen the number of undernourished people around the world (FAO 2020). Further exacerbating this food security problem, crop productivity itself also suffers great threats from stresses, such as drought stress, nutrient stress, and salinity stress, which reduce the yield at various locations by more than 50% (Anami et al. 2020). Moreover, crops frequently suffer from a combination of stress (Dresselhaus and Hückelhoven 2018), which further causes challenges for food production. In order to allow for sustainable agricultural production and mitigate the threat of global food shortages, the impact of these stressors needs to be monitored and alleviated.

Water stress, in the form of droughts, has been identified as the most serious threat for global agriculture, approximately affecting 40% of the world's land area (Dunn et al. 2020). Between 1980 and 2020, droughts have caused economic damages of around $6 billion per year in the United States, exceeding damages from other weather and climate disasters (Smith 2020). Likewise, in China, the average annual economic damage due to drought was $12.8 billion during 2006-2015 (Su et al. 2018). In addition to drought, salinity has emerged as a major factor limiting the productivity of crops. Southwest United States, southern Asia (including India and Pakistan), eastern Asia (Western China), eastern Australia, and northwest Africa are the most affected areas (FAO/IIASA/ISRIC/ISSCAS/JRC 2012; Ivushkin et al. 2019; Koohafkan 2012). The United Nations Food and Agriculture Organization (FAO) has estimated that 11% of the global irrigated area (34 Mha) is currently affected by different levels of salinity. Therein, China, the United States, Pakistan, and India hold more than 60% of the total area (21 Mha).

While presently, drought and salinity already pose tremendous challenges for food production, it has been forecasted that both stressors will increase both spatially and in severity. Climate change will increase the frequency and severity of drought events in numerous regions (Cook et al. 2015; Mosley 2015; Schwalm et al. 2017; Trenberth et al. 2013), leading to dramatic impacts on crop growth and productivity (Trenberth et al. 2013). Specifically, higher temperatures and lower humidity have been shown to lead to an increasing water demand (in the form of crop evapotranspiration) and a reduced water availability from effective precipitation, while simultaneously, a lower and infrequent effective precipitation significantly reduces water availability, thereby negatively affecting food production (Mimi and Jamous 2010). Similarly, it has been suggested that salinity will impact 50% of the

cultivated land by 2050 (Butcher et al. 2016). Soil salinity levels have been shown to increase in arid lands because fresh water is not available to drain accumulated salts (Rozema and Flowers 2008), thus acting as a practically irreversible process. Moreover, soil salinization has been shown to increase with the expansion of agriculture to semi-arid and arid regions (Cramer et al. 2007; Oki and Kanae 2006; Rozema and Flowers 2008). Therefore, the increase in drought frequency and soil salinity under climate change further exacerbates the threat to crop production.

Drought and salinity cannot be seen independently of each other. As an aspect of water quality, salinity has been proven to increase during drought periods (Hrdinka et al. 2012; Mosley 2015; van Vliet and Zwolsman 2008). Specifically, it has been shown that due to lower river levels, hydrological drought significantly increases the salinity in rivers (Jones and van Vliet 2018; Mosley 2015). Consequently, increased drought frequency and severity will exacerbate the accumulation of salinization and adversely affect crop yield and sustainable agricultural development (Wang et al. 2013b). As such, there are already numerous areas in the world where both drought and salinity stress co-occur (Figure 2.1). Furthermore, due to sea level rise in the future, cultivated land (and in particular coastal lowlands) will have a higher probability to suffer from both drought and salinity stress (Corwin 2020; Gopalakrishnan et al. 2019; Katschnig et al. 2013; Pankova and Konyushkova 2014). Therefore, drought and salinity should not be viewed independently, and the impacts of joint drought and salinity stress on agricultural production should be investigated.

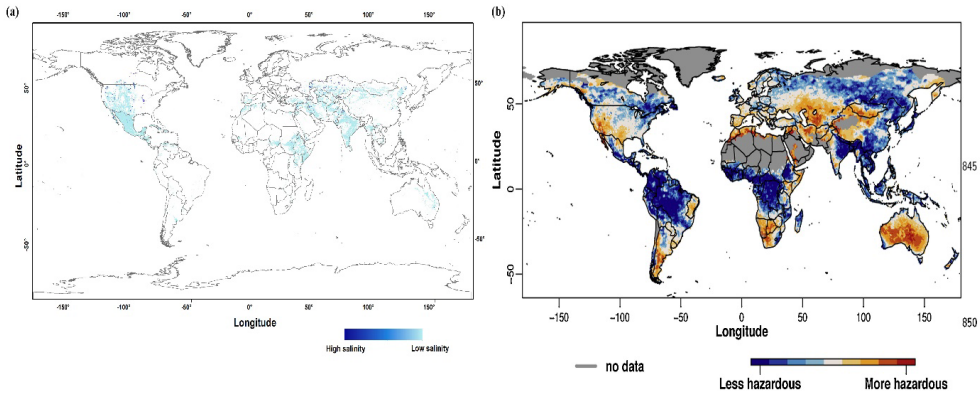

Figure 2.1 Global distribution of drought and salinity. In panel (a), the global map of soil salinity change is shown [10], while in panel (b) the global map of drought hazard (Carrão et al. 2016) is shown. Global soil salinity map was extracted from [10] and then transformed to the plate carrée projection by ArcGIS.

Remote sensing (RS) is a key method for monitoring crop health due to its capability to monitor and detect effective changes of large areas at a relatively low

cost, in comparison to traditional methods (Wu et al. 2015). For this purpose, several vegetation indices (VIs) such as the Normalized Difference Vegetation Index (NDVI) (Tucker 1979), the Perpendicular Vegetation Index (PVI) (Rondeaux et al. 1996), and the Soil Adjusted Vegetation Index (SAVI) (Huete 1988) have been developed in the past to monitor agricultural production. In addition, drought (impact) indicators have been developed that account for seasonality effects (based on long-term standardized observations), e.g., the Vegetation Condition Index (VCI) (Kogan 1995b), the Vegetation Health Index (VHI) (Kogan 1997), and the Normalized Difference Water Index (NDWI) anomalies (Gao 1996). However, each of these drought indicators has specific limitations that limit its applicability as early warning signals of drought (Liu et al. 2016). As a consequence, results vary among different indices, and most applications with these indicators focus on local scales and individual crop types. As such, no comprehensive vegetation index has been developed that can be applied globally to investigate drought impact consistently (Liu et al. 2016). Similar to drought monitoring, vegetation indices, used to monitor crop salinity stress, are also affected by limitations regarding noise, halophyte presence, and spatial resolution (Allbed and Kumar 2013; Metternicht and Zinck 2003). In response, a more comprehensive measurement of the reflectance spectrum representing crop traits is required to monitor crop growth and health as affected by stress. In this regard, it has been shown that hyperspectral data have a strong potential to detect biophysical and biochemical parameters (Serbin et al. 2015; Serbin et al. 2016). In addition, various studies highlighted that other (multi-spectral) RS methods (e.g., microwave, thermal infrared (TIR), hyperspectral) show great promise in characterizing vegetation stress (Gerhards et al. 2019; Vereecken et al. 2012). However, the number of studies focusing on this is limited, and only part of these investigations focused on agricultural RS applications (Homolova et al. 2013; Weiss et al. 2020), while studies on the relationship between crop traits and spectral properties in relation to under drought or salinity stress are even more limited. Therefore, an in-depth analysis of the reflectance spectrum of crop traits under stress is required to better identify plant drought and salinity stress by remote sensing.

The main objective of the study is to evaluate the current state and shortcomings in the RS monitoring of crops under drought and/or salinity stress. Based on a comprehensive analysis, we evaluate the potential of remote sensing to identify and assess agricultural ecosystems under drought and salinity stress through vegetation indices and plant traits.

2.2 Methodology

To evaluate the current state of monitoring drought and salinity stress by RS, we applied a thorough systematic review of recent scientific publications. For this, we

(a) collected a large representative set of scientific publications, and (b) analyzed their results to identify the response patterns in vegetation indices and plant traits. For the analysis of plant traits, we classified them according to underlying plant functions (relating to primary production, hydrological processes, and osmosis). This allows us to coherently investigate the potential of remote sensing for monitoring the salinity/drought impact on biological pathways/processes.

2.2.1 Creating representative database through a systematic review

In order to facilitate the analysis of a representative set of recent publications, we adopted an optimized systematic review approach (Berger et al. 2018). Specifically, we focused on scientific peer-reviewed papers published between 2005 and 2020 through the Web of Science (WOS) and Google Scholar (GS) (Figure 2.2). This approach first requires the definition of a representative set of keywords. For our study, these keywords were “remote sensing”, “drought”, “salinity”, “agriculture”, and “traits”, as well as their synonyms (such as RS, food security, etc.). Afterwards, publications were selected from WOS and GS according to the occurrence of combinations of these keywords in the title, abstract, author keywords, and keywords plus, to create a first selection of publications, leading to 1184 selected records. Then, this set of publications was screened to capture only papers that analyzed (a) the impact of drought/salinity stress on VIs/traits of crops by remote sensing, and (b) included information on the spectral wavelength on which the analysis was based. This resulted in 78 unique records. Next, through snowballing these records (to capture papers that were missed in the first step), an additional 49 publications were obtained. In total, 115 publications (Table S2-1) fitting these criteria were identified after removing 12 duplicates. More details on each step are provided in the supplementary information (Figure S2-1). Maps of co-authors and co-occurrences based on the results of the systematic review were created through VOSviewer (Figure S2-2).

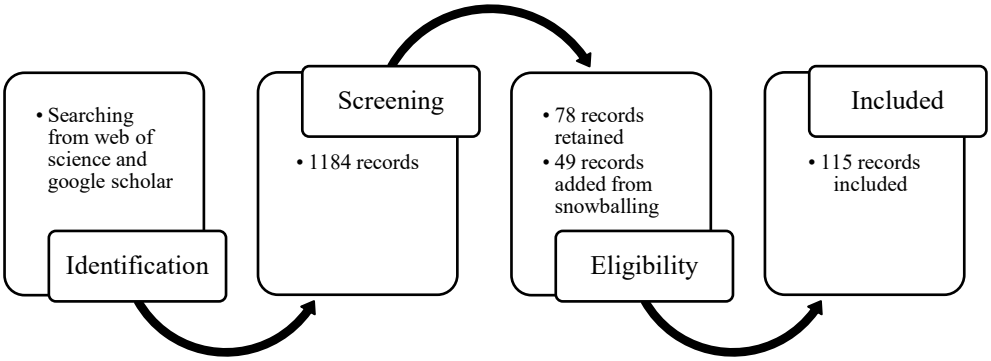

Figure 2.2 Flowchart of the systematic review.

2.2.2 Extraction of drought/salinity stress information

From the full set of publications on drought and salinity stress of agricultural crops, we extracted the correlation strengths between vegetation indices/crop traits responding to drought and salinity stress and spectral bands/wavelengths. Finally, 348 correlations were found, among which 102 traits were wavelength correlations, 171 were VIs-wavelength correlations, and 75 traits were VIs correlations. All 171 VIs-wavelength correlations that we found focused on drought, and no reviewed study provided correlations for salinity stress.

2.2.3 Classification of plant traits and vegetation indices

After the creation of our representative set of publications, we clustered the traits into four groups to relate the impact of drought/salinity stress on biological processes. Specifically, we classified the traits together on the basis of their definitions and the functional processes involved (Niinemets 2015; Pérez-Harguindeguy et al. 2013). This provided us with four clusters, namely biomass traits, photosynthesis traits, water traits, and osmosis traits. Afterwards, each cluster was further divided into RS (directly measurable by RS) and In-RS (indirectly derived by RS) (Table 2.1).

Table 2.1 Classification of plant traits included in this study.

Group	RS methods	Traits							
Biomass traits	RS	LMA	LAI	--	--	--	--	--	--
	In-RS	FS	SDW	BDW	BFW	--	--	--	--

Photosynthesis traits	RS	Chl	Chla/Chlb	--	--	--	--	--	--
	In-RS	A	Pn	ΔF/Fm	Chl*ΔF /Fm	--	--	--	--
Water traits	RS	LCT	CWC	RWC	EWT	CWM	--		
	In-RS	Gs	LOP	Ψp	LWP	Ψs	E	Tl - Tair	--
Osmosis traits	RS	--	--	--	--	--	--	--	--
	In-RS	Na^+	Cl^-	K^+	Ca^{2+}	K^+/Na^+	TSS	TA	TSS/ TA

Notes: leaf mass per unit area (LMA), leaf Area Index (LAI), fruit size (FS), shoot dry weight (SDW), biomass dry weight (BDW), biomass fresh weight (BFW), stomatal conductance (Gs), net gas exchange (A), leaf total chlorophyll (Chl), the quantum yield of photosystem II efficiency (ΔF/Fm), net photosynthesis rate (Pn), the difference between leaf and air temperature (Tl -Tair), transpiration rate (E), leaf water potential (LWP), stem water potential (Ψs), leaf osmotic potential (LOP), leaf canopy temperature (LCT), canopy water content (CWC), relative water content (RWC), leaf equivalent water thickness (EWT), pressure potential (Ψp), canopy water mass (CWM), Na^+ contents in leaf (Na^+), Cl^- contents in leaf (Cl^-), K^+ contents in leaf (K^+), Ca^{2+} contents in leaf (Ca^{2+}), total soluble solids (TSS), tritatable acidity (TA). RS methods: directly derived by remote sensing (RS), indirectly derived by remote sensing (In-RS).

In addition to individual plant functional traits, well-known RS vegetation indices have been related to the responses to drought and/or salinity stress. For consistency, we clustered the results of these studies on the basis of a functional classification, resulting in xanthophyll indices, water content indices, carotenoid indices and greenness indices (Table 2.2).

Table 2.2 Classification, explanation, and equations of different vegetation indices (VIs) included in this study.

VIs	Meaning	Equation	Reference
Xanthophyll Indices			
PRI570	Photochemical reflectance index	(R531 - R570) / (R531 +R570)	(Gamon et al. 1992)
PRI515	Photochemical reflectance index	(R531 - R515) / (R531 +R515)	(Hernández-Clemente et al. 2011)
PRI586	Photochemical reflectance index	(R531 – R586) / (R531 + R586)	(Panigada et al. 2014)
PRI600	Photochemical reflectance index	(R531-R602) / (R531 + R602)	(Hernández-Clemente et al. 2011)
PRI670	Photochemical reflectance index	(R531-R668) / (R531 + R668)	(Hernández-Clemente et al. 2011)
Water Content Indices			
WI	Water index	R900 / R970	(Peñuelas et al. 1993)
CWSI	Crop Water Stress Index	CWSI = (Tleaf - Twet) / (Tdry - Twet)	(Idso et al. 1981)
Carotenoid Indices			
R520/R500	Carotenoid concentration		(Zarco-Tejada et al. 2012)
R515/R570	Carotenoid concentration		(Zarco-Tejada et al. 2012)
Greenness Indices			

OSAVI	Optimized Soil-Adjusted Vegetation Index	(R800 −R670) / (R800 + R670 + 0.16)	(Rondeaux et al. 1996)
TCARI	The Transformed Chlorophyll Absorption in Reflectance Index	TCARI = 3 · [(R700 − R670) − 0.2 · (R700 − R550) · (R700/R670)]	(Haboudane et al. 2002)
TCARI/OSAVI	Normalized by OSAVI to obtain	TCARI/OSAVI = [3 · [(R700 − R670) − 0.2 · (R700 − R550) · (R700/R670)]]/ [(1 + 0.16) · (R800 − R670) / (R800 + R670 + 0.16)]	(Haboudane et al. 2002)
CIgreen	Green chlorophyll index	(R750 / R550)–1	(Gitelson et al. 2005)
CIred edge	Red edge chlorophyll index	(R750 / R710)–1	(Gitelson et al. 2005)
SR	Simple ratio	R800 / R670	(Asrar et al. 1985)
Red edge ratio index		R700 / R670	(Zarco-Tejada et al. 2013b)
VOG1	The chlorophyll a +b index	R740 / R720	(Vogelmann et al. 1993)
ZM	The chlorophyll a +b index	R750 / R710	(Zarco-Tejada et al. 2001)

Notes: R means the reflectance of the band and T means temperature. While NDVI has been used frequently for drought monitoring at a regional scale, we did not include it in this review. The reasoning for this is that NDVI is considered as a greenness index related to chlorophyll instead of the water status of the vegetation. In support of this interpretation, NDVI has not been found to respond to rainfall or major precipitation events during the crop growth period (Rahimzadeh-Bajgiran et al. 2012; Rahimzadeh Bajgiran et al. 2008). Therefore, NDVI was not included in the review.

2.2.4 Analyses of Vegetation Responses

After all functional clusters were defined, we aggregated the results from the different papers for each functional cluster (of VIs and plant traits) and proceeded to analyze their correlations. We first analyzed the spectral signatures of VIs under drought and their strengths. Afterwards, the distribution of spectral signatures of each functional traits cluster was investigated in the range of 400–2800 nm. Finally, we analyzed the correlations of different clusters of VIs and plant traits.

2.3 Results

2.3.1 Spectral signatures of vis under drought stress

We found a wide range of correlations for the four clusters of VIs (defined within the spectral range of 500–1050 nm) under drought stress, as highlighted in Figure 2.3. Specifically, xanthophyll indices showed their highest R^2 at 531 nm (R^2max = 0.80) and 570–600 nm (R^2max = 0.80), while greenness indices showed their highest R^2 at 550 nm (R^2max = 0.70), 670 nm (R^2max = 0.76), 700–750 nm (R^2max = 0.78), and 800 nm (R^2max = 0.76), and water indices showed their highest R^2 at 900 nm (R^2max = 0.72) and 970 nm (R^2max = 0.72). For carotenoid indices, no such region could be identified due to mostly low correlations ($0.20 \leq R^2 \leq 0.49$).

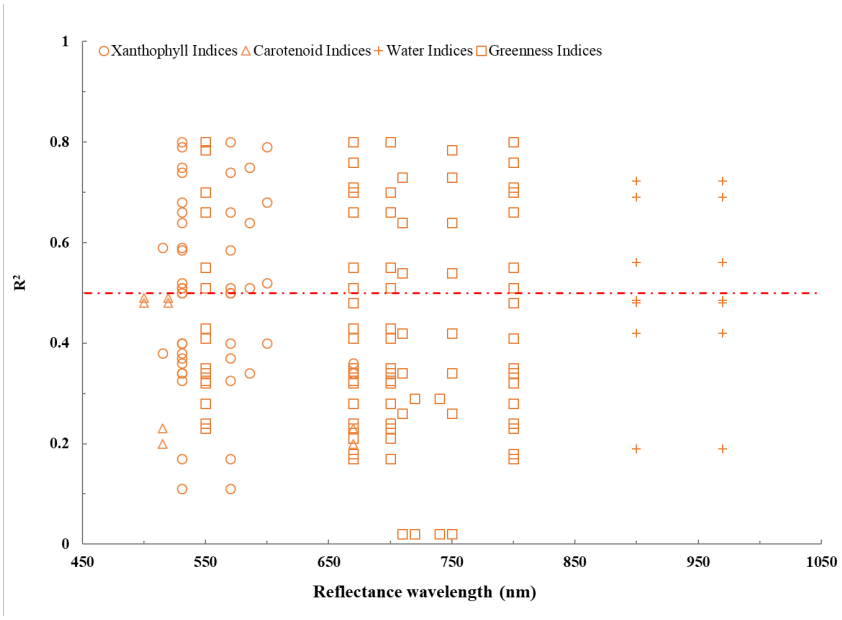

Figure 2.3 Relationships between R^2 and wavelength of different VIs clusters under drought stress. The red line indicates that $R^2 > 0.50$.

While we could identify specific regions where individual VIs provided a maximum sensitivity, we also found variation in this sensitivity. Although we identified studies that highlighted the potential of specific VIs for drought monitoring, we also found other studies reporting low R^2 ($R^2 < 0.50$) for the same VIs and wavelengths. Thus, there are undeniable limitations to identifying vegetation health using VIs under drought stress.

2.3.2 Spectral signatures of plant traits under drought and salinity stress

The reviewed studies focusing on plant trait signals showed that these crop responses were not constrained to specific wavelengths. Biomass, photosynthesis, water, and osmosis clusters of traits were identified across the full spectral range. These clusters showed few spectral patterns, even for those trait clusters that were supposedly directly measurable by RS (Figure 2.4). The only recognizable trends concern the osmosis traits cluster (with a significant response to salinity stress), with a slight tendency to occur more frequently at 550–750 nm, and the biomass traits and water traits occurring at 1400–1850 nm. As far as the few observations for drought do allow, those patterns did not seem to deviate much from those for salinity (Figure 2.4).

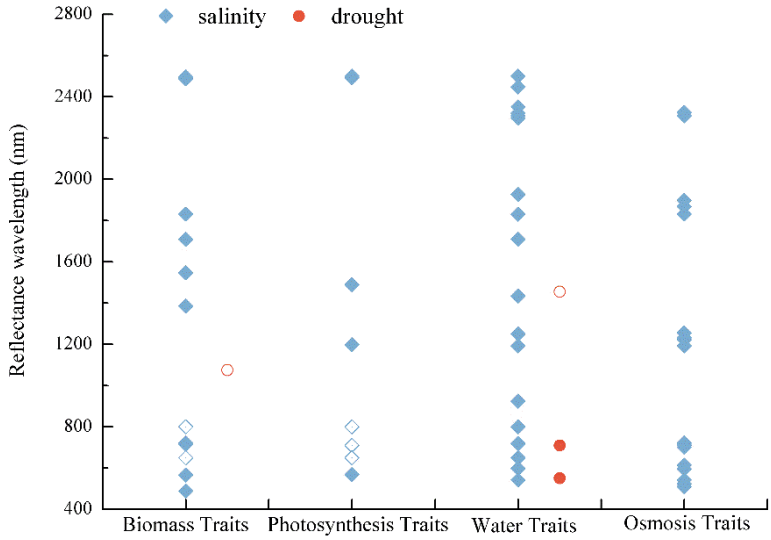

Figure 2.4 Drought and salinity stress responses of different trait clusters across the reflectance spectrum based on relationships with $R^2 > 0$. Solid symbols indicate traits directly measured by RS; empty symbols are related to traits indirectly measured by RS.

Moreover, while plant traits are more directly related to plant functioning and thus to stress, the correlations between the plant traits and the (drought and salinity) stress were not necessarily stronger (Figure 2.5). Biomass traits showed to have high R^2 value to salinity stress at around 720 nm (R^2max = 0.74), 1300–1800 nm (R^2max = 0.88), and around 2500 nm (R^2max = 0.88). Photosynthesis traits had high R^2 values at 710 nm (R^2max = 0.97), 800 nm (R^2max = 0.89), 1200 nm, and around 2500 nm (R^2max = 0.75). Interestingly, for both biomass and photosynthesis traits, the indirectly derived plant traits had generally higher R^2 values than the directly measurable RS traits. For water traits, we found different patterns from biomass traits and photosynthesis traits, with high R^2 widely distributed between 500 and 2500 nm (R^2max = 0.78). While high R^2 peaked in the 600–800 nm range, they were also highly variable ($0.02 \leq R^2 \leq 0.78$). In contrast, osmosis traits (only indirectly retrievable) showed a very promising performance (all with $R^2 > 0.50$) across the entire region of 500-2300 nm. Thus, it seemed that osmosis traits were most directly related to salinity stress responses. For drought stress, the number of studies that presented the wavelengths they used was too limited to draw clear conclusions. In general though, neither the range of R^2 values nor the wavelengths at which traits responded to drought stress deviated much from those for salinity stress.

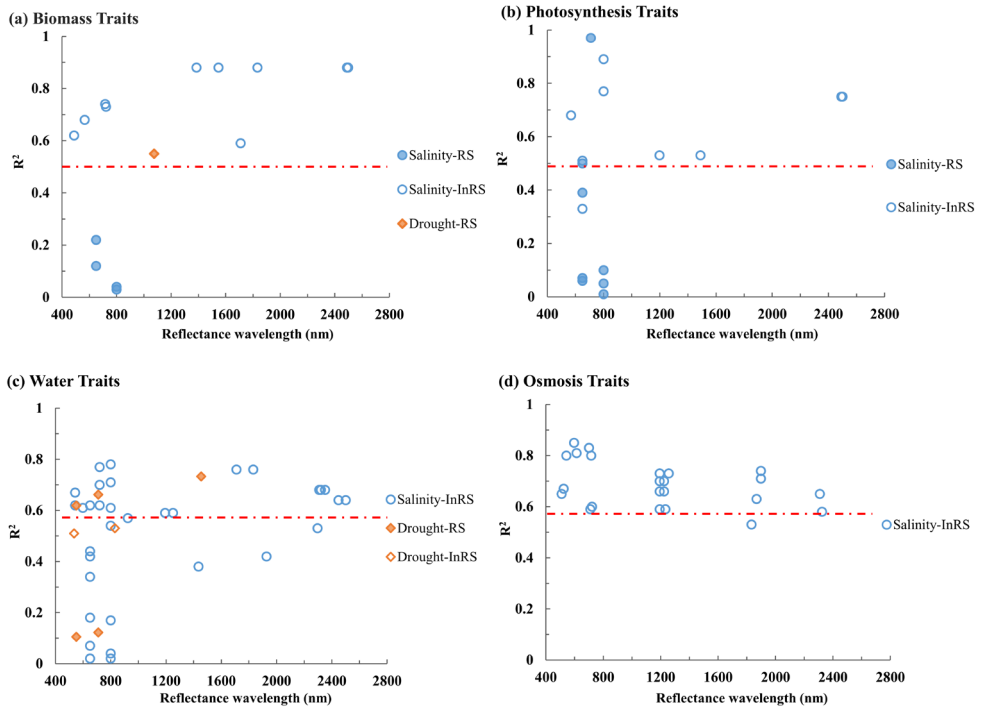

Figure 2.5 Relationship between R^2 and wavelength of different trait clusters under drought/salinity stress. RS identifies traits that can be directly measured by RS; InRS identifies traits that can be indirectly measured by RS. The red line indicates $R^2 > 0.50$.

2.3.3 The relationship between vis and plant traits

Vegetation indices have been shown to strongly correlate with individual plant traits (e.g., LAI and Chl), but the linkage between VIs, spectral reflectance, and crop traits remains inadequately understood. Thus, we analyzed the relationship between VIs and plant traits, and the results are shown in Table 2.3. For biomass traits, LAI showed high correlations with xanthophyll indices (R^2max = 0.66) and greenness indices (R^2max = 0.71) (particularly for OSAVI). Photosynthesis traits were also highly correlated with xanthophyll indices (R^2max = 0.68) and greenness indices (R^2max = 0.70). Especially, ΔF/Fm was highly correlated with TCARI/OSAVI (R^2max = 0.70). Water traits showed a wide range of correlations ($0.02 \leq R^2 \leq 0.80$) with VIs. Therein, Tl − Tair was highly correlated with PRI570 ($R^2 = 0.74$), PRI600 ($R^2 = 0.79$), and TCARI/OSAVI ($R^2 = 0.80$). CWC was highly correlated to three VIs, including WI ($R^2 = 0.72$), CIgreen ($R^2 = 0.78$), and CIred edge ($R^2 = 0.73$). EWTcanopy was highly correlated to PRI586 ($R^2 = 0.75$) and OSAVI ($R^2 = 0.76$). LWP was highly correlated to CWSI ($R^2 = 0.78$) and Gs was highly correlated with CWSI ($R^2 = 0.77$). Osmosis traits were mainly highly correlated with PRI570 (R^2max = 0.50). Thus, in general, the four trait clusters

were highly correlated with xanthophyll indices ($0.50 \leq R^2max \leq 0.79$), while they showed lower correlations with carotenoid indices ($0.20 \leq R^2 \leq 0.49$). Furthermore, water traits were correlated stronger with water indices ($0.42 \leq R^2 \leq 0.78$) than with the other three trait groups ($0.19 \leq R^2 \leq 0.49$). Greenness indices showed high correlations with biomass traits ($R^2max = 0.71$), photosynthesis traits ($R^2max = 0.70$), and water traits ($R^2max = 0.80$) but not with osmosis traits ($R^2max = 0.35$). However, despite these general patterns, Table 2.3 also shows that variability in the relationships is high.

Table 2.3 The relationship between traits and VIs under drought stress

VIs	Biomass Traits		Photosynthesis Traits			Water Traits					Osmosis Traits				
	LAI*	FS	Chl*	ΔF/Fm	Chl×ΔF/Fm	Tl - Tair	CWC*	RWC*	EWT*	EWTcanopy*	LWP	Gs	TSS	TA	TSS/TA
Xanthophyll Indices															
PRI570	0.66	0.11	--	--	0.40	0.74	--	0.51	--	--	0.37	0.59	0.17	0.50	0.50
PRI515	--	--	--	--	--	--	--	--	--	--	0.38	0.59	--	--	--
PRI586	0.64	--	--	0.51	0.34	--	--	--	--	0.75	--	--	--	--	--
PRI600	0.40	--	--	0.68	--	0.79	--	0.52	--	--	--	--	--	--	--
PRI670	--	--	--	0.34	0.36	--	--	--	--	--	--	--	--	--	--
Carotenoid Indices															
R520/R500	--	--	--	--	--	--	--	--	--	--	0.48	0.49	--	--	--
R515/R670	--	--	--	--	--	--	--	--	--	--	0.20	0.23	--	--	--
Water Content Indices															
WI	0.49	--	--	0.48	0.19	0.69	0.72	0.42	--	0.56	--	--	--	--	--
CWSI	--	--	--	--	--	--	--	--	--	--	0.78	0.77	--	--	--
Greenness Indices															
OSAVI	0.71	--	--	0.48	0.32	--	--	--	--	0.76	--	--	--	--	--
TCARI	--	--	0.43	--	--	--	--	--	--	--	0.325	0.32	--	--	--
TCARI/OSAVI	0.34	0.32	0.66	0.70	0.51	0.80	--	0.41	0.55	--	0.28	0.23	0.24	0.35	0.28
CIgreen	--	--	--	--	--	--	0.78	--	--	--	--	--	--	--	--
CIred edge	0.64	--	--	0.42	--	0.54	0.73	0.34	--	--	--	--	--	--	--
SR	--	0.18	--	--	--	--	--	--	--	--	--	--	0.28	0.34	0.17
Red edge ratio index	--	--	--	--	--	--	--	--	--	--	--	0.21	--	--	--
VOG1	--	--	--	--	--	--	--	--	--	--	0.02	0.29	--	--	--
ZM	--	--	--	--	--	--	--	--	--	--	0.02	0.26	--	--	--

Note: bold numbers indicate that R^2 >0.50. * means the traits could be directly measured by RS.

2.4 Discussion

In this study, we systematically evaluated the usefulness of current monitoring approaches (i.e., vegetation indices and plant traits) for evaluating vegetation responses to drought and salinity stress. Vegetation indices have been developed to monitor vegetation health conditions since the 1980s (Rahimzadeh-Bajgiran et al. 2012), and a review of drought indices can be found in (Zargar et al. 2011). In contrast, only over the past two decades, remote sensing techniques have advanced enough to retrieve plant traits, increasingly leading to remote sensing applications to monitor plant traits to characterize both natural vegetation and crop functioning (Moreno-Martínez et al. 2018). However, a systematic review on the extent to which these metrics can pick up drought and salinity stress has so far been missing.

Our study reveals that most VIs reviewed are not accurate and consistent enough to detect changes in crop temporal and spatial responses under stress. This finding coincides with previous studies (Liu et al. 2016) that showed that simple VIs were hardly able to detect the impact of drought on crops. A possible explanation for this is that most VIs do not directly reflect the mechanism of crop responses to stress. While many VIs are related to (normalized) features of e.g., greenness, carotenoid, or xanthophyll concentrations, it seems that these features do not only vary because of the actual drought and salinity stress but also under the influence of various other local conditions. This may explain the wide range of R^2 values in relation to drought or salinity stress. In order to comprehensively monitor stress, we should therefore focus on exploring the spectral characteristics of crop tolerance and stress response mechanisms to truly reflect the crop health condition under stress.

Plant traits might provide an approach to measure these stress mechanisms, given that traits have proven to be indicators of plant and ecosystem functioning. While previous studies showed that RS could potentially address plant traits, in particular traits related to photosynthetic process, canopy structure, and leaf biochemistry (Homolova et al. 2013; Weiss et al. 2020), there are a few plant traits studies that focus on drought and salinity stress. More specifically, the number of drought and salinity studies evaluating plant traits is much lower than those using VIs. Irrespective of this dichotomy, our systematic review shows that neither the wavelengths at which traits are detected nor the strength of the relationship to drought and salinity stress is consistent within or between traits of different crops. In fact, a wide range of wavelengths used to detect plant traits was found (Homolova et al. 2013), which suggests that most relationships to spectral signatures are indirect at best. These indirect relationships, and thus the potential for confounding factors, may provide a partial explanation for the large variance we found in R^2 values and the generally low explained variance. One of those confounding factors concerns that crop (biomass and water) responses to salinity

are to some extent similar to those to drought. This confounding factor leads to confusion in some results and has hitherto not been accounted for in previous studies. Furthermore, the relationship between traits and stress is further complicated by the fact the drought and salinity tolerance mechanisms of crops are complicated and multivariate.

An exception to the low and varied R^2 values is the osmotic traits as detected (indirectly) by remote sensing. In all evaluated studies, osmotic traits were strongly related to salinity stress. This phenomenon is linked to crop response mechanisms and is -in contrast to biomass and water responses- unique to salinity stress. Salinity stress inflicts damage to plants due to (a) the disruption of the ionic equilibrium, (b) an osmotic imbalance, and thereby (c) a decreased photosynthesis due to the toxicity of Na^+. Likewise, evidence shows that an increased expression of K^+, Ca^{2+}, Salt Overly Sensitive (SOS) pathways, and glycine betaine are related to salinity stress tolerance (Mahajan and Tuteja 2005; Niu et al. 1995; Yeo 1998). Both drought and salinity stress cause osmotic stress and decrease cytosolic as well as vacuolar volumes. In the case of drought, this osmotic stress is the result of a displacement of membrane proteins and disruptions in cellular metabolism (Mahajan and Tuteja 2005). In addition, reactive oxygen species are produced, which have adverse effects on cellular structures and metabolism (Bartels and Sunkar 2005). Therefore, the responses of plants to drought and salinity are identical at the early stage. Consequently, osmotic traits show a high potential as a suitable indicator for drought and salinity stress RS monitoring. In particular, promising results have been found for detecting ionic concentrations of sodium, potassium, and chloride (El-Hendawy et al. 2019b; Zhang et al. 2017). Unfortunately, though, it seems that our understanding at which wavelengths the osmotic traits are expressed is still limited.

As highlighted in the previous paragraph, plant functioning under stress is affected by various pathways. From that perspective, instead of focusing on individual VIs or traits, an alternative approach to monitoring drought and salinity stress is the consideration of multiple trait responses simultaneously. Although stresses have been investigated using many aspects, previous studies rarely utilized multiple variables to assess these pathways. Radiative transfer models (RTMs) may be particularly useful to retrieve such multiple variables from remote sensing observations. RTMs have been developed to study the relationship between vegetation biochemical and biophysical properties, and hyperspectral reflectance (Bayat et al. 2016; Botha et al. 2006). In the forward mode, RTMs simulate the vegetation spectrum based on known spectral signatures of vegetation biochemical and biophysical properties. Likewise, RTMs can retrieve vegetation properties from reflectance data in the inverse mode (Jacquemoud 2000; Lu et al. 2020a; Timmermans et al. 2009). Indeed, RTM inversion has been successfully applied to

monitor the changes in plant traits and reflectance upon drought (Bayat et al. 2016). By monitoring multiple traits simultaneously, through the inversion of RTMs, it will become possible to evaluate how multiple traits in concert are affected by drought and/or salinity stress. This may also provide additional insights into the plant strategies to deal with drought and/or salinity stress. Unfortunately, though, the ill-posedness of the inversion problem commonly puts major constraints on the generic applicability of RTMs for crop monitoring. Another major constraint, in the context of this review, is that osmosis traits are difficult to measure directly by remote sensing. Dissolved salts such as Na^+, Cl^-, K^+, and Ca^{2+} are not directly tractable, although NaCl has a clearly defined spectrum in the infrared spectrum. This strongly limits its incorporation within RTMs, which indeed only focus on a limited number of vegetation traits such as LAI, Chl, and CWC. More research will be needed to evaluate the prospects of physical modeling of radiative transfer under the influence of known stress response mechanisms. Traditional multi- or high-spectral field sensors to investigate the impacts of drought and salinity on crops in relation to in situ observed traits related to these stresses will be the way forward here.

A final limitation to monitoring plant traits in response to drought and salinity stress is the spatiotemporal and spectral resolution of current satellites. Low spatiotemporal resolution and revisit periods are two main restraints for current satellite sensor applications in crop management (Berni et al. 2009), although this has strongly improved with the launch of the Sentinels satellites. The spectral resolution is currently probably more limiting. The inconsistency across multiple sensors of different satellites does not allow combining them in one retrieval (Liu et al. 2016). Hyperspectral missions, such as those foreseen in EnMAP, may provide such information. This may be particularly interesting if combined with Light Detection and Ranging (LiDAR) information (e.g., from Global Ecosystem Dynamics Investigation (GEDI)) or high-resolution information on temperature (e.g., the Ecosystem Spaceborne Thermal Radiometer Experiment on Space Station (ECOSTRESS)). However, also, for a fruitful incorporation of such information sources, it will be essential to first characterize the spectral properties of traits directly related to the plant responses to drought and salinity stress. This will reduce the impacts of confounding factors that currently seem to dominate the patterns obtained, as seems apparent from Figures 2.3-2.5.

2.5 Conclusions

Based on a systematic review, we conclude that a significant number of challenges remain before RS can be used to monitor drought and salinity stress on crop health. Specifically, we found that VIs are insufficiently accurate to consistently estimate these effects. For plant traits, we found some positive correlations for individual

cases, confirming that plant traits indeed reflect stress response mechanisms. However, these cases were too few to accurately monitor the pathways for drought and salinity stress. Furthermore, we found that both spectral wavelengths and the strength of the relationship to drought and salinity stress varied strongly. Osmosis traits appear to be the exception to this and consequently have the potential to be used for monitoring the pathways along which drought and salinity impact crops. However, osmosis traits cannot be directly measured by RS. In order to fully capture the biophysical/biochemical pathways of drought/salinity stress on crop health, future research should focus on (1) advancing our capability to simultaneously monitor (through multi-sensor frameworks) the suite of crop traits that are connected to the different pathways affected by drought and salinity, and (2) expanding our characterization of the spectral properties of osmotic traits (through optimized RTMs).

2.6 Author contributions

Conceptualization, J.T., P.M.v.B., and W.W.; methodology, J.T., W.W., and P.M.v.B.; investigation, W.W.; writing—original draft preparation, W.W.; writing—review and editing, P.M.v.B., J.T. and Q.C.; supervision, P.M.v.B. and J.T. All authors have read and agreed to the published version of the manuscript.

2.7 Supporting information

Figure S2-1 The flowchart of the systematic review

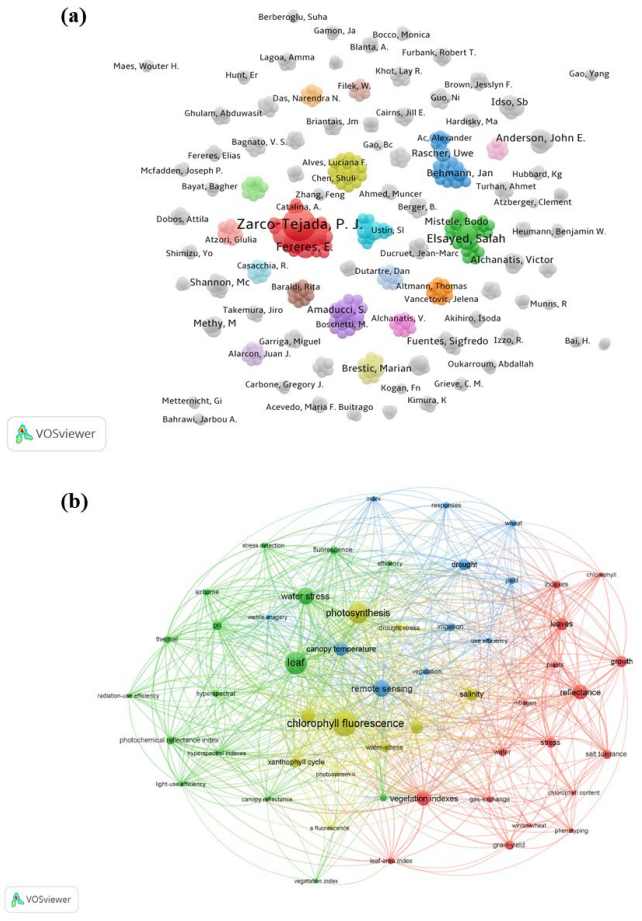

Figure S2-2 Maps of co-authors and co-occurrences from the results of the systematic review. A bubble and a tag constitute an element. The size of an element depends on the number of nodes, the strength of the line, and the number of citations. The color of an element represents the cluster to which it belongs, and different clusters are represented by different colors. In the co-author map, it shows the network of co-authorship links between 115 publications from the systematic review. The "bubbles" represent authors. The size of an author bubble represents the number of publications. Colors represent authors groups that are clustered by co-authorship links (Perianes-Rodriguez et al. 2016; Van Eck and Waltman 2011, 2014).

It was noticed that very few people are focusing on the topic of using remote sensing to monitor crop response to drought and salt stress. Also, the connections among most authors were rather weak. Also, there was a very limited number of studies focusing on monitoring crop traits responses to drought and salinity using remote sensing techniques as the co-occurrence map showed that the connection of plant traits and spectra was rather weak. Therefore, we conclude that these topics need further investigation.

Table S2-1 115 publications identified from the systematic review

No.	Title	Reference
1	Detection of early plant stress responses in hyperspectral images	(Behmann et al. 2014)
2	A crop-specific drought index for corn: I. Model development and validation	(Meyer et al. 1993)
3	A field experiment on spectrometry of crop response to soil salinity	(Leone et al. 2007)
4	A PRI-based water stress index combining structural and chlorophyll effects: Assessment using diurnal narrow-band airborne imagery and the CWSI thermal index	(Zarco-Tejada et al. 2013b)
5	Advanced phenotyping offers opportunities for improved breeding of forage and turf species	(Walter et al. 2012)
6	Advances in Remote Sensing of Agriculture: Context Description, Existing Operational Monitoring Systems and Major Information Needs	(Atzberger 2013)
7	Aerial canopy temperature differences between fast- and slow-wilting soya bean genotypes	(Bai and Purcell 2018)
8	Agricultural drought monitoring: Progress, challenges, and prospects	(Liu et al. 2016)
9	Anatomy of a local-scale drought: Application of assimilated remote sensing products, crop model, and statistical methods to an agricultural drought study	(Mishra et al. 2015)
10	Application of vegetation index and brightness temperature for drought detection	(Kogan 1995a)
11	Application of visible and near-infrared spectrophotometry for detecting salinity effects on wheat leaves (*Triticum aestivum* L.)	(Mokhtari M. H. et al. 2014)
12	Applying hyperspectral imaging to explore natural plant diversity towards improving salt stress tolerance	(Sytar et al. 2017)
13	Assessing canopy PRI for water stress detection with diurnal airborne imagery	(Suarez et al. 2008)
14	Assessing canopy PRI from airborne imagery to map water stress in maize	(Rossini et al. 2013)
15	Assessment of Photochemical Reflectance Index as a Tool for Evaluation of Chlorophyll Fluorescence Parameters in Cotton and Peanut Cultivars Under Water Stress Condition	(Yoshizumi et al. 2010)
16	Assessment of the water status of mandarin and peach canopies using visible multispectral imagery	(Kriston-Vizi et al. 2008)
17	Associated changes in physiological parameters and spectral reflectance indices in olive (*Olea europaea* L.) leaves in response to different levels of water stress	(Sun et al. 2008)
18	Biophysical properties and biomass production of elephant grass under saline conditions	(Wang et al. 2002a)
19	Broadband Spectral Reflectance Models of Turfgrass Species and Cultivars to Drought Stress	(Jiang and Carrow 2007)
20	Can chlorophyll-a fluorescence parameters be used as bio-indicators to distinguish between drought and salinity stress in *Tilia cordata Mill*	(Kalaji et al. 2018)
21	Canopy temperature as a crop water stress indicator	(Jackson et al. 1981)

22	Characterization of Crop Canopies and Water Stress Related Phenomena using Microwave Remote Sensing Methods: A Review	(Vereecken et al. 2012)
23	Chlorophyll fluorescence performance of sweet almond [Prunus dulcis (Miller) D. Webb] in response to salinity stress induced by NaCl	(Ranjbarfordoei et al. 2006)
24	Chlorophyll, anthocyanin, and gas exchange changes assessed by spectroradiometry in *Fragaria chiloensis* under salt stress.	(Garriga et al. 2014)
25	Comparative evaluation of the Vegetation Dryness Index (VDI), the Temperature Vegetation Dryness Index (TVDI) and the improved TVDI (iTVDI) for water stress detection in semi-arid regions of Iran	(Rahimzadeh-Bajgiran et al. 2012)
26	Computational water stress indices obtained from thermal image analysis of grapevine canopies	(Fuentes et al. 2012)
27	Crop yield prediction under soil salinity using satellite derived vegetation indices	(Satir and Berberoglu 2016)
28	Data fusion of spectral, thermal and canopy height parameters for improved yield prediction of drought stressed spring barley	(Rischbeck et al. 2016)
29	Detecting salinity stress in tall fescue based on single leaf spectrum	(Gao and Li 2012)
30	Detecting water stress effects on fruit quality in orchards with time-series PRI airborne imagery	(Suárez et al. 2010)
31	Detection of water stress in an olive orchard with thermal remote sensing imagery	(Sepulcre-Canto et al. 2006)
32	Detection of water stress in orchard trees with a high-resolution spectrometer through chlorophyll fluorescence In-Filling of the O2-A band	(Pérez-Priego et al. 2005)
33	Determining the Canopy Water Stress for Spring Wheat Using Canopy Hyperspectral Reflectance Data in Loess Plateau Semiarid Regions	(Wang et al. 2015)
34	Drought and Salinity Impacts on Bread Wheat in a Hydroponic Culture: A Physiological Comparison	(Movahhedi Dehnavi et al. 2017)
35	Drought stress effects on photosystem I content and photosystem II thermotolerance analyzed using Chl a fluorescence kinetics in barley varieties differing in their drought tolerance	(Oukarroum et al. 2009)
36	Early drought stress detection in cereals: Simplex Volume Maximization for hyperspectral image analysis	(Römer et al. 2012)
37	Effect of different concentrations of diluted seawater on yield and quality of lettuce	(Turhan et al. 2014)
38	Effects of four types of sodium salt stress on plant growth and photosynthetic apparatus in sorghum leaves	(Zhang et al. 2018)
39	Effects of saline reclaimed waters and deficit irrigation on Citrus physiology assessed by UAV remote sensing	(Romero-Trigueros et al. 2017)
40	Effects of salinity on physiological responses and the photochemical reflectance index in two co-occurring coastal shrubs	(Zinnert et al. 2012)
41	Estimating crop water stress with ETM+ NIR and SWIR data	(Ghulam et al. 2008)
42	Estimating growth and photosynthetic properties of wheat grown in simulated saline field conditions using hyperspectral	(El-Hendawy et al. 2019a)

	reflectance sensing and multivariate analysis	
43	Estimating Yields of Salt- and Water-Stressed Forages with Remote Sensing in the Visible and Near Infrared	(Poss et al. 2006)
44	Estimation of Canopy Water Content by Means of Hyperspectral Indices Based on Drought Stress Gradient Experiments of Maize in the North Plain	(Zhang and Zhou 2015)
45	Estimation of Water Stress in Grapevines Using Proximal and Remote Sensing Methods	(Matese et al. 2018)
46	Evaluation of agronomic traits and spectral reflectance in Pacific Northwest winter wheat under rain-fed and irrigated conditions	(Gizaw et al. 2016)
47	Evaluation of Hyperspectral Reflectance Parameters to Assess the Leaf Water Content in Soybean	(Kovar et al. 2019)
48	Evaluation of wavelengths and spectral reflectance indices for high-throughput assessment of growth, water relations and ion contents of wheat irrigated with saline water	(El-Hendawy et al. 2019b)
49	Fluorescence excitation spectra of drought resistant and sensitive genotypes of triticale and maize	(Grzesiak et al. 2007)
50	Fluorescence Spectroscopy to Detect Water Stress in Orange Trees	(Lins et al. 2005)
51	Fluorescence, PRI and canopy temperature for water stress detection in cereal crops	(Panigada et al. 2014)
52	Fluorescence, temperature and narrow-band indices acquired from a UAV platform for water stress detection using a micro-hyperspectral imager and a thermal camera	(Zarco-Tejada et al. 2012)
53	Fluorescence-based sensing of drought-induced stress in the vegetative phase of four contrasting wheat genotypes	(Bürling et al. 2013)
54	Genes and salt tolerance: bringing them together	(Munns 2005)
55	Ground-based canopy sensing for detecting effects of water stress in cotton	(Stamatiadis et al. 2010)
56	High-throughput field phenotyping in dry bean using small unmanned aerial vehicle based multispectral imagery	(Sankaran et al. 2018)
57	Hyperspectral Reflectance Response of Freshwater Macrophytes to Salinity in a Brackish Subtropical Marsh	(Tilley et al. 2007)
58	Hyperspectral remote sensing of salinity stress on red (*Rhizophora mangle*) and white (*Laguncularia racemosa*) mangroves on Galapagos Islands	(Song et al. 2011)
59	Hyperspectral remote sensing to assess the water status, biomass, and yield of maize cultivars under salinity and water stress	(Elsayed and Darwish 2017)
60	Identifying leaf traits that signal stress in TIR spectra	(Acevedo et al. 2017)
61	Image-Derived Traits Related to Mid-Season Growth Performance of Maize Under Nitrogen and Water Stress	(Dodig et al. 2019)
62	Imaging chlorophyll fluorescence with an airborne narrow-band multispectral camera for vegetation stress detection	(Zarco-Tejada et al. 2009)
63	Integrating satellite optical and thermal infrared observations for improving daily ecosystem functioning estimations during a drought episode	(Bayat et al. 2018)
64	Interpretation of salinity and irrigation effects on soybean	(Wang et al. 2002b)

	canopy reflectance in visible and near-infrared spectrum domain	
65	Landsat images and crop model for evaluating water stress of rainfed soybean	(Sayago et al. 2017)
66	Leaf chlorophyll fluorescence, reflectance, and physiological response to freshwater and saltwater flooding in the evergreen shrub, *Myrica cerifera*	(Naumann et al. 2008b)
67	Leaf-rolling in maize crops: from leaf scoring to canopy-level measurements for phenotyping	(Baret et al. 2018)
68	Linking leaf chlorophyll fluorescence properties to physiological responses for detection of salt and drought stress in coastal plant species	(Naumann et al. 2007)
69	Linking physiological responses, chlorophyll fluorescence and hyperspectral imagery to detect salinity stress using the physiological reflectance index in the coastal shrub, *Myrica cerifera*	(Naumann et al. 2008a)
70	Measurement of leaf relative water content by infrared reflectance	(Hunt Jr et al. 1987)
71	Melon crops (*Cucumis melo* L., cv. Tendral) grown in a mediterranean environment under saline-sodic conditions: Part I. Yield and quality	(Tedeschi et al. 2011)
72	Meta-analysis assessing potential of steady-state chlorophyll fluorescence for remote sensing detection of plant water, temperature and nitrogen stress	(Alexander et al. 2015)
73	Modelling PRI for water stress detection using radiative transfer models	(Suarez et al. 2009)
74	Monitoring agricultural drought for arid and humid regions using multi-sensor remote sensing data	(Rhee et al. 2010)
75	Monitoring stomatal conductance of *Jatropha curcas* seedlings under different levels of water shortage with infrared thermography	(Maes et al. 2011)
76	Monitoring water stress and fruit quality in an orange orchard under regulated deficit irrigation using narrow-band structural and physiological remote sensing indices	(Stagakis et al. 2012)
77	Monitoring yield and fruit quality parameters in open-canopy tree crops under water stress. Implications for ASTER	(Sepulcre-Canto et al. 2007)
78	Natural selection and neutral evolutionary processes contribute to genetic divergence in leaf traits across a precipitation gradient in the tropical oak *Quercus oleoides*	(Ramírez-Valiente et al. 2018)
79	NDWI—A normalized difference water index for remote sensing of vegetation liquid water from space	(Gao 1996)
80	New phenotyping methods for screening wheat and barley for beneficial responses to water deficit	(Munns et al. 2010)
81	Normalizing the stress-degree-day parameter for environmental variability	(Idso et al. 1981)
82	Perspectives for Remote Sensing with Unmanned Aerial Vehicles in Precision Agriculture	(Maes and Steppe 2019)
83	Phenotyping for Abiotic Stress Tolerance in Maize	(Masuka et al. 2012)
84	Photochemical reflectance index as a mean of monitoring early water stress	(Sarlikioti et al. 2010)

85	Photochemistry, remotely sensed physiological reflectance index and de-epoxidation state of the xanthophyll cycle in *Quercus coccifera* under intense drought	(Peguero-Pina et al. 2008)
86	Photosynthetic gas exchange, chlorophyll fluorescence and some associated metabolic changes in cowpea (*Vigna unguiculata*) during water stress and recovery	(Souza et al. 2004)
87	Potential and constraints of different seawater and freshwater blends as growing media for three vegetable crops	(Atzori et al. 2016)
88	Radiation use efficiency, chlorophyll fluorescence, and reflectance indices associated with ontogenic changes in water limited Chenopodium quinoa leaves	(Winkel et al. 2002)
89	Recovery responses of photosynthesis, transpiration, and stomatal conductance in kidney bean following drought stress	(Miyashita et al. 2005)
90	Relationships between net photosynthesis and steady-state chlorophyll fluorescence retrieved from airborne hyperspectral imagery	(Zarco-Tejada et al. 2013a)
91	Relationships between stomatal behavior, spectral traits and water use and productivity of green peas (*Pisum sativum* L.) in dry seasons	(Nemeskéri et al. 2015)
92	Remote sensing of soil salinity: potentials and constraints	(Metternicht and Zinck 2003)
93	Risk identification of agricultural drought for sustainable Agroecosystems	(Dalezios et al. 2014)
94	Salinity tolerance and the decoupling of resource axis plant traits	(Eallonardo Jr et al. 2013)
95	Seasonal and drought-related changes in leaf area profiles depend on height and light environment in an Amazon forest	(Smith et al. 2019)
96	Seasonal patterns of reflectance indices, carotenoid pigments and photosynthesis of evergreen chaparral species	(Stylinski et al. 2002)
97	Simple reflectance indices track heat and water stress-induced changes in steady-state chlorophyll fluorescence at the canopy scale	(Dobrowski et al. 2005)
98	Soil salinity mapping and hydrological drought indices assessment in arid environments based on remote sensing techniques	(Elhag and Bahrawi 2017)
99	Spatial–spectral processing strategies for detection of salinity effects in cauliflower, aubergine and kohlrabi	(Rud et al. 2013)
100	Spectral assessments of wheat plants grown in pots and containers under saline conditions	(Hackl et al. 2013)
101	Spectral indicators for salinity effects in crops: a comparison of a new green-indigo ratio with existing indices	(Rud et al. 2011)
102	Spectral indices for the detection of salinity effects in melon plants	(Hernández et al. 2014)
103	Spectral Reflectance for Indirect Selection and Genome-Wide Association Analyses of Grain Yield and Drought Tolerance in North American Spring Wheat	(Gizaw et al. 2018)
104	Steady-State and Maximum Chlorophyll Fluorescence Responses to Water Stress in Grapevine Leaves: A New Remote Sensing System	(Flexas et al. 2000)
105	The influence of diluted seawater and ripening stage on the	(Sgherri et al. 2007)

	content of antioxidants in fruits of different tomato genotypes	
106	The influence of soil salinity, growth form, and leaf moisture on the spectral radiance o	(Klemas and Smart 1983)
107	The Photochemical Reflectance Index (PRI) as a water-stress index	(Thenot et al. 2002)
108	The relationships between electrical conductivity of soil and reflectance of canopy, grain, and leaf of rice in northeastern Thailand	(Touch et al. 2015)
109	The use of infrared thermal imaging as a non-destructive screening tool for identifying drought-tolerant lentil genotypes	(Biju et al. 2018)
110	The Vegetation Drought Response Index (*VegDRI*): A New Drought Monitoring Approach for Vegetation	(Wardlow et al. 2008)
111	Thermal and Narrowband Multispectral Remote Sensing for Vegetation Monitoring From an Unmanned Aerial Vehicle	(Berni et al. 2009)
112	Use of thermal and visible imagery for estimating crop water status of irrigated grapevine	(Möller et al. 2007)
113	Using paired thermal and hyperspectral aerial imagery to quantify land surface temperature variability and assess crop stress within California	(Shivers et al. 2019)
114	Utilization of a high-throughput shoot imaging system to examine the dynamic phenotypic responses of a C-4 cereal crop plant to nitrogen and water deficiency over time	(Neilson et al. 2015)
115	Water stress detection in potato plants using leaf temperature, emissivity, and reflectance	(Gerhards et al. 2016)

Chapter 3

Monitoring the combined effects of drought and salinity stress on crops using remote sensing in the Netherlands

Wen Wen, Joris Timmermans, Qi Chen, Peter M. van Bodegom

Hydrology and Earth System Sciences, 2022, 26: 4537–4552.

https://doi.org/10.5194/hess-26-4537-2022

Abstract

Global sustainable agricultural systems are under threat, due to increasing and co-occurring drought and salinity stresses. Combined effects of these stresses on agricultural crops have traditionally been evaluated in small-scale experimental studies. Consequently, large-scale studies need to be performed to increase our understanding and assessment of the combined impacts in agricultural practice in real-life scenarios. This study aims to provide a new monitoring approach using remote-sensing observations to evaluate the joint impacts of drought and salinity on crop traits. In our tests over the Netherlands at a large spatial scale (138.74 km^2), we calculated five functional traits for both maize and potato from Sentinel-2 observations, namely leaf area index (LAI), the fraction of absorbed photosynthetically active radiation (FAPAR), the fraction of vegetation cover (FVC), leaf chlorophyll content (Cab), and leaf water content (Cw). Individual and combined effects of the stresses on the seasonal dynamics in crop traits were determined using both one-way and two-way analyses of variance (ANOVAs). We found that both stresses (individual and co-occurring) affected the functional traits of both crops significantly (with R^2 ranging from 0.326 to 0.796) though with stronger sensitivities to drought than to salinity. While we found exacerbating effects within co-occurrent stresses, the impact level depended strongly on the moment in the growing season. For both crops, LAI, FAPAR, and FVC dropped the most under severe drought stress conditions. The patterns for Cab and Cw were more inhibited by co-occurring drought and salinity. Consequently, our study constitutes a way towards evaluating drought and salinity impacts in agriculture, with the possibility of potential large-scale application for sustainable food security.

3.1 Introduction

Food production is required to increase by 70% to satisfy the growing population demand by the year 2050 (Godfray et al. 2010). Meanwhile, food security is becoming increasingly threatened due to the increasing abiotic stresses under the influence of global climate change; abiotic stresses including drought, soil salinity, nutrient stress, and heavy metals are estimated to constrain crop productivity by 50%-80% (Shinozaki et al. 2015). Of these stresses, drought and salinity stress have been identified as the two main factors to limit crop growth, affecting respectively 40% and 11% of the global irrigated areas (Dunn et al. 2020; FAO 2020). With drought and salinity forecasted to increase spatially and in severity (Rozema and Flowers 2008; Schwalm et al. 2017; Trenberth et al. 2013), and with predictions of higher co-occurrence around the world (Corwin 2020; Jones and van Vliet 2018; Wang et al. 2013b), food production will be more deeply challenged by both stresses.

Numerous small-scale experimental studies for a large variety of crops have shown that the impact of co-occurring drought and salinity stress is exacerbated. Co-occurrence of drought and salinity stress is found to decrease the yield of spinach (Ors and Suarez 2017) and the forage grass *Panicum antidotale* (Hussain et al. 2020) more compared with the occurrence of one of these stresses only. Likewise, cotton root growth tends to be more inhibited under the co-occurrence of drought and salinity than by isolated occurrences (Zhang et al. 2013). Similarly, the exacerbating effect of co-occurring stresses limits both maize reproductive growth and grain formation (Liao et al. 2022). While these studies demonstrate the exacerbating effects of co-occurring drought and salinity stress, they have limitations in projecting the impact towards real farmers' conditions due to their small-scale experimental nature. Thus, there is still a significant knowledge gap concerning the large-scale evaluation of the combined impacts of drought and salinity.

Remote sensing (RS) provides a huge potential to close this knowledge gap due to its capability to monitor continuous large areas at frequent intervals. For this, remote sensing has traditionally used vegetation indices, such as the Normalized Difference Vegetation Index (NDVI) (Tucker 1979). However, such indices provide limited information on how the impact is achieved (e.g. in Chapter 2) and how it can be mitigated. With the launch of better multispectral and high-resolution satellite sensors (such as Sentinel-2), new RS methods (e.g., hyperspectral, thermal infrared, and microwave) have been identified to detect stress in both natural vegetation (Gerhards et al. 2019; Vereecken et al. 2012) as well as in agricultural applications (Homolova et al. 2013; Weiss et al. 2020). Specifically, these new RS methods allow for the retrieval of plant traits that directly link to plant processes,

such as leaf biochemistry and photosynthetic processes, and thereby provide high potential for agricultural applications. RS plant traits of specific interest to monitor crop health include leaf area index (LAI) (Wengert et al. 2021), canopy chlorophyll content (Cab*LAI) (Gitelson et al. 2005), canopy water content (Cw*LAI) (Kriston-Vizi et al. 2008), the fraction of absorbed photosynthetically active radiation (FAPAR) (Zhang et al. 2015), and the fraction of vegetation cover (FVC) (Yang et al. 2018). Canopy chlorophyll content and mean leaf equivalent water thickness (EWT) of maize differed remarkably under drought stress using hyperspectral remote-sensing data (Zhang and Zhou 2015). Using a lookup-table approach, LAI and chlorophyll content of wheat obtained from a radiative transfer model showed potential to assess drought levels (Richter et al. 2008). However, while there have been several attempts to monitor the response of crop health with either a drought or salinity focus, not much research has taken these factors into account simultaneously (Chapter 2).

In this study, we propose a novel approach to estimate, compare, and evaluate the impacts of drought, salinity, and their combination on crop traits using remote sensing. To allow for a detailed evaluation of this approach, we applied it to analyze the impacts of the 2018 summer drought in the Netherlands on agricultural crops. In this, a stress co-occurrence map was created by overlaying a high-resolution drought map of 2018 with a groundwater salinity map. Then, we characterized the response of maize and potato to different stress conditions based on five plant traits (LAI, FAPAR, FVC, Cab, and Cw). Two-way analyses of variance (ANOVAs) were adopted to test the main effects and the interactive effect between stress combinations and time on crop traits. Moreover, the effect of drought and salinity on crop traits was determined across the growing season with one-way ANOVAs. Consequently, this approach facilitates the simultaneous monitoring of crop health at various scales (regional, national, and continental) across multiple stresses (drought and salinity) and multiple species.

3.2 Methodology

To achieve our aim of monitoring the impacts of (co-occurring) drought and salinity on agricultural production, we developed a new approach to estimate crop traits from remote-sensing observations. Specifically, we developed an approach that integrates image-processing techniques, such as image classification, co-registration, land surface parameter retrieval, and time-series analysis (Figure 3.1). Using these techniques, we were able to estimate the drought, salinity, and crop growth.

To allow for a detailed evaluation, we focused on the 2018 summer drought in the Netherlands. This period was selected because of the extreme drought that affected a large part of Europe (Masante et al. 2018). Within parts of the selected area,

salinity was reported to increase during that same period (Broekhuizen 2018). Hence this study area provides us with the opportunity to investigate the combined impacts of these stresses on crops. In the following paragraphs, we provide more information on the specific processing steps.

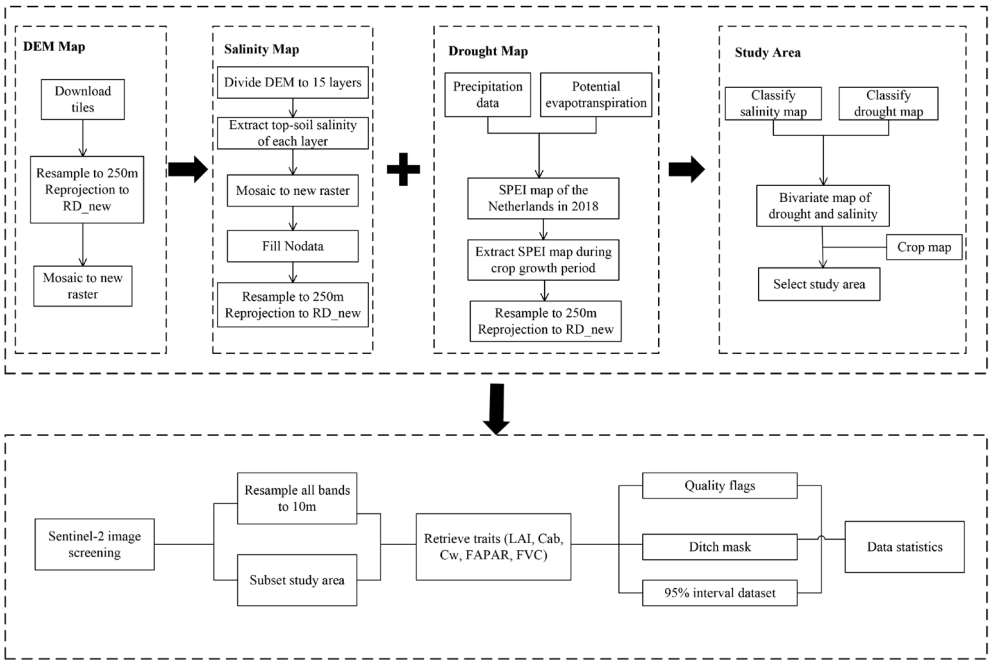

Figure 3.1 Technical workflow of the maps and data framework.

3.2.1 Study area and data

3.2.1.1 Drought map

A drought map of the Netherlands in 2018 was created based on the standardized precipitation evapotranspiration index (SPEI) drought index, which was calculated from long-term precipitation data and potential evapotranspiration, from 2004 to 2018 (Chen et al. 2022). Specifically, SPEI was estimated using a 3-month sliding time window, as this was found best to investigate the impacts on the local ecosystems. We have extracted SPEI-3 data from 1 April to 30 October, in total of 214 days, as this coincided with the crop growth period of both maize and potato. Then, the drought map was resampled to 250m resolution using the nearest neighbor interpolation and reprojected to RD_new projection. The RD_new projection (EPSG:28992) is a projected coordinate reference system of the Netherlands. All maps were projected to RD_new projection to create consistent data layers. We defined -1 and -1.5 as daily thresholds for different drought severity classes according to previous classifications (McKee et al. 1993; Tao et al.

2014). Thus, (cumulative) SPEI for no drought should be between -214 and 0, SPEI for moderate drought should be between -321 and -214, and for severe drought, SPEI should be lower than -321 when calculated for the whole growing period (Figure 3.2a).

3.2.1.2 Salinity map

A topsoil salinity map of the Netherlands was created based on a nationwide fresh-salt groundwater dataset, which derived chloride concentrations as a salinity indicator (https://data.nhi.nu/, last access: 8 April 2021). To obtain the salinity map of the topsoil, 15 layers of the groundwater salinity were extracted from the 3D groundwater salinity map. For each location, the layer closest to the location's corresponding elevation (according to the digital elevation model), i.e., closest to the soil surface, was selected. The salinity map was resampled to 250m resolution and reprojected to RD_new projection Ultimately, the salinity map was classified into three levels namely no-salinity (0.1 $g \cdot L^{-1}$to 0.8 $g \cdot L^{-1}$), moderate salinity (0.8 $g \cdot L^{-1}$ to 2.5 $g \cdot L^{-1}$), severe salinity (>= 2.5 $g \cdot L^{-1}$) according to the salt-resistant capacity of various crops cultivated in the Netherlands (Mulder 2018; Stuyt 2016) (Figure 3.2b).

3.2.1.3 Crop map

The crop map of the Netherlands in 2018 was collected from the Key Register of Parcels (BRP) of the Netherlands Enterprise Agency (https://www.pdok.nl/introductie/-/article/basisregistratie-gewaspercelen-brp-). The crop map was resampled to 250m resolution and reprojected to RD_new projection (Figure 3.2d).

3.2.1.4 Co-occurrence map of drought and salinity

The drought map and the salinity map were overlain to evaluate co-occurrences of drought and salinity of the Netherlands in 2018 (Figure 3.2c). By classifying the three stress levels for the individual occurrences, we obtained nine stress classes of co-occurring drought and salinity, namely no stress, moderate drought only (MD), severe drought only (SD), moderate salinity only (MS), severe salinity only (SS), moderate drought and moderate salinity (MD+MS), moderate drought and severe salinity (MD+SS), severe drought and moderate salinity (SD+MS), and severe drought and severe salinity (SD+SS).

3.2.1.5 Study area selection

Based on the national map of the Netherlands (Figure 3.2c), a single region with similar soil type, climate, tillage systems, and irrigation methods was chosen to minimize the interference of these factors on the observed trait expressions. The

province of North Holland was selected because it contained the most (seven out of nine) combinations of drought and salt stress (Figure 3.2c), namely no stress, MD, SD, MS, SS, MD+MS, and SD+SS. Moreover, both maize and potato were cultivated across all stress combinations in this province. For further analysis, MS and SS were grouped into a new class of salinity stress since the area of MS and SS was quite limited. Therefore, six classes of stress combinations, namely no stress, MD, SD, salinity (MS+SS), MD+MS, and MD+SS, were analyzed for the study area.

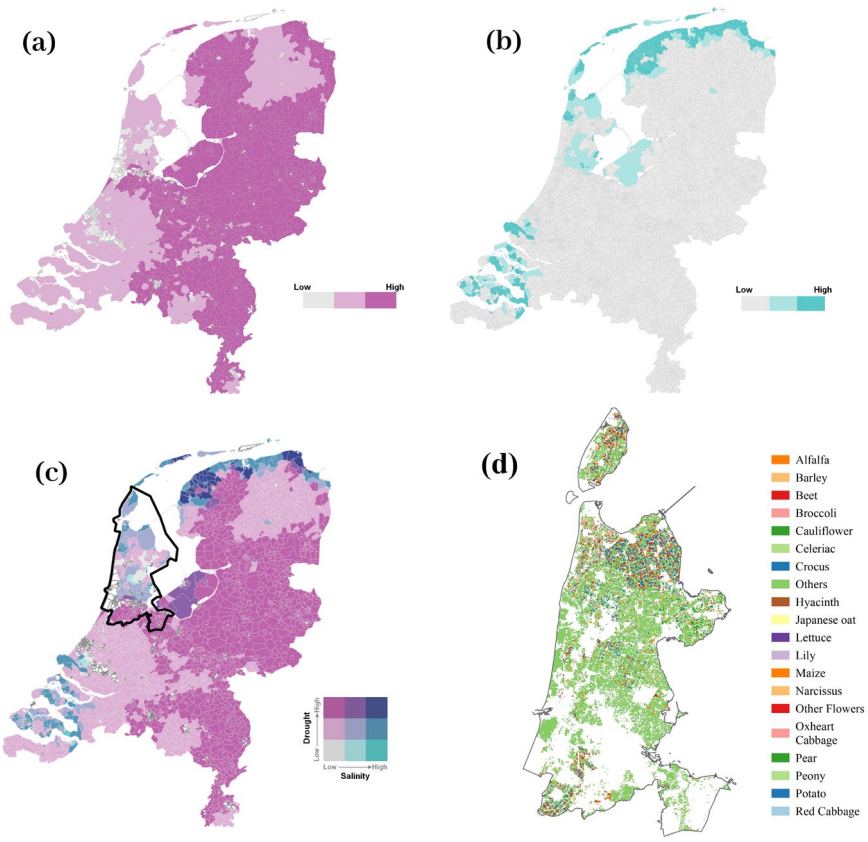

Figure 3.2 Map of the Netherlands overlaying a) drought and b) salinity to show c) the co-occurrence of drought and salinity in 2018. The selected study area is indicated by black lines in panel c. d) The associated crop map of the study area in 2018.

3.2.2 Traits retrieval

3.2.2.1 Satellite data

The Sentinel-2 mission consists of two satellites equipped with the high-resolution Multispectral Instrument (MSI) in the same orbit. This sensor acquires 13 spectral

bands (with varying spatial resolutions) in the visible and near-infrared spectrum at 5 days of revisit times (ESA 2015). In our study, we used both the 10 and 20m Level 2A observations, downloaded from the Copernicus Open Access Hub (https://scihub.copernicus.eu/, last access: 20 May 2021), to facilitate the requirement of the Sentinel Application Platform (SNAP) toolbox for both optical and near-infrared observations to be available for determining the functional traits. To create consistency across the bands, those with a 20m resolution (B5, B6, B7, B8A, B11, and B12) were resampled to the 10m resolution of B3 and B4. In total, eight cloud-free scenes were found (21 April 2018, 6 May 2018, 26 May 2018, 30 June 2018, 15 July 2018, 13 September 2018, 13 October 2018, and 28 October 2018) to cover the crop growth cycle. Although additional cloud-free scenes were found in August (4, 9, 14, 19, 24, and 29 August 2018), none were of high quality, and we therefore chose to omit August from our analysis.

3.2.2.2 Trait selection

Plant traits (e.g., LAI, FAPAR, FVC, Cab, and Cw) were selected in consideration of their corresponding impacts on crop functioning and their potential for assessment by remote sensing. LAI is a critical vegetation structural trait related to various plant functioning processes, such as primary productivity, photosynthesis, and transpiration (Asner et al. 2003; Boussetta et al. 2012; Fang et al. 2019; Jarlan et al. 2008). FAPAR depends on vegetation structure, energy exchange, and illumination conditions, while FAPAR is also an important parameter to assess primary productivity (Liang 2020; Weiss et al. 2016). FVC is a promising parameter corresponding to the energy balance process such as temperature and evapotranspiration (Weiss et al. 2016). Cab is an effective indicator of stress and is strongly related to photosynthesis and resource strategy (Croft et al. 2017). Cw plays an important role in transpiration, stomatal conductance, photosynthesis, and respiration (Bowman 1989; Zhu et al. 2017), as well as in drought assessment (Steidle Neto et al. 2017).

3.2.3 Dataset processing

The biophysical processor within the SNAP toolbox derives the five traits, namely LAI, FAPAR, FVC, canopy chlorophyll content (CCC), and canopy water content (CWC), for each pixel from the Sentinel-2 top of canopy reflectance data at a 10m resolution for each month. This processor utilizes an artificial neural network (ANN) approach, trained using the PROSAIL simulated database (Weiss et al. 2016). This training utilized canopy traits rather than leaf traits (estimated by multiplication with LAI) to improve their neural network performance. To obtain their leaf counterparts (Cw and Cab), to create fully independent variables, CCC and CWC thus need to be divided by LAI to obtain Cab (i.e., CCC/LAI) and Cw (i.e., CWC/LAI). Pixels with quality flags were eliminated from the dataset. It was

observed that in April no crop had yet been planted. Instead, we observed that only along the edge of the plots, e.g., in ditches, was vegetation found. This feature was used to generate a ditch map and mask out pixels in trait maps for the other months. For each variable and each date, only data within the 95% confidence interval were taken to increase data robustness.

3.2.4 Analysis

Since the pixel counts of the six classes of stress combinations, namely no stress, MD, SD, salinity, MDCMS, and MDCSS, were (highly) different, drought and salinity were not considered two independent factors. Instead, a two-way analysis of variance (ANOVA) was applied to test the main effects and the interactive effect between stress combinations (consisting of six levels) and time (5 months) on each individual crop trait. Significant effects of the main stress condition were investigated through post hoc tests to test whether interaction effects between drought and salinity had occurred. Two-way ANOVAs were run separately for each trait and each crop type (maize and potato) as we expected different patterns. In the Netherlands, potato and maize are planted between mid-April and early May. Crops are surfacing in May and harvested in October. Therefore, to evaluate the response of crops to stresses across the growing season, the effect of drought and salinity on crop traits was determined for May, June, July, and September with a one-way ANOVA. Tukey's honest significant difference (HSD) post hoc tests were performed to identify the differences among the six stress combinations. All statistical analyses were performed with SPSS 27.0 (SPSS Inc., USA).

3.3 Results

3.3.1 Stress impacts depend on the moment in the growing season

The two-way ANOVAs revealed strong effects of date and stress level on the five traits with effect sizes of the response (R^2) ranging from 0.326 to 0.796 for the five traits, which was similar for maize and potato. For both maize and potato, R^2 values were lowest for Cab and highest for LAI, FAPAR, and FVC. For maize, we found a significant main effect of both date and stress ($p < 0.05$) for Cab, Cw, FAPAR, and FVC. In contrast, LAI was not significantly different across the different stress conditions. For potato, all main effects of date and stress were significant for all five crop traits (Table 3.1).

For all traits and both crops, the interaction between the effects of time and stress conditions was significant ($p < 0.05$) (Table 3.1), indicating that the impact of stress depended on the moment in the growing season. Despite the significant interaction terms, the partial Eta squared values (Table 3.1) showed that the effects of time in the growing season were much stronger than those of stress or the interaction of date and stress. The effects of date for maize were stronger than for

potato. Interestingly, the effects of the interaction between date and stress were stronger than those of the main effects of stress, suggesting strong time-specific impacts of stress on the crop traits investigated. The interaction terms were strongest for FVC.

Table 3.1 Two-way ANOVA for different crop traits by time series and stress interactions.

Crops	Traits	Factors	F	*p*	Partial Eta Squared	R^2
Maize	LAI	date	2144.5	0.000	0.636	0.766
		stress	1.4	0.226	0.001	
		date*stress	8.5	0.000	0.033	
	Cab	date	333.9	0.000	0.222	0.326
		stress	10.7	0.000	0.008	
		date*stress	3.6	0.000	0.015	
	Cw	date	952.1	0.000	0.449	0.590
		stress	9.9	0.000	0.007	
		date*stress	4.0	0.000	0.017	
	FAPAR	date	1865.9	0.005	0.603	0.738
		stress	3.3	0.000	0.002	
		date*stress	8.5	0.000	0.033	
	FVC	date	2022.5	0.000	0.622	0.761
		stress	22.1	0.000	0.015	
		date*stress	28.7	0.000	0.105	
Potato	LAI	date	752.1	0.000	0.273	0.782
		stress	13.7	0.000	0.006	
		date*stress	8.1	0.000	0.020	
	Cab	date	96.4	0.000	0.050	0.329
		stress	54.2	0.000	0.024	
		date*stress	8.7	0.000	0.023	
	Cw	date	347.4	0.000	0.158	0.571
		stress	68.1	0.000	0.030	
		date*stress	10.3	0.000	0.027	
	FAPAR	date	612.7	0.000	0.234	0.744
		stress	25.8	0.000	0.011	
		date*stress	14.0	0.000	0.034	
	FVC	date	844.0	0.000	0.297	0.796
		stress	18.8	0.000	0.008	
		date*stress	13.6	0.000	0.033	

Note: F indicates the test statistic of the F-test; p indicates whether the effect is statistically significant in comparison to the significance level ($p < 0.05$); Partial Eta Squared indicates the effect size of different factors; R^2 indicates the percentage that the model coincides with the data.

3.3.2 Response of LAI, FAPAR, and FVC to drought and salinity

Given the significance of both date and stress and their interactions, subsequent one-way ANOVAs were performed to compare the effects of drought and salinity on LAI, FAPAR, and FVC for maize and potato in May, June, July, and September separately (Figure 3.3). The patterns for LAI, FAPAR, and FVC were very similar, although they differ in detail and were therefore treated together.

For maize, all of LAI, FAPAR, and FVC obtained their lowest value under MD+SS stress conditions in May. In June, both LAI and FVC dropped the most under salinity stress and it was significantly ($p < 0.05$) different from MD, MD+MS, and MD+SS conditions, but not significantly different from no-stress conditions. In contrast, FAPAR also reached its lowest value (under MD+MS stress conditions) in June but had a significant difference ($p < 0.05$) compared with no stress conditions. Both in July and September, LAI, FAPAR, and FVC all had the lowest value under SD conditions, and the difference was significant compared with no-stress conditions.

For potato, LAI, FAPAR, and FVC had the lowest ($p < 0.05$) value under MD+MS and MD+SS stress conditions in May. In June, LAI, FAPAR as well as FVC reached the lowest value under SD conditions and were significantly lower than in most other stress conditions even though the difference was not significant from no-stress conditions. In July, there was a tendency for LAI, FAPAR, and FVC to be lower under stress conditions, although none of the effects were significant. In September, however, LAI, FAPAR, and FVC significantly decreased under MD, MD+MS, and MD+SS conditions, and the difference was significant compared with no-stress conditions. In addition, the difference was not significant among these three stress conditions.

Therefore, both for maize and potato, LAI, FAPAR, and FVC dropped the most under SD stress conditions when they reached their respective maximum value, compared with other stress conditions. At the same time, maize and potato were more sensitive to drought than salinity since no significant change was observed between drought conditions and conditions with a combination of drought and salinity stress.

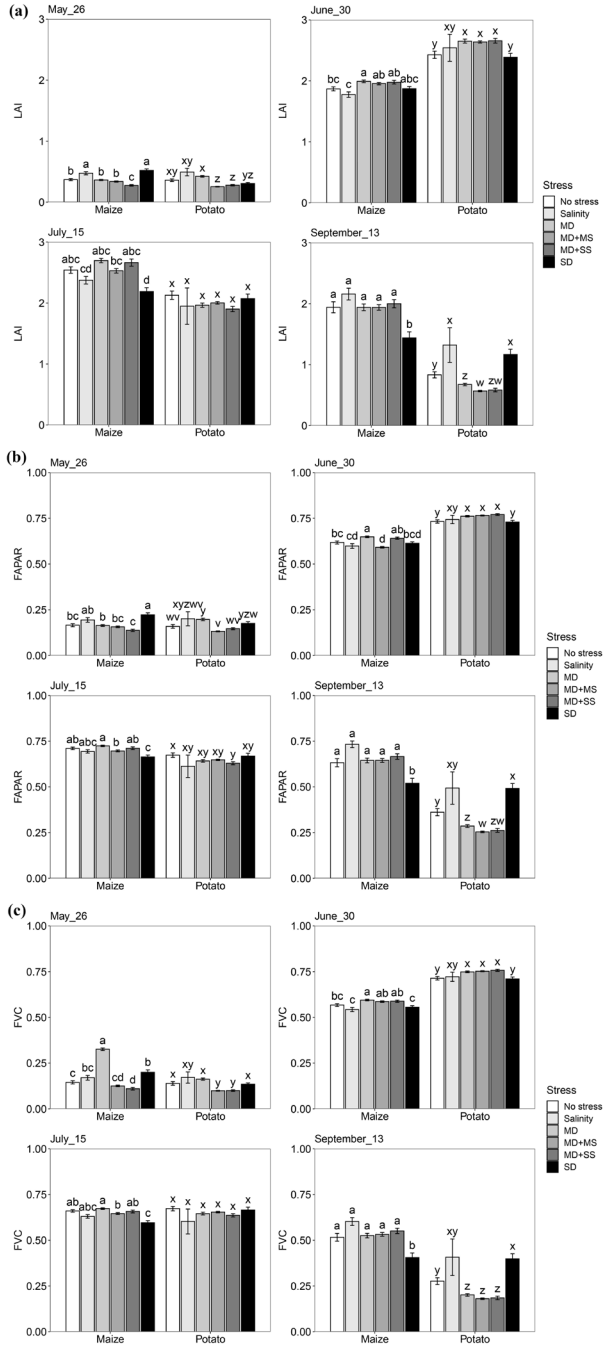

Figure 3.3 Expressions of LAI, FAPAR, and FVC under various stress conditions in May, June, July, and September 2018. Different letters in each panel indicate significant differences ($p < 0.05$). MD, moderate drought only; Salinity, salinity only; MD+MS, moderate drought, and moderate salinity; MD+SS, moderate drought and severe salinity (MD+SS); SD, severe drought only.

3.3.3 Response of leaf chlorophyll and water content to drought and salinity

The one-way ANOVAs revealed that there were significant ($p < 0.05$) impacts of the various stress conditions on Cab and Cw (Figure 3.4). For maize, Cab obtained its lowest value under salinity stress in May and June while it was not significantly different from no-stress conditions. However, in July, Cab reached the lowest value under MD+MS conditions although the difference was not significant from other stress conditions. There were no significant changes observed for Cab in September. For potato, Cab dropped the most under salinity conditions in May although the difference was not significant from no-stress conditions. Furthermore, Cab significantly decreased under MD+SS conditions in June and July, compared with other conditions. Although Cab dropped the most under salinity conditions in September, the difference was not significantly different from other conditions. In addition, compared with no stress, potato had the lowest Cab under MD+SS conditions while there was no significant difference between MD+SS and salinity conditions in most growing periods.

Cw decreased under all stress conditions in May, June, and July for both maize and potato, except for SD conditions in May, compared with no-stress conditions. At the same time, Cw reached its lowest value under MD+SS conditions and it was significantly different from under no-stress conditions. Nonetheless, there were different changes for maize and potato in September. Cw was not significantly different among any conditions for maize while it was the lowest under salinity conditions for potato.

Therefore, this analysis illustrates that salinity affected maize less than drought since crop responses were more obvious to drought than salinity for Cw. In contrast, salinity showed a more severe effect on maize and potato at the early growth stages for Cab. Meanwhile, Cab was affected by co-occurring drought and salinity in June and July for potato. It seems that there was a non-additive effect of drought and salinity for Cw since the changes were not significant between MD+MS, MD+SS, MD, and salinity conditions.

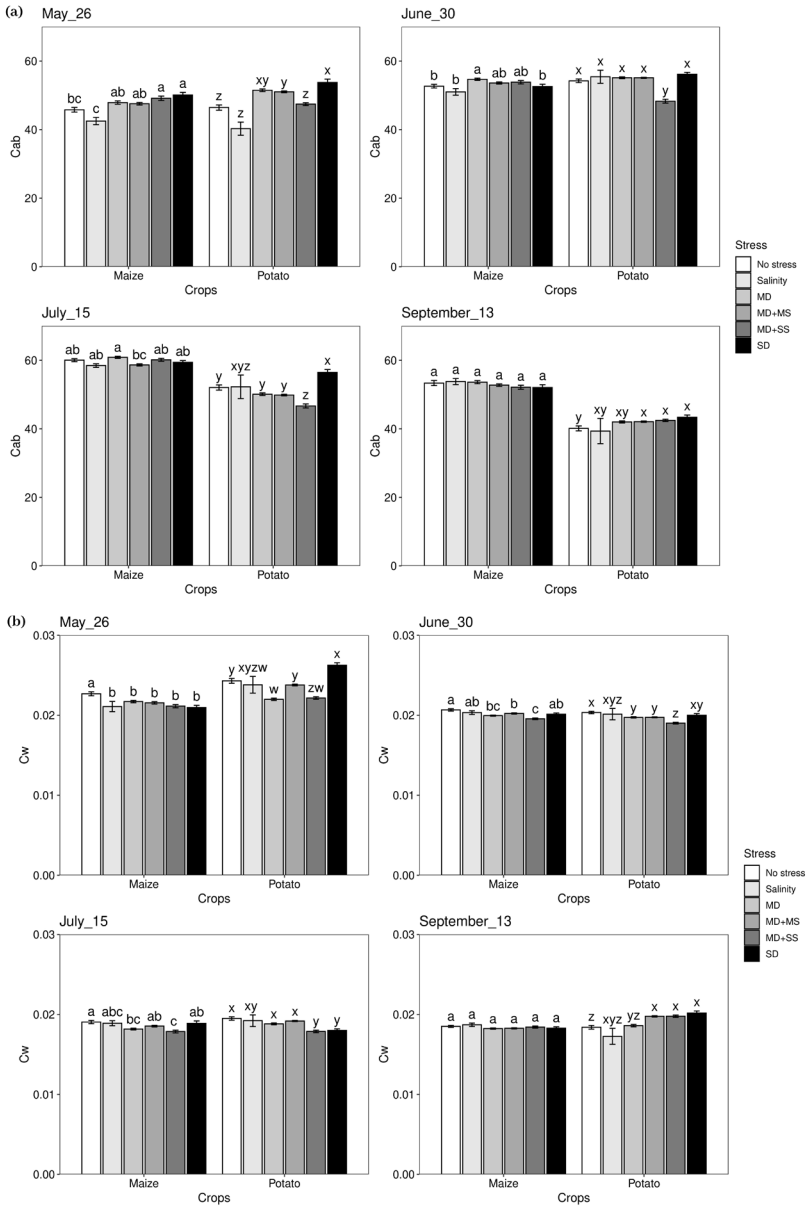

Figure 3.4 Expressions of Cab and Cw under various stress conditions in May, June, July, and September 2018. Different letters in each panel indicate significant differences ($p < 0.05$). MD, moderate drought only; Salinity, salinity only; MD+MS, moderate drought, and moderate salinity; MD+SS, moderate drought and severe salinity (MD+SS); SD, severe drought only.

3.4 Discussion

In this study, we quantified the large-scale impacts of co-occurring drought and salinity on a variety of crop traits using satellite remote sensing. We observed that -in contrast to our expectations- the impacts of salinity were not highly pronounced at this scale, with most strong impacts originating due to drought stress during the 2018 drought. At specific moments in the growing season, salinity and/or the combined effects of salinity and drought pronouncedly affected individual crop traits. In this way, with increasing salinity driven by more intensive droughts, water allocation should not only be governed by the amount of water shortage but also the salinity of the remaining water. In this paper, we provide the first evidence that those impacts can be monitored through remote sensing. This might provide a basis towards a monitoring system for multiple crops with multiple stresses as well as better governance policies to ameliorate this problem.

3.4.1 Drought stress is more important than salinity stress in farmers' conditions

The exacerbating effects of co-occurrent drought and salinity (Figure 3.3 and Figure 3.4) that we found are consistent with findings of small-scale experiments (e.g. greenhouses). Consistent with our results, synergistic effects of co-occurring water stress and salinity stress have been found on maize reproductive growth and grain formation in a field study (Liao et al. 2022). Spinach (*Spinaciaoleracea* L., cv. Racoon) yield decreased more under co-occurring water-salinity stress in comparison with separate water stress and salinity (Ors and Suarez 2017). The co-occurring drought and salinity stress was more harmful to cotton root growth compared to their individual effects (Zhang et al. 2013). Moreover, the combined negative effect of drought and salinity stress on *Panicum antidotale* was stronger than that of single stress (Hussain et al. 2020). Our research showed that the outcomes of these small-scale experimental studies also apply to real large-scale environments, where different sources of variance are present. Specifically, we show that in real farmers' conditions, the co-occurrence of drought and salinity indeed can constitute a severe threat due to its interactive effects on crop growth.

In addition, we evaluated whether drought or salinity stress has more impact on crop performance. We observed that maize and potato were generally more sensitive to drought than salinity in this study (Figure 3.3 and Figure 3.4). This is consistent with results of previous studies that highlight that drought impacts are generally more detrimental than salinity stress for crops, e.g. for sesame (*Sesamum indicum*) (Harfi et al. 2016), *Mentha pulegium* L. (Azad et al. 2021), durum wheat (Sayar et al. 2010), grass pea (Tokarz et al. 2020), and sweet sorghum (Patane et al. 2013). However, given that the threshold of salinity at which crop damage occurs (according to the FAO guidelines (Ayers and Westcot 1985)) was surpassed in all

situations in which salinity stress was imposed (including in our study), we initially expected salinity to be a stronger explanatory variable than drought. As such, salinity impacts on crop performance (by the FAO) may have been overestimated. Indeed, in an experimental field situation in which drought stress was carefully avoided, higher thresholds of salinity-induced damage were observed for potato (van Straten et al. 2021).

In combination, the results from our study (supported by results from other studies) suggest that salinity particularly induces adverse effects when co-occurring with drought stress. The impact of water stress on photosynthesis and the biomass of plants was extenuated by salinity since salinity enhances the synthesis of ATP and NADPH by promoting photosynthetic pigments and photosystem II efficiency. The impacts of combined drought and salinity stress on plant growth, chlorophyll content, water use efficiency, and photosynthesis were less severe compared to drought alone. This indicates compensating effects on carbon assimilation due to osmotic adjustments induced by Na^+ and Cl^- (Hussain et al. 2020). Thus, the detrimental effect of single drought stress on crop growth is considered to be mitigated by salinity.

3.4.2 Drought and salinity stress differ between growth stages

The responses to drought and salinity stress were different at different growth stages of the crops. This was expressed by the significant interactions between the effects of time and stress conditions for all of our crop responses (Table 3.1). We found that during the grain filling (maize) and tuber bulking phase (potato), the sensitivities of these crops are expressed distinctly in the non-harvested aboveground tissues (Figure 3.3 and Figure 3.4), with clear differences in the remote sensing plant traits.

Given that we were not able to monitor the harvestable products, multiple mechanisms may explain these patterns. The relatively high leaf coverage (as related to LAI, FAPAR, and FVC) at salinity and severe drought conditions at the end of the growing season may be an expression of a compensation process. Specifically, early and prolonged drought could have led to more assimilates allocated to non-harvestable potato parts for drought resistance since the number of tubers reduced (Jefferies 1995; Schittenhelm et al. 2006). In that case, we should consider their higher leaf coverage at the end of the season as a survival mechanism, rather than true drought tolerance, leading to reduced tuber yields (Daryanto et al. 2016b). Future studies that combine remote sensing with harvesting data may be able to evaluate this mechanism in more detail.

In our study, different response patterns of maize and potato occurred to the different stresses over the growing season. This is consistent with previous studies

focusing on the impact of drought and/or salinity onsets. For potato, it has been suggested that tuber yields particularly decreased when drought stress occurs during the vegetative and tuber initiation stages than during the tuber bulking stage (Wagg et al. 2021), although another study observed the reverse pattern (Daryanto et al. 2016b). For maize, on the other hand, drought seems to have the most detrimental impact during the maturation stage (Mi et al. 2018; Zhang et al. 2019), and the reproductive phase (Daryanto et al. 2016a; Daryanto et al. 2017). Considering the additional co-varying factors within our 'real-life' study, it is very probable that we were able to detect similar effects. This suggests that we may use satellite remote sensing -albeit less spatially precise than e.g. sensing through drones- as a cost-effective early warning signal for detecting drought and salinity stress at moments during the growing season when differences in crop performance are still subtle.

3.4.3 Crop responses to stress can be better understood with a multi-trait approach

In addition to facilitating the evaluation of crop performance during multiple stages of the growing season (in contrast to most destructive methods), remote sensing also allows a multi-trait approach to better understand the mechanisms involved in crop responses. Each of the five traits is associated with different functions of plants that might be individually impacted by the different stresses. Therefore, focusing on only one individual metric (as commonly done, see Chapter 2 for a review) limits our capacity to gain full insight into drought and salinity responses. Hence, given that individual crop traits may respond differently to drought and salinity reflecting its stress resistance and tolerance strategy, the evaluation of these distinct responses may help to understand this strategy.

In this study, Cw was consistently lower in all drought and salinity treatments as compared to no-stress conditions in May, June, and July. Indeed, this is a common response of plants in response to drought and salinity (e.g. Chapter 2). In this respect, it is interesting that no decrease in Cw was observed at the end of the growing season, in September. Whether the phenomenon is related to the survival mechanism mentioned above or to the lower transpiration demands at the end of the season because of lower aboveground biomass, cannot be concluded from these data. Some evidence pointing to the survival mechanism is the finding (Ghosh et al. 2001; Levy 1992) that the leaf dry matter increased for potato under drought/salinity stress (like in our study) while the dry matter of the tubers appeared to have a greater decline.

With respect to chlorophyll contents, we observed a decline in Cab under salinity conditions in May and the MS+SS treatment in June and July, while no decrease was observed in any of the treatments exposed to drought only. This indicates that

while total leaf area was not (much) affected by salinity, the salinity did negatively affect crop performance. It has been reported that chlorophyll content in maize was significantly reduced upon salinity, along with other plant traits including plant height, shoot/root biomass, and leaf numbers (Fatima et al. 2021; Mahmood et al. 2021). Likewise, similar patterns were obtained in potato plants in saline soil (Efimova et al. 2018). Hence, this implies that soil salinity tends to negatively affect crop growth and restrict nutrient uptake.

Cab and Cw responses to drought and salinity were distinct from responses of LAI, FAPAR, and FVC (Figure 3.3 and Figure 3.4). LAI, FAPAR, and FVC showed similar patterns to stress due to their highly physical correlation (Hu et al. 2020). The different patterns of Cw and Cab point to different drought and salinity resistance strategy components associated with these traits: LAI (and FAPAR/FVC) reflect the decrease in biomass due to stress, partly because stress directly and negatively impacts growth and partly because having lower biomass decreases the evapotranspiration demands of the crop, which increases the resilience of the crop to deal with drought. Cw represents another pathway to reduce evapotranspiration demands, i.e. by reducing the amount of water per gram of leaves. Also, this response may be a direct effect of the more negative pressure heads due to drought or due to increased osmotic pressures (due to salinity). It may also be part of the adaptive strategy of the crop to increase its resilience. Cab also responds to drought and salinity, but in its own way, i.e. by adapting its photosynthetic capacity while being affected by a lower stomatal conductance (due to drought and/or salinity). See e.g. Wright et al. (2003) for a framework explaining these nitrogen-water interactions.

In addition, our approach gives the insight to analyze the effect of stresses on yield based on the five traits, even though yield cannot directly be derived from remote sensing. Traits including Cab, LAI, and FAPAR, have been used (either separately or in combination) as a proxy for final yield estimates from remote sensing in many studies. For instance, NDVI -which is based on the combination of LAI and Cab- is extensively used to estimate crop yield (Huang et al. 2014; Mkhabela et al. 2011; Vannoppen et al. 2020). Also, LAI itself has been used for predicting the final yield (Dente et al. 2008; Doraiswamy et al. 2005; Sun et al. 2017). Meanwhile, Cab and FAPAR were also proven to be highly correlated with crop yield (Ghimire et al. 2015; López-Lozano et al. 2015). Thus, while yield cannot be estimated directly from remote sensing or ground truth data at the desired high spatial resolution, our indicators do relate to yield and can be used in more application-based contexts to inform on yield impacts.

3.4.4 Implications for future research and management

The number of studies that evaluate the effects of drought and salinity stress on crops is limited (Chapter 2). In general, studies focus on small-scale experimental studies under strict control of all variables with only a limited number of crops (Hussain et al. 2020; Ors and Suarez 2017). To our knowledge, this is the first study that uses satellite remote sensing to investigate drought and salinity impacts for a large area under real-life conditions necessary for constructing stress management policies.

In such real-life conditions, as investigated here, irrigation of crops is commonly applied as management practice during drought events to reduce the severity of drought impacts (Deb et al. 2022; Lu et al. 2020b). In this study, however, we have evidence that irrigation did not play a major role in the patterns found since all croplands included in our research area were identified as rainfed cropland (according to the ESA/CCI land cover map in 2018; https://maps.elie.ucl.ac.be/CCI/viewer/, last access: 19 April 2022). In addition, while farmers in the area are known to irrigate their cropland, the Dutch government announced a temporary national irrigation ban in 2018 (for various areas including our research area) to spare water (Perry de Louw 2020). As a consequence, we could not analyze the impacts of irrigation management on the combined effects of drought and salinity. This might potentially be solved by investigating other drought historic events with moderate severity in Europe, such as the year 2003 (Ciais et al. 2005) or 2015 (Ionita et al. 2017) in Europe, when such a ban was not executed. Unfortunately, satellite remote sensing observations with the required 20-30m resolutions of these events are limited, as Sentinel-2 was only launched in 2015 and the Landsat satellites provide a too coarse temporal resolution.

Likewise, the impacts of salinity and drought are moderated by crop selection. Traditionally, farmers do not plant highly vulnerable crops in moderate/high salinity areas. In fact, we found crops sensitive to salinity such as apple (Ivanov 1970) and broccoli (Bernstein and Ayers 1949) to be abundant in non-saline areas but only little in saline areas. To ensure an accurate evaluation of salinity impacts, we only investigated those crops with a significant abundance in all available stress conditions. More sensitive crops might even respond more strongly.

3.5 Conclusions

In this study, we present the first attempt to evaluate the real-life effects of drought, salinity, and their combination on crop health using multiple traits from remote sensing monitoring during 2018 over the Netherlands. Our approach gives new insights for monitoring crop growth under co-occurring stresses at a large scale

with high-resolution data. We found that while in general temporal patterns -reflecting crop growth dynamics- were stronger than effects of stress conditions, stress impacts depended on the time of the growing season. Furthermore, we also found that the temporal dynamics in crop responses to drought and salinity were different for maize vs. potato. In general, the five investigated traits were more negatively affected by a combination of drought and salinity stress compared to individual stress. Meanwhile, both maize and potato responded more prominently to drought, thus demonstrating a stronger sensitivity, than to salinity. Specifically, LAI, FAPAR, and FVC dropped the most under severe drought stress conditions. Consequently, the proposed new approach poses a facilitated way for simultaneously monitoring the effect of drought and salinity on crops in large-scale agricultural applications.

3.6 Author contributions

Conceptualization, JT, PVB, and WW; methodology, JT, QC, WW, and PVB.; investigation, WW and QC; writing--original draft preparation, WW; writing--review and editing, PVB. and JT; supervision, PVB, and JT All authors have read and agreed to the published version of the manuscript.

Chapter 4

Evaluating crop-specific responses to salinity and drought stress from remote sensing

Wen Wen, Joris Timmermans, Qi Chen, Peter M. van Bodegom

International Journal of Applied Earth Observation and Geoinformation, 2022, 26: 4537–4552.
https://doi.org/10.1016/j.jag.2023.103438

Abstract

Food security is projected to be threatened by increasing co-occurring stresses (e.g., drought and salinity) under global climate change. To mitigate major impacts on food production, the tolerances and vulnerabilities of crops to these threats need to be characterized. The aim of this research is to assess the tolerances of crops to the combination of drought and salinity stress across plant functions under real-life settings. Using five traits, we evaluated the impacts of drought and salinity tolerance on a multitude of crops throughout the United States. We assessed the dominant stress as well as the onset of combined and individual effects of drought and salinity from March to October. We indeed observed that stress impacts strongly depended on time. In addition, we observed that crops were more sensitive to combined salinity and drought than to individual stresses, although stress impacts significantly varied between time and species. Of the individual traits, LAI was triggered first by stresses, followed by FVC and FAPAR, and Cw and Cab were the last to respond to stresses. In comparison to other species, almond demonstrated greater resilience to combined drought and salinity, whereas soybean and maize were more drought tolerant. In combination, our study provides a way of assessing the tolerance of various crops to co-occurrent stresses both independently and in combination. By allowing applications to other co-occurring stresses and vegetation types, our approach creates a quantitative foundation to inform sustainable food production.

4.1 Introduction

Crops are continuously exposed to a variety of abiotic stresses. Extreme occurrences including floods, droughts, and heat waves are forecasted to increase as a result of global climate change (Wang et al. 2022). These occurrences not only directly lower agricultural yield but also increase the susceptibility of crop production to future events (Zscheischler et al. 2018). Salinity and drought are two major factors that constrain crop yield and are expected to increase in frequency. By 2050, salinity is expected to affect half of the arable land, most of which is on dry or semi-arid land (Angon et al. 2022). More frequent droughts will further increase yield loss risk in the future, with rice, soybeans, wheat, and maize being particularly vulnerable (Leng and Hall 2019). Therefore, food security is expected to be more threatened by the co-occurrence of stress (i.e. salinity and drought) under global climate change. Although singular stress impacts on crops have been extensively studied, co-occurrence stress impacts are still considered challenging due to their complexity (Mehrabi et al. 2022). Thus, to mitigate major impacts on food production, the tolerances and vulnerabilities of crops to these threats need to be characterized.

Traditionally, the tolerance of crops is estimated for a limited number of crop types in highly controlled small-scale experiments. Maas and Grattan (1999) published a list of salt tolerance of 81 crops based on the electrical conductivity of the saturated paste (EC_e) under simulated conditions. However, there is evidence showing that the tolerance of some crops to salinity had been underestimated in such conditions (van Straten et al. 2021). Apart from isolated drought or salinity stress, several studies evaluated the tolerance of combined drought and salinity stress of various crops. In contrast, in wheat, the combination of mild salinity and drought stress was found to cause a stronger inhibition of wheat yield compared with singular stress (Paul et al. 2019). However, in these pot experiments, there was a large difference among various wheat cultivars concerning their tolerance to combined drought and salinity stress (Paul et al. 2019). Suarez et al. (2019) estimated the salt tolerance of grape rootstock in a simulated water stress environment for four years. They came to the conclusion that it was difficult to forecast the combined impacts of salinity and water stress based on the quantification of isolated effects of salinity or water stress from tests. Therefore, it is important to evaluate the simultaneous response to co-occurring stressors in real-life scenarios for a wide range of crop types.

Plant traits can serve as indicators for assessing crop health and crop responses, given that plant traits are associated with various plant functions involving leaf biochemistry and biophysics processes as well as photosynthetic processes. Leaf area index (LAI), the fraction of absorbed photosynthetically active radiation (FAPAR), and the fraction of vegetation cover (FVC) are critical traits related to

primary productivity, vegetation structure, photosynthesis, and transpiration (Asner et al. 2003; Fang et al. 2019; Weiss et al. 2016). Leaf chlorophyll content (Cab) is closely related to the process of photosynthesis and resource management strategy (Croft et al. 2017). Leaf water content (Cw) is a trait related to transpiration, stomatal conductance, and the respiration process and has been linked to drought impacts on crops in many studies (Bowman 1989; Zhu et al. 2017). LAI, FAPAR, and Cab have been shown to have a strong correlation with crop yield and are thus used to estimate final yield (Dente et al. 2008; Doraiswamy et al. 2005; Ghimire et al. 2015; López-Lozano et al. 2015). Therefore, to enhance our understanding of actual agricultural tolerances, and associated plant functioning, it is crucial to evaluate the performance of functional traits in real-life.

Remote sensing has a great potential for monitoring stresses on a large scale, if current challenges are met (Jiao et al. 2021; West et al. 2019). In particular for agricultural applications, satellites with multispectral sensors in high-resolution, such as Sentinel-2, allow stress detection based on retrieved plant traits (Weiss et al. 2020). Two common approaches to retrieving plant traits relevant for analyzing plant stress effects rely on statistical and physical modeling (Bayat et al. 2016). Statistical approaches involve parametric regressions based on the relationship between spectral bands/vegetation indices (VIs) and functional traits as linked to vegetation stress. Moreover, physical modeling approaches, such as radiative transfer models (RTM), show promising potential to retrieve plant traits related to stress from remote sensing (Wocher et al. 2020). Traits including LAI, FAPAR, FVC, Cw, and Cab retrieved from remote sensing have been applied to evaluate the response of vegetation to either drought or salinity stress (Bayat et al. 2016; Zhang et al. 2020). Instead of relying on individual traits to evaluate crop resistance mechanisms, remote sensing has demonstrated a way to monitor crop responses to stresses based on a multi-trait approach (Berger et al. 2022). Therefore, compared to most destructive methods with restricted capacity to detect mechanisms of stress in crops, remote sensing is a crucial tool that can simultaneously monitor plant functional traits across a wide range of crop types. Moreover, with remote sensing, such monitoring can be achieved over large spatial scales, at high temporal resolution, and in real-life agricultural settings. However, despite attempts to assess the impact of drought and salinity stress on crops using remote sensing traits, these studies are often limited in terms of the number of traits, crop types, and individual stress factors considered.

This study addresses the challenge of simultaneously evaluating the response of diverse crops to the co-occurrence of drought and salinity stress in real-life settings at a large scale. To achieve this, we generated a comprehensive co-occurrence map of drought and salinity across the entire United States. To isolate the effects of stress, we employed a pair-wise method to compare stressed and unstressed

observations while eliminating the impacts of other factors including soil, climate zone, and region. Based on five retrieved traits including LAI, FVC, FAPAR, Cw, and Cab using Sentinel-2 observations, we characterized the response of eight crops to various drought and salinity stress conditions, as well as their interactions with other impacting factors throughout the growing season. We also analyzed the onset of stress (drought, salinity, and their combination) on five traits for each crop individually. Ultimately, our study provides valuable guidance to local farmers and governments by supplying timely information on crop responses to co-occurring stresses, both individually and collectively.

4.2 Methodology

According to the U.S. Drought Monitor (USDM), drought attacked the USA on a national scale throughout 2021 (NCEI and NOAA 2021). Around half of the contiguous USA experienced different strengths of drought from January onwards, and the west and middle of the USA which are typically used for farming crops suffered more severe drought (NCEI and NOAA 2021). In this study, we integrated multiple techniques to evaluate the response of diverse crops to salinity and drought stress at various levels simultaneously across the contiguous USA. In a previous paper (Chapter 3), we developed a novel approach to evaluate the expression of five crop traits under salinity and drought stress conditions in the Netherlands for only two crops. In this study, by adopting a pair-wise method to assess trait expressions concerning drought, salinity, and their combined impacts compared to non-stressed conditions, we captured stress impacts more precisely for a much larger range of crops and spatial conditions (Figure 4.1 and Figure S4-1).

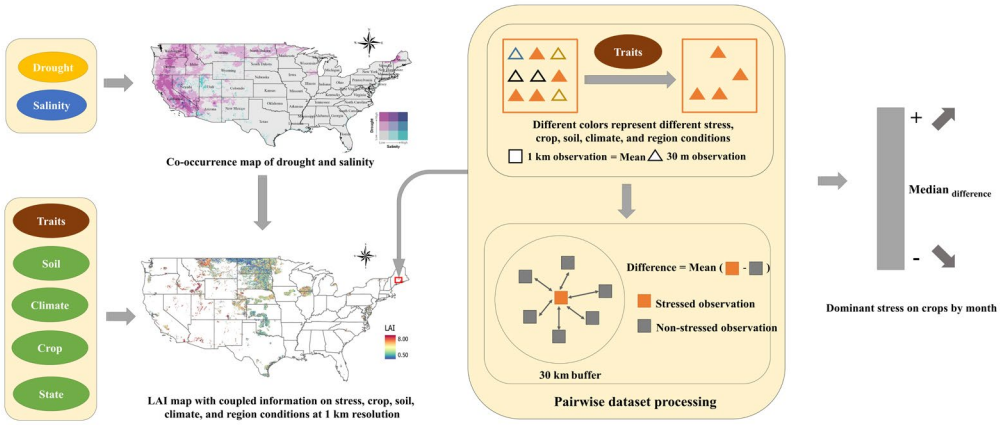

Figure 4.1 Conceptualisation of the technical workflow.

4.2.1 Study area and stress map

4.2.1.1 Drought map

A drought map of the contiguous USA in 2021 was generated based on the standardized precipitation evapotranspiration index (SPEI) drought index. The monthly SPEI with 3-month sliding time windows was collected from The West Wide Drought Tracker (https://wrcc.dri.edu/wwdt/about.php) (Abatzoglou et al. 2017). We extracted SPEI-3month data from March to October to coincide with various crop growth periods. Next, SPEI-3month maps for each month were combined to create the drought map for 2021. Then, the drought map with NAD 1983 Contiguous USA Albers projection was resampled to 30m resolution by using nearest neighbor interpolation. We define -8 and -12 as cumulative SPEI thresholds for no drought (-8 to 0), moderate drought (-12 to -8), and severe drought (< -12) in the whole growth season (McKee et al. 1993; Tao et al. 2014) (Figure 4.2a).

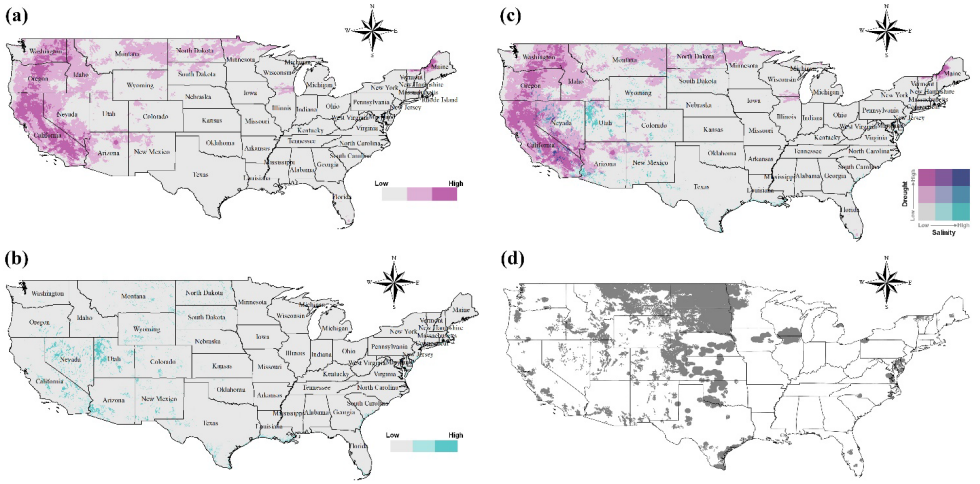

Figure 4.2 a) Drought map in the contiguous USA in 2021. b) Salinity map in the contiguous USA in 2021. c) co-occurrence map of drought and salinity in the contiguous USA in 2021. d) Map of stress-no stress pairs at 1km resolution.

4.2.1.2 Salinity map

A soil salinity map of the United States was generated from Gridded National Soil Survey Geographic Data (gNATSGO) (https://www.nrcs.usda.gov/wps/portal/nrcs/detail/soils/survey/geo/?cid=nrcseprd1464625). We extracted the attribute Electrical Conductivity (EC) data for the topsoil with a 30m map unit raster. Based on EC, we developed the soil salinity map using the lookup function. Afterwards, the soil salinity map was reclassified to three levels namely no-salinity (0 $dS \cdot m^{-1}$ to 4 $dS \cdot m^{-1}$), moderate salinity (4 $dS \cdot m^{-1}$

to 8 $dS \cdot m^{-1}$), and severe salinity (> 8 $dS \cdot m^{-1}$) according to estimated salinity effects on crop growth (Richards 1954) (Figure 4.2b).

4.2.1.3 Co-occurrence map of drought and salinity

The co-occurrence of drought and salinity map for the COUNS in 2021 was created by overlaying the drought map and soil salinity map (Figure 4.2c). Given separative three levels of drought (no drought, moderate drought, and severe drought) and salinity stress (no salinity, moderate salinity, and severe salinity) (section 4.2.1.1 and section 4.2.1.2), we obtained nine classes of stress combinations, namely no stress, moderate salinity only (MS), severe salinity only (SS), moderate drought only (MD), severe drought only (SD), moderate salinity and moderate drought (MS+MD), moderate salinity and severe drought (SD+MS), severe salinity and moderate drought (MD+SS), and severe salinity and severe drought (SD+SS). In some cases, there were limited salinity observations for specific combination conditions. Therefore, these observations were merged with the closest classification into an overall category. For instance, MS+MD and SS+MD were reclassified to the MD+Salinity category.

4.2.2 Crop dataset

4.2.2.1 Crop map

The crop map of the contiguous USA in 2021 was collected from the Cropland Data Layer program (CDL) in the United States Department of Agriculture (USDA) (https://www.nass.usda.gov/Research_and_Science/Cropland/Release/index.php). The crop map is in 30m resolution with NAD 1983 Contiguous USA Albers projection.

4.2.2.2 Crop selection

To ensure the highest availabilities of pairs subjected to multiple levels of stress throughout the growing season, eight crops including alfalfa, almond, grape, maize, sorghum, soybean, spring wheat, and sugar beet, were selected out of over 70 crop types because they contained most pairs of observations with comparable stress combinations (Table S4-1). These eight crops were classified into three categories according to their tolerance for drought and salinity stress from the literature (Table S4-2).

4.2.3 Remote sensing traits retrieval

In this study, we derived geospatial maps of functional traits by using remote sensing. We used Sentinel-2 observations composited scenes in 60m resolution (sun azimuth, sun zenith, view azimuth mean, view zenith mean, B03, B04, B05, B06, B07, B08A, B11, and B12) with 10-days periods (from 11^{th} to 20^{th}) for each

month from The Sentinel-2 Global Mosaic 2 (S2GM-2) service (https://s2gm.land.copernicus.eu/mosaic-hub). Then, all scenes were processed by the biophysical processor in the Sentinel Application Platform (SNAP) toolbox API for python to retrieve five traits namely LAI, FVC, FAPAR, canopy water content (CWC), and canopy chlorophyll content (CCC) for each observation. Trait tiles were purged of observations raised with quality flags. After that, maps for the contiguous USA for each trait were accomplished by mosaicking all trait tiles from March to October to capture the full phenology of each crop. CCC and CWC were divided by LAI to acquire the independent leaf counterparts Cab (=CCC / LAI) and Cw (=CWC / LAI). To eliminate outliers for Cab and Cw created by extremely low values of LAI, observations with LAI values lower than 0.5 were excluded from the calculation of Cw and Cab. In order to maintain consistency for all five trait maps, LAI, FAPAR, and FVC maps were additionally screened for observations of LAI values less than 0.5.

4.2.4 Pairwise dataset processing

We adopted a pairwise method to eliminate the impacts of potentially confounding factors as much as possible. To ensure capturing representative crop responses on the basis of high-resolution data (section 4.2.3), we defined our pixels at 1km resolution. For this purpose, the crop map in 30m resolution was resampled to 1km using majority interpolation. The drought and salinity maps were resampled to 1km using the nearest neighbor interpolation. Subsequently, a fishnet comprising attributes of stress conditions, soil type, climate zone, state, and crop type, was created in 1 km resolution. Next, within a 30 km buffer, each observation in a stressed condition at the 1km resolution fishnet was coupled with several non-stressed observations that met the same criteria (crop type, soil taxonomy, climate zone, and state). The threshold of the buffer was determined by a semi-variogram based on LAI considering the spatial correlations and the presence of multiple stress combinations. To calculate the corresponding trait value for the 1km resolution fishnet, we extracted observations in a 30m resolution map with the same five attributes as the fishnet using raster calculator. Then, the average trait value at 1km resolution was determined by the mean value of the traits in 30m resolution using the zonal statistic. Next, we quantified the difference between stressed and non-stressed observations for the five traits based on the available pairs in the 1km resolution fishnet (Figure 4.2d) using the field calculation. Finally, we calculated the mean difference in trait values of each stressed observation involved in multiple pairs with unstressed conditions according to its unique (stressed observation) ID.

4.2.5 Data analysis

To minimize the impact of outliers, the median value for each stress class for five traits was calculated across the growth period. Considering the planting and harvest time of crops differs in the southern and northern part regions of the contiguous USA, we evaluated the response of crops to salinity and drought stress on crop traits from March to October to capture the whole growing period for different crops. The main effect of factors -stress condition, time, soil type, climate zone, state, and crop types) and their two-way interaction effects on each trait were determined by an analysis of variance (ANOVA) with SPSS 27.0. Post-hoc tests were performed to determine the significance of individual levels within factors. Partial Eta Square was determined to indicate the effect size of different factors. Since the interaction effects with crop type were omnipresent and to understand those better, we subsequently ran ANOVAs for each crop individually (Table S4-4 and Table S4-5). For eight crops, ANOVAs on stress condition, time, soil type, climate zone, state, and their two-way interactions were conducted for each trait, respectively. Since the interactions of other factors with stress were consistently smaller than those with time, we focused on the two-way ANOVAs of stress and time in the results. In addition, to evaluate which type of stress - salinity, drought, and combined salinity and drought - has the strongest impact on crops, the dominant stress without considering different strengths of stress was determined based on the median value of each trait throughout the growing season. Meanwhile, the onset of stress was determined as the first time during the growing season when a negative impact was observed on an individual trait. The onset of drought, salinity, and combined stress for eight crops was estimated for all five traits.

4.3 Results

4.3.1 Crop response commonalities to stress

The two-way ANOVAs of stress and time revealed a strongly time-dependent impact of stress on the five traits, as expressed by strong interaction effects (Figure 4.3). Each trait varied significantly ($p < 0.05$) over time for soybean, maize, almond, alfalfa, sugar beet, and spring wheat. However, the impact of time was always insignificant for sorghum. Stress significantly ($p < 0.05$) impacted FAPAR, FVC, and LAI for all crops. Except in Cw for sorghum, and in Cab for soybean and spring wheat, other crops had significant ($p < 0.05$) differences in Cab and Cw in all stress conditions across the growing season. In addition, for all traits and crops, the impacts of stress varied significantly ($p < 0.05$) over time except in Cw and LAI for sorghum. Among all crops, we found that both the main effect and interaction effect were always significant ($p < 0.05$) in all five traits for maize, almond, alfalfa, and sugar beet, indicating that the impacts of drought and salinity on their performance depended on the moment in the growing season. Interestingly,

sorghum had the highest number of insignificant effects of both the main effect of stress and time as well as their interaction effect for the five traits. In particular, Cw was not significant ($p < 0.05$) in either main effects or interaction effects, suggesting sorghum had a stronger resilience to drought and salinity over the whole growing season. Moreover, time and stress were similarly important (as expressed by the partial eta square value) across five traits for soybean, maize, almond, spring wheat, and sorghum. In general, time, stress, and time*stress explained more of the variance in the trait values for grape, almond, alfalfa, sugar beet, and sorghum compared to soybean, maize, and spring wheat, indicating stronger impacts on the first group of crops. Furthermore, the interaction effect between stress and time was more important or equally important as the separate main effects, indicating that the impact of stress showed complicated dynamics that highly depended on the moment of the growing season.

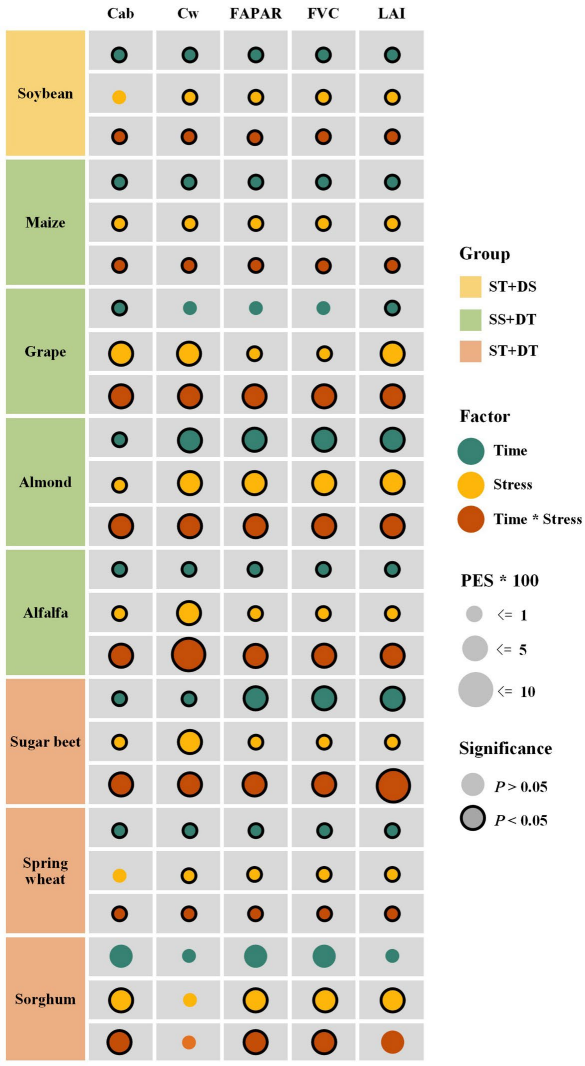

Figure 4.3 Results from two-way ANOVAs for different crop traits by stress, time, and their interactions, highlighting which effects are significant and which are not. ST+DS indicates salt-tolerant and drought-sensitive crops; SS+DT indicates salt-sensitive and drought-tolerant crops; ST+DT indicates salt-tolerant and drought-tolerant crops; PES indicates the partial eta square, i.e. the strength of the relationship.

4.3.2 Crop structural trait differences to stress in the growing season

Given the strong interaction effects of stress and time, the effects of salinity and drought on LAI, FVC, and FAPAR for crops from March to October were evaluated separately (Figure 4.4 and Figure S4-2). The patterns for FVC and FAPAR were similar to the pattern for LAI, even though the impacts of stresses were stronger for LAI throughout the growing season compared to FAPAR and

FVC. Therefore, they are presented in the supplementary information (Figure S4-3, Figure S4-4, Figure S4-7, and Figure S4-8).

Figure 4.4 The pattern of LAI, expressing the severest stress conditions in different months. ST+DS indicates salt-tolerant and drought-sensitive crops; SS+DT indicates salt-sensitive and drought-tolerant crops; ST+DT indicates salt-tolerant and drought-tolerant crops; in strength, low indicates a difference between stress pixels and control pixels smaller than 0.1 m^2 leaf per m^2 surface, moderate indicates a difference between stress pixels and control pixels between 0.1 m^2 leaf per m^2 surface and 0.5 m^2 leaf per m^2 surface, and high indicates a difference between stress pixels and control pixels greater than 0.5 m^2 leaf per m^2 surface; positive effect and negative effect indicate the direction of the pair-wise differences between stress pixels and control pixels.

The patterns of LAI, FVC, and FAPAR under drought and salinity stress varied strongly between different crops and at different moments (Figure 4.4, Figure S4-2, and Figure S4-3) as well as between different states (Figure S4-9, Figure S4-10, and Figure S4-11). For all crops, the combination of salinity and drought stress commonly had the biggest impact on the performance of LAI, FAPAR, and FVC over the whole growing season, even though occasionally in parts of the growing season positive effects on individual traits were observed. Drought stress alone had the lowest amount of impact among the three stress factors (and particularly affected sorghum). These results suggest that in general salinity was more important in determining crop performance than drought. Salinity stress showed

negative impacts on all crops for LAI in all months. However, for FAPAR and FVC, salinity stress showed positive impacts on almond, alfalfa, and sorghum during the growing season (Figure S4-2).

The importance of individual and combined stresses varied among the different crops. In many crops, the combination of stresses really mattered. However, for almond and sorghum, there were only independent drought and salinity stress impacts on LAI, FVC, and FAPAR throughout the whole growing season. All crops except for grape and sugar beet responded consistently negatively to stresses for LAI from April to August. Thus, the responses of crops to drought and salinity differed between species and over time. Importantly, none of these patterns seemed to relate to their perceived tolerance to salinity or drought (Table S4-2).

4.3.3 Crop physiological traits difference to stress in the growing season

The patterns of Cab and Cw under salinity and drought stress varied between different crops and at different moments (Figure 4.5, Figure 4.6, Figure S4-5, and Figure S4-6) as well as between different states (Figure S4-12, and Figure S4-13). For all crops, the combined drought and salinity stress had the highest impact as the severest stress for Cab over the whole growing season. Drought stress alone was the most important stress factor in the least number of occasions. For almond and sorghum, only drought and salinity stress alone impacted Cab. Salinity stress tended to show positive impacts on soybean, almond, and sugar beet for Cab at the beginning and end of the growing season. Also, drought stress and the combination of salinity and drought stress showed negative impacts as well as positive impacts on crops for Cab without clear patterns in terms of the timing of the positive and negative effects. Crops including maize, almond, and alfalfa, responded negatively to stresses for Cab from April to August. All crops showed complex dynamic responses to stresses for Cab from March to October.

Figure 4.5 The pattern of Cab (Chlorophyll a/b), expressing the severest stress conditions in different months. ST+DS indicates salt-tolerant and drought-sensitive crops; SS+DT indicates salt-sensitive and drought-tolerant crops; ST+DT indicates salt-tolerant and drought-tolerant crops; in strength, low indicates a difference between stress pixels and control pixels smaller than 1 ug.cm^{-2}, moderate indicates a difference between stress pixels and control pixels between 1 ug.cm^{-2} and 5 ug.cm^{-2}, high indicates a difference between stress pixels and control pixels greater than 5 ug.cm^{-2}; positive effect and negative effect indicate the direction of the pair-wise differences between stress pixels and control pixels.

Similar to Cab, Cw was mostly affected by the combination of salinity and drought stress over the whole growing season, while drought stress alone occurred in the least number of occasions as the most important stress factor among all crops. Interestingly, sorghum was the only crop that was most impacted by the independent effects of salinity and drought stress for Cw across the whole growing season. Drought stress always caused negative impacts on Cw, except for spring wheat and sorghum. In contrast, salinity stress and combined salinity and drought stress showed both negative and positive impacts on crops for Cw during the growing season, the direction of the impact as well as the most important stress factor varied strongly over time. Crops including maize, grape, alfalfa, and spring

wheat responded consistently negatively to stresses for Cw in the later phase of the growing season, i.e., from July to October.

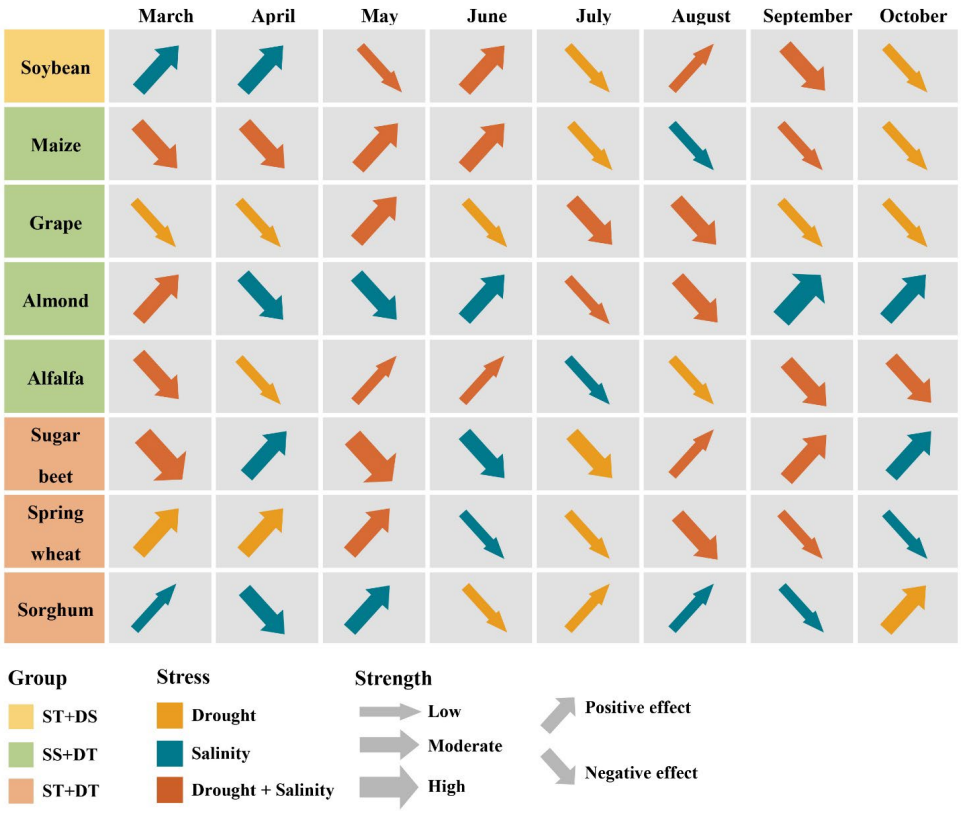

Figure 4.6 The pattern of Cw (concentration of water in leaves), expressing the severest stress conditions in different months. ST+DS indicates salt-tolerant and drought-sensitive crops; SS+DT indicates salt-sensitive and drought-tolerant crops; ST+DT indicates salt-tolerant and drought-tolerant crops; in strength, low indicates a difference between stress pixels and control pixels smaller than 0.001 $g.cm^{-2}$, moderate indicates a difference between stress pixels and control pixels between 0.001 $g.cm^{-2}$ and 0.005 $g.cm^{-2}$, high indicates a difference between stress pixels and control pixels greater than 0.005 $g.cm^{-2}$; positive effect and negative effect indicate the direction of the pair-wise differences between stress pixels and control pixels.

4.3.4 The onset of drought and salinity impacts in the growing season

As crops responded in different ways to salinity and drought stress, the onset of stresses was analyzed to further compare the differences among crops and traits (Figure 4.7). We found for most crops that stress impacts were triggered in March and April, indicating on average crops suffered from stresses throughout most of the growing season. Although the onset of separate drought and salinity differed among crops as well as among traits, the onset of all crops to combined drought and salinity stress was similar to or later than drought for all traits except for Cab in

alfalfa. Furthermore, among the five traits, LAI was the first trait to respond to stresses for all crops, except for almond under combined salinity and drought stress conditions. FAPAR and FVC showed similar onset timing to stress. On average, Cw and Cab were the last to respond to stresses, compared to other traits.

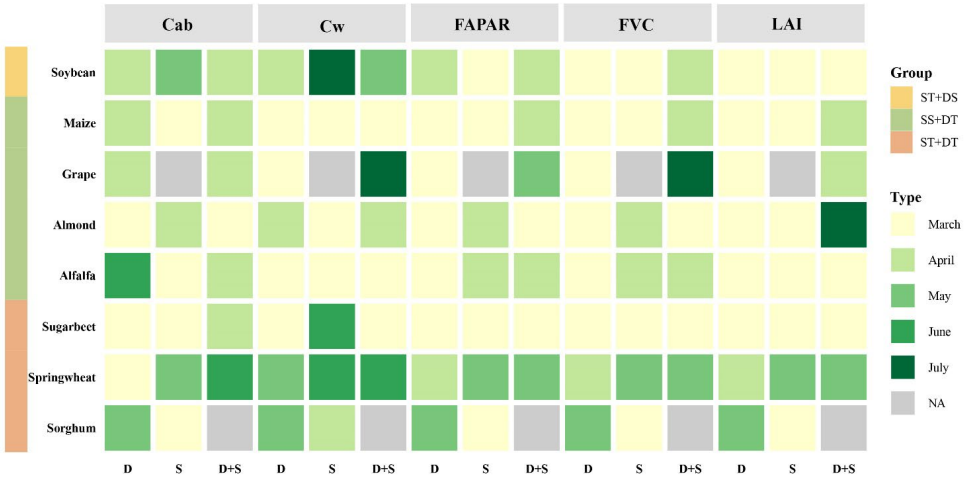

Figure 4.7 The onset of crop responses to stresses in the growing season. D indicates drought stress; S indicates salinity stress; D+S indicates combined drought and salinity stress; ST+DS indicates salt-tolerant and drought-sensitive crops; SS+DT indicates salt-sensitive and drought-tolerant crops; ST+DT indicates salt-tolerant and drought-tolerant crops.

4.4 Discussion

4.4.1 Crop responses to salinity and drought differ between species and growth stages

A key finding of our research is that the combined effects of drought and salinity stress on crop growth are more pronounced than the effects of drought or salinity stress individually. Consistent with our previous study (Chapter 3) and various small-scale experiments, co-occurring salinity and drought showed exacerbating effects on crop traits in most cases (Ors and Suarez 2017; Zhang et al. 2013).

While exacerbated impacts of co-occurring stresses are commonly observed, we additionally show how the impacts of stresses on crops vary strongly over the growing season (Figure 4.4, Figure 4.5, and Figure 4.6), a finding that would not be possible to obtain from small-scale experiments focusing on yield impacts only. Moreover, even the dominant stress on crop traits varied throughout the growing season. This indicates that the crop responses to drought and salinity are highly dependent on the moment. Such variation is consistent with physiological

knowledge showing that the sensitivity to specific drivers depends on the growth stage (Saqib et al. 2013). For instance, previous studies showed that drought has a higher impact on maize during the reproductive phase (Daryanto et al. 2017), while the impacts of drought stress were strongest during the tuber bulking phase in potato (Chapter 3). Such impacts of (drought and salinity) stress are not commonly evaluated but are of crucial importance to evaluating those impacts and for taking mitigating measures. Our study shows how we can use remote sensing as a convenient tool to enable real-time dynamic monitoring and evaluating crop performance to regulate crop management.

Aside from the significant impact of the moment in the growing season, drought and salinity also affect crops differently depending on their species. A number of controlled experiments studies have shown that a variety of crops such as barley (Toker et al. 1999), reed (Sánchez et al. 2015), durum wheat (Houshmand et al. 2014), etc., respond differently to salinity and drought. Likewise, seven pepper accessions showed a wide variability of responses to salinity, drought, and their combination treatments (López-Serrano et al. 2017) These different responses of crops to drought and salinity likely link to their differences in tolerance to these stresses, which were shown in this study through the trait expressions of the various crops studied. For instance, almond -known to be sensitive to salinity and tolerant to drought- showed a higher sensitivity to salinity stress for LAI, FVC, FAPAR, and Cab during the growing season than to drought and or the combination of drought and salinity (Figure 4.4, Figure S4-2, Figure S4-3, and Figure 4.5), while sorghum responded more strongly to drought. Nevertheless, the responses of individual crops to salinity and drought stress were not fully consistent with expected tolerances based on controlled experiments. For instance, sorghum was expected to be tolerant to both drought and salinity (but mainly responded to drought) and almond was expected to be mainly sensitive to salinity. Thus, given the multitude of responses for different traits and crops that might not always be consistent with assumed tolerance to these stresses, our study shows that a comprehensive evaluation of responses to drought and salinity in a real-life agricultural setting across multiple crop types, growth conditions, and management is essential. In light of the projected future increase in drought and salinity stress, our remote sensing approach may be an appropriate tool to give timely guidance to government and local farmers.

4.4.2 Patterns in growth stage-dependent responses to stress

Although the responses of crops to drought and salinity differed between species and growth stages, there were commonalities among various crop types. In general, for all eight crops, LAI was triggered first by drought and salinity stress, followed by FVC and FAPAR, and Cw and Cab were the last to respond (Figure 4.7).

Therefore, it indicates that -depending on the growth stage- crops employ a different strategy to resist drought and salinity or vary in the sensitivity of traits to these stresses. Generally, our results suggest that most crops prefer to remove some leaves first before decreasing the vegetation cover as a whole to capture as much sunlight as possible, maintaining energy and nutrient uptake. When they cannot deal with water stress anymore, they reduce leaf chlorophyll content and leaf water content at last. This general sequence in trait responses -which we describe for the first time- with chlorophyll and leaf water responding when conditions get severe for a longer period of time, may explain why several studies concluded that chlorophyll content has a high correlation with drought or salinity stress (Schlemmer et al. 2005). Our results, showing that LAI responds first, explain why LAI -as the most well-known trait- provides a highly sensitive stress detection for vegetation (Li et al. 2022). Given their similar responsiveness, also FAPAR and FVC have the capability to determine and monitor stress impact on crop growth (Cammalleri et al. 2022; Mohammed and Algarni 2020).

Given that crops employ different strategies to resist drought and salinity stress (section 4.4.1) and given the growth-stage dependent trait responses to drought and salinity (this section), our study shows the importance of evaluating multiple traits simultaneously. Several studies focus on the spatiotemporal variation of individual traits, but the responses of crops from the beginning to the end of the growing season are rarely considered or compared. This limited coverage in time and traits may limit their findings to the restricted range of crop varieties and growth stages. Instead, in this study, we obtained a detailed description of crop tolerances to drought and salinity thanks to the combination of multiple measurements during the growing season and the assessment of multiple traits simultaneously. Such quantification is of importance for understanding crop responses to stress in real-life agricultural systems.

4.4.3 Local impacts on crop responses to salinity and drought stress

Despite the strong significance of all patterns described above, the effect sizes of the crop responses to salinity and drought stress were limited. Additionally accounting for the potential effects of differences in soil type, climate zone, and region between our observation pairs hardly improved our explanatory power of the effects of stress (Figure 4.3, Table S4-4, and Table S4-5), even though local conditions affected crop responses to stress (Figure S4-9, Figure S4-10, Figure S4-11, Figure S4-12, and Figure S4-13). The interaction effects of e.g. soil type or climate zone with stress were however significant in many cases (Table S4-5). This may be explained by the fact that soil moisture and soil salinity variations are known to be controlled by various factors, including soil type, climatic conditions, and local management policy (Ben Ahmed et al. 2012). Ben Rouina et al. (2007)

pointed out that the response of the olive tree to drought stress varied in soil type, due to the higher water-holding capacity in clay soils than in sandy soils. In most crops and for the five traits investigated, the impacts of soil type on the effects of stress were stronger than the impacts of climate zones or specific regions thereon. Together, they provide a partial explanation for the strong variation in crop responses to salinity and drought stress in the contiguous USA. However, even soil type did not affect the expression of impacts of salinity or drought stress as much as time did. This reinforces our assessment of the importance of time-dependent impacts of drought and salinity stress (section 4.4.1) and the generic patterns in the timing of the trait responses (section 4.4.2). In combination, our results indicate that a high variation in responses to drought and salinity is an outcome of the complex interaction of different crop responses and strategies over time in a broad spectrum of environmental conditions.

4.4.4 Future implications

The remote sensing approach developed and employed in this study to evaluate crop tolerance to combined salinity and drought stress by assessing multiple traits linked to crop performance also provides possibilities for application to other stress combinations (e.g., flood, heat, frost). Given the general nature of the traits used and of its generic assessment methodology, such applications are not only feasible for crops but for all kinds of vegetation types. Our approach is complementary to existing small-scale and experimental approaches by focusing on large-scale settings in local agricultural settings. Our approach shows that it is able to capture the high variation in crop performance in the contiguous USA at relatively high resolution. This suggests that it can be an interesting approach for local farmers or the government to timely assess crop health. In this way, it gives farmers an open-source tool to monitor crop growth conditions and adjust field management based on evidence. For larger to global scale applications, our approach allows evaluating food security and associated stress factors to may constrain food security, many of which are likely to become more prominent in the near future.

4.5 Conclusions

In this study, we evaluated the responses of multiple crops to salinity, drought, and their combination based on five functional traits across the entire U.S. continent throughout crop growing season in 2021 from remote sensing. We found that stress impacts were highly dependent on the moment in the growing season. Moreover, different crops showed divergent responses to these stresses over time. In general, crops were more sensitive to the combined effects of salinity and drought stress compared to the individual effects of salinity and drought stress. Most crops first reduced their primary production capacity through reducing LAI before reducing water or chlorophyll contents. In combination, we established a quantitative

foundation for simultaneously assessing the responses of various crops to the occurrence of stresses, alone and collectively at large scale and under actual agricultural conditions. Consequently, we contribute to monitor food security and guide food production in a timely and non-destructive way by remote sensing.

4.6 Author contributions

Wen Wen: Conceptualization, Methodology, Investigation, Writing, and Reviewing. Joris Timmermans: Conceptualization, Methodology, Supervision, Writing, and Reviewing. Qi Chen: Methodology and Reviewing. Peter M. van Bodegom: Conceptualization, Methodology, Supervision, Writing, and Reviewing.

4.7 Supporting information

Table S4-1. Number of observation pairs in the final selection for crops during the growing season from March to October.

	March	April	May	June	July	August	September	October	Total
Soybean	405	1500	6994	13810	18402	22975	21824	12392	98302
Maize	911	2827	6227	10293	14460	16228	16341	9497	76784
Alfalfa	1678	4265	8144	8402	6932	6517	7702	5868	49508
Spring wheat	14	35	3298	11391	9093	6925	7695	5604	44055
Sugar beet	101	140	289	755	1014	1187	1153	1036	5675
Almond	405	728	709	705	707	705	699	739	5397
Grape	340	352	391	452	466	527	587	622	3737
Sorghum	9	12	58	111	176	180	144	127	817

Table S4-2. Crop stress-tolerance characteristics.

Crop	Drought tolerance (Idowu et al. 2012; Wei et al. 2018)	Salinity tolerance (Grieve et al. 2011)	Category
Soybean	drought-sensitive (DS)	salinity-tolerant (ST)	ST+DS
Maize	drought-tolerant (DT)	salinity-sensitive (SS)	SS+DT
Grape	drought-tolerant (DT)	salinity-sensitive (SS)	SS+DT
Almond	drought-tolerant (DT)	salinity-sensitive (SS)	SS+DT
Alfalfa	drought-tolerant (DT)	salinity-sensitive (SS)	SS+DT
Sugar beet	drought-tolerant (DT)	salinity-tolerant (ST)	ST+DT
Spring wheat	drought-tolerant (DT)	salinity-tolerant (ST)	ST+DT
Sorghum	drought-tolerant (DT)	salinity-tolerant (ST)	ST+DT

Table S4-3. Two-way ANOVA results by time series and stress interactions for different crop traits (sig.= significance with ** $p < 0.01$; * $p < 0.05$; ns = not significant).

Crops	Factors	LAI		FAPAR		FVC		Cab		Cw	
		sig.	Partial Eta Squared	sig.	Partial Eta Squared	sig.	Partial Eta Squared	sig.	Partial Eta Squared	sig.	Partial Eta Squared
Alfalfa	time	**	0.001	**	0.001	**	0.001	**	0.001	**	0.001
	stress	**	0.002	**	0.002	**	0.002	**	0.004	**	0.013
	time*stress	**	0.012	**	0.014	**	0.014	**	0.014	**	0.073
Almond	time	**	0.007	*	0.030	*	0.004	*	0.003	**	0.010
	stress	**	0.014	**	0.016	**	0.020	*	0.004	**	0.018
	time*stress	**	0.037	**	0.036	**	0.035	**	0.030	**	0.045
Grape	time	*	0.007	ns	0.003	ns	0.003	*	0.005	ns	0.001
	stress	**	0.010	*	0.004	*	0.005	**	0.012	**	0.010
	time*stress	**	0.048	**	0.028	**	0.033	**	0.027	**	0.028
Maize	time	**	0.000	**	0.001	**	0.001	**	0.001	**	0.001
	stress	**	0.001	**	0.001	**	0.001	**	0.001	*	0.000
	time*stress	**	0.003	**	0.002	**	0.002	**	0.002	**	0.002
Sorghum	time	ns	0.007	ns	0.014	ns	0.011	ns	0.010	ns	0.006
	stress	**	0.026	*	0.014	*	0.015	*	0.018	ns	0.001
	time*stress	ns	0.020	*	0.028	*	0.026	*	0.035	ns	0.009
Soybean	time	**	0.001	**	0.000	**	0.001	**	0.002	**	0.001
	stress	**	0.000	**	0.000	**	0.000	ns	0.000	**	0.000
	time*stress	**	0.001	**	0.001	**	0.001	**	0.002	**	0.001
Spring wheat	time	**	0.001	**	0.001	**	0.001	**	0.003	**	0.002
	stress	*	0.000	*	0.000	*	0.000	ns	0.000	*	0.000
	time*stress	**	0.002	**	0.002	**	0.002	**	0.002	**	0.001
Sugar beet	time	**	0.023	**	0.014	**	0.019	**	0.006	**	0.006
	stress	**	0.007	**	0.005	**	0.007	**	0.008	**	0.010
	time*stress	**	0.053	**	0.028	**	0.033	**	0.026	**	0.040

Table S4-4. Multi-way ANOVA for different crop traits including only main effects of time, stress, soil type, climate zone, and state (sig. = significance with ** $p < 0.01$; * $p < 0.05$; ns = not significant).

Crops	Factors	Cab		Cw		FAPAR		FVC		LAI	
		sig.	Partial Eta Squared	sig.	Partial Eta Squared	sig.	Partial Eta Squared	sig.	Partial Eta Squared	sig.	Partial Eta Squared
Alfalfa	time	**	0.004	**	0.011	**	0.002	**	0.004	**	0.002
	stress	**	0.002	**	0.011	**	0.001	**	0.001	**	0.001
	soil type	**	0.012	**	0.005	**	0.010	**	0.010	**	0.005
	climate zone	**	0.003	**	0.002	**	0.002	**	0.002	**	0.002
	state	**	0.006	**	0.009	**	0.005	**	0.005	**	0.004
Almond	time	**	0.039	**	0.055	**	0.081	**	0.084	**	0.067
	stress	**	0.005	**	0.010	*	0.003	**	0.007	**	0.006
	soil type	**	0.078	**	0.115	**	0.050	**	0.040	**	0.040
	climate zone	**	0.030	**	0.075	**	0.013	**	0.013	**	0.020
	state	--	--	--	--	--	--	--	--	--	--
Grape	time	**	0.013	**	0.016	**	0.047	**	0.051	**	0.087
	stress	**	0.014	**	0.015	**	0.006	*	0.004	*	0.004
	soil type	**	0.025	**	0.023	**	0.042	**	0.045	**	0.044
	climate zone	**	0.077	**	0.019	**	0.078	**	0.096	**	0.137
	state	ns	0.000	*	0.004	**	0.007	**	0.010	**	0.029
Maize	time	**	0.007	**	0.004	**	0.004	**	0.004	**	0.005
	stress	**	0.002	*	0.000	**	0.001	**	0.001	**	0.001
	soil type	**	0.003	**	0.008	**	0.003	**	0.003	**	0.004
	climate zone	**	0.001	**	0.001	**	0.001	**	0.001	**	0.001
	state	**	0.003	**	0.004	**	0.002	**	0.002	**	0.003
Sorghum	time	**	0.037	ns	0.015	**	0.053	**	0.044	**	0.037
	stress	*	0.009	ns	0.000	ns	0.001	ns	0.001	ns	0.000
	soil type	*	0.026	ns	0.008	ns	0.016	ns	0.013	*	0.020
	climate zone	ns	0.013	ns	0.008	ns	0.014	ns	0.012	*	0.028
	state	*	0.026	*	0.019	ns	0.015	ns	0.014	**	0.040
Soybean	time	**	0.011	**	0.006	**	0.004	**	0.004	**	0.007
	stress	**	0.001	ns	0.000	**	0.001	**	0.001	**	0.001
	soil type	**	0.001	**	0.001	**	0.003	**	0.004	**	0.005
	climate zone	**	0.000	**	0.000	**	0.000	**	0.000	*	0.000
	state	**	0.002		0.001	**	0.001	**	0.001	**	0.001

Spring Wheat	time	**	0.014	**	0.002	**	0.004	**	0.003	**	0.006
	stress	**	0.002	ns	0.000	**	0.000	**	0.001	**	0.001
	soil type	**	0.005	**	0.003	**	0.002	**	0.003	**	0.005
	climate zone	**	0.001	ns	0.000	**	0.002	**	0.002	**	0.002
	state	**	0.002	*	0.001	**	0.002	**	0.001	**	0.003
Sugar beet	time	**	0.073	**	0.029	**	0.051	**	0.066	**	0.089
	stress	ns	0.001	**	0.015	*	0.002	*	0.002	*	0.003
	soil type	ns	0.002	*	0.004	**	0.006	**	0.006	**	0.006
	climate zone	*	0.002	**	0.004	**	0.004	**	0.004	**	0.010
	state	**	0.009	**	0.005	**	0.009	**	0.008	**	0.016

Table S4-5. Multi-way ANOVA for different crop traits including main effects of time, stress, soil type, climate zone, and states and the interactions of stress and time with other factors (sig. = significance, ** $p < 0.01$; * $p < 0.05$; ns = not significant).

Crops	Factors	Cab		Cw		FAPAR		FVC		LAI	
		sig.	Partial Eta Squared	sig.	Partial Eta Squared	sig.	Partial Eta Squared	sig.	Partial Eta Squared	sig.	Partial Eta Squared
Alfalfa	time	ns	0.000	*	0.000	*	0.000	*	0.000	*	0.000
	stress	ns	0.000	ns	0.000	ns	0.000	ns	0.000	ns	0.000
	soil type	**	0.000	**	0.002	**	0.003	**	0.003	**	0.002
	climate zone	*	0.002	**	0.001	ns	0.000	ns	0.000	*	0.000
	state	**	0.001	**	0.002	**	0.002	**	0.002	**	0.002
	time*stress	**	0.006	**	0.026	**	0.009	**	0.004	**	0.006
	time*soil type	**	0.013	**	0.026	**	0.018	**	0.022	**	0.018
	time*state	**	0.014	**	0.027	**	0.019	**	0.020	**	0.022
	time*climate zone	**	0.007	**	0.013	**	0.007	**	0.008	**	0.008
	stress*soil type	**	0.008	**	0.002	**	0.006	**	0.007	**	0.006
	stress*climate zone	*	0.001	**	0.001	*	0.001	ns	0.001	ns	0.001
	stress*state	**	0.006	**	0.003	**	0.005	**	0.006	**	0.005
Almond	time	**	0.012	**	0.008	**	0.005	**	0.007	**	0.019
	stress	**	0.008	**	0.011	**	0.007	**	0.013	**	0.013
	soil type	**	0.017	**	0.025	**	0.017	**	0.016	**	0.017
	climate zone	**	0.022	**	0.013	**	0.019	**	0.025	**	0.035
	state	--	--	--	--	--	--	--	--	--	--
	time*stress	**	0.020	**	0.027	**	0.018	**	0.018	**	0.022
	time*soil type	**	0.060	**	0.094	**	0.061	**	0.056	**	0.043
	time*state	--	--	--	--	--	--	--	--	--	--
	time*climate zone	**	0.055	**	0.064	**	0.046	**	0.047	**	0.066
	stress*soil type	*	0.005	**	0.006	**	0.008	**	0.009	**	0.010
	stress*climate zone	**	0.008	**	0.006	*	0.004	**	0.009	**	0.010
	stress*state	--	--	--	--	--	--	--	--	--	--
Maize	time	*	0.000	**	0.000	ns	0.000	ns	0.000	*	0.000
	stress	*	0.000	*	0.000	ns	0.000	ns	0.000	*	0.000
	soil type	**	0.001	**	0.003	**	0.001	**	0.002	**	0.002
	climate zone	*	0.000	ns	0.000	ns	0.000	ns	0.000	*	0.000
	state	**	0.001	**	0.002	**	0.001	**	0.001	**	0.001
	time*stress	**	0.002	**	0.001	**	0.001	**	0.001	**	0.001
	time*soil type	**	0.032	**	0.018	**	0.021	**	0.021	**	0.033
	time*state	**	0.015	**	0.016	**	0.011	**	0.011	**	0.018
	time*climate zone	**	0.005	**	0.003	**	0.004	**	0.004	**	0.005
	stress*soil type	**	0.001	ns	0.000	**	0.001	**	0.001	**	0.002
	stress*climate zone	ns	0.000	**	0.001	*	0.000	*	0.001	**	0.001
	stress*state	**	0.001	*	0.001	**	0.001	**	0.001	**	0.002
	time	**	0.010	*	0.005	**	0.011	**	0.010	*	0.007
	stress	*	0.004	ns	0.002	ns	0.002	*	0.003	**	0.007

Grape	soil type	**	0.038	**	0.018	**	0.042	**	0.045	**	0.061
	climate zone	**	0.041	**	0.010	**	0.029	**	0.026	**	0.030
	state	ns	0.000	*	0.003	*	0.002	*	0.003	**	0.010
	time*stress	**	0.013	*	0.011	*	0.011	**	0.013	**	0.018
	time*soil type	**	0.102	**	0.043	**	0.054	**	0.054	**	0.061
	time*state	*	0.005	*	0.004	**	0.006	**	0.007	*	0.004
	time*climate zone	**	0.065	**	0.034	**	0.072	**	0.082	**	0.142
	stress*soil type	ns	0.001	*	0.001	ns	0.000	ns	0.000	ns	0.000
	stress*climate zone	**	0.009	**	0.008	ns	0.001	ns	0.001	ns	0.001
	stress*state	ns	0.000	ns	0.000	ns	0.000	ns	0.000	ns	0.000
Sorghum	time	*	0.021	ns	0.014	*	0.025	*	0.024	*	0.024
	stress	ns	0.007	ns	0.001	ns	0.003	ns	0.006	ns	0.002
	soil type	*	0.022	ns	0.006	*	0.020	*	0.019	**	0.035
	climate zone	ns	0.003	ns	0.004	ns	0.003	ns	0.005	ns	0.003
	state	*	0.015	ns	0.007	ns	0.010	ns	0.013	ns	0.008
	time*stress	**	0.049	ns	0.012	*	0.036	*	0.035	*	0.033
	time*soil type	ns	0.032	ns	0.029	*	0.059	ns	0.056	ns	0.034
	time*state	ns	0.016	ns	0.011	ns	0.016	ns	0.022	ns	0.033
	time*climate zone	ns	0.021	ns	0.008	ns	0.038	ns	0.035	ns	0.031
	stress*soil type	*	0.021	ns	0.010	ns	0.010	*	0.016	*	0.018
	stress*climate zone	ns	0.002	ns	0.001	ns	0.001	ns	0.000	ns	0.000
	stress*state	ns	0.001	ns	0.001	ns	0.001	ns	0.002	ns	0.006
Soybean	time	*	0.000	*	0.000	*	0.000	*	0.000	**	0.000
	stress	ns	0.000	ns	0.000	ns	0.000	ns	0.000	ns	0.000
	soil type	*	0.000	**	0.001	ns	0.000	*	0.000	ns	0.000
	climate zone	ns	0.000	**	0.000	ns	0.000	ns	0.000	ns	0.000
	state	**	0.000	*	0.000	*	0.000	*	0.000	*	0.000
	time*stress	**	0.001	**	0.001	*	0.001	**	0.001	**	0.001
	time*soil type	**	0.013	**	0.011	**	0.009	**	0.009	**	0.010
	time*state	**	0.007	**	0.005	**	0.005	**	0.005	**	0.006
	time*climate zone	**	0.002	**	0.001	**	0.002	**	0.002	**	0.002
	stress*soil type	ns	0.000	ns	0.000	ns	0.000	ns	0.000	*	0.000
	stress*climate zone	*	0.000	*	0.000	*	0.000	**	0.000	*	0.000
	stress*state	*	0.000	*	0.000	*	0.000	*	0.000	**	0.000
Spring wheat	time	**	0.001	**	0.002	**	0.001	**	0.001	**	0.003
	stress	ns	0.000	*	0.000	ns	0.000	ns	0.000	*	0.000
	soil type	**	0.001	**	0.003	ns	0.000	*	0.001	**	0.001
	climate zone	**	0.001	ns	0.000	ns	0.000	ns	0.000	*	0.000
	state	*	0.000	*	0.000	*	0.000	*	0.000	*	0.001
	time*stress	**	0.003	**	0.001	*	0.001	*	0.001	*	0.001
	time*soil type	**	0.011	**	0.010	**	0.008	**	0.007	**	0.011
	time*state	**	0.007	**	0.003	**	0.007	**	0.007	**	0.011
	time*climate zone	**	0.005	**	0.002	**	0.004	**	0.004	**	0.005
	stress*soil type	*	0.001	*	0.001	ns	0.000	ns	0.000	ns	0.001
	stress*climate zone	ns	0.000	ns	0.000	ns	0.000	ns	0.000	ns	0.000
	stress*state	**	0.001	ns	0.000	*	0.001	*	0.001	**	0.001

	time	ns	0.002	*	0.003	ns	0.003	ns	0.001	ns	0.001
	stress	ns	0.001	ns	0.001	**	0.004	*	0.003	**	0.004
	soil type	*	0.003	*	0.003	ns	0.002	*	0.002	ns	0.001
	climate zone	ns	0.001	**	0.003	*	0.002	*	0.002	**	0.007
	state	ns	0.001	**	0.005	*	0.003	*	0.003	**	0.006
	time*stress	*	0.007	**	0.009	**	0.010	**	0.011	**	0.012
Sugar	time*soil type	**	0.015	**	0.020	**	0.017	**	0.019	**	0.017
beet	time*state	**	0.014	**	0.012	**	0.020	**	0.020	**	0.019
	time*climate zone	**	0.007	*	0.005	**	0.012	**	0.012	**	0.012
	stress*soil type	*	0.002	ns	0.001	ns	0.001	ns	0.001	**	0.004
	stress*climate zone	ns	0.001	ns	0.001	ns	0.001	ns	0.001	*	0.003
	stress*state	ns	0.001	*	0.002	*	0.003	**	0.003	**	0.005

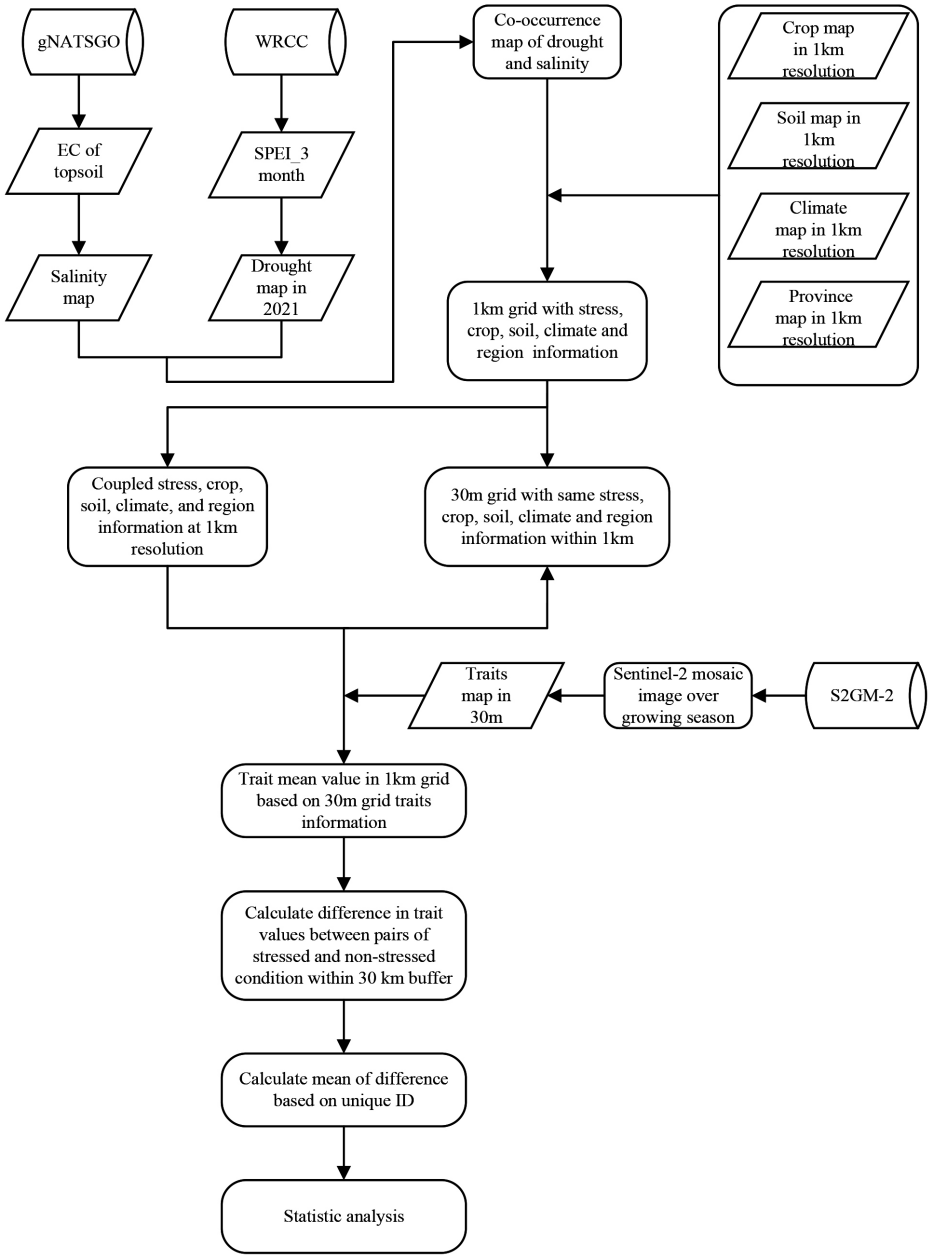

Figure S4-1 Technical workflow of pairwise dataset processing.

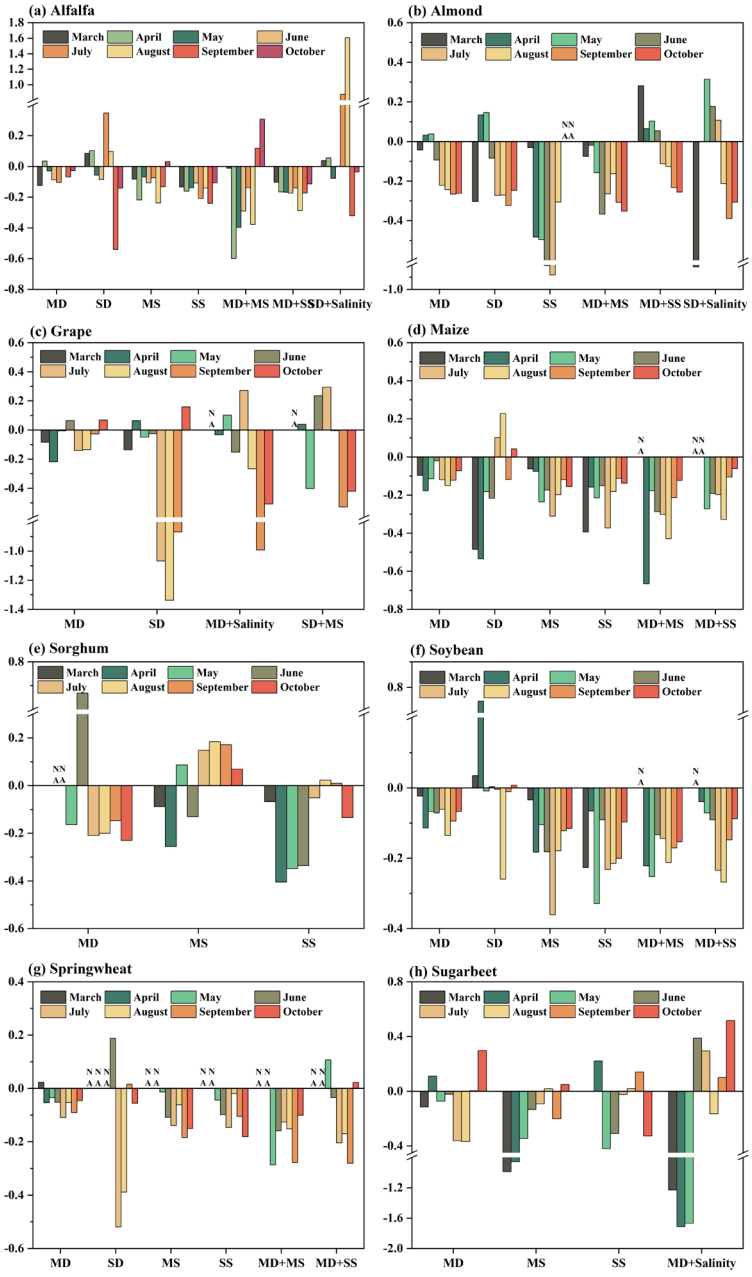

Figure S4-2. Expressions of LAI under various stress conditions for eight crops from March to October in 2021. MS, moderate salinity only; SS, severe salinity only; MD, moderate drought only; SD, severe drought only; MD+MS, moderate drought and moderate salinity; SD+MS, severe drought and moderate salinity; MD+SS, moderate drought and severe salinity; SD+SS, severe drought and severe salinity; MD+Salinity, moderate drought and salinity; SD+Salinity, severe drought and salinity; NA, the stress condition is not applicable to that month.

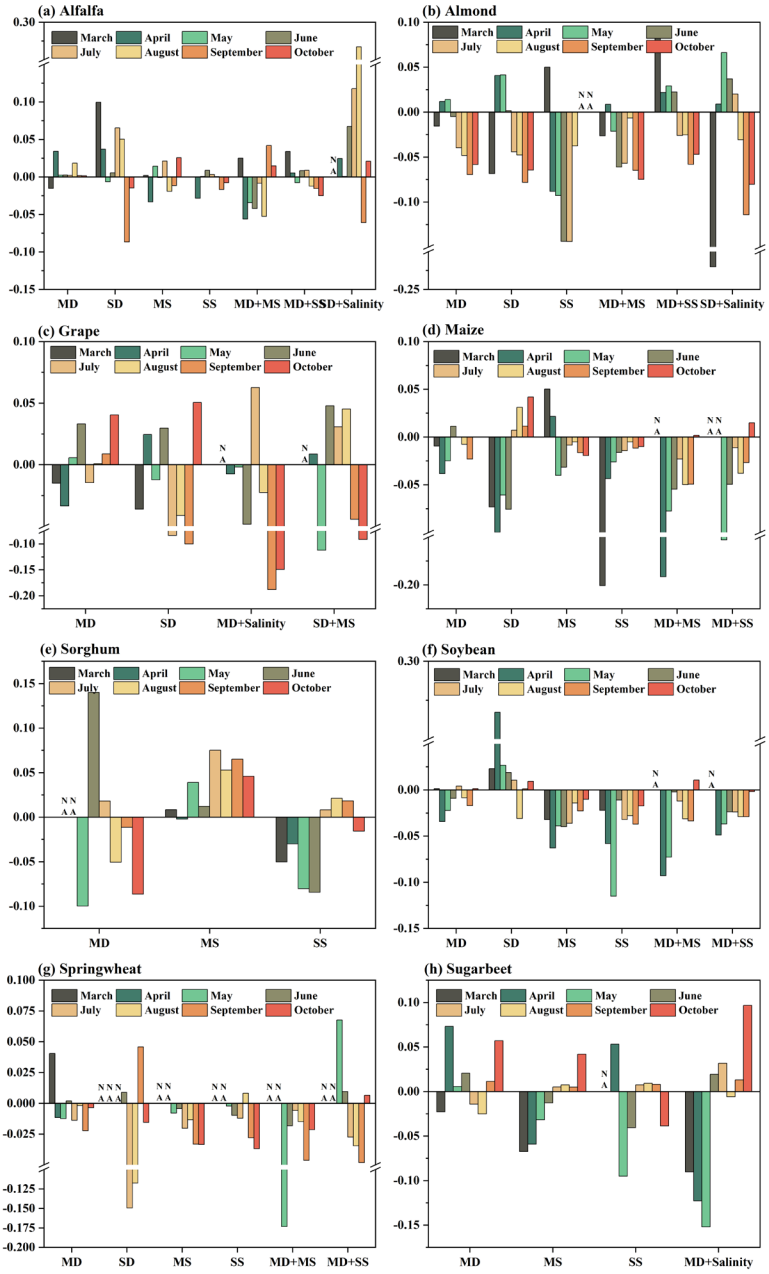

Figure S4-3. Expressions of FAPAR under various stress conditions for eight crops from March to October in 2021. MS, moderate salinity only; SS, severe salinity only; MD, moderate drought only; SD, severe drought only; MD+MS, moderate drought and moderate salinity; SD+MS, severe drought and moderate salinity; MD+SS, moderate drought and severe salinity; SD+SS, severe drought and severe salinity; MD+Salinity, moderate drought and salinity; SD+Salinity, severe drought and salinity; NA, the stress condition is not applicable to that month.

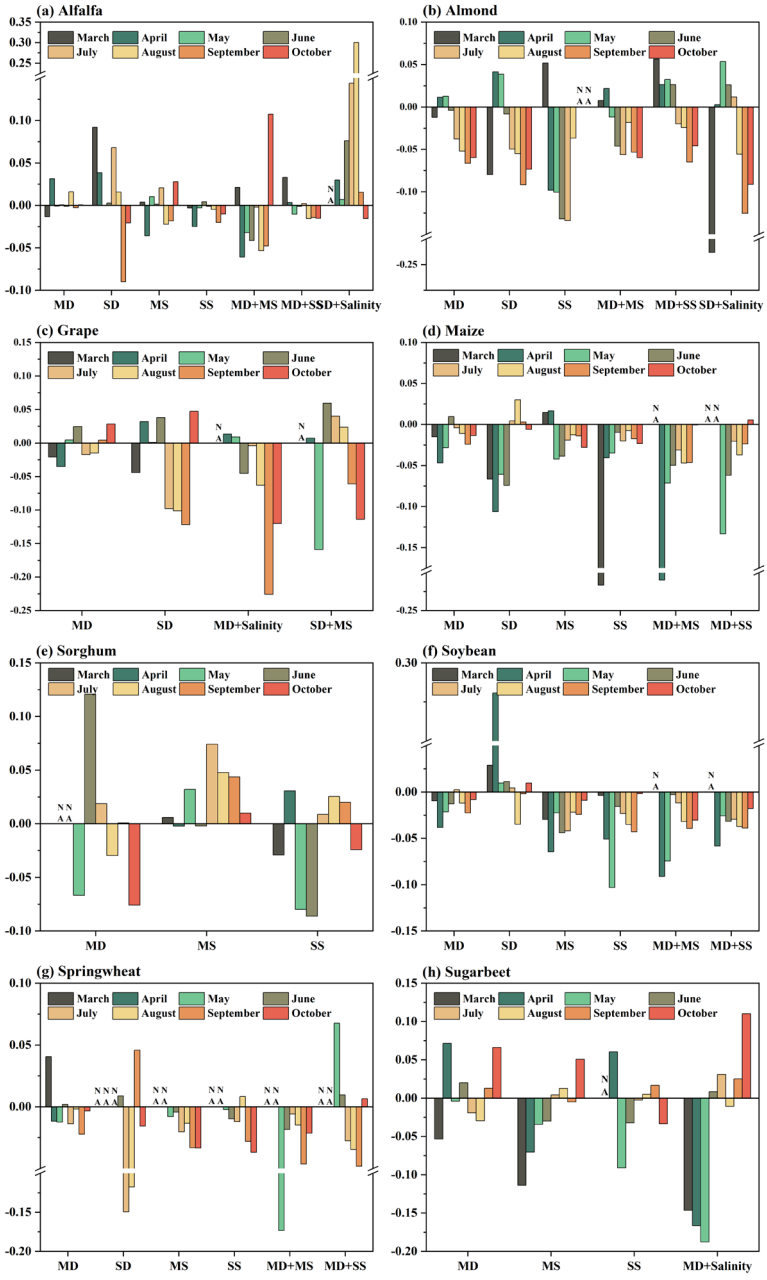

Figure S4-4. Expressions of FVC under various stress conditions for eight crops from March to October in 2021. MS, moderate salinity only; SS, severe salinity only; MD, moderate drought only; SD, severe drought only; MD+MS, moderate drought and moderate salinity; SD+MS, severe drought and moderate salinity; MD+SS, moderate drought and severe salinity; SD+SS, severe drought and severe salinity; MD+Salinity, moderate drought and salinity; SD+Salinity, severe drought and salinity; NA, the stress condition is not applicable to that month.

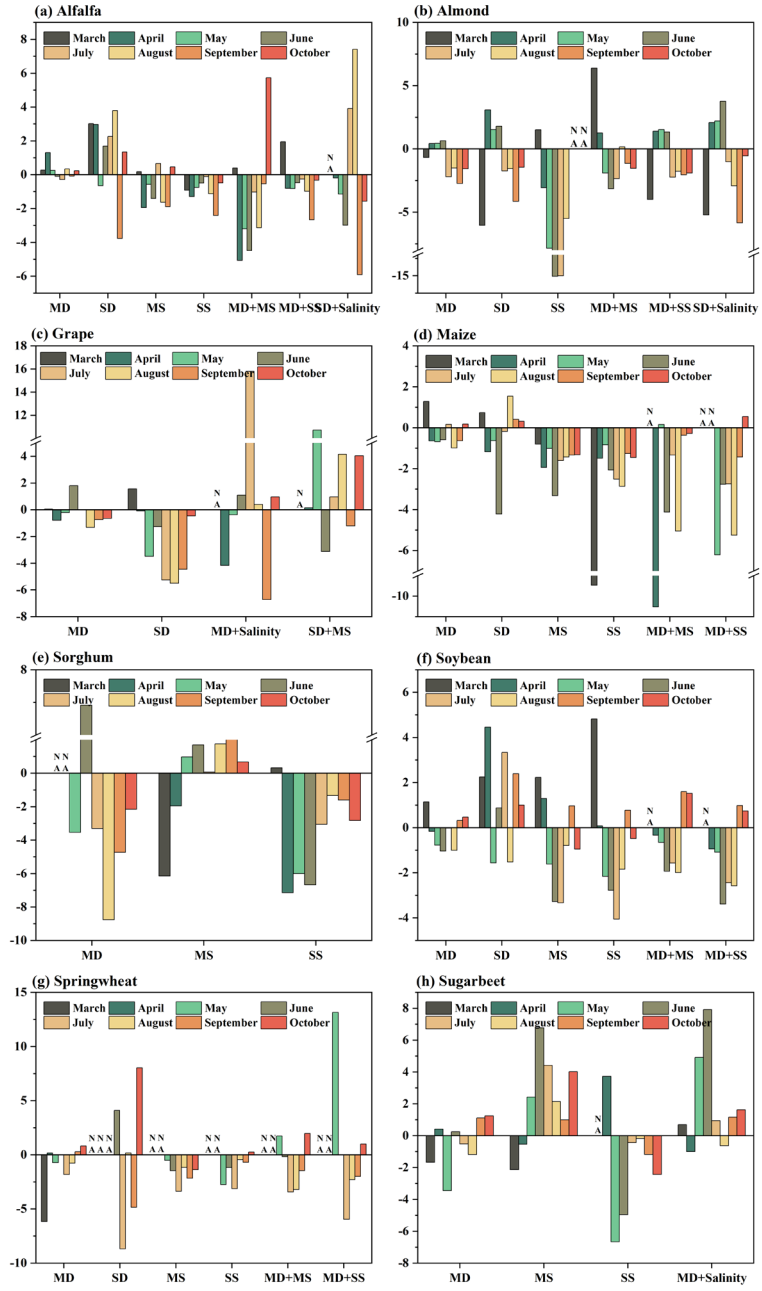

Figure S4-5. Expressions of Cab under various stress conditions for eight crops from March to October in 2021. MS, moderate salinity only; SS, severe salinity only; MD, moderate drought only; SD, severe drought only; MD+MS, moderate drought and moderate salinity; SD+MS, severe drought and moderate salinity; MD+SS, moderate drought and severe salinity; SD+SS, severe drought and severe salinity; MD+Salinity, moderate drought and salinity; SD+Salinity, severe drought and salinity; NA, the stress condition is not applicable to that month.

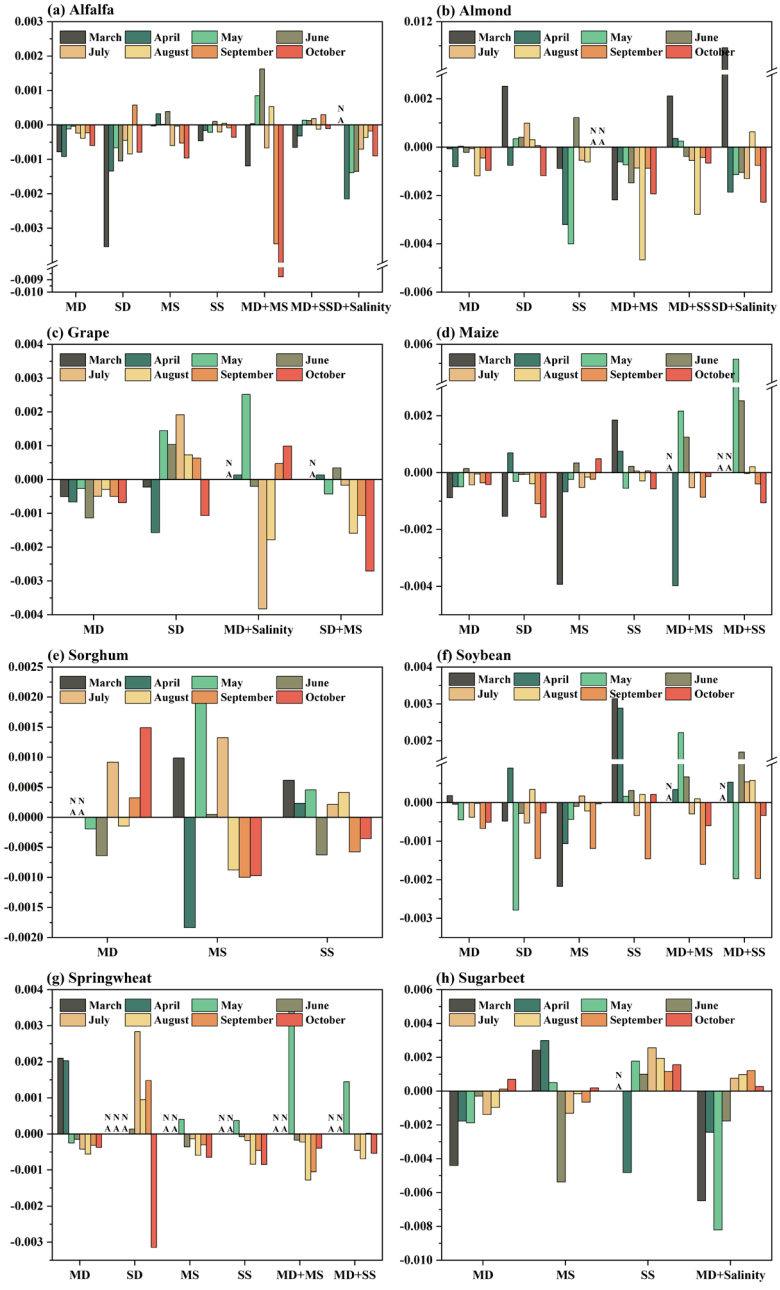

Figure S4-6. Expressions of Cw under various stress conditions for eight crops from March to October in 2021. MS, moderate salinity only; SS, severe salinity only; MD, moderate drought only; SD, severe drought only; MD+MS, moderate drought and moderate salinity; SD+MS, severe drought and moderate salinity; MD+SS, moderate drought and severe salinity; SD+SS, severe drought and severe salinity; MD+Salinity, moderate drought and salinity; SD+Salinity, severe drought and salinity; NA, the stress condition is not applicable to that month.

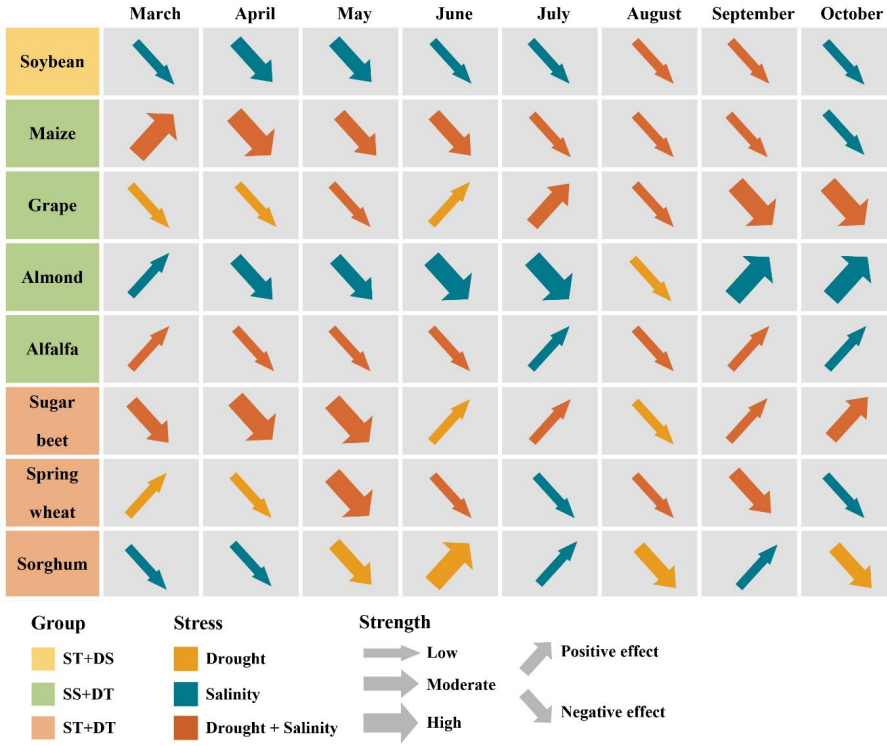

Figure S4-7. The pattern of FAPAR, expressing the severest stress conditions in different months. ST+DS indicates salt-tolerant and drought-sensitive crop; SS+DT indicates salt-sensitive and drought-tolerant crop; ST+DT indicates salt-tolerant and drought-tolerant crop; in strength, low indicates a difference between stress pixels and control pixels smaller than 0.05 (unitless), moderate indicates a difference between stress pixels and control pixels between 0.05 and 0.1, high indicates a difference between stress pixels and control pixels greater than 0.1; positive effect and negative effect indicate the direction of the pair-wise differences between stress pixels and control pixels.

Figure S4-8. The pattern of FVC, expressing the severest stress conditions in different months. ST+DS indicates salt-tolerant and drought-sensitive crop; SS+DT indicates salt-sensitive and drought-tolerant crop; ST+DT indicates salt-tolerant and drought-tolerant crop; in strength, low indicates a difference between stress pixels and control pixels smaller than 0.05 (unitless), moderate indicates a difference between stress pixels and control pixels between 0.05 and 0.1, high indicates a difference between stress pixels and control pixels greater than 0.1; positive effect and negative effect indicate the direction of the pair-wise differences between stress pixels and control pixels.

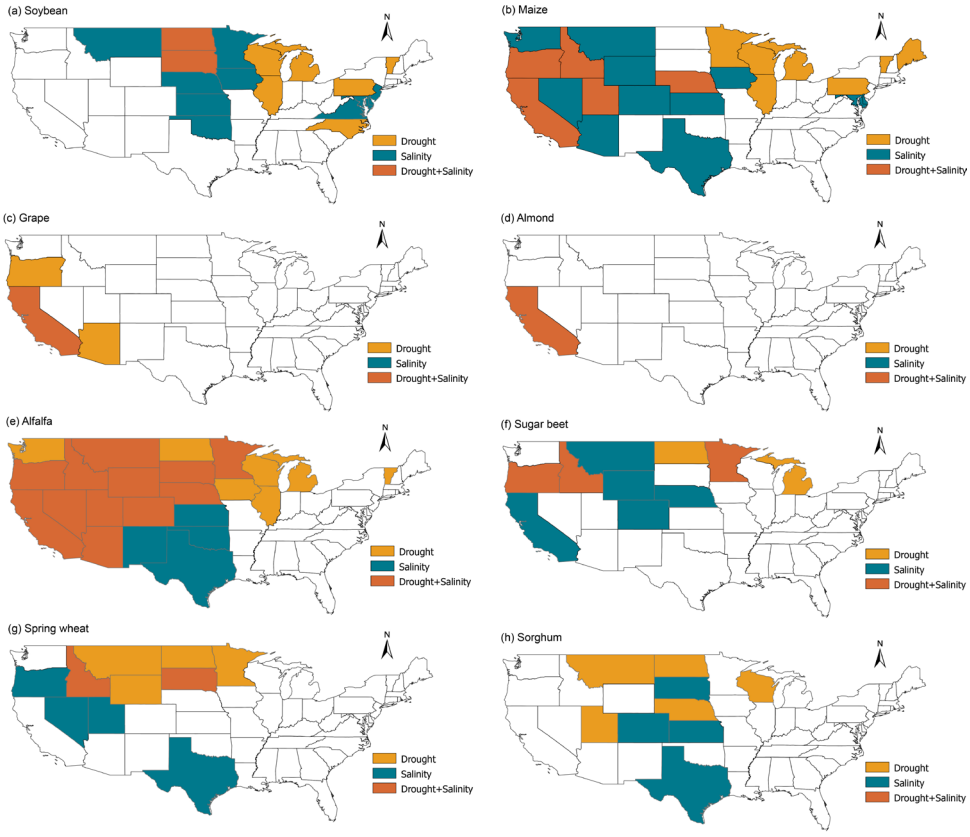

Figure S4-9. The spatial variation of LAI by states for eight crops.

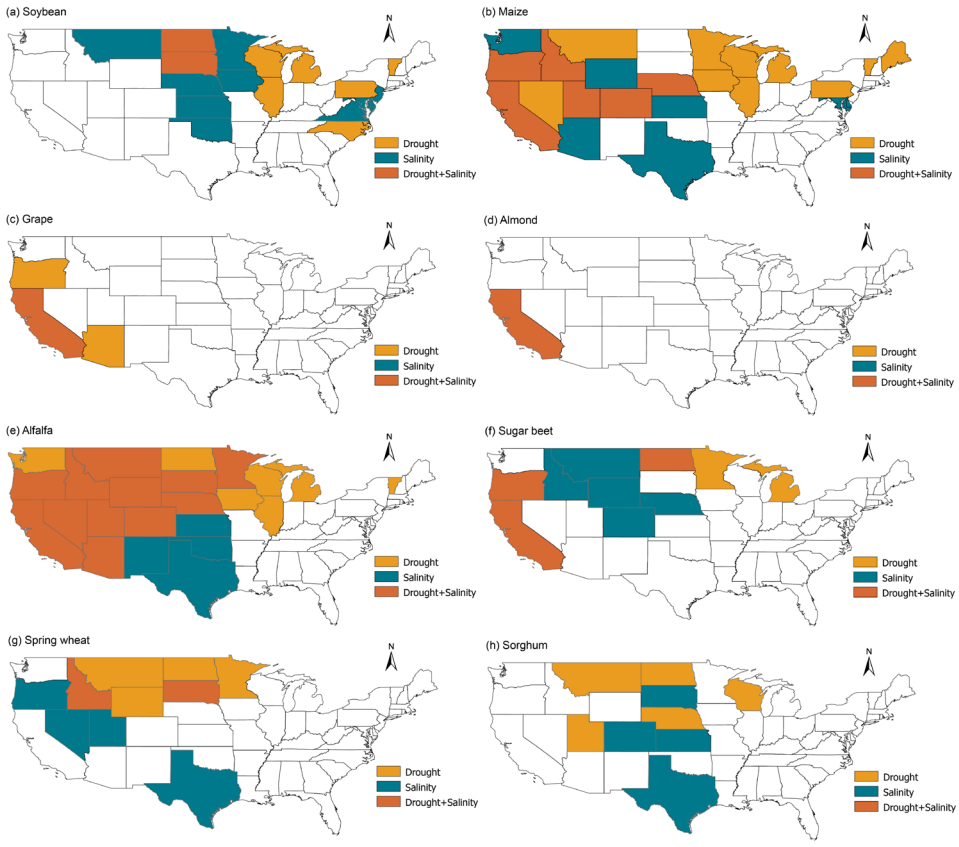

Figure S4-10. The spatial variation of FAPAR by states for eight crops.

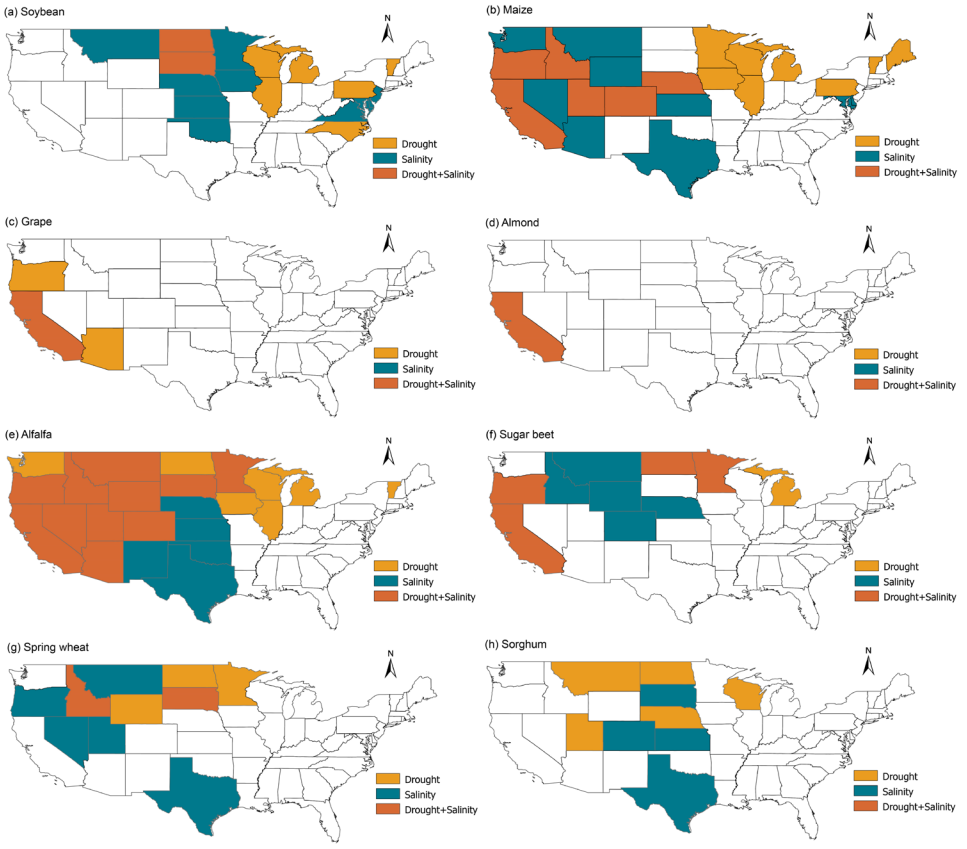

Figure S4-11. The spatial variation of FVC by states for eight crops.

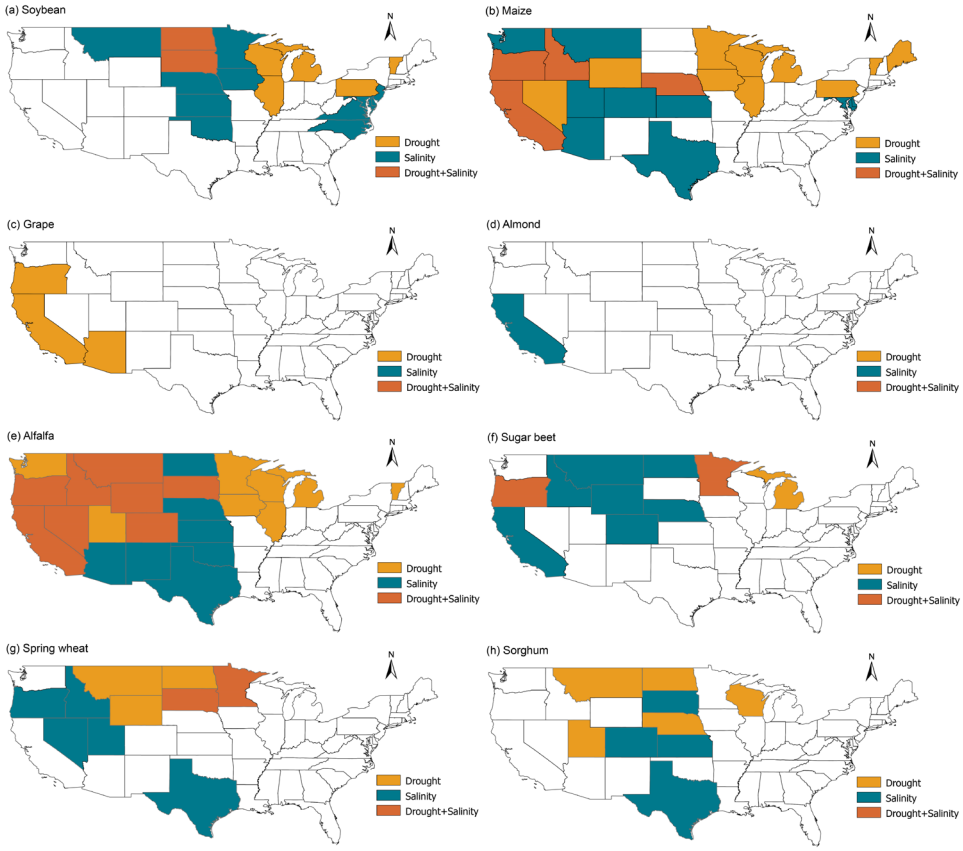

Figure S4-12. The spatial variation of Cab by states for eight crops.

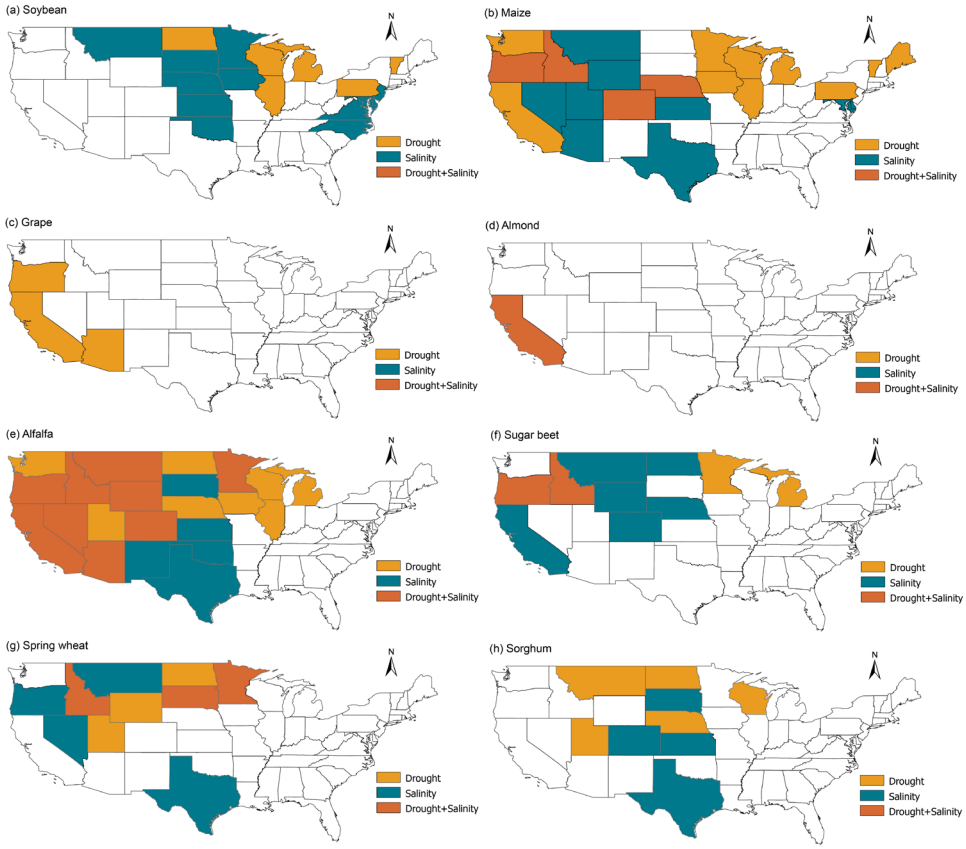

Figure S4-13. The spatial variation of Cw by states for eight crops.

Chapter 5

Prospects of salt-tolerant potato to increase food productivity towards a zero hunger world

Wen Wen, Joris Timmermans, Daan Hooimeijer, Peter M. van Bodegom

In preparation

Abstract

Sustainable agriculture and food security are critical aspects of the sustainable development goals (SDGs), but they are increasingly vulnerable to the impacts of global climate change. While salt-induced stress on crop growth and food production has been extensively studied, the quantification of the contribution of the utilization of saline soil to agricultural production (i.e., saline farming) on a global scale is still highly uncertain. This study aims to address this gap by evaluating the local and regional suitability areas for salt-tolerant potato cultivation in affected soils, thereby assessing the contribution of salt-tolerant potatoes to the current and future SDGs. We found that Oceania, out of all other continents, currently exhibits the greatest potential for enhancing food production through salt-tolerant potato cultivation in salt-affected soils. In particular, Australia emerges as the country with the most substantial increase in the local suitability and regional suitability area. Meanwhile, Kazakhstan, the Russian Federation, Iraq, and Lesotho also possess the capacity to address food shortage challenges and work towards achieving SDG targets by utilizing salt-tolerant potato cultivation. Furthermore, under various future scenarios, the extent of local suitability area for salt-tolerant potato will consistently expand despite the increasing severity of soil salinity. Hence, also under future climatic and salinity conditions, salt-tolerant crops may help to enhance food production and to successfully achieve SDG targets (with a 100% increase for countries like Kazakhstan and the Russian Federation) across various future scenarios. In combination, our study provides a way of evaluating salt-tolerant potato as a proxy of saline farming, enabling enhanced food production in salt-affected soils, thereby establishing the backbone for promoting saline farming practices, with the ultimate goal of ensuring food security and enhancing agricultural resilience.

5.1 Introduction

To ensure a safe and sustainable future for all, the United Nations (UN) has established the sustainable development goals (SDGs) for 2030, with sustainable agriculture and food security being essential components. Within this framework, SDG-2 specifies aims to improve agriculture system resilience to e.g. climate change, drought, and soil quality, to ensure sustainable food production by 2030 (UN 2015). To attain SDG-2 requires significant improvements to agricultural production both in terms of size and efficiency. However, SDG-2 is also persistently challenged by frequently occurring extreme events, sluggish economics, conflicts, inequality, and poverty. Hence, despite considerable progress, the world remains off track in achieving the zero hunger world goal under global climate change and there are still 1/10 people suffering from hunger in 2021 (UN 2022). Therefore, there is a pressing need for improved agricultural practices and optimal utilization of the available land area to ensure food security.

Salt affects approximately 11% of the world's irrigated area while soil salinity is projected to increase to 50% of the arable land by 2050 (Butcher et al. 2016; FAO 2011). Most of these increases are on arid or semi-arid lands where increasingly frequent extreme events (e.g., drought) are projected to increase soil salinity impacts (Chapter 2). Meanwhile, the availability of water suitable for irrigation is projected to be exacerbated in the coastal area due to sea-level rise and seawater intrusion in the near future (Chen and Mueller 2018). Salinity is a major pressure limiting crop growth and yield, resulting in an annual economic loss of 27.3 billion US dollars globally (Qadir et al. 2014). Thus, improving the utilization of salt-affected soils can be a critical step to contribute to a sustainable agricultural system. Although various attempts have been made to assess salt-affected soil areas at a regional scale or global scale (Corwin and Scudiero 2019; Hassani et al. 2021), there is not any regional or global analysis to couple soil salinity with food productivity in a quantitative way.

To address this challenge, salt farming has emerged as a new practice to promote crop utilization and contribute to food security in the present and foreseeable future. Salt-affected soils have been reclaimed through applications of various amendments, halophytes, and microorganisms, and optimizations in land use as well as irrigation and drainage strategies (Mukhopadhyay et al. 2021). Next to reclaiming salt-affected soils, cultivating salt-tolerant crops is a promising solution to tackle this problem (Rozema and Flowers 2008). Crops such as rice, wheat, maize, etc., have been screened for salt-tolerant genotypes with stable productivities (Farooq et al. 2015; Genc et al. 2019; Reddy et al. 2017). However, most of these salt-tolerant cereal cultivars have been primarily tested in local experimental settings, indicating a limited understanding of salt-tolerant crops'

application on a large scale. Compared to these cereals, potato delivers higher calories per unit of water (Renault and Wallender 2000). Salt-tolerant potato, in particular, has a high value due to its high productivity and water-use efficiency allowing it to better utilize salt-affected soils (van Straten et al. 2020;2022).

Currently, several studies indicated that the cropland suitability for saline farming on the global and regional scale. A study using Global Agro-Ecological Zones (GAEZ) was conducted to evaluate potato suitability at a global scale based on the crop suitability index (FAO and IIASA 2012). However, neither the land suitability for salt-tolerant crops in moderate saline areas nor the potential impacts of such cultivation on global food productivity have been estimated over the world. Therefore, the estimation of suitable areas for salt-tolerant crops (e.g. potatoes) provides a critical foundation for the utilization of salt-affected soils for saline farming.

In response, we aim to evaluate the suitable area for salt-tolerant potato in salt-affected soils and assess the potential of cultivating salt-tolerant potato in these areas with respect to the UN sustainable development goals for the present and the near future in this study. For this, we generated a global suitability map for salt-tolerant potato taking multiple constraining factors including land cover, soil quality, and essential potato growing conditions into account. Then, the contribution of salt-tolerant potato was estimated at the continent level and country level to highlight the areas that benefit most towards achieving their SDGs. Moreover, in order to evaluate the future contribution of salt-tolerant potato, the changes in potentially suitable areas of salt-tolerant potato cultivation between the current state and different future scenarios were further analyzed. Consequently, our study provides insights into a better utilization of salt-affected soils by cultivating salt-tolerant potato to improve food security and agriculture resilience.

5.2 Methodology

5.2.1 Data collection

5.2.1.1 Land cover map

A global land cover map was obtained from the GlobCover Portal (http://due.esrin.esa.int/page_globcover.php). The land cover map was generated by observations from the MERIS sensor in 300m resolution with the ENVISAT satellite mission. The land cover map included 22 classes which we reclassified as suitable or not suitable for crop cultivation based on the possibilities for agriculture practices (Table S5-1). Four classes were defined as suitable land types for potato cultivation, and given new code=1, water bodies were designated to code = 2, and the rest classes were designated to code = 0 (not suitable) (Table S5-3). The land

cover map was resampled to 0.83 degrees with WGS84 projection using interpolation based on the majority method.

5.2.1.2 Potato distribution map

A potato harvest map in 2010 was created from the MapSPAM data center (https://mapspam.info/index.php/data/). The potato harvest dataset was reclassified to code 1(= distributed area, harvest area > 0 ha) and code 0 (= non-distributed area, harvest area > 0 ha). Afterward, based on the reclassified soil salinity map, we identified the area within 30 km surrounding current potato production lands as the buffer area (code = 2) (Table S5-3). Due to data limitations, this study did not take farmers' willingness for potato cultivation into account. Instead, it is assumed that in areas close to current potato production lands, the likelihood of potato adoption is high as it is presumably part of the local tradition.

5.2.1.3 World map

The world country map was obtained from ArcGIS HUB, named "World Countries (Generalized)" provided by ESRI (https://services.arcgis.com/P3ePLMYs2RVChkJx/arcgis/rest/services/World_Countries_(Generalized)/FeatureServer) for the world shapefile in 2022.

5.2.1.4 Soil quality map

Based on the soil parameters published by the Harmonized World Soil Database (HWSD), six soil attributes for crop cultivation, including nutrient availability (SQ1), nutrient retention capacity (SQ2), rooting conditions (SQ3), oxygen availability to roots (SQ4), toxicities (SQ6), and workability (SQ7) were extracted (https://www.fao.org/soils-portal/soil-survey/soil-maps-and-databases/harmonized-world-soil-database-v12/en/). Each of the six soil qualities was distributed into seven quantitative classes, including no or slight limitations=code 1, moderate limitations = code 2, sever limitations = code 3, very severe limitations = code 4, mainly non-soil = code 5, permafrost area = code 6, water bodies = code 7 (Fischer et al. 2008). All six soil quality maps were reclassified to two new classes, namely suitable (code = 1, no or slight limitations) or not suitable area (code = 0, all other classifications) (Table S5-2). The six soil quality maps were resampled to 0.83 degree with WGS84 projection using the interpolation of the nearest method.

5.2.1.5 Soil salinity map

A soil salinity map was created based on excess salts (SQ5) in HWSD (https://www.fao.org/soils-portal/soil-survey/soil-maps-and-databases/harmonized-world-soil-database-v12/en/). Soil salinity is measured by Electric Conductivity (EC, dS/m) or saturation of the exchange complex with sodium ions (Fischer et al.

2008). Future soil salinity maps were created based on four scenarios at a 0.5° resolution, including Representative Concentration Pathways (RCP) 4.5, RCP 8.5, Shared Socio-economic Pathways 2 (SSP2)-4.5, and SSP5-8.5 for two periods (the 2050s and 2100s) (Hassani et al. 2021). The RCP 4.5 and RCP 8.5 scenarios represent radiative forcing of 4.5 and 8.5 W m−2 in the year 2100 compared to pre-industrial conditions in the ensemble of CMIP5 (Coupled Model Inter-comparison Project Phase 5) data project with eight Global Circulation Models (GCMs) outputs. The SSP 2-4.5 and SSP 5-8.5 scenarios represent the projections forced by RCP 4.5 and RCP 8.5 global forcing pathways for SSP2 and SSP5 to the ensemble of CMIP6 (CMIP Phase 6) with eight Global Circulation Models (GCMs) outputs. Soil salinity maps of the current state and future scenarios were resampled to 0.83 degree with WGS84 projection using the interpolation of the nearest method.

5.2.1.6 Salt-tolerant potato suitability for salinity

Although the salt tolerance of potato is defined as 1.7 dS/m according to FAO investigation, some potato varieties are more tolerant of salinity than expected. Based on several years of field experiments, potato variety '927' showed no yield reduction up to 5.9 dS/m salinity level (de Vos et al. 2016; Oosterbaan 2019; van Straten et al. 2021). Considering that crops would probably already be grown when soil salinity varies between 0 dS/m to 2 dS/m, there is no added value for salt-tolerant potato to be cultivated there. So, the salt-tolerant potato's profitable salinity range was defined between 2.0 dS/m and 6.0 dS/m. Moreover, considering there is no distinction within "severe limitations - 4 dS/m to 8 dS/m-" of soil salinity (SQ5) from FAO, the soil salinity maps were reclassified to three classes, namely code0 = not suitable (< 2 dS/m or > 8 dS/m), code1 = high-suitable salinity (2 dS/m to 4 dS/m), and code2 = moderate-suitable salinity (4 dS/m to 8 dS/m) (Table S3).

5.2.2 The algorithm of soil suitability for salt-tolerant potato

The suitable map was generated based raster calculator in ArcGIS Pro using the following equation:

$$\text{Suitability index} = \text{LSAL} \times \text{LLC} \times \text{LPD} \times \text{LNA} \times \text{LNRC} \times \text{LRC} \times \text{LOAR} \times \text{LTOX} \times \text{LWOR} \quad (1)$$

LSAL = layer of soil salinity, LLC = layer of landcover, LPD = layer of potato distribution, LNA= layer of nutrient availability, LNRC = layer of nutrient retention capacity, LRC = layer of rooting conditions, LOAR = layer of oxygen availability to roots, LTOX = layer of toxicities, LWOR = layer of workability.

Thus, the local suitability area was determined on the occasions of LSALH =1 (high-suitable salinity, 2 dS/m to 4 dS/m) or LSALM = 2 (moderate-suitable salinity, 4 dS/m to 8 dS/m) with other layers' codes equalling 1. Though LPD = 1

suggests the presence of potato cultivation in the pixel, it should be noted that there are also salt-affected parts within the pixel. Meanwhile, the regional suitability area was determined when occurring in the buffer area close to current potato fields (LPD = 2) while LSALH =1(high-suitable salinity, 2 dS/m to 4 dS/m) or LSALM = 2 (moderate-suitable salinity, 4 dS/m to 8 dS/m), and other layers' codes equalling 1. According to different constraints, the suitability map was grouped into 12 categories (Table S5-4). Finally, the local suitability area and the regional suitability area were calculated at the continent level and country level based on zonal statistics in ArcGIS Pro (Figure 5.1).

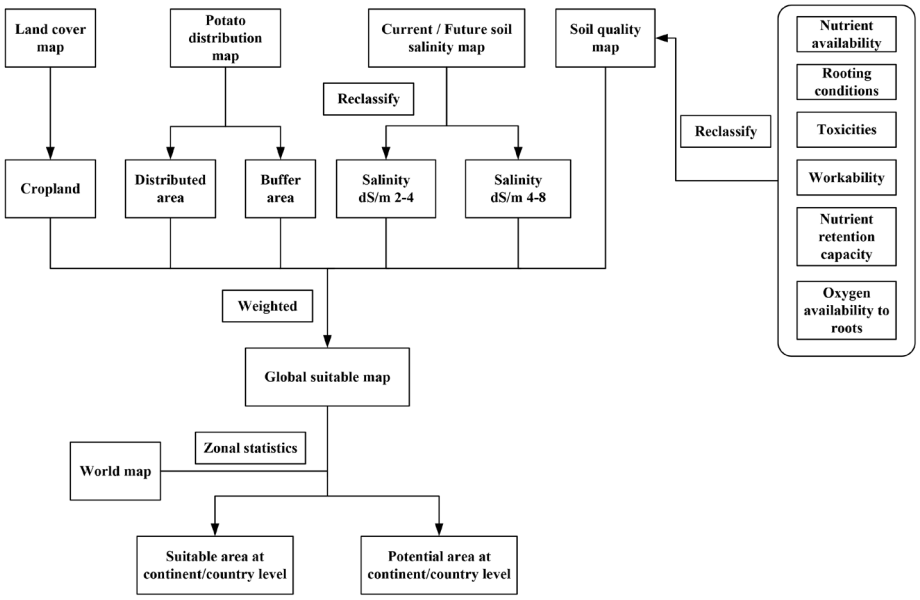

Figure 5.1 Technical workflow of the maps and data framework.

5.2.3 Data analysis

To investigate the contribution of salt-tolerant potato to salt-affected soils at the current state and in future scenarios at the global scale, the availability was calculated based on the following equation:

$$\text{PCTi} = \frac{Area_i}{Area_p + Area_i} \times 100\% \quad (2)$$

Where PCTi is the percentage, Areap is the current potato harvest area (https://mapspam.info/index.php/data/), and Areai is the local /regional suitability area of the salt-tolerant potato.

According to the latest sustainable development goals report in 2022 by the United Nations (UN 2022), it is evident that approximately 1 in 10 people globally are currently experiencing hunger, while almost 1 in 3 people lack consistent access to sufficient food. In response, international frameworks, such as the "Kunming-Montreal Global Biodiversity Framework" (GBF), aim to enhance the resilience of agricultural systems and improve food security (CBD 2022) for the year 2030. Specifically, Target 10 of the GBF, emphasizes that 30% of the world's land requires restoration to ensure sustainable management of the agriculture system. Thus, given the current gap in food production in terms of SDG 2 and GBF, we define 10% and 30% increasement as two thresholds to analyze the contribution of salt-tolerant potato cultivating in salt-affected areas. By focusing on the 10% and 30% increasement in food production, we aim to assess the viability and potential of this salt-tolerant crop in achieving the objectives of both SDG 2 and GBF. To investigate the critical countries where salt-tolerant potato helps to achieve the SDGs and GBF in the near future, the contribution was calculated based on the following equation:

$$\text{PCTt} = \frac{Area_i}{Area_{total}} \times 100\% \quad (3)$$

Where PCTt is the percentage, Areai is the local/regional suitability area of the salt-tolerant potato, and Areatotal is the total harvest area of all crops in 2021 (https://www.fao.org/faostat/en/#data/QCL).

The relative change between the local/regional suitability area under future scenarios and the current state was calculated based on the following equation:

$$\text{PCTr} = \frac{Area_f}{Area_f + Area_i} \times 100\% \quad (4)$$

Where PCTr is the relative change, Areaf is the future local/regional suitability area of the salt-tolerant potato, and Areai is the current local/regional suitability area of the salt-tolerant potato. In order to be consistent with the future soil salinity map' resolution, we compare the relative change at 0.5° (~ 55km) resolution. Given the coarse pixel size of the scenarios, both local and regional suitability were aggregated for future scenarios.

5.3 Results

5.3.1 Global suitability of salt-tolerant potato for salt-affected area

A global suitability map of salt-tolerant potato in salt-affected areas was created, as shown in Figure 5.2a. The highest suitability areas were concentrated around Kazakhstan, the Russian Federation, and northern India while some pieces were

distributed in the western part of Australia. Thus, compared to other continents, Asia showed a larger extent of local suitability area for salt-tolerant cultivation.

In order to compare the contributions of salt-tolerant potato to salt-affected areas among different continents and countries, the availability of productive land for saline potato farming was further analyzed (Figure 5.2b and Figure 5.2c). Here, Oceania showed the highest availability of local and regional suitability areas, allowing to increase potato production by 99.24% and 98.28% in the local suitability area of highly (dS/m 2-4) and moderately (dS/m 4-8) saline conditions, and by 97.50% and 94.35% in regional suitability area of highly (dS/m 2-4), and moderately (dS/m 4-8) saline conditions, respectively. In contrast, Europe has the lowest availability in both locally and regionally suitable areas, with 44.08% more local land available that is highly suitable (dS/m 2-4), and 2.51% that is moderately suitable (dS/m 4-8), and 17.09% more regional land available that is highly suitable (dS/m 2-4), and 0.85% that is moderately suitable (dS/m 4-8).

At the country level, we found the top 15 countries (i.e., Australia, Mozambique, Pakistan, Argentina, Iran, Kazakhstan, India, Russian Federation, Canada, Senegal, United States, Zimbabwe, Chad, Spain, and Syria) that benefit greatly from cultivating salt-tolerant potatoes. Among these countries, Australia has the highest potential, with land area increases of 99.43% in the local suitability area (dS/m 2-4), 98.11% in the local suitability area (dS/m 4-8), 98.67% in the regional suitability area (dS/m 2-4), and 95.69% in the regional suitability area (dS/m 4-8), respectively. Interestingly, Senegal does not have any local suitability area for salt-tolerant potato while Senegal showed notable regional suitability areas at the current state. In addition, Chad had only local suitability areas at two salinity levels without any regional suitability areas.

Overall, Oceania had the highest possibility to improve food production while Europe had the least capacity for increasing production by salt-tolerant potato cultivation in salt-affected soils.

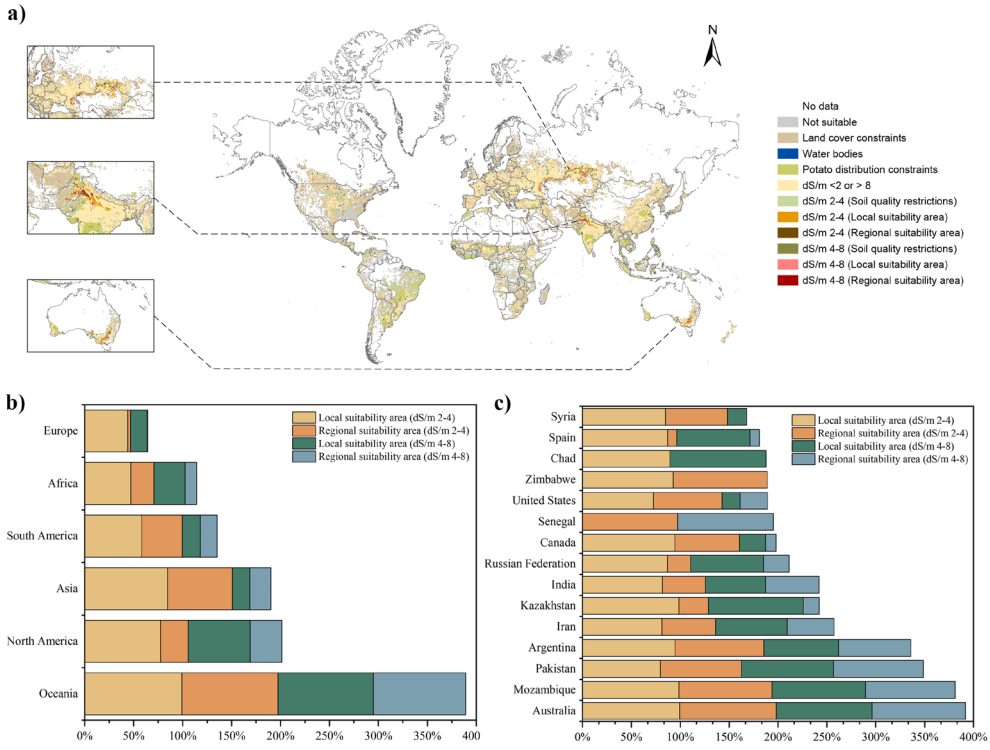

Figure 5.2 a) Global suitability map for the salt-tolerant potato. b) The availability of local and regional suitability areas for salt-tolerant potato at the continent level. c) The availability of local and regional suitability areas for salt-tolerant potato at the country-level.

5.3.2 Contribution of salt-tolerant potato to SDGs

As there were various countries showing promising potential to increase food production by better utilizing salt-affected soils, the contribution of local suitability and regional suitability areas for achieving SDGs was analyzed (Figure 5.3a and Figure 5.3b). When making use of the local suitability area for saline potato farming, Kazakhstan, the Russian Federation, Australia, Iraq, and Lesotho could already achieve their SDG2 targets (of a 10% increase to deal with current food shortages).

In particular, Kazakhstan showed the highest possibility for achieving the SDG2 target as well as the GBF target thanks to its availability of 41.88% local suitability area compared to the current crop harvested area. Based on the sum of the local suitability and regional suitability area, additional countries including New Zealand, Mozambique, and Pakistan can succeed in achieving the SDG2 target while Kazakhstan was still the only country that can accomplish the GBF target.

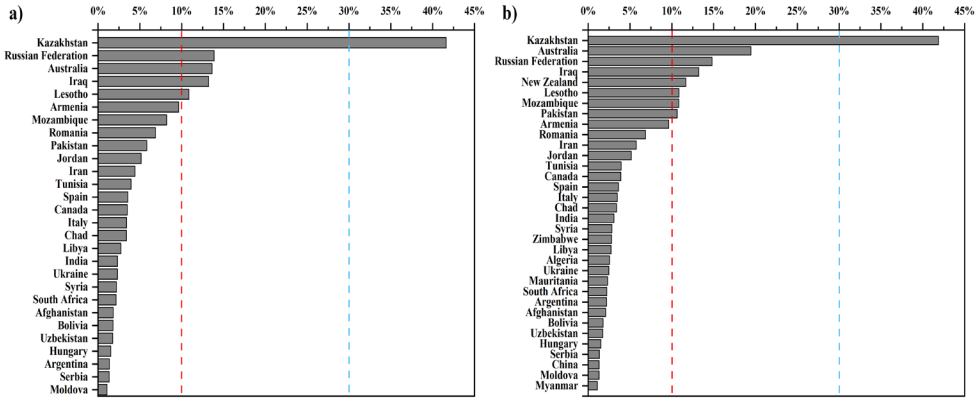

Figure 5.3 The critical countries with a high contribution of salt-tolerant potato in terms of a) the local suitability area, b) local suitability area + regional suitability area. The red line (10%) indicates the SDG2 target in the 2030 agenda. The Blue line (30%) indicates the GBF target for 2030.

5.3.3 Global suitability of salt-tolerant potato in the future

Given that soil salinity was projected to increase with global climate change, the relative change in the local suitability areas for salt-tolerant potato cultivation under future scenarios was evaluated for two different future periods, namely 2050 and 2100 (Figure 5.4). The relative change patterns of the four scenarios were similar, even though they differed in detail. Thus, the relative change under RCP85 was chosen to represent the local suitability area changes in the future while other results are presented in the supplementary information (Figure S5-1). In both periods, more salt-affected soil was detected under different future scenarios (i.e. the area with dS/m 2-4 and dS/m 4-8 will increase more than the area with dS/m>8) and therefore resulted in consistently increased the local suitability area for salt-tolerant potato in comparison to the present. Although the local suitability area in Asia was the largest under the four scenarios, North America was projected to have the average highest increase compared with the current local suitability area. Meanwhile, South America showed overall the lowest increase in the local suitability area in future scenarios both for 2050 and 2100. Moreover, there was a higher increase in the local suitability area in dS/m 2-4 in Asia and Europe while other continents including South America, Oceania, Africa, and North America showed a higher incense in the local suitability area in dS/m 4-8 in 2050 as well as 2100.

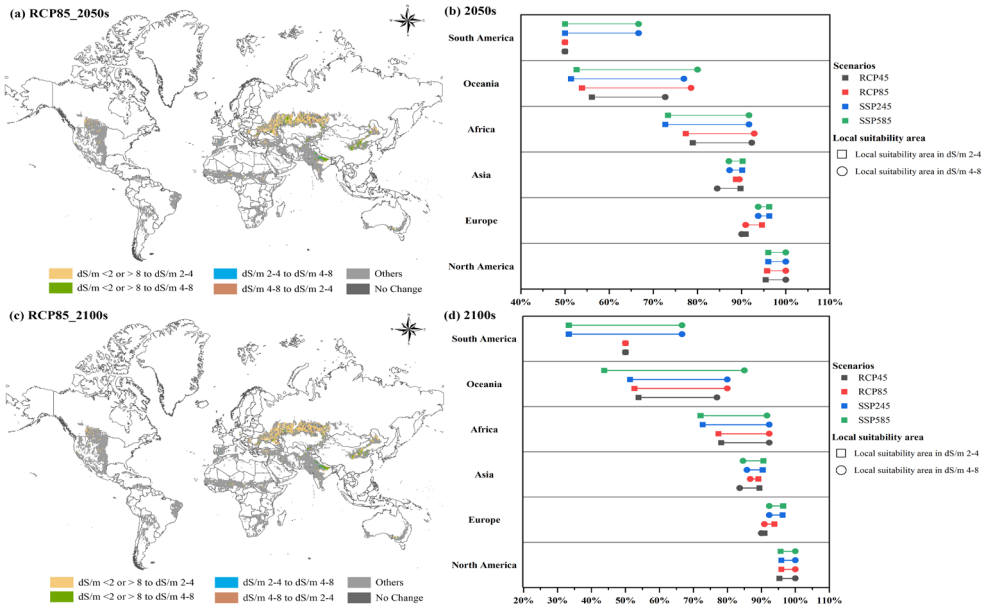

Figure 5.4 (a) Relative change in suitability for saline farming under the RCP85 scenario in the 2050s. (b) The increase in the local suitability area for salt-tolerant potato in the 2050s under different scenarios at the continent level. (c) Relative change in suitability in the 2100s under the RCP85 scenario. (d) The increase in the local suitability area for salt-tolerant potato in 2100s under different scenarios at the continent level.

5.3.4 Contributions of salt-tolerant potato to SDGs in the future

As all continents showed an increase in the local suitability area for salt-tolerant potato, the contribution of these increases for the sustainability targets was analyzed (Figure 5.5). The contributions varied slightly for the different future scenarios. In general, the contributions were higher for most countries under the SSP245 and SSP585 scenarios, compared to the RCP45 and RCP85 scenarios. There were 20 countries with an average increase of over 10% (i.e. achieving SDG-2) under different scenarios in the 2050s and 2100s around the world. Kazakhstan, Russian Federation, Ukraine, Hungry, and Romania were projected to be the top 5 countries with an average high increase of more than 30% both in the 2050s and 2100s. These increases indicate that these countries achieve their GBF target as well. There was even an increase of over 100% for Kazakhstan and the Russian Federation under all scenarios in the 2050s and 2100s. Therefore, Kazakhstan, the Russian Federation, Ukraine, Hungry, and Romania were critical countries to improve food production and achieve sustainable agriculture system by cultivating salt-tolerant potato in salt-affected soil in the future. Moreover, Kazakhstan and the Russian Federation even showed significant potential to secure sustainable food production with over 100% increasement by extending salt-tolerant potato cultivation in the salt-affected area across all four scenarios.

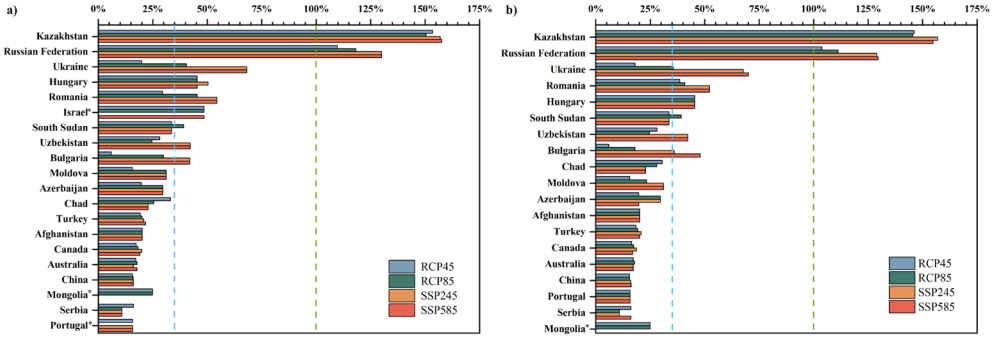

Figure 5.5 The critical countries with high contributions of salt-tolerant potato in a) 2050s, b) 2100s. The blue line (30%) indicates the GBF target for 2030. The green line (100%) indicates doubling the current harvested area. * indicates absent scenarios for that country.

5.4 Discussion

5.4.1 Hotspot areas for salt-tolerant potato cultivation

Among the six continents, Oceania had the highest relative amounts of the local suitability area for saline farming while Asia had the largest (absolute) area for growing salt-tolerant potato on salt-affected soil (Figure 5.2). Salt-affected area has been mapped regionally and globally using various technologies. Asia is commonly identified as the continent with the highest risks of saline soils in the current state and the near future (e.g. Ivushkin et al. 2019; Hassani et al. 2020). Nevertheless, considering the current potato cultivated area, Oceania showed higher potential than Asia, for promoting salt-tolerant potato on salt-affected soil given its suitability. This might be due to the current relatively low potato cultivation in Oceania with only 0.5% market share in global potato production (Bartosz Mickiewicz et al. 2022).

At the country level, Australia, Mozambique, Pakistan, Argentina, Iran, Kazakhstan, India, Russian Federation, Canada, Senegal, United States, Zimbabwe, Chad, Spain, and Syria were critical countries with high capacity for enhancing food production by promoting salt-tolerant potato cultivation in salt-affected soil (Figure 5.2). This is in line with various studies indicating that these countries have a significant salt-induced soil degradation problem (e.g. Hassani et al. 2020) and major economic costs due to salt-induced soil degradation (Qadir et al. 2014; Rengasamy, 2002; Rengasamy, 2006). Moreover, consistent with our results, Russia, Argentina, China, the United States, and Kazakhstan were identified as the most promising countries to develop saline agriculture (ECe > 4 dS/m) based on an analysis taking suitable conditions for agriculture into account (Negacz et al. 2022). Therefore, these hotspot areas with a high potential to better utilize salt-affected soil by cultivating

salt-tolerant potato match with the high-risk areas in terms of soil salinity while their potential strength might differ due to their current potato cultivation status.

Our assessment of the regional suitability contribution of salt-tolerant potato for global food production in salt-affected areas is based on limitations due to salt tolerance only. However, over 70% of the global salt-affected soil area is distributed in arid and semi-arid regions, including but not limited to Pakistan, India, Australia, Egypt, and Central Asia (Li et al. 2016). Thus, most regions that suffer from soil salinity stress are expected to experience the frequently compounded impact of both drought and salinity (Chapter 2 & Chapter 3). In this study, the threshold of salt-tolerant potato was determined under strict conditions without drought. Given that the side effect of drought is excluded in our current analysis, the local suitability area might be overestimated for arid and semi-arid regions unless irrigation water is available. Another critical assumption is that farmers close to or in buffer areas of 30km around current potato production regions are willing to adopt (salt-tolerant) potato cultivation. This assumption may be most likely for developing nations that struggle with food security. In contrast, developed countries may prefer high-value halophytes with high-end markets such as Salicornia, which fetches up to 12 GBP/kg in the United Kingdom (Negacz et al. 2021). Despite these assumptions, we believe that the results of our study are generally robust.

5.4.2 The role of salt-tolerant potato towards SDGs

Cultivating salt-tolerant potato is a promising way to close the current food production gap to achieve SDG-2 targets for various countries. Negacz et al. (2021) conclude that saline agriculture can foster achieving SDGs, especially for SDG2 and SDG8 in saline soils for those regions with high salt-induced problems and that struggle with food security and water scarcity. These countries were estimated to have to increase over 10% of the current food production to satisfy their food requirements with an increasing population. Countries like Kazakhstan (and others) show that they may easily comply with such requirements when embracing salt-tolerant potato (Figure 5.3). According to FAO (2017), the salt-affected irrigation area in Kazakhstan is about 19.6% of the total irrigated area and has grown by almost 44% in 20 years (1997-2017). Although innovative technologies e.g., drainage, allowed to reclaim soil salinity and maintain crop production (FAO 2022a; Tanirbergenov et al. 2020), the cost and efficiency need to be further evaluated. This study suggests and provides an alternative solution for improving sustainable food supply through cultivating salt-tolerant potato in salt-affected soils.

Cultivating salt-tolerant potato does not only benefit food production within the SDG-2 target but also contributes to achieving the GBF target. Salinity has shown negative impacts on plant species variety and below-ground biodiversity, including

the quantity and activity of soil microbes (IPCC 2019; Rahman et al. 2011). In order to control soil salinity and reduce its adverse effects on biodiversity, the replacement by salinity-tolerant species and revegetation where necessary have been adopted as main measures in forest systems (IPCC 2019; Rahman 2020). Likewise, we found that salt-tolerant crop cultivation may be profitable for achieving the GBF target (e.g. target 10) by preventing soil degradation, especially for the regions that suffered from salt-induced stress. In addition to increasing the revenue through greater yields than with conventional crops, the management of saline soils can mitigate economic and climate migration (SDG 8) (Negacz et al. 2021). Moreover, managing soil salinization is essential to accomplishing SDG15 "Life on Land", with particular emphasis on target 15.3 -combat desertification, and restore degraded land and soil- (Singh 2021). Meanwhile, saline farming may reduce the demand for high-quality irrigation water, which facilitates having enough drinking water (SDG6) (Keesstra et al. 2018) for other agricultural applications. Therefore, considering SDGs in close connection to each other shows that salt-tolerant potato is not only a proxy for success in food production (SDG2), but can also make a crucial contribution to other SDGs.

5.4.3 Salt farming contributes to a sustainable future world

In addition, our study also shows how salt-tolerant potato growth may have a notable contribution to sustainable food production with future climate change. It is expected that salt-affected soils are growing at a rate of 1-2 Mhectares per year (Abbas et al. 2013) and the rate was predicted to speed up shortly as a result of climate change (Hassani et al. 2021). Interestingly, despite the increase in salinity, there will be more suitable areas for salt-tolerant potato (Figure 5.4 and Figure S5-1), suggesting that the increase in moderate saline areas is larger than the increase in severely affected areas. This provides additional opportunities for saline farming. The changes observed in the local suitability area, while transitioning from the current state to different future scenarios, exhibited a degree of resemblance. However, a stronger increase in the local suitability area was evident under CMIP6 models (SSP245 and SSP585) compared to CMIP5 models (RCP4.5 and RCP8.5). This difference can be driven by different predictors and GCMs involved in CMIP5 and CMIP6 models (Eyring et al. 2016; Hassani et al. 2021).

Saline farming, which salt-tolerant potato is a part of, contributes to creating a more sustainable world. In this study, salt-tolerant potato showed to be a promising crop to improve food production in salt-affected areas both in the current state and future scenarios and therefore achieving various sustainability targets in different ways (Figure 5.4 and Figure 5.5). Salicornia, as a typical halophyte, was identified as one the most important genera that have high adaptability to saline environments and therefore applied could be in food, pharmacy, bioenergy, and ecology field as a

sustainable crop (Cárdenas-Pérez et al. 2021). However, saline farming is more than growing Salicornia but also has a potential contribution to food security as a whole (e.g. salt-tolerant potato). There have been several studies conducted to test the opportunity of producing food through saline farming based on several salt-tolerant crops including rice, barley, quinoa, beetroot, etc. (de Vos et al. 2021; ICBA 2015; Wang et al. 2013b). Although these studies demonstrated the potential application of divergent salt-tolerant crops for saline farming, they were currently fragmented in space, only covering a limited area. Given the impact of climate change, saline farming would be a promising global solution for salt-affected regions. Thus, our study provides a backbone to get more insight into how saline farming contributes to sustainable development with future climate change threats on a global scale.

5.5 Conclusions

In this study, we assessed the viability and potential of cultivating salt-tolerant potatoes in salt-affected soils, aiming to explore the role of salt-tolerant potato varieties in achieving sustainable development goals in the present and future climate. We found that Oceania showed the greatest potential for enhancing food production through salt-tolerant potato cultivation in salt-affected soils, while Europe demonstrated the lowest capacity for increasing production in this regard under the current state. Under different future scenarios, all continents show an expansion in the areas suitable for salt-tolerant potato cultivation. Moreover, we identified a number of countries that could crucially benefit through the promotion of salt-tolerant potato cultivation in salt-affected soils for enhancing food production. Specifically, Kazakhstan, the Russian Federation, Australia, Iraq, and Lesotho possess the capability to address their food shortage challenges and achieve sustainable development goals by cultivating salt-tolerant potatoes under the current state. Meanwhile, Kazakhstan, the Russian Federation, Ukraine, Hungary, and Romania were crucial countries by growing salt-tolerant potatoes in salt-affected soil for enhancing food production and achieving a sustainable agriculture system in the future. Consequently, our study proposed valuable insights into growing salt-tolerant potato to optimize the utilization of salt-affected soils, and therefore built the foundation for saline farming globally to secure food security and strengthen agricultural resilience.

5.6 Author contributions

Wen Wen: Conceptualization, Methodology, Investigation, Writing--original draft, Writing--review and editing. Joris Timmermans: Methodology, Supervision, Writing--review and editing. Daan Hooimeijer: Conceptualization, Methodology, Investigation. Peter M. van Bodegom: Conceptualization, Methodology, Supervision, Writing--review and editing.

5.7 Supporting information

Table S5-1. Reclassification of land cover classes

Value	Label	Reclassification
11	Post-flooding or irrigated croplands (or aquatic)	Suitable
14	Rainfed croplands	Suitable
20	Mosaic cropland (50-70%) / vegetation (grassland/shrubland/forest) (20-50%)	Suitable
30	Mosaic vegetation (grassland/shrubland/forest) (50-70%) / cropland (20-50%)	Suitable
40	Closed to open (>15%) broadleaved evergreen or semi-deciduous forest (>5m)	Not suitable
50	Closed (>40%) broadleaved deciduous forest (>5m)	Not suitable
60	Open (15-40%) broadleaved deciduous forest/woodland (>5m)	Not suitable
70	Closed (>40%) needleleaved evergreen forest (>5m)	Not suitable
90	Open (15-40%) needleleaved deciduous or evergreen forest (>5m)	Not suitable
100	Closed to open (>15%) mixed broadleaved and needleleaved forest (>5m)	Not suitable
110	Mosaic forest or shrubland (50-70%) / grassland (20-50%)	Not suitable
120	Mosaic grassland (50-70%) / forest or shrubland (20-50%)	Not suitable
130	Closed to open (>15%) (broadleaved or needleleaved, evergreen or deciduous) shrubland (<5m)	Not suitable
140	Closed to open (>15%) herbaceous vegetation (grassland, savannas or lichens/mosses)	Not suitable
150	Sparse (<15%) vegetation	Not suitable
160	Closed to open (>15%) broadleaved forest regularly flooded (semi-permanently or temporarily) - Fresh or brackish water	Not suitable
170	Closed (>40%) broadleaved forest or shrubland permanently flooded - Saline or brackish water	Not suitable
180	Closed to open (>15%) grassland or woody vegetation on regularly flooded or waterlogged soil - Fresh, brackish or saline water	Not suitable
190	Artificial surfaces and associated areas (Urban areas >50%)	Not suitable
200	Bare areas	Not suitable
210	Water bodies	Not suitable
220	Permanent snow and ice	Not suitable
230	No data (burnt areas, clouds)	Not suitable

Table S5-2. Classification of soil qualities. Only classes 1 to class 4 correspond to an evaluation of soil constraints for plant growth.

Qualitative classes	Salinity (dS/m)	Growth potential (%)	Organic carbon (%)	Impermeable layer (cm)	Cation exchange capacity (cmol/kg)	Obstacle to roots (cm)	Toxicities (pH)	$CaCO_3$ content (%)
1. No or slight limitations	< 2	80-100	> 2.0	0-150	> 40	60-80	5.5-7.2	< 2
2. Moderate limitations	2-4	60-80	1.2-2.0	80-150	20-40	40-60	7.2-8.5	2-5
3. Sever limitations	4-8	40-60	0.6-1.2	40-80	10-20	20-40	4.5-5.5	5-25
4. Very severe limitations	8-16	< 40	0.2-0.6	< 40	4-10	0-80	> 8.5	25-40
5. Mainly non-soil	> 16	0	< 0.2	0	< 4	0-20	< 4.5	> 40
6. Permafrost area	--	--	--	--	--	--	--	--
7. Water bodies	--	--	--	--	--	--	--	--

Table S5-3. Reclassification of constraint variables.

Data Layer	Raw value	Suitable y(1)/n(0)
Land cover	40-230	0
	11, 14, 20, 30	1
	210	2
Potato distribution	Buffer_30km	2
	1	1
	0	0
Excess salt (SQ5)	1, 4-7	0
	2 (2-4 dS/m)	1
	3 (4-8 dS/m)	2
Nutrient availability (SQ1)	2-7	0
	1	1
Nutrient retention capacity (SQ2)	2-7	0
	1	1
Rooting conditions (SQ3)	2-7	0
	1	1
Oxygen availability to roots (SQ4)	2-7	0
	1	1
Toxicities (SQ6)	2-7	0
	1	1
Workability (SQ7)	2-7	0
	1	1

Table S5-4. Labels of suitability index based on reclassifications of constraints.

Label	Necessary conditions
No data	$L_{all} = 0$
Not suitable	$L_x = 0$
Land cover constraints	$L_{LC} = 0$
Water bodies	$L_{LC} = 2$
Potato distribution constraints	$L_{LC} = 1$ and $L_{PD} = 0$
dS/m <2 or > 8	$L_{LC} = 1$, $L_{PD} = 1$, and $L_{SAL} = 0$
dS/m 2-4 (soil quality restrictions)	$L_{LC} = 1$, $L_{PD} = 1$, $L_{SALH} = 1$, and $L_x = 0$
Local area with high suitability (dS/m 2-4)	$L_{LC} = 1$, $L_{PD} = 1$, $L_{SALH} = 1$, $L_{NA} = 1$, $L_{NRC} = 1$, $L_{RC} = 1$, $L_{OAR} = 1$, $L_{TOX} = 1$, $L_{WOR} = 1$
Regional area with high suitability (dS/m 2-4)	$L_{LC} = 1$, $L_{PD} = 2$, $L_{SALH} = 1$, $L_{NA} = 1$, $L_{NRC} = 1$, $L_{RC} = 1$, $L_{OAR} = 1$, $L_{TOX} = 1$, $L_{WOR} = 1$
dS/m 4-8 (soil quality restrictions)	$L_{LC} = 1$, $L_{PD} = 1$, $L_{SALM} = 2$, and $L_x = 0$
Local area with moderate suitability (dS/m 4-8)	$L_{LC} = 1$, $L_{PD} = 1$, $L_{SALM} = 2$, $L_{NA} = 1$, $L_{NRC} = 1$, $L_{RC} = 1$, $L_{OAR} = 1$, $L_{TOX} = 1$, $L_{WOR} = 1$
Regional area with moderate suitability (dS/m 4-8)	$L_{LC} = 1$, $L_{PD} = 2$, $L_{SALM} = 2$, $L_{NA} = 1$, $L_{NRC} = 1$, $L_{RC} = 1$, $L_{OAR} = 1$, $L_{TOX} = 1$, $L_{WOR} = 1$

L_{SAL} = layer of soil salinity, L_{LC} = layer of landcover, L_{PD} = layer of potato distribution, L_{NA} = layer of nutrient availability, L_{NRC} = layer of nutrient retention capacity, L_{RC} = layer of rooting conditions, L_{OAR} = layer of oxygen availability to roots, L_{TOX} = layer of toxicities, L_{WOR} = layer of workability, L_x = any layers, L_{all} = all layers

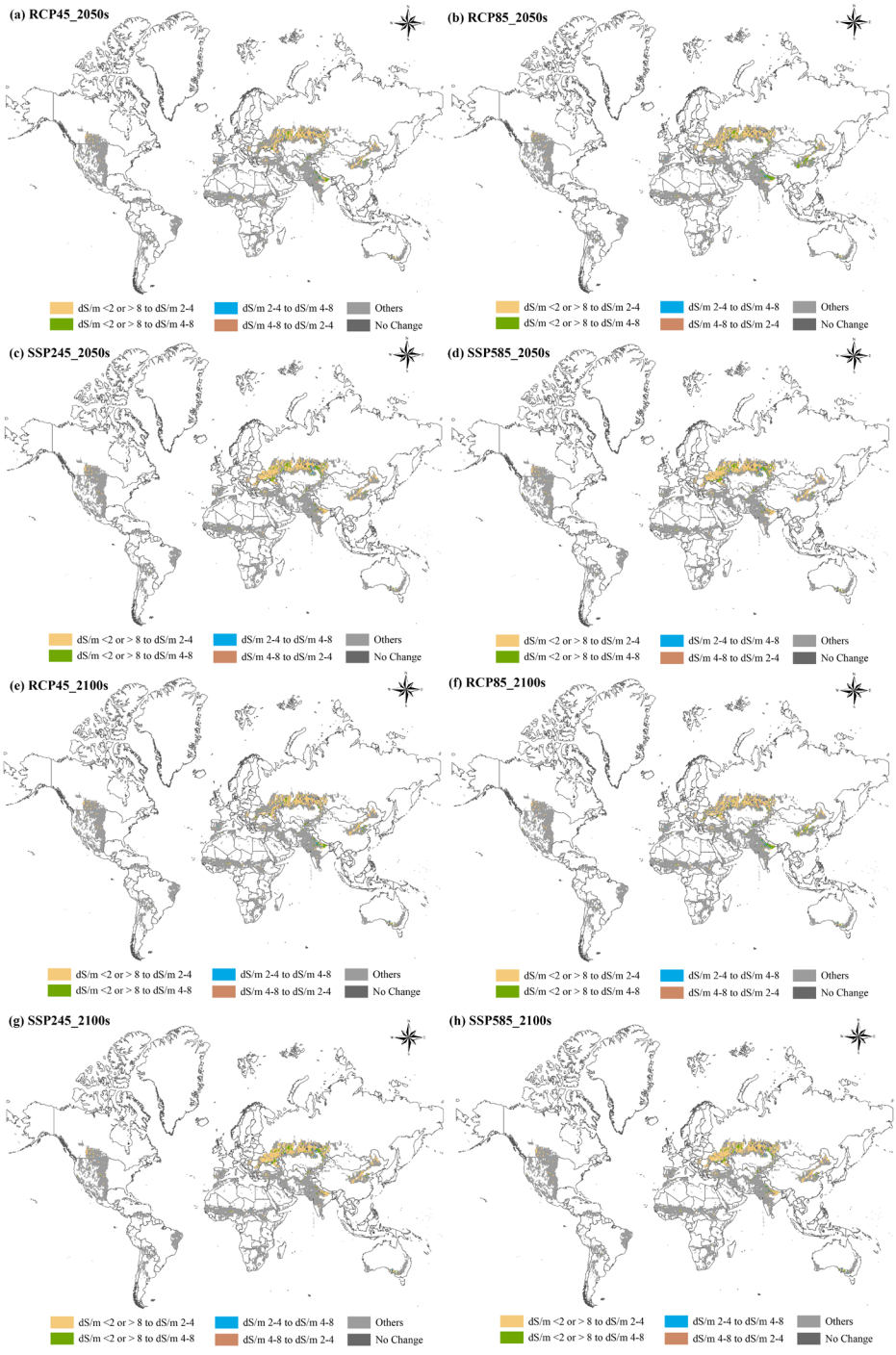

Figure S5-1. a) - d) maps of relative change in suitability in 2050 under different scenarios. e) - h) Relative change in suitability in 2100 under different scenarios.

Chapter 6

General discussion

Food security is projected to be challenged by the increasing co-occurrence of stresses with global climate change. Of these stresses drought and salinity are considered to be the main constraints for food production by their impacts on crop growth. Large-scale monitoring and quantification of the individual and combined impacts of drought and salinity stress on crop growth give rise to significant challenges related to spatial-temporal variability, data integration, crop variability, etc. Remote sensing offers potential solutions through detailed and timely detection of crop health. In this thesis, I evaluated the impact of drought and salinity stress on agriculture and sustainable development goals using remote sensing technology. Specifically, I assessed (i) which remote sensing features are available to monitor crops under drought and salinity stress, (ii) how drought and salinity stress on crop traits can be evaluated using remote sensing observations, (iii) what the tolerance of diverse crops in respect to drought and salinity stress was in real-life agriculture settings, and (iv) where cultivating salt-tolerant potato could be introduced to enhance global food production and secure. This chapter aims to synthesize the main findings of these research questions and provide a comprehensive discussion on the limitations and prospects for future studies, and implications to achieve sustainable development goals. Our insights can be used to enhance crop management and hence food security.

To answer the research question, I first reviewed the current capacity of remote sensing to detect the impacts of drought and salinity stress on crops based on the use of vegetation indices (VIs) and plant traits (Chapter 2). Next, a novel approach that utilized multiple plant traits derived from remote sensing data was used to estimate the effects of drought, salinity, and their combination on crop growth in the Netherlands (Chapter 3). Based on the approach developed in Chapter 3, the tolerance of eight different crops to drought, salinity, and their combined stress was assessed across the entire U.S. continent throughout the crop growing season from sentinel-2 observations (Chapter 4). Finally, to answer where the biggest opportunity exists (with respect to achieving Sustainable Development Goal 2), I quantified the potential of enhancing food production by cultivating salt-tolerant potato species in salt-affected areas under present and future scenarios (Chapter 5).

The findings of this thesis highlight the potential of remote sensing-derived traits for evaluating crop growth under stress conditions (explored in more detail in section 6.1). Through a systematic review, positive correlations were identified between specific plant traits and stress response mechanisms, indicating the potential of plant traits as indicators (Chapter 2). However, the spectral signals related to drought and salinity stress exhibited inconsistencies across various crop traits due to variations in growth stage, soil properties, stress severity and duration, and environmental conditions. In response, a novel workflow that integrates multiple traits derived from remote sensing was developed to evaluate the real-life

impacts of drought, salinity, and their combined influence on crop growth in the Netherlands (Chapter 3). By employing a pair-wise method within this workflow, I quantified the stress impacts over a select range of crops and growth conditions. Afterwards, I upscaled this workflow to cover a wider range of crops and spatial conditions and applied it across the entire U.S. continent throughout the crop growing season in 2021 (Chapter 4). In this analysis, I found stress impacts to be significantly dependent on the specific moment in the growing season, with crops are generally more sensitive to the combined effects of salinity and drought stress compared to the singular stress (Chapter 3 & Chapter 4). Nevertheless, the observed stress impacts showed significant variations over time and among different crop species. Notably, most crops experienced an initial reduction in primary production capacity through a decrease in Leaf Area Index (LAI) before experiencing reductions in water or chlorophyll contents (Chapter 4). Finally, we assessed how the above-mentioned information could be used in combating food insecurity by identifying areas where salt-tolerant crops (i.e., potato) could be cultivated. Out of six continents, Oceania was found to exhibit the greatest potential for enhancing food production through better utilization of the salt-affected area (Chapter 5). In addition, Kazakhstan, the Russian Federation, Australia, Iraq, and Lesotho also show a potential to address their food shortage challenges and achieve sustainable development goals by cultivating salt-tolerant potatoes. Furthermore, under various future scenarios, the local suitability area for salt-tolerant potato consistently expanded, with Kazakhstan, the Russian Federation, Ukraine, Hungary, and Romania emerging as crucial countries to enhance food production and accomplish SDG targets. In combination, the thesis shows from review to application how remote sensing techniques may be applied to detect stress responses and mitigate the impacts of those stresses on global crop production.

Despite proving the potential to detect stress responses of crops with functional traits by remote sensing, I found that the effectiveness of such monitoring varied across different plant species and growth stages (Chapter 2, Chapter 3, and Chapter 4). Consequently, there are several challenges left open that need to be addressed in future studies. One such challenge is the need for a better understanding of representative traits that can accurately reflect specific stress conditions at specific moments during the growing season (Chapter 2, Chapter 3, and Chapter 4). This challenge will be explained in more detail in section 6.1. Moreover, current remote sensing for agricultural applications still faces challenges regarding spatial-temporal resolutions and integration of multi-platform data. These limitations and the prospects to deal with them will be treated in section 6.2. Remote sensing is promising to effectively monitor the achievement of SDGs and ensure food security on a global scale, involving different stakeholders and policymakers (Chapter 5). My suggestion to implement these societal implications is treated in

section 6.3. Overall, this comprehensive investigation explored various aspects of remote sensing-based monitoring of crop responses to stress, offering valuable insights into the viability of using remote sensing for improving food security and addressing sustainable development goals.

6.1 Open challenges regarding the Trait-based evaluation method

Plant functional traits are associated with various adaptation pathways to the environment, as they indicate a set of plant features that represent strategies for a variety of stress conditions (Andrew et al. 2022). Thus, plant functional traits allow us to quantify the extent of the adaptation to various environmental pressures (i.e., drought and salinity stress). Connecting vegetation function (including primary production) with environmental stress by trait-based evaluation methods has shown to provide significant promises (Zakharova et al. 2019). Functional traits are intimately linked to stress tolerance, carbon storage, water regulation, and climate regulation (Lavorel and Grigulis 2012). Thus, functional trait-based research plays a pivotal role in comprehending the structure and function of agroecosystems including crop productivity, agroecosystem dynamics, non-crop biodiversity, other biogeochemical cycles, and crop vulnerability to climate change (Martin et al. 2015). However, large-scale research on functional traits across a wide variety of crops remains quite limited. For instance, leaf economics trait information is unavailable for over 70% of the important agricultural species in the TRY database (Martin et al. 2015).

Even though trait-based methods show promising potential to evaluate stress impacts on plants, it remains challenging to identify a proper selection of appropriate traits that detect specific signals for different stresses (Griffin-Nolan et al. 2018). Specifically, diverse stresses may manifest similar symptoms in plants (He et al. 2020), while different plant strategies (to resist these stresses) might lead to different expressions of functional traits (even for the same stress). According to Chaves et al. (2009), most plant species tend to lower transpiration and avoid more severe stress by decreasing their leaf area both for drought and salinity stress. Functional traits such as specific leaf area (SLA), leaf dry matter content (LDMC), leaf area (LA), turgor loss point (TLP), relative water content (RWC), leaf chlorophyll content (Cab) are essential for plant drought tolerance (Kramp et al. 2022; Mwamahonje et al. 2021). Meanwhile, most of these traits are used to evaluate salinity stress impacts as well (Zhou et al. 2021). In addition, it was reported that any abiotic stress decreases leaf size (El-Moneim et al. 2020). Likewise, there is no significant difference in the expression of traits for drought vs. salinity in our study (Chapter 2, Chapter 3, and Chapter 4).

Salinity (in the first growing phase) affects plants in a comparable way as droughts, namely through water stress/osmotic stress. Therefore, additional traits are required

to make these distinctions. For example, salinity also has clear impacts with regard to toxic stress/ion stress (Munns 2002). Thus, the traits related to toxic stress tolerance may provide a breakthrough to distinguish salinity stress from drought stress. In melon plants, the levels of phenylalanine, histidine, proline, and the Na^+/K^+ ratio emerge as key distinguishing traits for salinity tolerance (Chevilly et al. 2021). Moreover, the Na^+/K^+ ratio is one of the most important traits in controlling salinity tolerance in rice (Kanawapee et al. 2012) while Na^+/K^+ was not significantly affected in wheat (Garcia et al. 1997; Pires et al. 2015). In addition, physiological traits related to chlorophyll fluorescence might be another option to distinguish drought and salinity stress impacts, as these stresses are found to have varying effects on photosynthetic performance (Lazarevic et al. 2021). Meanwhile, Lazarevic et al. (2021) pointed out that the plant growth stage during which the stress impacts the plant is another factor that needs to be taken into account when choosing a set of traits to differentiate plant tolerance mechanisms between drought and salinity stress. Likewise, the impact of drought and salinity on crop traits is found to be highly dependent on the moment in the growing season (Chapter 3 & Chapter 4). Moreover, although LAI, FAPAR, and FVC exhibit comparable patterns in response to drought and salinity stress, Cab and Cw appear to have distinct patterns from other traits (Chapter 3 & Chapter 4). Thus, distinct traits representing different stress strategies are varied in species, between stress strengths as well as between growth stages.

Given trait multifunctionality, traits may not line up with environmental gradients as expected when only taking the tolerance of individual stress into account (Sack and Buckley 2020). Indeed, plant stresses frequently occur in combination, and thus a functional trait confers tolerances to multiple stresses simultaneously. In general, co-occurrence stresses (e.g. salinity and drought stress) exert a more pronounced negative impact on plant growth (Chapter 3 & Chapter 4), photosynthesis, ionic balance, and oxidative balance, compared to the effects of either stress alone (Angon et al. 2022). However, it is important to note that in certain cases, salinity may have a more pronounced negative effect than drought stress, while in other instances, drought stress may outweigh the impact of salinity (Angon et al. 2022; Ibrahim et al. 2019; Zhou et al. 2021). In addition, Sack and Buckley (2020) indicated that the relative importance of multifunctional traits is highly contingent on the environmental context such as stress levels and their interactions under the co-occurrence stress environment. LAI, FAPAR, and FVC exhibited the most significant reductions under severe drought stress conditions for both maize and potato crops, underscoring their heightened sensitivity to drought compared to salinity (Chapter 3). Moreover, the interaction effects of stress (e.g., drought and salinity) and environmental factors (e.g., soil type and climate zone) were significant in many cases (Chapter 4), indicating that the severity of stress and its impact on crops were affected by diverse environmental conditions. Therefore,

when assessing plant tolerance to co-occurrence stress using a traits-based approach, it is important to consider a number of variables, including the plant species, the severity and duration of each stress, and the specific physiological responses of the plant to the combined stress conditions.

Network theory presents an effective approach toward resolving the relationships among multiple plant traits and their significance (He et al. 2020). The concept of plant traits networks (PTNs) provides a multidimensional framework for comprehensively evaluating the responses of plants across diverse lineages, life forms, ontogenetic stages, and environmental conditions (He et al. 2020). In plant trait networks, certain economic traits were found more important than other traits. Particularly in dryland ecosystems, where nutrients and water are scarce, plants prioritize those links between their economic traits that increase the effectiveness of storing carbon and nitrogen and thus enhance their resilience against shortages and their competitiveness (Wang et al. 2023b; Wilcox et al. 2021). However, this is not valid for all conditions. For example, herbaceous plants emphasize the connections between structural traits to increase leaf structural resilience and to lessen physical damage from drought, whereas woody plants favor connections between economic traits to resist drought stress (Wang et al. 2023b). Although various studies have analyzed the key traits for plant functioning based on PTNs, the application to agriculture systems is still unclear and there is no comprehensive framework established to quantify the relative significance of each trait function under co-occurrence stress environmental circumstances. Even so, our results on multiple crops suggest that these herbaceous crops exhibit a prioritization of reducing their structural traits including LAI, FAPAR, and FVC, before undergoing reductions in water or chlorophyll contents (Chapter 4). This demonstrates leaf water content and leaf chlorophyll content are considered to be key traits for agricultural crops to maintain crop health and resilience to drought and salinity stress at an early stage.

Overall, the trait-based method has proven to be a promising way to evaluate plant tolerances to diverse stresses. Hence there is a great opportunity for creating a system that can monitor crops in real-time across a wide variety of crops at various scales (local, regional, national, and global). This system requires however a spatial and temporal resolution that is presently not offered by traditional monitoring platforms. To address this need, the integration of remote sensing technologies, such as satellites, offers a compelling solution to extend the implementation of trait-based methods in agriculture. By leveraging remote sensing capabilities, timely and comprehensive monitoring of agricultural systems can be achieved, enabling a more effective and efficient evaluation of crop responses to stresses on a broader spatial and temporal scale.

6.2 Prospects of remote sensing for agricultural applications

Remote sensing has become increasingly relevant in the field of sustainable agriculture and emerged to improve food security in developing countries with its global coverage characteristics (Berger et al. 2022). With enhanced spatial, temporal, and spectral capacities based on various launched platforms and sensors, remote sensing studies, focused on agricultural applications, have increased significantly (Weiss et al. 2020). Although remote sensing technologies show significant advantages compared to traditional methods, there are constraints that remain to limit their application in agriculture.

High-resolution maps for stresses and crops are still not fully available at a global e xtent. While high-resolution stress maps (e.g. drought and salinity) have been gener ated using remote sensing observations, they focus mostly on regional or continent al extents. For example, Aadhar and Mishra (2017) created a drought map for Sout h Asia based on the Standardized precipitation index (SPI) and Standardized Precip itation Evapotranspiration Index (SPEI). AghaKouchak et al. (2015) reviewed the p rogress of monitoring drought using satellite remote sensing observations, highlight ing the limitations including data continuity, unquantified uncertainty, sensor chang es, community acceptability, and data maintenance in drought monitoring by curren t satellite missions for the application at different regions. And while specific count ries have developed their local-scale programs to track crop systems, such as the N etherlands (Key Register of Parcels (BRP), https://www.pdok.nl/introductie/-/article/ basisregistratie-gewaspercelen-brp-) (as used in Chapter 3) and the United States (Cropland Data Layer program (CDL), https://www.nass.usda.gov/Research_and_ Science/Cropland/Release/index.php) (as used in Chapter 4), similar maps at differ ent locations are not widely accessible. This significantly limits the monitoring of c rop performance under salinity and drought stress, and the quantification of food se curity in developing countries. To address this issue, high-resolution crop maps nee d to be created. Compared with other maps (e.g., stress map, landcover map, etc.), crop mapping asks for higher spatial resolution (e.g., 10m ~ 30m) considering the d iversity of crop types and fragmented cultivation plots. Although there is a program Global Agricultural Monitoring Initiative-Best Available Crop Specific Masks (GE OGLAM-BACS) that generates crop type map at 0.05 degree on a global scale, it o nly contains four main crop types (wheat, maize, rice, and soybeans) and have certa in limitations (Becker-Reshef et al. 2023). Additionally, differences in phenology, c ultivation practices, cloud cover, and weather across different regions pose challeng es to the quality and quantity of satellite images for crop mapping (Wu et al. 2023). As new-generation satellite spectrometers (e.g. HysIRI spectrometer) characterized by high spatial resolution (8-30 m) and spectral resolution (~10 nm) are being laun ched, future applications in precision farming and environmental monitoring are pr omising to be enhanced in the coming years (Lassalle 2021). With such crop maps,

coupled with (remote sensing derived) maps of environmental stresses, approaches such as those developed in this thesis may be further refined and globally applied.

Remote sensed traits show potential for evaluating crop responses to stress. Various trait retrieval methods have been investigated to detect plant responses to stress by optical remote sensing observations (Verrelst et al. 2015). Most approaches are developed based on parametric regressions, specifically employing spectral bands, vegetation indices (VIs), and spectral ratios to establish correlations with functional traits associated with plant stress (Berger et al. 2022). However, the number of traits that can be directly retrieved from remote sensing imagery is limited. For instance, osmotic traits were found to be promising to detect drought and salinity stress, but so far neither parametric approaches nor physically based methods (i.e., radiative transfer models (RTMs)) have been able to retrieve these traits with remote sensing. Instead, in our approach we relied on traits that could be quantified by RTMs. PROSAIL is a well-known RTM that integrates a leaf optical properties model (PROSPECT) (Jacquemoud and Baret 1990) and a canopy bidirectional reflectance model (SAIL) (Verhoef 1984). PROSAIL has been widely to estimate canopy biophysical, and structural traits in agriculture at different scales (Chaabouni et al. 2021). For future research, it would be interesting to evaluate whether additional traits such as osmotic traits may be derived from RTMs. Additionally, it becomes possible to retrieve biochemical traits based on a modified RTM. For instance, Zhu et al. (2014) developed a modified PROSPECT model integrating the specific absorption coefficient of the copper ion to retrieve copper ion traits. Therefore, by integrating RTMs with local experimental results of indirect traits' optical properties, it is projected to be more effective in retrieving stress-related traits. With the launch of multi-sensor satellites (e.g. Sentinel-2) with a short revisit period, the spatial-temporal resolution has been enhanced. This thesis evaluates crop response to stress only based on satellite remote sensing (Chapter 3 & Chapter 4). Apart from satellite remote sensing, other remote sensing technologies including microwave data and unmanned aerial vehicles (UAVs) play a crucial role in providing valuable insights for agricultural applications. Active microwave radiometers have predominantly been employed for the characterization of various biophysical traits, water content, leaf area index (LAI), vegetation height, aboveground biomass, crop type mapping, and monitoring crop growth (Vereecken et al. 2012). Meanwhile, UAV-based remote sensing (UAV-RS) shows high potential to complement and validate satellite remote sensing thanks to its high spatial resolution and high frequency, and economical friendly (Wang et al. 2023a). Zhou et al. (2020) quantified soybean traits under drought stress based on UAV imagery to identify drought tolerance genotypes.

Another new development involves the integration of remote sensing data from multiple platforms and sensors. Through this integration, a more comprehensive

and detailed understanding of the intricate interaction of stress combinations and affected crop traits can be obtained (Berger et al. 2022). The synergistic utilization of optical and microwave data enables the detection of more accurate and additional land surface properties and traits. Also, microwave observations can be interpreted and corrected using optical data and the resulting parameters (Vereecken et al. 2012). Numerous approaches have been proposed to integrate remote sensing data from multiple platforms, encompassing microwave data (both active and passive), as well as optical data spanning from visible, near-infrared, and thermal spectra (Vereecken et al. 2012). However, there are several factors that need to be considered for this integrated framework application. Data collected from various sensors for the same location often exhibit redundancy. This redundancy arises from the distinct characteristics and physical diffusion mechanisms inherent in different sensors (Le Hegarat-Mascle et al. 2000; Li et al. 2021). As a result, multiple sensors may capture similar or overlapping information, leading to a significant amount of time consumption to fuse remote sensing data. This time-consuming process can potentially limit the efficiency of data analysis and interpretation. Moreover, the integration framework involves data from various platforms/sensors, each with distinct spatial and spectral resolutions, acquisition frequencies, and calibration procedures. This heterogeneity necessitates meticulous data preprocessing and calibration to ensure compatibility and consistency during integration (Mura et al. 2015).

In addition, by combining remote sensing data with artificial intelligence techniques like Machine Learning (ML), it is possible to identify and predict crop trait changes with stress. Lassalle (2021) reviewed six categories of machine learning algorithms including Partial Least Square Regression (PLSR), Random Forest (RF), Linear or Quadratic Discriminant Analysis (LDA/QDA), Support Vector Machines (SVM), Neural Networks (NNs), and Elastic net (ENET) regression. These algorithms were utilized to monitor plant stress using hyperspectral remote sensing. Ion traits including Na^{+}, Cl^{-}, K^{+}, and Ca^{2+} concertation were determined for wheat with salinity stress by employing PLSR on canopy reflectance data (El-Hendawy et al. 2019b). ML has demonstrated a strong performance in detecting crop stress signals at an early stage using hyperspectral data (Zarco-Tejada et al. 2018). These algorithms have also shown their relevance in distinguishing between different stresses that have similar effects on plant reflectance (Lassalle et al. 2019). Furthermore, certain machine learning algorithms are capable of handling nonlinear relationships between stress intensity and the spectral response of plants, thus providing new opportunities for quantitative monitoring (Lassalle 2021). Finally, the integration of ML and RTM has shown promise in accurately and rapidly mapping crop traits across extensively cultivated regions (Danner et al. 2021). This way, this combination of techniques highlights

the potential to quantity and monitor stress-related crop traits at the global scale (Berger et al. 2022; Verrelst et al. 2019).

Finally, combining crop growth models with remote sensed traits enables timely and accurately predict stress impact on food security in crop production. Crop growth models simulate the relationship between crop physiological processes and the environment, aiming to assess the potential impacts of climate change on crop growth and yield in different regions (Kasampalis et al. 2018). Gaining early insights into the impacts of extreme weather events on crops can assist farmers and decision-makers in minimizing risks and enhancing food security. However, current crop growth models have certain limitations. They lack spatial scale information and suffer from the absence or inaccuracy of relevant data such as soil conditions and weather parameters (Kasampalis et al. 2018; Palosuo et al. 2011; Wallach et al. 2006). To enhance yield predictions by crop models, remote sensing technology can provide the missing spatial information required by crop growth models. Variables in the crop growth model can be replaced or adjusted using remote sensing data through data assimilation (Maas 1988). A review conducted by Jin et al. (2018) highlighted the capability of assimilating remote sensing data to enhance the accuracy of predictions and estimations in crop growth models, ultimately leading to improved understanding and management of agricultural systems. Hence, more accurate predictions of crop growth and yield may in the future be achieved by integrating remote sensing data with crop models, thereby improving agricultural production and ensuring food security.

6.3 Implications to sustainability goals

Remote sensing can significantly contribute to achieving the Sustainable Development Goals (SDGs) by providing data to track the progress of key indicators and assess policy efficiency. Specifically, three major gaps in SDGs indicators are expected to be filled by integrating remote sensing data, including environmental indicators, multi-resolution spatial indicators, and indicators coupling environmental and societal or economic data (Cochran et al. 2020; Griggs et al. 2014; Scott and Rajabifard 2017). With respect to securing SDG 2 (zero hunger), remote sensing earth observations can strengthen the monitoring of food security by providing crop growth models with timely input variables to better predict crop production. Already several international monitoring systems, such as the GEOGLAM, have been developed to track crop growth and evaluate the progress toward achieving SDG 2(Singh Parihar et al. 2012). The GEOGLAM Crop Monitor provides monthly assessments of crop conditions for wheat, maize, rice, and soybeans in 49 countries (Anderson et al. 2017), and thereby creates the ability to use its products within SDG indicators (e.g. target 2.C) (Anderson et al. 2017; Whitcraft et al. 2019). In addition, the Crop Monitor for Early Warning

(CM4EM) within GEOGLAM monitors the risk of food insecurity in over 80 countries, and serves as an early warning tool for agriculture monitoring, enhancing resilience to climate-related extreme events (Becker-Reshef et al. 2020). Through this, CM4EM is possible to detect crop growth in a drought-stressed environment and provide timely updates on food production challenges (Becker-Reshef et al. 2020). This way, CM4EM contributes towards not only SDG 2 (target 2.1), but also SDG 1(target 1.5), SDG 3 (target 3.D), and SDG 13 (target 13.3) (Becker-Reshef et al. 2020). However, these international monitoring systems focus solely on droughts without incorporating the effects of salinity. Co-occurring drought and salinity give rise to a more pronounced -inhibitory- impact on crop growth (Chapter 3 & Chapter 4) than their individual impacts. Given the increasing possibility of co-occurring drought and salinity stress with climate change, there is a compelling need to take these co-occurring stresses into account and enhance our understanding of crop monitoring on a global scale. By integrating the evaluation of salinity impact on crops with the current GEOGLAM framework, it provides crucial open-source benefits to diverse stakeholders engaged in agricultural research, policy, and practice. Notably, in arid and semi-arid regions where water scarcity and soil salinization pose formidable barriers to sustainable crop production, leveraging the GEOGLAM program with the integration of salinity evaluation can prove instrumental in developing targeted strategies for resilient agriculture.

As part of the SDGs, improving agricultural resilience and food production within limited arable land under global climate change is a significant challenge to addressing food security. In this regard, saline agriculture poses a promising future to enhance the utilization of salt-affected areas. Specifically, saline agriculture is considered to significantly contribute to achieving several SDGs, including food security (SDG 2), freshwater resources utilization (SDG 6), sustainable livelihoods (SDG 8), climate change adaption (SDG 13), and life on Land (SDG15) (Negacz et al. 2021; Singh 2021). The most promising areas for saline agriculture are Africa, the Middle East, Central Asia, the United States, and Australia (Negacz et al. 2022). Additionally, Kazakhstan, the Russian Federation, Australia, Iraq, and Lesotho exhibit significant potential to address their food shortage challenges and work towards achieving sustainable development goals through the cultivation of salt-tolerant potatoes (Chapter 5). Given these regions with different soil properties, climate conditions, and water availability, salt-tolerant variates of major crops (e.g. potato) in addition to halophytes (e.g. Salicornia europaea) are accessible options for broader application at the global scale, particularly for developing countries (Chapter 5). However, given the high frequency of co-occurrent stress (e.g. salinity and drought), saline agriculture needs to further take the risk of co-occurring impacts (e.g., with drought) into account. Therefore, this asks for understanding and managing the combined effects of stress on crop productivity, soil health, water

availability, and overall system resilience to ensure sustainable and effective agricultural practices in saline environments. With the impact of climate change, there will be an expansion of suitable areas for saline farming in response to the increase in salinity. Salt-tolerant potato, as a part of saline farming, is proven to be a promising crop to improve food production in salt-affected areas both in the current state and future scenarios, and therefore achieving various sustainability targets in different ways (Chapter 5). By quantifying the contribution of saline farming to sustainable development in the face of impending climate change threats on a global scale, it provides valuable insights into optimizing the utilization of salt-affected soils. Consequently, it establishes a foundation for the promotion and widespread implementation of saline farming practices, bolstering food security and fortifying agricultural resilience at the global scale.

6.4 Concluding remarks

Remote sensing has shown promise in monitoring crop growth and health using vegetation indices (VIs) and plant functional traits, although the results may vary depending on spectral wavelengths and stress intensity. Plant functional traits derived from remote sensing data can serve as proxies for monitoring the effects of drought and salinity stress on crop health, as they align closely with vegetation processes. A novel approach was developed to quantify the impact of drought, salinity, and their combination on multiple crops at a large scale using remote sensing traits. The impact of stress varies across species, growth stages, and stress conditions. The interaction between drought and salinity stress is complex, and their combined effect generally exacerbates the impact on crops compared to individual stress. Most crops tend to reduce their primary production capacity before experiencing reductions in water and chlorophyll content. In order to mitigate the impact of salinity on crop productivity and improve food production, salt-tolerant potato -as a proxy of saline agriculture-, can contribute to enhancing the use of salt-affected areas and support the achievement of SDG2. This thesis provides a promising perspective on the application of remote sensing in agriculture systems to monitor food production with stress and improve agricultural resilience.

References

Aadhar, S., & Mishra, V. (2017). High-resolution near real-time drought monitoring in South Asia. Sci. Data, 4, 170145. https://doi.org/10.1038/sdata.2017.145.

Abatzoglou, J.T., McEvoy, D.J., & Redmond, K.T. (2017). The west wide drought tracker: drought monitoring at fine spatial scales. Bull. Am. Meteorol. Soc., 98, 1815-1820. https://wrcc.dri.edu/wwdt/about.php.

Abbas, A., Khan, S., Hussain, N., Hanjra, M.A., & Akbar, S. (2013). Characterizing soil salinity in irrigated agriculture using a remote sensing approach. Phys. Chem. Earth, 55-57, 43-52. https://doi.org/10.1016/j.pce.2010.12.004.

Acevedo, M.F.B., Groen, T.A., Hecker, C.A., & Skidmore, A.K. (2017). Identifying leaf traits that signal stress in TIR spectra. ISPRS J. Photogramm. Remote Sens., 125, 132-145. https://doi.org/10.1016/j.isprsjprs.2017.01.014.

AghaKouchak, A., Farahmand, A., Melton, F.S., Teixeira, J., Anderson, M.C., Wardlow, B.D., & Hain, C.R. (2015). Remote sensing of drought: progress, challenges and opportunities. Rev. Geophys., 53, 452-480. https://doi.org/10.1002/2014RG000456.

Alexander, A., Zbyněk, M., Julie, O., Alexander, G., Uwe, R., & Gina, M. (2015). Meta-analysis assessing potential of steady-state chlorophyll fluorescence for remote sensing detection of plant water, temperature and nitrogen stress. Remote Sens. Environ., 168, 420-436. https://doi.org/10.1016/j.rse.2015.07.022.

Allbed, A., & Kumar, L. (2013). Soil salinity mapping and monitoring in arid and semi-arid regions using remote sensing technology: a review. Adv. Remote Ses., 02, 373-385. http://dx.doi.org/10.4236/ars.2013.24040.

Anami, B.S., Malvade, N.N., & Palaiah, S. (2020). Classification of yield affecting biotic and abiotic paddy crop stresses using field images. Inf. Process. Agric., 7, 272-285. https://doi.org/10.1016/j.inpa.2019.08.005.

Anderegg, W.R.L., Trugman, A.T., Bowling, D.R., Salvucci, G., & Tuttle, S.E. (2019). Plant functional traits and climate influence drought intensification and land–atmosphere feedbacks. Proc. Natl. Acad. Sci. U.S.A., 116, 14071-14076. https://doi.org/10.1073/pnas.1904747116.

Anderson, K., Ryan, B., Sonntag, W., Kavvada, A., & Friedl, L. (2017). Earth observation in service of the 2030 agenda for sustainable development. Geo-Spat. Inf. Sci., 20, 77-96. https://doi.org/10.1080/10095020.2017.1333230.

Andrew, S.C., Gallagher, R.V., Wright, I.J., & Mokany, K. (2022). Assessing the vulnerability of plant functional trait strategies to climate change. Glob. Ecol. Biogeogr., 31, 1194-1206. https://doi.org/10.1111/geb.13501.

Angon, P.B., Tahjib-Ul-Arif, M., Samin, S.I., Habiba, U., Hossain, M.A., & Brestic, M. (2022). How do plants respond to combined drought and salinity stress? A systematic review. Plants (Basel), 11, 2884. https://doi.org/10.3390/plants11212884.

Arun-Chinnappa, K.S., Ranawake, L., & Seneweera, S. (2017). Impacts and management of temperature and water stress in crop plants. In P.S. Minhas, J. Rane, & R.K. Pasala (Eds.), Abiotic Stress Management for Resilient Agriculture (pp. 221-233). Singapore: Springer Singapore. https://doi.org/10.1007/978-981-10-5744-1_9.

Asner, G.P., Scurlock, J.M.O., & Hicke, J.A. (2003). Global synthesis of leaf area index observations: implications for ecological and remote sensing studies. Glob. Ecol. Biogeogr., 12, 191-205. https://doi.org/10.1046/j.1466-822X.2003.00026.x.

Asrar, G., Kanemasu, E.T., Jackson, R.D., & Pinter, P.J. (1985). Estimation of total above-ground phytomass production using remotely sensed data. Remote Sens. Environ., 17, 211-220. https://doi.org/10.1016/0034-4257(85)90095-1.

Atzberger, C. (2013). Advances in remote sensing of agriculture: context description, existing operational monitoring systems and major information needs. Remote Sens., 5, 949-981. https://doi.org/10.3390/rs5020949.

Atzori, G., Nissim, W.G., Caparrotta, S., Masi, E., Azzarello, E., Pandolfi, C., Vignolini, P., Gonnelli, C., & Mancuso, S. (2016). Potential and constraints of different seawater and freshwater blends as growing media for three vegetable crops. Agric. Water Manag., 176, 255-262. https://doi.org/10.1016/j.agwat.2016.06.016.

Audil, G., Ajaz Ahmad, L., & Noor Ul Islam, W. (2019). Biotic and abiotic stresses in plants. In O. Alexandre Bosco de (Ed.), Abiotic and Biotic Stress in Plants (p. Ch. 1). Rijeka: IntechOpen. https://doi.org/10.5772/intechopen.85832.

Ayers, R.S., & Westcot, D.W. (1985). Water quality for agriculture. Food and Agriculture Organization of the United Nations Rome. https://www.waterboards.ca.gov/water_issues/programs/tmdl/records/state_board/1985/ref2648.pdf.

Azad, N., Rezayian, M., Hassanpour, H., Niknam, V., & Ebrahimzadeh, H. (2021). Physiological mechanism of salicylic acid in Mentha pulegium L. Under salinity and drought stress. Braz. J. Bot., 44, 359-369. https://doi.org/10.1007/s40415-021-00706-y.

Bai, H., & Purcell, L. (2018). Aerial canopy temperature differences between fast-and slow-wilting soya bean genotypes. J. Agron. Crop Sci., 204, 243-251. https://doi.org/10.1111/jac.12259.

Baret, F., Madec, S., Irfan, K., Lopez, J., Comar, A., Hemmerlé, M., Dutartre, D., Praud, S., & Tixier, M.H. (2018). Leaf-rolling in maize crops: from leaf scoring to canopy-level measurements for phenotyping. J. Exp. Bot., 69, 2705-2716. https://doi.org/10.1093/jxb/ery071.

Bartels, D., & Sunkar, R. (2005). Drought and salt tolerance in plants. Crit. Rev. Plant Sci., 24, 23-58. https://doi.org/10.1080/07352680590910410.

Bartosz Mickiewicz, Ekaterina Volkova, & Jurczak, R. (2022). The Global Market for Potato and Potato Products in the Current and Forecast Period. Eur. Res. Stud., 740-751. https://doi.org/10.35808/ersj/3062.

Basso, B., & Liu, L. (2019). Seasonal crop yield forecast: methods, applications, and accuracies. (pp. 201-255). https://doi.org/10.1016/bs.agron.2018.11.002.

Bayat, B., van der Tol, C., & Verhoef, W. (2016). Remote sensing of grass response to drought stress using spectroscopic techniques and canopy reflectance model inversion. Remote Sens., 8, 557-581. https://doi.org/10.3390/rs8070557.

Bayat, B., van der Tol, C., & Verhoef, W. (2018). Integrating satellite optical and thermal infrared observations for improving daily ecosystem functioning estimations during a drought episode. Remote Sens. Environ., 209, 375-394. https://doi.org/10.1016/j.rse.2018.02.027.

Becker-Reshef, I., Barker, B., Whitcraft, A., Oliva, P., Mobley, K., Justice, C., & Sahajpal, R. (2023). Crop type maps for operational global agricultural monitoring. Sci. Data, 10, 172. https://doi.org/10.1038/s41597-023-02047-9.

Becker-Reshef, I., Justice, C., Barker, B., Humber, M., Rembold, F., Bonifacio, R., Zappacosta, M., Budde, M., Magadzire, T., Shitote, C., Pound, J., Constantino, A., Nakalembe, C., Mwangi, K., Sobue, S., Newby, T., Whitcraft, A., Jarvis, I., & Verdin, J. (2020). Strengthening agricultural decisions in countries at risk of food insecurity: The GEOGLAM Crop Monitor for Early Warning. Remote Sens. Environ., 237, 11153. https://doi.org/10.1016/j.rse.2019.111553.

Behmann, J., Steinrücken, J., & Plümer, L. (2014). Detection of early plant stress responses in hyperspectral images. ISPRS J. Photogramm. Remote Sens., 93, 98-111. https://doi.org/10.1016/j.isprsjprs.2014.03.016.

Ben Ahmed, C., Magdich, S., Ben Rouina, B., Boukhris, M., & Ben Abdullah, F. (2012). Saline water irrigation effects on soil salinity distribution and some physiological responses of field

grown Chemlali olive. J. Environ. Manage., 113, 538-544. https://doi.org/10.1016/j.jenvman.2012.03.016.

Ben Rouina, B., Trigui, A., d'Andria, R., Boukhris, M., & Chaieb, M. (2007). Effects of water stress and soil type on photosynthesis, leaf water potential and yield of olive trees (Olea europaea L. cv. Chemlali Sfax). Aust. J. Exp. Agr., 47, 1484-1490. https://doi.org/10.1071/Ea05206.

Berger, K., Atzberger, C., Danner, M., D'Urso, G., Mauser, W., Vuolo, F., & Hank, T. (2018). Evaluation of the PROSAIL model capabilities for future hyperspectral model environments: A review study. Remote Sens., 10, 85-101. https://doi.org/10.3390/rs10010085.

Berger, K., Machwitz, M., Kycko, M., Kefauver, S.C., Van Wittenberghe, S., Gerhards, M., Verrelst, J., Atzberger, C., van der Tol, C., Damm, A., Rascher, U., Herrmann, I., Paz, V.S., Fahrner, S., Pieruschka, R., Prikaziuk, E., Buchaillot, M.L., Halabuk, A., Celesti, M., Koren, G., Gormus, E.T., Rossini, M., Foerster, M., Siegmann, B., Abdelbaki, A., Tagliabue, G., Hank, T., Darvishzadeh, R., Aasen, H., Garcia, M., Pocas, I., Bandopadhyay, S., Sulis, M., Tomelleri, E., Rozenstein, O., Filchev, L., Stancile, G., & Schlerf, M. (2022). Multi-sensor spectral synergies for crop stress detection and monitoring in the optical domain: A review. Remote Sens. Environ., 280, 113198. https://doi.org/10.1016/j.rse.2022.113198.

Berni, J., Zarco-Tejada, P.J., Suarez, L., & Fereres, E. (2009). Thermal and narrowband multispectral remote sensing for vegetation monitoring from an unmanned aerial vehicle. IEEE Trans. Geosci. Remote Sens., 47, 722-738. https://doi.org/10.1109/tgrs.2008.2010457.

Bernstein, L., & Ayers, A. (1949). Salt tolerance of cabbage and broccoli. In, United States Salinity Laboratory Report to Collaborators, Riverside, CA (p. 39). https://www.ars.usda.gov/arsuserfiles/20360500/pdf_pubs/P1567.pdf.

Biju, S., Fuentes, S., & Gupta, D. (2018). The use of infrared thermal imaging as a non-destructive screening tool for identifying drought-tolerant lentil genotypes. Plant Physiol. Biochem., 127, 11-24

Bontemps, S., Defourny, P., Radoux, J., Van Bogaert, E., Lamarche, C., Achard, F., Mayaux, P., Boettcher, M., Brockmann, C., & Kirches, G. (2013). Consistent global land cover maps for climate modelling communities: current achievements of the ESA's land cover CCI. In, Proceedings of the ESA living planet symposium, Edimburgh (pp. 9-13). https://articles.adsabs.harvard.edu/pdf/2013ESASP.722E..62B.

Boryan, C., Yang, Z., Mueller, R., & Craig, M. (2011). Monitoring US agriculture: the US department of agriculture, national agricultural statistics service, cropland data layer program. Geocarto Int., 26, 341-358. https://doi.org/10.1080/10106049.2011.562309.

Botha, E.J., Zebarth, B.J., & Leblon, B. (2006). Non-destructive estimation of potato leaf chlorophyll and protein contents from hyperspectral measurements using the PROSPECT radiative transfer model. Can. J. Plant. Sci., 86, 279-291. https://doi.org/10.4141/P05-017.

Boussetta, S., Balsamo, G., Beljaars, A., Kral, T., & Jarlan, L. (2012). Impact of a satellite-derived leaf area index monthly climatology in a global numerical weather prediction model. Int. J. Remote Sens., 34, 3520-3542. https://doi.org/10.1080/01431161.2012.716543.

Bowman, W.D. (1989). The relationship between leaf water status, gas-exchange, and spectral reflectance in cotton leaves. Remote Sens. Environ., 30, 249-255. https://doi.org/10.1016/0034-4257(89)90066-7.

Broekhuizen, A. (2018). 'Storm duurt dagen, droogte duurt maanden'. In: Dutch Ministry of Infrastructure and Water Management

Bürling, K., Cerovic, Z.G., Cornic, G., Ducruet, J.-M., Noga, G., & Hunsche, M. (2013). Fluorescence-based sensing of drought-induced stress in the vegetative phase of four contrasting wheat genotypes. Environ. Exp. Bot., 89, 51-59. https://doi.org/10.1016/j.envexpbot.2013.01.003.

Butcher, K., Wick, A.F., DeSutter, T., Chatterjee, A., & Harmon, J. (2016). Soil salinity: A threat to global food security. Agron. J., 108, 2189-2200. https://doi.org/10.2134/agronj2016.06.0368.

Calvao, T., & Pessoa, M. (2015). Remote sensing in food production: a review. Emirates Journal of Food and Agriculture, 27. https://doi.org/10.9755/ejfa.v27i2.19272.

Cammalleri, C., McCormick, N., & Toreti, A. (2022). Analysis of the relationship between yield in cereals and remotely sensed fAPAR in the framework of monitoring drought impacts in Europe. Nat. Hazards Earth Syst. Sci., 22, 3737-3750. https://doi.org/10.5194/nhess-22-3737-2022.

Cammalleri, C., Verger, A., Lacaze, R., & Vogt, J.V. (2019). Harmonization of GEOV2 fAPAR time series through MODIS data for global drought monitoring. Int. J. Appl. Earth Obs. Geoinf., 80, 1-12. https://doi.org/10.1016/j.jag.2019.03.017.

Cárdenas-Pérez, S., Piernik, A., Chanona-Pérez, J.J., Grigore, M.N., & Perea-Flores, M.J. (2021). An overview of the emerging trends of the Salicornia L. genus as a sustainable crop. Environ. Exp. Bot., 191. https://doi.org/10.1016/j.envexpbot.2021.104606.

Carrão, H., Naumann, G., & Barbosa, P. (2016). Mapping global patterns of drought risk: An empirical framework based on sub-national estimates of hazard, exposure and vulnerability. Glob. Environ. Change, 39, 108-124. https://doi.org/10.1016/j.gloenvcha.2016.04.012.

Caruso, C.M., Maherali, H., & Martin, R.A. (2019). A meta-analysis of natural selection on plant functional traits. Int. J. Plant Sci., 181, 44-55. https://doi.org/10.1086/706199.

CBD (2022). Decision Adopted by the Conference of the Parties to the Convention on Biological Diversity. In 15/4. Kunming-Montreal Global Biodiversity Framework. In. https://www.cbd.int/doc/decisions/cop-15/cop-15-dec-04-en.pdf.

Chaabouni, S., Kallel, A., & Houborg, R. (2021). Improving retrieval of crop biophysical properties in dryland areas using a multi-scale variational RTM inversion approach. International Journal of Applied Earth Observation and Geoinformation, 94, 102220. https://doi.org/10.1016/j.jag.2020.102220.

Chaves, M.M., Flexas, J., & Pinheiro, C. (2009). Photosynthesis under drought and salt stress: regulation mechanisms from whole plant to cell. Ann. Bot., 103, 551-560. https://doi.org/10.1093/aob/mcn125.

Chen, J., & Mueller, V. (2018). Coastal climate change, soil salinity and human migration in Bangladesh. Nat. Clim. Chang., 8, 981-985. https://doi.org/10.1038/s41558-018-0313-8.

Chen, Q., Timmermans, J., Wen, W., & van Bodegom, P.M. (2022). A multi-metric assessment of drought vulnerability across different vegetation types using high-resolution remote sensing. Sci. Total Environ., 832, 154970. https://doi.org/10.1016/j.scitotenv.2022.154970.

Chevilly, S., Dolz-Edo, L., Martinez-Sanchez, G., Morcillo, L., Vilagrosa, A., Lopez-Nicolas, J.M., Blanca, J., Yenush, L., & Mulet, J.M. (2021). Distinctive traits for drought and salt Stress tolerance in melon (Cucumis melo L.). Front. Plant Sci., 12, 777060. https://doi.org/10.3389/fpls.2021.777060.

Ciais, P., Reichstein, M., Viovy, N., Granier, A., Ogée, J., Allard, V., Aubinet, M., Buchmann, N., Bernhofer, C., Carrara, A., Chevallier, F., De Noblet, N., Friend, A.D., Friedlingstein, P., Grünwald, T., Heinesch, B., Keronen, P., Knohl, A., Krinner, G., Loustau, D., Manca, G., Matteucci, G., Miglietta, F., Ourcival, J.M., Papale, D., Pilegaard, K., Rambal, S., Seufert, G., Soussana, J.F., Sanz, M.J., Schulze, E.D., Vesala, T., & Valentini, R. (2005). Europe-wide reduction in primary productivity caused by the heat and drought in 2003. Nature, 437, 529-533. https://doi.org/10.1038/nature03972.

Cochran, F., Daniel, J., Jackson, L., & Neale, A. (2020). Earth observation-based ecosystem services indicators for national and subnational reporting of the sustainable development goals. Remote Sens. Environ., 244, 1-111796. https://doi.org/10.1016/j.rse.2020.111796.

Colombo, R., Meroni, M., Marchesi, A., Busetto, L., Rossini, M., Giardino, C., & Panigada, C. (2008). Estimation of leaf and canopy water content in poplar plantations by means of hyperspectral indices and inverse modeling. Remote Sens. Environ., 112, 1820-1834. https://doi.org/10.1016/j.rse.2007.09.005.

Cook, B.I., Ault, T.R., & Smerdon, J.E. (2015). Unprecedented 21st century drought risk in the American Southwest and Central Plains. Sci. Adv., 1, e1400082. https://doi.org/10.1126/sciadv.1400082.

Cornelissen, J.H.C., Lavorel, S., Garnier, E., Díaz, S., Buchmann, N., Gurvich, D.E., Reich, P.B., Steege, H.t., Morgan, H.D., Heijden, M.G.A.v.d., Pausas, J.G., & Poorter, H. (2003). A handbook of protocols for standardised and easy measurement of plant functional traits worldwide. Aust. J. Bot., 51, 335-380. https://www.publish.csiro.au/bt/BT02124.

Corwin, D.L. (2020). Climate change impacts on soil salinity in agricultural areas. Eur. J. Soil Sci., 72, 842-862. https://doi.org/10.1111/ejss.13010.

Corwin, D.L., & Scudiero, E. (2019). Chapter One - Review of soil salinity assessment for agriculture across multiple scales using proximal and/or remote sensors. In D.L. Sparks (Ed.), Advances in Agronomy (pp. 1-130): Academic Press. https://doi.org/10.1016/bs.agron.2019.07.001.

Cramer, G.R., Ergul, A., Grimplet, J., Tillett, R.L., Tattersall, E.A., Bohlman, M.C., Vincent, D., Sonderegger, J., Evans, J., Osborne, C., Quilici, D., Schlauch, K.A., Schooley, D.A., & Cushman, J.C. (2007). Water and salinity stress in grapevines: early and late changes in transcript and metabolite profiles. Funct. Integr. Genomics, 7, 111-134. https://doi.org/10.1007/s10142-006-0039-y.

Croft, H., Chen, J.M., Luo, X., Bartlett, P., Chen, B., & Staebler, R.M. (2017). Leaf chlorophyll content as a proxy for leaf photosynthetic capacity. Glob. Change Biol., 23, 3513-3524. https://doi.org/10.1111/gcb.13599.

Dai, A. (2011). Drought under global warming: a review. Wiley Interdiscip. Rev. Clim. Change, 2, 45-65. https://doi.org/10.1002/wcc.81.

Dai, A. (2013). Increasing drought under global warming in observations and models. Nat. Clim. Chang., 3, 52-58. https://doi.org/10.1038/nclimate1633.

Dalezios, N., Blanta, A., Spyropoulos, N., & Tarquis, A. (2014). Risk identification of agricultural drought for sustainable agroecosystems. Nat. Hazards Earth Syst. Sci., 14, 2435. https://doi.org/10.5194/nhess-14-2435-2014.

Danner, M., Berger, K., Wocher, M., Mauser, W., & Hank, T. (2021). Efficient RTM-based training of machine learning regression algorithms to quantify biophysical & biochemical traits of agricultural crops. ISPRS J. Photogramm. Remote Sens., 173, 278-296. https://doi.org/10.1016/j.isprsjprs.2021.01.017.

Daryanto, S., Wang, L., & Jacinthe, P.A. (2016a). Global synthesis of drought effects on maize and wheat production. PLoS One, 11, e0156362. https://doi.org/10.1371/journal.pone.0156362.

Daryanto, S., Wang, L.X., & Jacinthe, P.A. (2016b). Drought effects on root and tuber production: A meta-analysis. Agric. Water Manag., 176, 122-131. https://doi.org/10.1016/j.agwat.2016.05.019.

Daryanto, S., Wang, L.X., & Jacinthe, P.A. (2017). Global synthesis of drought effects on cereal, legume, tuber and root crops production: A review. Agric. Water Manag., 179, 18-33. https://doi.org/10.1016/j.agwat.2016.04.022.

Dasgupta, S., Hossain, M.M., Huq, M., & Wheeler, D. (2015). Climate change and soil salinity: The case of coastal Bangladesh. Ambio, 44, 815-826. https://doi.org/10.1007/s13280-015-0681-5.

de Vos, A., Andres Parra González, & Bruning, B. (2021). Case Study: Putting Saline Agriculture into Practice – A Case Study from Bangladesh. Future of Sustainable Agriculture in Saline Environments: Routledge, Taylor & Francis Group, London. https://doi.org/10.1201/9781003112327.

de Vos, A., Bruning, B., van Straten, G., Oosterbaan, R., Rozema, J., & van Bodegom, P. (2016). Crop salt tolerance under controlled field conditions in The Netherlands, based on trials conducted at Salt Farm Texel. In: Salt Farm Texel. https://edepot.wur.nl/409817.

Deb, P., Moradkhani, H., Han, X., Abbaszadeh, P., & Xu, L. (2022). Assessing irrigation mitigating drought impacts on crop yields with an integrated modeling framework. J. Hydrol., 609, 127760. https://doi.org/10.1016/j.jhydrol.2022.127760.

Dente, L., Satalino, G., Mattia, F., & Rinaldi, M. (2008). Assimilation of leaf area index derived from ASAR and MERIS data into CERES-Wheat model to map wheat yield. Remote Sens. Environ., 112, 1395-1407. https://doi.org/10.1016/j.rse.2007.05.023.

Diepen, C.A.V., Wolf, J., Keulen, H.V., & Rappoldt, C. (1989). WOFOST: a simulation model of crop production. Soil Use Manag., 5, 16-24. https://doi.org/10.1111/j.1475-2743.1989.tb00755.x.

Dobrowski, S., Pushnik, J., Zarco-Tejada, P.J., & Ustin, S. (2005). Simple reflectance indices track heat and water stress-induced changes in steady-state chlorophyll fluorescence at the canopy scale. Remote Sens. Environ., 97, 403-414. https://doi.org/10.1016/j.rse.2005.05.006.

Dodig, D., Bozinovic, S., Nikolić, A., Zoric, M., Vancetovic, J., Ignjatovic-Micic, D., Delic, N., Weigelt-Fischer, K., Junker, A., & Altmann, T. (2019). Image-derived traits related to mid-season growth performance of maize under nitrogen and water stress. Front. Plant Sci., 10, 814. https://doi.org/10.3389/fpls.2019.00814.

Doraiswamy, P.C., Sinclair, T.R., Hollinger, S., Akhmedov, B., Stern, A., & Prueger, J. (2005). Application of MODIS derived parameters for regional crop yield assessment. Remote Sens. Environ., 97, 192-202. https://doi.org/10.1016/j.rse.2005.03.015.

Dresselhaus, T., & Hückelhoven, R. (2018). Biotic and abiotic stress responses in crop plants. Agronomy, 8, 267-273. https://doi.org/10.3390/agronomy8110267.

Dunn, R.J.H., Stanitski, D.M., Gobron, N., Willett, K.M., Ades, M., Adler, R., Allan, R., Allan, R.P., Anderson, J., Argüez, A., Arosio, C., Augustine, J.A., Azorin-Molina, C., Barichivich, J., Barnes, J., Beck, H.E., Becker, A., Bellouin, N., Benedetti, A., Berry, D.I., Blenkinsop, S., Bock, O., Bosilovich, M.G., Boucher, O., Buehler, S.A., Carrea, L., Christiansen, H.H., Chouza, F., Christy, J.R., Chung, E.S., Coldewey-Egbers, M., Compo, G.P., Cooper, O.R., Covey, C., Crotwell, A., Davis, S.M., de Eyto, E., de Jeu, R.A.M., VanderSat, B.V., DeGasperi, C.L., Degenstein, D., Di Girolamo, L., Dokulil, M.T., Donat, M.G., Dorigo, W.A., Durre, I., Dutton, G.S., Duveiller, G., Elkins, J.W., Fioletov, V.E., Flemming, J., Foster, M.J., Frey, R.A., Frith, S.M., Froidevaux, L., Garforth, J., Gupta, S.K., Haimberger, L., Hall, B.D., Harris, I., Heidinger, A.K., Hemming, D.L., Ho, S.-p., Hubert, D., Hurst, D.F., Hüser, I., Inness, A., Isaksen, K., John, V., Jones, P.D., Kaiser, J.W., Kelly, S., Khaykin, S., Kidd, R., Kim, H., Kipling, Z., Kraemer, B.M., Kratz, D.P., La Fuente, R.S., Lan, X., Lantz, K.O., Leblanc, T., Li, B., Loeb, N.G., Long, C.S., Loyola, D., Marszelewski, W., Martens, B., May, L., Mayer, M., McCabe, M.F., McVicar, T.R., Mears, C.A., Menzel, W.P., Merchant, C.J., Miller, B.R., Miralles, D.G., Montzka, S.A., Morice, C., Mühle, J., Myneni, R., Nicolas, J.P., Noetzli, J., Osborn, T.J., Park, T., Pasik, A., Paterson, A.M., Pelto, M.S., Perkins-Kirkpatrick, S., Pétron, G., Phillips, C., Pinty, B., Po-Chedley, S., Polvani, L., Preimesberger, W., Pulkkanen, M., Randel, W.J., Rémy, S., Ricciardulli, L., Richardson, A.D., Rieger, L., Robinson, D.A., Rodell, M., Rosenlof, K.H., Roth, C., Rozanov, A., Rusak, J.A., Rusanovskaya, O., Rutishäuser, T., Sánchez-Lugo, A., Sawaengphokhai, P., Scanlon, T., Schenzinger, V., Schladow, S.G., Schlegel, R.W., Schmid, M.E., Selkirk, H.B., Sharma, S., Shi, L., Shimaraeva, S.V., Silow, E.A., Simmons, A.J., Smith, C.A., Smith, S.L., Soden, B.J., Sofieva, V., Sparks, T.H., Stackhouse, P.W., Steinbrecht, W., Streletskiy, D.A., Taha, G., Telg, H., Thackeray, S.J., Timofeyev, M.A., Tourpali, K., Tye, M.R., van der A, R.J., van der Schalie, R.V.B.V., van der SchrierW. Paul, G., van der Werf, G.R., Verburg, P., Vernier, J.-P., Vömel, H., Vose, R.S., Wang, R., Watanabe, S.G., Weber, M., Weyhenmeyer, G.A., Wiese, D., Wilber, A.C., Wild, J.D., Wong, T., Woolway, R.I., Yin, X., Zhao, L., Zhao, G., Zhou, X., Ziemke, J.R., & Ziese, M. (2020). Global climate-state of the climate in 2019. State of the climate in 2019, 101, S9-S128. https://doi.org/10.1175/bams-d-20-0104.1.

Eallonardo Jr, A.S., Leopold, D.J., Fridley, J.D., & Stella, J.C. (2013). Salinity tolerance and the decoupling of resource axis plant traits. J. Veg. Sci., 24, 365-374. https://doi.org/10.1111/j.1654-1103.2012.01470.x.

Eckardt, N.A., Cutler, S., Juenger, T.E., Marshall-Colon, A., Udvardi, M., & Verslues, P.E. (2022). Focus on climate change and plant abiotic stress biology. The Plant Cell, 35, 1-3. https://doi.org/10.1093/plcell/koac329.

Efimova, M.V., Kolomeichuk, L.V., Boyko, E.V., Malofii, M.K., Vidershpan, A.N., Plyusnin, I.N., Golovatskaya, I.F., Murgan, O.K., & Kuznetsov, V.V. (2018). Physiological mechanisms of Solanum tuberosum L. Plants' tolerance to chloride salinity. Russ. J. Plant Physiol., 65, 394-403. https://doi.org/10.1134/S1021443718030020.

El-Hendawy, S., Al-Suhaibani, N., Alotaibi, M., Hassan, W., Elsayed, S., Tahir, M.U., Mohamed, A.I., & Schmidhalter, U. (2019a). Estimating growth and photosynthetic properties of wheat grown in simulated saline field conditions using hyperspectral reflectance sensing and multivariate analysis. Sci. Rep., 9, 1-15. https://doi.org/10.1038/s41598-019-52802-5.

El-Hendawy, S.E., Al-Suhaibani, N.A., Hassan, W.M., Dewir, Y.H., Elsayed, S., Al-Ashkar, I., Abdella, K.A., & Schmidhalter, U. (2019b). Evaluation of wavelengths and spectral reflectance indices for high-throughput assessment of growth, water relations and ion contents of wheat irrigated with saline water. Agric. Water Manag., 212, 358-377. https://doi.org/10.1016/j.agwat.2018.09.009.

El-Moneim, D.A., Alqahtani, M.M., Abdein, M.A., & Germoush, M.O. (2020). Drought and salinity stress response in wheat: physiological andTaNACgene expression analysis in contrasting Egyptian wheat genotypes. Plant Biotechnol. J., 47, 1-14. https://doi.org/10.5010/jpb.2020.47.1.001.

El hasini, S., Iben. Halima, O., El. Azzouzi, M., Douaik, A., Azim, K., & Zouahri, A. (2019). Organic and inorganic remediation of soils affected by salinity in the Sebkha of Sed El Mesjoune – Marrakech (Morocco). Soil Tillage Res., 193, 153-160. https://doi.org/10.1016/j.still.2019.06.003.

Elhag, M., & Bahrawi, J.A. (2017). Soil salinity mapping and hydrological drought indices assessment in arid environments based on remote sensing techniques. Geosci. Instrum. Methods Data Syst., 6, 149-158. https://doi.org/10.5194/gi-6-149-2017.

Elsayed, S., & Darwish, W. (2017). Hyperspectral remote sensing to assess the water status, biomass, and yield of maize cultivars under salinity and water stress. Bragantia, 76, 62-72. https://doi.org/10.1590/1678-4499.018.

ESA (2015). Sentinel-2 User Handbook. https://sentinels.copernicus.eu/documents/247904/685211/Sentinel-2_User_Handbook.pdf/8869acdf-fd84-43ec-ae8c-3e80a436a16c?t=1438278087000.

Eswar, D., Karuppusamy, R., & Chellamuthu, S. (2021). Drivers of soil salinity and their correlation with climate change. Curr. Opin. Environ. Sustain., 50, 310-318. https://doi.org/10.1016/j.cosust.2020.10.015.

Eyring, V., Bony, S., Meehl, G.A., Senior, C.A., Stevens, B., Stouffer, R.J., & Taylor, K.E. (2016). Overview of the Coupled Model Intercomparison Project Phase 6 (CMIP6) experimental design and organization. Geosci. Model Dev., 9, 1937-1958. https://doi.org/10.5194/gmd-9-1937-2016.

Fang, H., Baret, F., Plummer, S., & Schaepman-Strub, G. (2019). An overview of global leaf area index (LAI): methods, products, validation, and applications. Rev. Geophys., 57, 739-799. https://doi.org/10.1029/2018RG000608.

FAO (2002). The state of food insecurity in the world 2001. In. Rome, Italy. https://www.fao.org/3/y1500e/y1500e02.htm.

FAO (2009). High level expert forum—how to feed the world in 2050. In: Food and Agriculture Organization of the United Nations (FAO) Rome, Italy.

https://www.fao.org/fileadmin/templates/wsfs/docs/expert_paper/How_to_Feed_the_World_in_2050.pdf.
FAO (2011). The state of the world's land and water resources for food and agriculture: Managing systems at risk. In: Earthscan. https://www.fao.org/land-water/solaw2021/en/.
FAO (2017). AQUASTAT Database. In F.L.a.W. Division (Ed.). http://www.fao.org/aquastat/en/.
FAO (2022a). Halt soil salinization, boost soil productivity In, Proceedings of the Global Symposium on Salt-affected Soils. Rome. https://doi.org/10.4060/cb9565en.
FAO (2022b). The state of food security and nutrition in the world 2022. In. Rome, Italy. https://doi.org/10.4060/cc0639en.
FAO, & IIASA (2012). Crop suitability index (value) for high input level rain-fed white potato. In F.a. IIASA (Ed.). http://gisweb.ciat.cgiar.org/RTBMaps/docs/metadata/Menu_RTBCrops/Potato_Suitability_Index.pdf.
FAO, I., UNICEF, WFP and WHO (2020). The state of food security and nutrition in the world 2020. In, Transforming food systems for affordable healthy diets. Rome: FAO. https://doi.org/10.4060/ca9692en.
FAO/IIASA/ISRIC/ISSCAS/JRC (2012). Harmonized World Soil Database (version 1.2). In FAO (Ed.). Rome, Italy and Laxenburg, Austria.
Farooq, M., Hussain, M., Wakeel, A., & Siddique, K.H.M. (2015). Salt stress in maize: effects, resistance mechanisms, and management. A review. Agron. Sustain. Dev., 35, 461-481. https://doi.org/10.1007/s13593-015-0287-0.
Farooq, M., Wahid, A., Kobayashi, N., Fujita, D., & Basra, S.M.A. (2009). Plant drought stress: effects, mechanisms and management. Agron. Sustain. Dev., 29, 185-212. https://doi.org/10.1051/agro:2008021.
Fatima, A., Hussain, S., Hussain, S., Ali, B., Ashraf, U., Zulfiqar, U., Aslam, Z., Al-Robai, S.A., Alzahrani, F.O., Hano, C., & El-Esawi, M.A. (2021). Differential morphophysiological, biochemical, and molecular responses of maize hybrids to salinity and alkalinity stresses. Agronomy, 11, 1150. https://doi.org/10.3390/agronomy11061150.
Fischer, G., Nachtergaele, F., Prieler, S., Van Velthuizen, H., Verelst, L., & Wiberg, D. (2008). Global agro-ecological zones assessment for agriculture (GAEZ 2008). IIASA, Laxenburg, Austria and FAO, Rome, Italy, 10.
Flexas, J., Briantais, J.-M., Cerovic, Z., Medrano, H., & Moya, I. (2000). Steady-state and maximum chlorophyll fluorescence responses to water stress in grapevine leaves: a new remote sensing system. Remote Sens. Environ., 73, 283-297. https://doi.org/10.1016/S0034-4257(00)00104-8.
Fuentes, S., De Bei, R., Pech, J., & Tyerman, S. (2012). Computational water stress indices obtained from thermal image analysis of grapevine canopies. Irrig. Sci., 30, 523-536. https://doi.org/10.1007/s00271-012-0375-8.
Gamon, J.A., Penuelas, J., & Field, C.B. (1992). A narrow-waveband spectral index that tracks diurnal changes in photosynthetic efficiency. Remote Sens. Environ., 41, 35-44. https://doi.org/10.1016/0034-4257(92)90059-S.
Gao, B.C. (1996). NDWI—A normalized difference water index for remote sensing of vegetation liquid water from space. Remote Sens. Environ., 58, 257-266. https://doi.org/10.1016/S0034-4257(96)00067-3.
Gao, Y., & Li, D. (2012). Detecting salinity stress in tall fescue based on single leaf spectrum. Sci. Hortic., 138, 159-164. https://doi.org/10.1016/j.scienta.2012.02.018.
Garcia, A., Rizzo, C.A., Ud-Din, J., Bartos, S.L., Senadhira, D., Flowers, T.J., & Yeo, A.R. (1997). Sodium and potassium transport to the xylem are inherited independently in rice, and the mechanism of sodium: potassium selectivity differs between rice and wheat. Plant Cell Environ., 20, 1167-1174. https://doi.org/10.1046/j.1365-3040.1997.d01-146.x.

Garriga, M., Retamales, J.B., Romero-Bravo, S., Caligari, P.D., & Lobos, G.A. (2014). Chlorophyll, anthocyanin, and gas exchange changes assessed by spectroradiometry in Fragaria chiloensis under salt stress. J. Integr. Plant Biol., 56, 505-515. https://doi.org/10.1111/jipb.12193.

Genc, Y., Taylor, J., Lyons, G., Li, Y., Cheong, J., Appelbee, M., Oldach, K., & Sutton, T. (2019). Bread wheat with high salinity and sodicity tolerance. Front. Plant Sci., 10, 1280. https://doi.org/10.3389/fpls.2019.01280.

Gerhards, M., Rock, G., Schlerf, M., & Udelhoven, T. (2016). Water stress detection in potato plants using leaf temperature, emissivity, and reflectance. Int. J. Appl. Earth Obs. Geoinf., 53, 27-39. https://doi.org/10.1016/j.jag.2016.08.004.

Gerhards, M., Schlerf, M., Mallick, K., & Udelhoven, T. (2019). Challenges and future perspectives of multi-/hyperspectral thermal infrared remote sensing for crop water-stress detection: a review. Remote Sens., 11, 1240-1264. https://doi.org/10.3390/rs11101240.

Ghimire, B., Timsina, D., & Nepal, J. (2015). Analysis of chlorophyll content and its correlation with yield attributing traits on early varieties of maize (Zea mays L.). J. Maize Res. Dev., 1, 134-145. https://doi.org/10.3126/jmrd.v1i1.14251.

Ghosh, S.C., Asanuma, K., Kusutani, A., & Toyota, M. (2001). Effect of salt stress on some chemical components and yield of potato. Soil Sci. Plant Nutr., 47, 467-475. https://doi.org/10.1080/00380768.2001.10408411.

Ghulam, A., Li, Z.-L., Qin, Q., Yimit, H., & Wang, J. (2008). Estimating crop water stress with ETM+ NIR and SWIR data. Agric. For. Meteorol., 148, 1679-1695. https://doi.org/10.1016/j.agrformet.2008.05.020.

Gitelson, A.A., Vina, A., Ciganda, V., Rundquist, D.C., & Arkebauer, T.J. (2005). Remote estimation of canopy chlorophyll content in crops. Geophys. Res. Lett., 32, L08403. https://doi.org/10.1029/2005GL022688.

Gizaw, S.A., Garland-Campbell, K., & Carter, A.H. (2016). Evaluation of agronomic traits and spectral reflectance in Pacific Northwest winter wheat under rain-fed and irrigated conditions. Field Crops Res., 196, 168-179. https://doi.org/10.1016/j.fcr.2016.06.018.

Gizaw, S.A., Godoy, J.G.V., Pumphrey, M.O., & Carter, A.H. (2018). Spectral reflectance for indirect selection and genome-wide association analyses of grain yield and drought tolerance in north American spring wheat. Crop Sci., 58, 2289-2301. https://doi.org/10.2135/cropsci2017.11.0690.

Godfray, H.C., Beddington, J.R., Crute, I.R., Haddad, L., Lawrence, D., Muir, J.F., Pretty, J., Robinson, S., Thomas, S.M., & Toulmin, C. (2010). Food security: the challenge of feeding 9 billion people. Science, 327, 812-818. https://doi.org/10.1126/science.1185383.

Gopalakrishnan, T., Hasan, M., Haque, A., Jayasinghe, S., & Kumar, L. (2019). Sustainability of coastal agriculture under climate change. Sustainability, 11. https://doi.org/10.3390/su11247200.

Grieve, C.M., Grattan, S.R., & Maas, E.V. (2011). Plant Salt Tolerance. Agricultural Salinity Assessment and Management (pp. 405-459). https://doi.org/10.1061/9780784411698.ch13.

Griffin-Nolan, R.J., Bushey, J.A., Carroll, C.J.W., Challis, A., Chieppa, J., Garbowski, M., Hoffman, A.M., Post, A.K., Slette, I.J., Spitzer, D., Zambonini, D., Ocheltree, T.W., Tissue, D.T., & Knapp, A.K. (2018). Trait selection and community weighting are key to understanding ecosystem responses to changing precipitation regimes. Funct. Ecol., 32, 1746-1756. https://doi.org/10.1111/1365-2435.13135.

Griggs, D., Smith, M.S., Rockström, J., Öhman, M.C., Gaffney, O., Glaser, G., Kanie, N., Noble, I., Steffen, W., & Shyamsundar, P. (2014). An integrated framework for sustainable development goals. Ecol. Soc., 19. http://dx.doi.org/10.5751/ES-07082-190449.

Grzesiak, M., Rzepka, A., Hura, T., Grzesiak, S., Hura, K., Filek, W., & Skoczowski, A. (2007). Fluorescence excitation spectra of drought resistant and sensitive genotypes of triticale and maize. Photosynthetica, 45, 606-611. https://ps.ueb.cas.cz/pdfs/phs/2007/04/23.pdf.

Haboudane, D., Miller, J.R., Tremblay, N., Zarco-Tejada, P.J., & Dextraze, L. (2002). Integrated narrow-band vegetation indices for prediction of crop chlorophyll content for application to precision agriculture. Remote Sens. Environ., 81, 416-426. https://doi.org/10.1016/S0034-4257(02)00018-4.

Hackl, H., Mistele, B., Hu, Y.C., & Schmidhalter, U. (2013). Spectral assessments of wheat plants grown in pots and containers under saline conditions. Funct. Plant Biol., 40, 409-424. https://doi.org/10.1071/fp12208.

Harfi, M.E., Hanine, H., Rizki, H., Latrache, H., & Nabloussi, A. (2016). Effect of drought and salt stresses on germination and early seedling growth of different color-seeds of sesame (Sesamum indicum). Int. J. Agric. Biol., 18, 1088-1094. https://doi.org/10.17957/ijab/15.0145.

Hassani, A., Azapagic, A., & Shokri, N. (2020). Predicting long-term dynamics of soil salinity and sodicity on a global scale. Proc. Natl. Acad. Sci. U.S.A., 117, 33017-33027. https://doi.org/10.1073/pnas.2013771117.

Hassani, A., Azapagic, A., & Shokri, N. (2021). Global predictions of primary soil salinization under changing climate in the 21st century. Nature Commun., 12, 6663. https://doi.org/10.1038/s41467-021-26907-3.

He, N., Li, Y., Liu, C., Xu, L., Li, M., Zhang, J., He, J., Tang, Z., Han, X., Ye, Q., Xiao, C., Yu, Q., Liu, S., Sun, W., Niu, S., Li, S., Sack, L., & Yu, G. (2020). Plant trait networks: improved resolution of the dimensionality of adaptation. Trends Ecol. Evol., 35, 908-918. https://doi.org/10.1016/j.tree.2020.06.003.

He, X., Estes, L., Konar, M., Tian, D., Anghileri, D., Baylis, K., Evans, T.P., & Sheffield, J. (2019). Integrated approaches to understanding and reducing drought impact on food security across scales. Curr. Opin. Environ. Sustain., 40, 43-54. https://doi.org/10.1016/j.cosust.2019.09.006.

Hernández-Clemente, R., Navarro-Cerrillo, R.M., Suárez, L., Morales, F., & Zarco-Tejada, P.J. (2011). Assessing structural effects on PRI for stress detection in conifer forests. Remote Sens. Environ., 115, 2360-2375. https://doi.org/10.1016/j.rse.2011.04.036.

Hernández, E.I., Melendez-Pastor, I., Navarro-Pedreño, J., & Gómez, I. (2014). Spectral indices for the detection of salinity effects in melon plants. Sci. Agric., 71, 324-330. https://doi.org/10.1590/0103-9016-2013-0338.

Homolova, L., Maenovsky, Z., Clevers, J.G.P.W., Garcia-Santos, G., & Schaeprnan, M.E. (2013). Review of optical-based remote sensing for plant trait mapping. Ecol. Complex., 15, 1-16. https://doi.org/10.1016/j.ecocom.2013.06.003.

Hopmans, J.W., Qureshi, A.S., Kisekka, I., Munns, R., Grattan, S.R., Rengasamy, P., Ben-Gal, A., Assouline, S., Javaux, M., Minhas, P.S., Raats, P.A.C., Skaggs, T.H., Wang, G., De Jong van Lier, Q., Jiao, H., Lavado, R.S., Lazarovitch, N., Li, B., & Taleisnik, E. (2021). Critical knowledge gaps and research priorities in global soil salinity. (pp. 1-191). https://doi.org/10.1016/bs.agron.2021.03.001.

Houshmand, S., Arzani, A., & Mirmohammadi-Maibody, S.A.M. (2014). Effects of salinity and drought stress on grain quality of durum wheat. Commun. Soil Sci. Plant Anal., 45, 297-308. https://doi.org/10.1080/00103624.2013.861911.

Hrdinka, T., Novický, O., Hanslík, E., & Rieder, M. (2012). Possible impacts of floods and droughts on water quality. J. Hydro-environ. Res., 6, 145-150. https://doi.org/10.1016/j.jher.2012.01.008.

Hu, Q., Yang, J., Xu, B., Huang, J., Memon, M.S., Yin, G., Zeng, Y., Zhao, J., & Liu, K. (2020). Evaluation of global decametric-resolution LAI, FAPAR and FVC estimates derived from Sentinel-2 imagery. Remote Sens., 12. https://doi.org/10.3390/rs12060912.

Huang, J., Wang, H., Dai, Q., & Han, D. (2014). Analysis of NDVI Data for crop identification and yield estimation. IEEE J. Sel. Top. Appl. Earth Obs. Remote Sens., 7, 4374-4384. https://doi.org/10.1109/JSTARS.2014.2334332.

Huete, A.R. (1988). A soil-adjusted vegetation index (SAVI). Remote Sens. Environ., 25, 295-309. https://doi.org/10.1016/0034-4257(88)90106-X.

Hunt Jr, E.R., Rock, B.N., & Nobel, P.S. (1987). Measurement of leaf relative water content by infrared reflectance. Remote Sens. Environ., 22, 429-435. https://doi.org/10.1016/0034-4257(87)90094-0.

Hussain, T., Koyro, H.W., Zhang, W., Liu, X., Gul, B., & Liu, X. (2020). Low salinity improves photosynthetic performance in Panicum Antidotale under drought stress. Front. Plant Sci., 11, 481. https://doi.org/10.3389/fpls.2020.00481.

Ibrahim, W., Qiu, C.W., Zhang, C., Cao, F., Shuijin, Z., & Wu, F. (2019). Comparative physiological analysis in the tolerance to salinity and drought individual and combination in two cotton genotypes with contrasting salt tolerance. Physiol. Plant., 165, 155-168. https://doi.org/10.1111/ppl.12791.

ICBA (2015). Quinoa for Marginal Environments, Project brief International Centre for Biosaline Agriculture. In ICBA (Ed.). https://www.biosaline.org/sites/default/files/Projectbrieffiles/Quinoa-Project_Brief-Final-2.pdf.

Idowu, O., Marsalis, M., & Flynn, R.P. (2012). Agronomic principles to help with farming during drought periods - guide a147. https://pubs.nmsu.edu/_a/A147.pdf.

Idso, S.B., Jackson, R.D., Pinter, P.J., Reginato, R.J., & Hatfield, J.L. (1981). Normalizing the stress-degreed-day parameter for environmental variability. Agric. Meteorol., 24, 45-55. https://doi.org/10.1016/0002-1571(81)90032-7.

Ionita, M., Tallaksen, L.M., Kingston, D.G., Stagge, J.H., Laaha, G., Van Lanen, H.A.J., Scholz, P., Chelcea, S.M., & Haslinger, K. (2017). The European 2015 drought from a climatological perspective. Hydrol. Earth Syst. Sci., 21, 1397-1419. https://doi.org/10.5194/hess-21-1397-2017.

IPCC, S.P. (2019). Climate change and land: an IPCC special report on climate change, desertification, land degradation, sustainable land management, food security, and greenhouse gas fluxes in terrestrial ecosystems. In. https://www.ipcc.ch/srccl/download/.

ISRIC (2023). Soil Geographic Databases. In. https://www.isric.org/explore/soil-geographic-databases.

ITPS, & FAO (2015). Status of the world's soil resources (SWSR)—Main report. In. Rome, Italy. https://www.fao.org/3/i5199e/I5199E.pdf.

Ivanov, V. (1970). Main principles of fruit crop salt resistance determination. Pochvovedenie, 4, 78-85

Ivushkin, K., Bartholomeus, H., Bregt, A.K., Pulatov, A., Kempen, B., & de Sousa, L. (2019). Global mapping of soil salinity change. Remote Sens. Environ., 231. https://doi.org/10.1016/j.rse.2019.111260.

Jackson, R.D., Idso, S., Reginato, R., & Pinter Jr, P. (1981). Canopy temperature as a crop water stress indicator. Water Resour. Res., 17, 1133-1138. https://doi.org/10.1029/WR017i004p01133.

Jacquemoud, S., & Baret, F. (1990). PROSPECT: A model of leaf optical properties spectra. Remote Sens. Environ., 34, 75-91. https://doi.org/10.1016/0034-4257(90)90100-Z.

Jacquemoud, S.B., C.; Poilve, H.; Frangi, J.P (2000). Comparsion of four radiative transfer models to simulate plant canopies reflectance: direct and inverse mode. Remote Sens. Environ., 74, 471-481. https://doi.org/10.1016/S0034-4257(00)00139-5.

Jamil, A., Riaz, S., Ashraf, M., & Foolad, M.R. (2011). Gene expression profiling of plants under salt stress. Crit. Rev. Plant Sci., 30, 435-458. https://doi.org/10.1080/07352689.2011.605739.

Jarlan, L., Balsamo, G., Lafont, S., Beljaars, A., Calvet, J.C., & Mougin, E. (2008). Analysis of leaf area index in the ECMWF land surface model and impact on latent heat and carbon fluxes: Application to West Africa. J. Geophys. Res. Atmos., 113, D24117. https://doi.org/10.1029/2007jd009370.

Jefferies, R. (1995). Physiology of crop response to drought. Potato ecology and modelling of crops under conditions limiting growth (pp. 61-74): Springer. https://doi.org/10.1007/978-94-011-0051-9.

Ji, L., & Peters, A.J. (2003). Assessing vegetation response to drought in the northern Great Plains using vegetation and drought indices. Remote Sens. Environ., 87, 85-98. https://doi.org/10.1016/S0034-4257(03)00174-3.

Jiang, Y., & Carrow, R.N. (2007). Broadband spectral reflectance models of turfgrass species and cultivars to drought stress. Crop Sci., 47, 1611-1618. https://doi.org/10.2135/cropsci2006.09.0617.

Jiao, W., Wang, L., & McCabe, M.F. (2021). Multi-sensor remote sensing for drought characterization: current status, opportunities and a roadmap for the future. Remote Sens. Environ., 256, 112313. https://doi.org/10.1016/j.rse.2021.112313.

Jin, X., Kumar, L., Li, Z., Feng, H., Xu, X., Yang, G., & Wang, J. (2018). A review of data assimilation of remote sensing and crop models. Eur. J. Agron., 92, 141-152. https://doi.org/10.1016/j.eja.2017.11.002.

Jones, E., & van Vliet, M.T.H. (2018). Drought impacts on river salinity in the southern US: Implications for water scarcity. Sci. Total Environ., 644, 844-853. https://doi.org/10.1016/j.scitotenv.2018.06.373.

Jones, J.W., Hoogenboom, G., Porter, C.H., Boote, K.J., Batchelor, W.D., Hunt, L.A., Wilkens, P.W., Singh, U., Gijsman, A.J., & Ritchie, J.T. (2003). The DSSAT cropping system model. Eur. J. Agron., 18, 235-265. https://doi.org/10.1016/S1161-0301(02)00107-7.

Kalaji, H.M., Račková, L., Paganová, V., Swoczyna, T., Rusinowski, S., & Sitko, K. (2018). Can chlorophyll-a fluorescence parameters be used as bio-indicators to distinguish between drought and salinity stress in Tilia cordata Mill? Environ. Exp. Bot., 152, 149-157. https://doi.org/10.1016/j.envexpbot.2017.11.001.

Kanawapee, N., Sanitchon, J., Lontom, W., & Threerakulpisut, P. (2012). Evaluation of salt tolerance at the seedling stage in rice genotypes by growth performance, ion accumulation, proline and chlorophyll content. Plant Soil, 358, 235-249. https://doi.org/10.1007/s11104-012-1179-6.

Karthikeyan, L., Chawla, I., & Mishra, A.K. (2020). A review of remote sensing applications in agriculture for food security: Crop growth and yield, irrigation, and crop losses. J. Hydrol., 586. https://doi.org/10.1016/j.jhydrol.2020.124905.

Kasampalis, D., Alexandridis, T., Deva, C., Challinor, A., Moshou, D., & Zalidis, G. (2018). Contribution of remote sensing on crop models: A review. J. Imaging, 4. https://doi.org/10.3390/jimaging4040052.

Katschnig, D., Broekman, R., & Rozema, J. (2013). Salt tolerance in the halophyte Salicornia dolichostachya Moss: Growth, morphology and physiology. Environ. Exp. Bot., 92, 32-42. https://doi.org/10.1016/j.envexpbot.2012.04.002.

Keesstra, S., Mol, G., de Leeuw, J., Okx, J., Molenaar, C., de Cleen, M., & Visser, S. (2018). Soil-related sustainable development goals: four concepts to make land degradation neutrality and restoration work. Land, 7, 133. https://doi.org/10.3390/land7040133.

Klemas, V., & Smart, R. (1983). The influence of soil salinity, growth form, and leaf moisture on the spectral radiance of Spartina Alterniflora canopies. Photogramm. Eng. Remote Sens., 49, 77-83. https://www.asprs.org/wp-content/uploads/pers/1983journal/jan/1983_jan_77-83.pdf.

Kogan, F.N. (1995a). Application of vegetation index and brightness temperature for drought detection. Adv. Space Res., 15, 91-100. https://doi.org/10.1016/0273-1177(95)00079-T.

Kogan, F.N. (1995b). Droughts of the late 1980s in the United-States as derived from NOAA polar-orbiting satellite data. Bull. Am. Meteorol. Soc., 76, 655-668. https://doi.org/10.1175/1520-0477(1995)076<0655:Dotlit>2.0.Co;2.

Kogan, F.N. (1997). Global drought watch from space. Bull. Am. Meteorol. Soc., 78, 621-636. https://doi.org/10.1175/1520-0477(1997)078<0621:Gdwfs>2.0.Co;2.

Koohafkan, P. (2012). Water and cereals in drylands. Routledge. http://dx.doi.org/10.1017/S0014479709990366.

Kousik, A., Aditya Pratap, S., Saju, A., Subhasis, M., & Sujaya, D. (2022). Drought stress: manifestation and mechanisms of alleviation in plants. Drought - Impacts and Management. Rijeka: IntechOpen. https://doi.org/10.5772/intechopen.102780.

Kovar, M., Brestic, M., Sytar, O., Barek, V., Hauptvogel, P., & Zivcak, M. (2019). Evaluation of hyperspectral reflectance parameters to assess the leaf water content in soybean. Water, 11. https://doi.org/10.3390/w11030443.

Kramp, R.E., Liancourt, P., Herberich, M.M., Saul, L., Weides, S., Tielborger, K., & Majekova, M. (2022). Functional traits and their plasticity shift from tolerant to avoidant under extreme drought. Ecology, 103, e3826. https://doi.org/10.1002/ecy.3826.

Kriston-Vizi, J., Umeda, M., & Miyamoto, K. (2008). Assessment of the water status of mandarin and peach canopies using visible multispectral imagery. Biosyst. Eng., 100, 338-345. https://doi.org/10.1016/j.biosystemseng.2008.04.001.

Lassalle, G. (2021). Monitoring natural and anthropogenic plant stressors by hyperspectral remote sensing: Recommendations and guidelines based on a meta-review. Sci. Total Environ., 788, 147758. https://doi.org/10.1016/j.scitotenv.2021.147758.

Lassalle, G., Fabre, S., Credoz, A., Hédacq, R., Borderies, P., Bertoni, G., Erudel, T., Buffan-Dubau, E., Dubucq, D., & Elger, A. (2019). Detection and discrimination of various oil-contaminated soils using vegetation reflectance. Sci. Total Environ., 655, 1113-1124. https://doi.org/10.1016/j.scitotenv.2018.11.314.

Lavorel, S., & Garnier, E. (2002). Predicting changes in community composition and ecosystem functioning from plant traits: revisiting the Holy Grail. Funct. Ecol., 16, 545-556. https://doi.org/10.1046/j.1365-2435.2002.00664.x.

Lavorel, S., & Grigulis, K. (2012). How fundamental plant functional trait relationships scale-up to trade-offs and synergies in ecosystem services. J. Ecol., 100, 128-140. https://doi.org/10.1111/j.1365-2745.2011.01914.x.

Lazarevic, B., Satovic, Z., Nimac, A., Vidak, M., Gunjaca, J., Politeo, O., & Carovic-Stanko, K. (2021). Application of phenotyping methods in detection of drought and salinity stress in Basil (Ocimum basilicum L.). Front. Plant Sci., 12, 629441. https://doi.org/10.3389/fpls.2021.629441.

Le Hegarat-Mascle, S., Quesney, A., Vidal-Madjar, D., Taconet, O., Normand, M., & Loumagne, C. (2000). Land cover discrimination from multitemporal ERS images and multispectral Landsat images: A study case in an agricultural area in France. Int. J. Remote Sens., 21, 435-456. https://doi.org/10.1080/014311600210678.

Leng, G., & Hall, J. (2019). Crop yield sensitivity of global major agricultural countries to droughts and the projected changes in the future. Sci. Total Environ., 654, 811-821. https://doi.org/10.1016/j.scitotenv.2018.10.434.

Leone, A., Menenti, M., Buondonno, A., Letizia, A., Maffei, C., & Sorrentino, G. (2007). A field experiment on spectrometry of crop response to soil salinity. Agric. Water Manag., 89, 39-48. https://doi.org/10.1016/j.agwat.2006.12.004.

Lesk, C., Rowhani, P., & Ramankutty, N. (2016). Influence of extreme weather disasters on global crop production. Nature, 529, 84-87. https://doi.org/10.1038/nature16467.

Levy, D. (1992). The response of potatoes (Solunum tuberosum L.) to salinity: plant growth and tuber yields in the arid desert of Israel. Ann. Appl. Biol., 120, 547-555. https://doi.org/10.1111/j.1744-7348.1992.tb04914.x.

Li, J., Liu, Z., Lei, X., & Wang, L. (2021). Distributed fusion of heterogeneous remote sensing and social media data: A review and new developments. Proc. IEEE, 109, 1350-1363. https://doi.org/10.1109/JPROC.2021.3079176.

Li, P., Wu, J., & Qian, H. (2016). Regulation of secondary soil salinization in semi-arid regions: a simulation research in the Nanshantaizi area along the Silk Road, northwest China. Environ. Earth Sci., 75. https://doi.org/10.1007/s12665-016-5381-3.

Li, W., Migliavacca, M., Forkel, M., Denissen, J.M.C., Reichstein, M., Yang, H., Duveiller, G., Weber, U., & Orth, R. (2022). Widespread increasing vegetation sensitivity to soil moisture. Nature Commun., 13, 3959. https://doi.org/10.1038/s41467-022-31667-9.

Liang, S.L.W., J. D. (2020). Chapter 11 - Fraction of absorbed photosynthetically active radiation. In S. Liang, & J. Wang (Eds.), Advanced Remote Sensing (Second Edition) (pp. 447-476): Academic Press. https://doi.org/10.1016/B978-0-12-815826-5.00011-8.

Liao, Q., Gu, S.J., Kang, S.Z., Du, T.S., Tong, L., Wood, J.D., & Ding, R.S. (2022). Mild water and salt stress improve water use efficiency by decreasing stomatal conductance via osmotic adjustment in field maize. Sci. Total Environ., 805, 150364. https://doi.org/10.1016/j.scitotenv.2021.150364.

Lins, E., Nunes, F., Gasparoto, M., Junior, J., Bagnato, V., & Marcassa, L. (2005). Fluorescence spectroscopy to detect water stress in orange trees. In, SBMO/IEEE MTT-S International Conference on Microwave and Optoelectronics, 2005. (pp. 534-537): IEEE. https://doi.org/10.1109/IMOC.2005.1580118.

Liu, H.Q., & Huete, A. (1995). A feedback based modification of the NDVI to minimize canopy background and atmospheric noise. IEEE Trans. Geosci. Remote Sens., 33, 457-465. https://doi.org/10.1109/TGRS.1995.8746027.

Liu, X., Zhu, X., Pan, Y., Li, S., Liu, Y., & Ma, Y. (2016). Agricultural drought monitoring: progress, challenges, and prospects. J. Geogr. Sci., 26, 750-767. https://doi.org/10.1007/s11442-016-1297-9.

López-Lozano, R., & Baruth, B. (2019). An evaluation framework to build a cost-efficient crop monitoring system. Experiences from the extension of the European crop monitoring system. Agric. Syst., 168, 231-246. https://doi.org/10.1016/j.agsy.2018.04.002.

López-Lozano, R., Duveiller, G., Seguini, L., Meroni, M., García-Condado, S., Hooker, J., Leo, O., & Baruth, B. (2015). Towards regional grain yield forecasting with 1km-resolution EO biophysical products: strengths and limitations at pan-European level. Agric. For. Meteorol., 206, 12-32. https://doi.org/10.1016/j.agrformet.2015.02.021.

López-Serrano, L., Penella, C., San-Bautista, A., López-Galarza, S., & Calatayud, A. (2017). Physiological changes of pepper accessions in response to salinity and water stress. Span. J. Agric. Res., 15, e0804. https://doi.org/10.5424/sjar/2017153-11147.

Lorenz, C., & Kunstmann, H. (2012). The hydrological cycle in three state-of-the-art reanalyses: Intercomparison and performance analysis. J. Hydrometeorol., 13, 1397-1420. https://doi.org/10.1175/JHM-D-11-088.1.

Lu, B., Dao, P.D., Liu, J., He, Y., & Shang, J. (2020a). Recent advances of hyperspectral imaging technology and applications in agriculture. Remote Sens., 12, 2659-2703. https://doi.org/10.3390/rs12162659.

Lu, J., Carbone, G.J., Huang, X., Lackstrom, K., & Gao, P. (2020b). Mapping the sensitivity of agriculture to drought and estimating the effect of irrigation in the United States, 1950–2016. Agric. For. Meteorol., 292-293, 108124. https://doi.org/10.1016/j.agrformet.2020.108124.

Maas, E.V., & Grattan, S. (1999). Crop yields as affected by salinity. Agric. Drain., 38, 55-108. https://doi.org/10.2134/agronmonogr38.c3.

Maas, S.J. (1988). Use of remotely-sensed information in agricultural crop growth models. Ecol. Model., 41, 247-268. https://doi.org/10.1016/0304-3800(88)90031-2.

Madadgar, S., AghaKouchak, A., Farahmand, A., & Davis, S.J. (2017). Probabilistic estimates of drought impacts on agricultural production. Geophys. Res. Lett., 44, 7799-7807. https://doi.org/10.1002/2017gl073606.

Maes, W.H., Achten, W.M.J., Reubens, B., & Muys, B. (2011). Monitoring stomatal conductance of Jatropha curcas seedlings under different levels of water shortage with infrared thermography. Agric. For. Meteorol., 151, 554-564. https://doi.org/10.3390/plants10071345.

Maes, W.H., & Steppe, K. (2019). Perspectives for Remote Sensing with Unmanned Aerial Vehicles in Precision Agriculture. Trends Plant Sci., 24, 152-164. https://doi.org/10.1016/j.tplants.2018.11.007.

Mahajan, S., & Tuteja, N. (2005). Cold, salinity and drought stresses: an overview. Arch. Biochem. Biophys., 444, 139-158. https://doi.org/10.1016/j.abb.2005.10.018.

Mahmood, U., Hussain, S., Hussain, S., Ali, B., Ashraf, U., Zamir, S., Al-Robai, S.A., Alzahrani, F.O., Hano, C., & El-Esawi, M.A. (2021). Morpho-physio-biochemical and molecular responses of maize hybrids to salinity and waterlogging during stress and recovery phase. Plants (Basel), 10, 1345. https://doi.org/10.3390/plants10071345.

Mantri, N., Patade, V., Penna, S., Ford, R., & Pang, E. (2012). Abiotic stress responses in plants: present and future. Abiotic stress responses in plants: metabolism, productivity and sustainability (pp. 1-19). https://doi.org/10.1007/978-1-4614-0634-1_1.

Martin, A.R., Isaac, M.E., & Manning, P. (2015). REVIEW: Plant functional traits in agroecosystems: a blueprint for research. J. Appl. Ecol., 52, 1425-1435. https://doi.org/10.1111/1365-2664.12526.

Masante D., B.P., McCormick N. (2018). Drought in Central-Northern Europe – August 2018. In (pp. 1-13): Report of the Copernicus European Drought Observatory (EDO) and Emergency Response Coordination Center (ERCC) Analytical Team https://edo.jrc.ec.europa.eu/documents/news/EDODroughtNews201808_Central_North_Europe.pdf.

Masuka, B., Araus, J.L., Das, B., Sonder, K., & Cairns, J.E. (2012). Phenotyping for abiotic stress tolerance in maize. J. Integr. Plant Biol., 54, 238-249. https://doi.org/10.1111/j.1744-7909.2012.01118.x.

Matese, A., Baraldi, R., Berton, A., Cesaraccio, C., Di Gennaro, S.F., Duce, P., Facini, O., Mameli, M.G., Piga, A., & Zaldei, A. (2018). Estimation of water stress in grapevines using proximal and remote sensing methods. Remote Sens., 10. https://doi.org/10.3390/rs10010114.

McKee, T.B., Doesken, N.J., & Kleist, J.R. (1993). The relationship of drought frequency and duration to time scales. 8th Conference on Applied Climatology, 179-184. https://www.droughtmanagement.info/literature/AMS_Relationship_Drought_Frequency_Duration_Time_Scales_1993.pdf.

Meena, M.D., Yadav, R.K., Narjary, B., Yadav, G., Jat, H.S., Sheoran, P., Meena, M.K., Antil, R.S., Meena, B.L., Singh, H.V., Singh Meena, V., Rai, P.K., Ghosh, A., & Moharana, P.C. (2019). Municipal solid waste (MSW): Strategies to improve salt affected soil sustainability: A review. Waste Manage., 84, 38-53. https://doi.org/10.1016/j.wasman.2018.11.020.

Mehrabi, Z., Delzeit, R., Ignaciuk, A., Levers, C., Braich, G., Bajaj, K., Amo-Aidoo, A., Anderson, W., Balgah, R.A., Benton, T.G., Chari, M.M., Ellis, E.C., Gahi, N.Z., Gaupp, F., Garibaldi, L.A., Gerber, J.S., Godde, C.M., Grass, I., Heimann, T., Hirons, M., Hoogenboom, G., Jain, M., James, D., Makowski, D., Masamha, B., Meng, S., Monprapussorn, S., Muller, D., Nelson, A., Newlands, N.K., Noack, F., Oronje, M., Raymond, C., Reichstein, M., Rieseberg, L.H., Rodriguez-Llanes, J.M., Rosenstock, T., Rowhani, P., Sarhadi, A., Seppelt, R., Sidhu, B.S., Snapp, S., Soma, T., Sparks, A.H., Teh, L., Tigchelaar, M., Vogel, M.M., West, P.C.,

Wittman, H., & You, L. (2022). Research priorities for global food security under extreme events. One Earth, 5, 756-766. https://doi.org/10.1016/j.oneear.2022.06.008.

Metternicht, G.I., & Zinck, J.A. (2003). Remote sensing of soil salinity: potentials and constraints. Remote Sens. Environ., 85, 1-20. https://doi.org/10.1016/s0034-4257(02)00188-8.

Meyer, S.J., Hubbard, K.G., & Wilhite, D.A. (1993). A crop-specific drought index for corn: I. Model development and validation. Agron. J., 85, 388-395. https://doi.org/10.2134/agronj1993.00021962008500020040x.

Mi, N., Cai, F., Zhang, Y.S., Ji, R.P., Zhang, S.J., & Wang, Y. (2018). Differential responses of maize yield to drought at vegetative and reproductive stages. Plant Soil Environ., 64, 260-267. https://doi.org/10.17221/141/2018-Pse.

Mimi, Z.A., & Jamous, S.A. (2010). Climate change and agricultural water demand: Impacts and adaptations. Afr. J. Environ. Sci. Technol., 4, 183-191. https://doi.org/10.4314/ajest.v4i4.56351.

Mishra, A.K., Ines, A.V.M., Das, N.N., Khedun, C.P., Singh, V.P., Sivakumar, B., & Hansen, J.W. (2015). Anatomy of a local-scale drought: Application of assimilated remote sensing products, crop model, and statistical methods to an agricultural drought study. J. Hydrol., 526, 15-29. https://doi.org/10.1016/j.jhydrol.2014.10.038.

Mittler, R. (2006). Abiotic stress, the field environment and stress combination. Trends Plant Sci., 11, 15-19. https://doi.org/10.1016/j.tplants.2005.11.002.

Miyashita, K., Tanakamaru, S., Maitani, T., & Kimura, K. (2005). Recovery responses of photosynthesis, transpiration, and stomatal conductance in kidney bean following drought stress. Environ. Exp. Bot., 53, 205-214. https://doi.org/10.1016/j.envexpbot.2004.03.015.

Mkhabela, M.S., Bullock, P., Raj, S., Wang, S., & Yang, Y. (2011). Crop yield forecasting on the Canadian Prairies using MODIS NDVI data. Agric. For. Meteorol., 151, 385-393. https://doi.org/10.1016/j.agrformet.2010.11.012.

Mohammed, W.E., & Algarni, S. (2020). A remote sensing study of spatiotemporal variations in drought conditions in northern Asir, Saudi Arabia. Environ. Monit. Assess., 192, 784. https://doi.org/10.1007/s10661-020-08771-8.

Mokhtari M. H., Sodaeezadeh H. R., Hakimzadeh M. A., & F., T. (2014). Application of visible and near-infrared spectrophotometry for detecting salinity effects on wheat leaves (Triticum aestivum L.). Agric. Eng. Int: CIRG Journal, 16, 35-42. https://cigrjournal.org/index.php/Ejounral/article/view/2814/1964.

Möller, M., Alchanatis, V., Cohen, Y., Meron, M., Tsipris, J., Naor, A., Ostrovsky, V., Sprintsin, M., & Cohen, S. (2007). Use of thermal and visible imagery for estimating crop water status of irrigated grapevine. J. Exp. Bot., 58, 827-838. https://doi.org/10.1093/jxb/erl115.

Moreno-Martínez, Á., Camps-Valls, G., Kattge, J., Robinson, N., Reichstein, M., van Bodegom, P., Kramer, K., Cornelissen, J.H.C., Reich, P., Bahn, M., Niinemets, Ü., Peñuelas, J., Craine, J.M., Cerabolini, B.E.L., Minden, V., Laughlin, D.C., Sack, L., Allred, B., Baraloto, C., Byun, C., Soudzilovskaia, N.A., & Running, S.W. (2018). A methodology to derive global maps of leaf traits using remote sensing and climate data. Remote Sens. Environ., 218, 69-88. https://doi.org/10.1016/j.rse.2018.09.006.

Mosley, L.M. (2015). Drought impacts on the water quality of freshwater systems; review and integration. Earth Sci. Rev., 140, 203-214. https://doi.org/10.1016/j.earscirev.2014.11.010.

Motohka, T., Nasahara, K.N., Oguma, H., & Tsuchida, S. (2010). Applicability of green-red vegetation index for remote sensing of vegetation phenology. In, Remote Sens. (pp. 2369-2387). https://doi.org/10.3390/rs2102369.

Movahhedi Dehnavi, M., Zarei, T., Khajeeyan, R., & Merajipoor, M. (2017). Drought and salinity impacts on bread wheat in a hydroponic culture: A physiological comparison. J. Plant Physiol. Breed., 7, 61-74. https://journals.tabrizu.ac.ir/article_6357_3ae4427db5a73b02b33f0f30fde7e8ae.pdf.

Mukhopadhyay, R., Sarkar, B., Jat, H.S., Sharma, P.C., & Bolan, N.S. (2021). Soil salinity under climate change: challenges for sustainable agriculture and food security. J. Environ. Manage., 280, 111736. https://doi.org/10.1016/j.jenvman.2020.111736.

Mulder, M., Hack-ten Broeke, M., Bartholomeus, R., van Dam, J., Heinen, M., van Bakel, J., Walvoort, D., Kroes, J., Hoving, I., Holshof, G., Schaap, J., Spruijt, J., Supit, I., de Wit, A., Hendriks, R., de Haan, J., van der Voort, M., & van Walsum, P. (2018). Waterwijzer Landbouw: instrumentarium voor kwantificeren van effecten van waterbeheer en klimaat op landbouwproductie. Stowa. https://edepot.wur.nl/464525.

Munns, R. (2002). Comparative physiology of salt and water stress. Plant Cell Environ., 25, 239-250. https://doi.org/10.1046/j.0016-8025.2001.00808.x.

Munns, R. (2005). Genes and salt tolerance: bringing them together. New Phytol., 167, 645-663. https://doi.org/10.1111/j.1469-8137.2005.01487.x.

Munns, R., James, R.A., Sirault, X.R., Furbank, R.T., & Jones, H.G. (2010). New phenotyping methods for screening wheat and barley for beneficial responses to water deficit. J. Exp. Bot., 61, 3499-3507. https://doi.org/10.1093/jxb/erq199.

Munns, R., & Tester, M. (2008). Mechanisms of salinity tolerance. Annu. Rev. Plant Biol., 59, 651-681. https://doi.org/10.1146/annurev.arplant.59.032607.092911.

Mura, M.D., Prasad, S., Pacifici, F., Gamba, P., Chanussot, J., & Benediktsson, J.A. (2015). Challenges and opportunities of ultimodality and data fusion in remote sensing. Proc. IEEE, 103, 1585-1601. https://doi.org/10.1109/JPROC.2015.2462751.

Mwamahonje, A., Eleblu, J.S.Y., Ofori, K., Feyissa, T., Deshpande, S., & Tongoona, P. (2021). Evaluation of traits' performance contributing to drought tolerance in sorghum. Agronomy, 11. https://doi.org/10.3390/agronomy11091698.

Myneni, R.B., Hoffman, S., Knyazikhin, Y., Privette, J.L., Glassy, J., Tian, Y., Wang, Y., Song, X., Zhang, Y., Smith, G.R., Lotsch, A., Friedl, M., Morisette, J.T., Votava, P., Nemani, R.R., & Running, S.W. (2002). Global products of vegetation leaf area and fraction absorbed PAR from year one of MODIS data. Remote Sens. Environ., 83, 214-231. https://doi.org/10.1016/S0034-4257(02)00074-3.

Naumann, J.C., Anderson, J.E., & Young, D.R. (2008a). Linking physiological responses, chlorophyll fluorescence and hyperspectral imagery to detect salinity stress using the physiological reflectance index in the coastal shrub, Myrica cerifera. Remote Sens. Environ., 112, 3865-3875. https://doi.org/10.1016/j.rse.2008.06.004.

Naumann, J.C., Young, D.R., & Anderson, J.E. (2007). Linking leaf chlorophyll fluorescence properties to physiological responses for detection of salt and drought stress in coastal plant species. Physiol. Plant., 131, 422-433. https://doi.org/10.1111/j.1399-3054.2007.00973.x.

Naumann, J.C., Young, D.R., & Anderson, J.E. (2008b). Leaf chlorophyll fluorescence, reflectance, and physiological response to freshwater and saltwater flooding in the evergreen shrub, Myrica cerifera. Environ. Exp. Bot., 63, 402-409. https://doi.org/10.1016/j.envexpbot.2007.12.008.

Nawar, S., Buddenbaum, H., & Hill, J. (2015). Digital mapping of soil properties using multivariate statistical analysis and ASTER data in an arid region. In, Remote Sens. (pp. 1181-1205). https://doi.org/10.3390/rs70201181.

NCEI, & NOAA (2021). Monthly drought report for annual 2021. https://www.ncei.noaa.gov/access/monitoring/monthly-report/drought/202113.

Negacz, K., Bruning, B., & Vellinga, P. (2021). Achieving multiple sustainable development goals through saline agriculture. Future of Sustainable Agriculture in Saline Environments (pp. 13-28). https://doi.org/10.1201/9781003112327-2.

Negacz, K., Malek, Ž., de Vos, A., & Vellinga, P. (2022). Saline soils worldwide: Identifying the most promising areas for saline agriculture. J. Arid Environ., 203. https://doi.org/10.1016/j.jaridenv.2022.104775.

Neilson, E.H., Edwards, A.M., Blomstedt, C., Berger, B., Møller, B.L., & Gleadow, R.M. (2015). Utilization of a high-throughput shoot imaging system to examine the dynamic phenotypic responses of a C4 cereal crop plant to nitrogen and water deficiency over time. J. Exp. Bot., 66, 1817-1832. https://doi.org/10.1093/jxb/eru526.

Nemeskéri, E., Molnár, K., Vígh, R., Nagy, J., & Dobos, A. (2015). Relationships between stomatal behaviour, spectral traits and water use and productivity of green peas (Pisum sativum L.) in dry seasons. Acta Physiol. Plant, 37, 34. https://doi.org/10.1007/s11738-015-1776-0.

Niinemets, U. (2015). Is there a species spectrum within the world-wide leaf economics spectrum? Major variations in leaf functional traits in the Mediterranean sclerophyll Quercus ilex. New Phytol., 205, 79-96. https://doi.org/10.1111/nph.13001.

Niu, X., Ray A. Bressan, Paul M. Hasegawa, & Pardo, J.M. (1995). lon homeostasis in NaCl stress environments. Plant Physiol., 109, 735-742. https://doi.org/10.1104/pp.109.3.735.

Oki, T., & Kanae, S. (2006). Global hydrological cycles and world water resources. Science, 313, 1068-1072. https://doi.org/10.1126/science.1128845.

Oosterbaan, R.J. (2019). The potato variety "927" tested at the Salt Farm Texel,The Netherlands, proved to be highly salt tolerant. In. https://www.researchgate.net/profile/Rj-Oosterbaan/publication/335789831_The_potato_variety_927_tested_at_the_Salt_Farm_TexelThe_Netherlands_proved_to_be_highly_salt_tolerant/links/5d7b474c4585155f1e3f0133/The-potato-variety-927-tested-at-the-Salt-Farm-Texel-The-Netherlands-proved-to-be-highly-salt-tolerant.pdf.

Ors, S., & Suarez, D.L. (2017). Spinach biomass yield and physiological response to interactive salinity and water stress. Agric. Water Manag., 190, 31-41. https://doi.org/10.1016/j.agwat.2017.05.003.

Oshunsanya, S.O., Nwosu, N.J., & Li, Y. (2019). Abiotic stress in agricultural crops under climatic conditions. Sustainable Agriculture, Forest and Environmental Management (pp. 71-100). https://doi.org/10.1007/978-981-13-6830-1_3.

Oukarroum, A., Schansker, G., & Strasser, R.J. (2009). Drought stress effects on photosystem I content and photosystem II thermotolerance analyzed using Chl a fluorescence kinetics in barley varieties differing in their drought tolerance. Physiol. Plant., 137, 188-199. https://doi.org/10.1111/j.1399-3054.2009.01273.x.

Palosuo, T., Kersebaum, K.C., Angulo, C., Hlavinka, P., Moriondo, M., Olesen, J.E., Patil, R.H., Ruget, F., Rumbaur, C., Takáč, J., Trnka, M., Bindi, M., Çaldağ, B., Ewert, F., Ferrise, R., Mirschel, W., Şaylan, L., Šiška, B., & Rötter, R. (2011). Simulation of winter wheat yield and its variability in different climates of Europe: A comparison of eight crop growth models. Eur. J. Agron., 35, 103-114. https://doi.org/10.1016/j.eja.2011.05.001.

Panigada, C., Rossini, M., Meroni, M., Cilia, C., Busetto, L., Amaducci, S., Boschetti, M., Cogliati, S., Picchi, V., Pinto, F., Marchesi, A., & Colombo, R. (2014). Fluorescence, PRI and canopy temperature for water stress detection in cereal crops. Int. J. Appl. Earth Obs. Geoinf., 30, 167-178. https://doi.org/10.1016/j.jag.2014.02.002.

Pankova, Y.I., & Konyushkova, M.V. (2014). Effect of global warming on soil salinity of the arid regions. Russ. Agric. Sci., 39, 464-467. https://doi.org/10.3103/s1068367413060165.

Patane, C., Saita, A., & Sortino, O. (2013). Comparative effects of salt and water stress on seed germination and early embryo growth in two cultivars of sweet sorghum. J. Agron. Crop Sci., 199, 30-37. https://doi.org/10.1111/j.1439-037X.2012.00531.x.

Paul, K., Pauk, J., Kondic-Spika, A., Grausgruber, H., Allahverdiyev, T., Sass, L., & Vass, I. (2019). Co-occurrence of mild salinity and drought synergistically enhances biomass and grain retardation in wheat. Front. Plant Sci., 10, 501. https://doi.org/10.3389/fpls.2019.00501.

Peguero-Pina, J.J., Morales, F., Flexas, J., Gil-Pelegrín, E., & Moya, I. (2008). Photochemistry, remotely sensed physiological reflectance index and de-epoxidation state of the xanthophyll

cycle in Quercus coccifera under intense drought. Oecologia, 156, 1. https://doi.org/10.1007/s00442-007-0957-y.

Peñuelas, J., Filella, I., Biel, C.,, Serrano, L., & Save, R. (1993). The reflectance at the 950–970 nm region as an indicator of plant water status. Int. J. Remote Sens., 1887-1905. https://doi.org/10.1080/01431169308954010.

Pérez-Harguindeguy, N., Díaz, S., Garnier, E., Lavorel, S., Poorter, H., Jaureguiberry, P., Bret-Harte, M.S., Cornwell, W.K., Craine, J.M., Gurvich, D.E., Urcelay, C., Veneklaas, E.J., Reich, P.B., Poorter, L., Wright, I.J., Ray, P., Enrico, L., Pausas, J.G., de Vos, A.C., Buchmann, N., Funes, G., Quétier, F., Hodgson, J.G., Thompson, K., Morgan, H.D., ter Steege, H., Sack, L., Blonder, B., Poschlod, P., Vaieretti, M.V., Conti, G., Staver, A.C., Aquino, S., & Cornelissen, J.H.C. (2013). New handbook for standardised measurement of plant functional traits worldwide. Aust. J. Bot., 61, 167-234. https://doi.org/10.1071/bt12225.

Pérez-Priego, O., Zarco-Tejada, P.J., Miller, J.R., Sepulcre-Cantó, G., & Fereres, E. (2005). Detection of water stress in orchard trees with a high-resolution spectrometer through chlorophyll fluorescence in-filling of the O/sub 2/-A band. IEEE Trans. Geosci. Remote Sens., 43, 2860-2869. https://doi.org/10.1109/TGRS.2005.857906.

Perianes-Rodriguez, A., Waltman, L., & Van Eck, N.J. (2016). Constructing bibliometric networks: A comparison between full and fractional counting. Journal of Informetrics, 10, 1178-1195. https://doi.org/10.1016/j.joi.2016.10.006.

Perry de Louw, V.K., Harry Massop, Ab Veldhuizen (2020). Beregening: Deltafact. In. Amersfoort Alterra - Soil, water and land use. https://library.wur.nl/WebQuery/wurpubs/fulltext/535694.

Pires, I.S., Negrao, S., Oliveira, M.M., & Purugganan, M.D. (2015). Comprehensive phenotypic analysis of rice (Oryza sativa) response to salinity stress. Physiol. Plant., 155, 43-54. https://doi.org/10.1111/ppl.12356.

Poss, J., Russell, W., & Grieve, C. (2006). Estimating yields of salt-and water-stressed forages with remote sensing in the visible and near infrared. J. Environ. Qual., 35, 1060-1071. https://doi.org/10.2134/jeq2005.0204.

Qadir, M., Quillerou, E., Nangia, V., Murtaza, G., Singh, M., Thomas, R.J., Drechsel, P., & Noble, A.D. (2014). Economics of salt-induced land degradation and restoration. Nat. Resour. Forum, 38, 282-295. https://doi.org/10.1111/1477-8947.12054.

Radanielson, A.M., Gaydon, D.S., Li, T., Angeles, O., & Roth, C.H. (2018). Modeling salinity effect on rice growth and grain yield with ORYZA v3 and APSIM-Oryza. Eur. J. Agron., 100, 44-55. https://doi.org/10.1016/j.eja.2018.01.015.

Radwan, T.M., Blackburn, G.A., Whyatt, J.D., & Atkinson, P.M. (2021). Global land cover trajectories and transitions. Sci. Rep., 11, 12814. https://doi.org/10.1038/s41598-021-92256-2.

Rahimzadeh-Bajgiran, P., Omasa, K., & Shimizu, Y. (2012). Comparative evaluation of the Vegetation Dryness Index (VDI), the Temperature Vegetation Dryness Index (TVDI) and the improved TVDI (iTVDI) for water stress detection in semi-arid regions of Iran. ISPRS J. Photogramm. Remote Sens., 68, 1-12. https://doi.org/10.1016/j.isprsjprs.2011.10.009.

Rahimzadeh Bajgiran, P., Darvishsefat, A.A., Khalili, A., & Makhdoum, M.F. (2008). Using AVHRR-based vegetation indices for drought monitoring in the Northwest of Iran. J. Arid Environ., 72, 1086-1096. https://doi.org/10.1016/j.jaridenv.2007.12.004.

Rahman, M.H., Lund, T., & Bryceson, I. (2011). Salinity impacts on agro-biodiversity in three coastal, rural villages of Bangladesh. Ocean Coast. Manag., 54, 455-468. https://doi.org/10.1016/j.ocecoaman.2011.03.003.

Rahman, M.M. (2020). Impact of increased salinity on the plant community of the Sundarbans Mangrove of Bangladesh. Community Ecol., 21, 273-284. https://doi.org/10.1007/s42974-020-00028-1.

Ramírez-Valiente, J.A., Deacon, N.J., Etterson, J., Center, A., Sparks, J.P., Sparks, K.L., Longwell, T., Pilz, G., & Cavender-Bares, J. (2018). Natural selection and neutral evolutionary processes contribute to genetic divergence in leaf traits across a precipitation gradient in the tropical oak Quercus oleoides. Mol. Ecol., 27, 2176-2192. https://doi.org/10.1111/mec.14566.

Ranjbarfordoei, A., Samson, R., & Van Damme, P. (2006). Chlorophyll fluorescence performance of sweet almond [Prunus dulcis (Miller) D. Webb] in response to salinity stress induced by NaCl. Photosynthetica, 44, 513-522. https://doi.org/10.1007/s11099-006-0064-z.

Rauff, K.O., & Bello, R. (2015). A review of crop growth simulation models as tools for agricultural meteorology. Agricultural Sciences, 6, 1098-1105. https://doi.org/10.4236/as.2015.69105.

Reddy, I.N.B.L., Kim, B.-K., Yoon, I.-S., Kim, K.-H., & Kwon, T.-R. (2017). Salt Tolerance in Rice: Focus on Mechanisms and Approaches. Rice Sci., 24, 123-144. https://doi.org/10.1016/j.rsci.2016.09.004.

Renault, D., & Wallender, W.W. (2000). Nutritional water productivity and diets. Agric. Water Manag., 45, 275-296. https://doi.org/10.1016/S0378-3774(99)00107-9.

Rhee, J., Im, J., & Carbone, G.J. (2010). Monitoring agricultural drought for arid and humid regions using multi-sensor remote sensing data. Remote Sens. Environ., 114, 2875-2887. https://doi.org/10.1016/j.rse.2010.07.005.

Richards, L.A. (1954). Diagnosis and improvement of saline and alkali Soils. Soil Sci., 78, 154. https://journals.lww.com/soilsci/Citation/1954/08000/Diagnosis_and_Improvement_of_Saline_and_Alkali.12.aspx.

Richter, K., Rischbeck, P., Eitzinger, J., Schneider, W., Suppan, F., & Weihs, P. (2008). Plant growth monitoring and potential drought risk assessment by means of Earth observation data. Int. J. Remote Sens., 29, 4943-4960. https://doi.org/10.1080/01431160802036268.

Rischbeck, P., Elsayed, S., Mistele, B., Barmeier, G., Heil, K., & Schmidhalter, U. (2016). Data fusion of spectral, thermal and canopy height parameters for improved yield prediction of drought stressed spring barley. Eur. J. Agron., 78, 44-59. https://doi.org/10.1016/j.eja.2016.04.013.

Römer, C., Wahabzada, M., Ballvora, A., Pinto, F., Rossini, M., Panigada, C., Behmann, J., Léon, J., Thurau, C., & Bauckhage, C. (2012). Early drought stress detection in cereals: simplex volume maximisation for hyperspectral image analysis. Funct. Plant Biol., 39, 878-890. https://doi.org/10.1071/FP12060.

Romero-Trigueros, C., Nortes, P.A., Alarcón, J.J., Hunink, J.E., Parra, M., Contreras, S., Droogers, P., & Nicolás, E. (2017). Effects of saline reclaimed waters and deficit irrigation on Citrus physiology assessed by UAV remote sensing. Agric. Water Manag., 183, 60-69. https://doi.org/10.1016/j.agwat.2016.09.014.

Rondeaux, G., Steven, M., & Baret, F. (1996). Optimization of soil-adjusted vegetation indices. Remote Sens. Environ., 55, 95-107. https://doi.org/10.1016/0034-4257(95)00186-7.

Rosenzweig, C., Elliott, J., Deryng, D., Ruane, A.C., Muller, C., Arneth, A., Boote, K.J., Folberth, C., Glotter, M., Khabarov, N., Neumann, K., Piontek, F., Pugh, T.A., Schmid, E., Stehfest, E., Yang, H., & Jones, J.W. (2014). Assessing agricultural risks of climate change in the 21st century in a global gridded crop model intercomparison. Proc. Natl. Acad. Sci. U.S.A., 111, 3268-3273. https://doi.org/10.1073/pnas.1222463110.

Rossini, M., Fava, F., Cogliati, S., Meroni, M., Marchesi, A., Panigada, C., Giardino, C., Busetto, L., Migliavacca, M., & Amaducci, S. (2013). Assessing canopy PRI from airborne imagery to map water stress in maize. ISPRS J. Photogramm. Remote Sens., 86, 168-177. https://doi.org/10.1016/j.isprsjprs.2013.10.002.

Rozema, J., & Flowers, T. (2008). Ecology. Crops for a salinized world. Science, 322, 1478-1480. https://doi.org/10.1126/science.1168572.

Rud, R., Shoshany, M., & Alchanatis, V. (2011). Spectral indicators for salinity effects in crops: a comparison of a new green indigo ratio with existing indices. Remote Sens. Lett., 2, 289-298. https://doi.org/10.1080/01431161.2010.520343.

Rud, R., Shoshany, M., & Alchanatis, V. (2013). Spatial–spectral processing strategies for detection of salinity effects in cauliflower, aubergine and kohlrabi. Biosyst. Eng., 114, 384-396. https://doi.org/10.1016/j.biosystemseng.2012.11.012.

Sack, L., & Buckley, T.N. (2020). Trait multi-functionality in plant stress response. Integr. Comp. Biol., 60, 98-112. https://doi.org/10.1093/icb/icz152.

Salmon, J.M., Friedl, M.A., Frolking, S., Wisser, D., & Douglas, E.M. (2015). Global rain-fed, irrigated, and paddy croplands: A new high resolution map derived from remote sensing, crop inventories and climate data. Int. J. Appl. Earth Obs. Geoinf., 38, 321-334. https://doi.org/10.1016/j.jag.2015.01.014.

Sánchez, E., Scordia, D., Lino, G., Arias, C., Cosentino, S.L., & Nogués, S. (2015). Salinity and water stress effects on biomass production in different Arundo donax L. Clones. Bioenergy Res., 8, 1461-1479. https://doi.org/10.1007/s12155-015-9652-8.

Sankaran, S., Zhou, J.F., Khot, L.R., Trapp, J.J., Mndolwa, E., & Miklas, P.N. (2018). High-throughput field phenotyping in dry bean using small unmanned aerial vehicle based multispectral imagery. Comput. Electron. Agric., 151, 84-92. https://doi.org/10.1016/j.compag.2018.05.034.

Saqib, M., Akhtar, J., Abbas, G., & Nasim, M. (2013). Salinity and drought interaction in wheat (Triticum aestivum L.) is affected by the genotype and plant growth stage. Acta Physiol. Plant, 35, 2761-2768. https://doi.org/10.1007/s11738-013-1308-8.

Sarlikioti, V., Driever, S., & Marcelis, L. (2010). Photochemical reflectance index as a mean of monitoring early water stress. Ann. Appl. Biol., 157, 81-89. https://doi.org/10.1111/j.1744-7348.2010.00411.x.

Satir, O., & Berberoglu, S. (2016). Crop yield prediction under soil salinity using satellite derived vegetation indices. Field Crops Res., 192, 134-143. https://doi.org/10.1016/j.fcr.2016.04.028.

Sayago, S., Ovando, G., & Bocco, M. (2017). Landsat images and crop model for evaluating water stress of rainfed soybean. Remote Sens. Environ., 198, 30-39. https://doi.org/10.1016/j.rse.2017.05.008.

Sayar, R., Bchini, H., Mosbahi, M., & Khemira, H. (2010). Response of durum wheat (Triticum durum Desf.) growth to salt and drought stresses. Czech J. Genet. Plant. Breed., 46, 54-63. https://doi.org/10.17221/85/2009-CJGPB.

Schittenhelm, S., Sourell, H., & Lopmeier, F.J. (2006). Drought resistance of potato cultivars with contrasting canopy architecture. Eur. J. Agron., 24, 193-202. https://doi.org/10.1016/j.eja.2005.05.004.

Schlemmer, M.R., Francis, D.D., Shanahan, J.F., & Schepers, J.S. (2005). Remotely measuring chlorophyll content in corn leaves with differing nitrogen levels and relative water content. Agron. J., 97, 106-112. https://doi.org/10.2134/agronj2005.0106.

Schwalm, C.R., Anderegg, W.R.L., Michalak, A.M., Fisher, J.B., Biondi, F., Koch, G., Litvak, M., Ogle, K., Shaw, J.D., Wolf, A., Huntzinger, D.N., Schaefer, K., Cook, R., Wei, Y., Fang, Y., Hayes, D., Huang, M., Jain, A., & Tian, H. (2017). Global patterns of drought recovery. Nature, 548, 202-205. https://doi.org/10.1038/nature23021.

Scott, G., & Rajabifard, A. (2017). Sustainable development and geospatial information: a strategic framework for integrating a global policy agenda into national geospatial capabilities. Geo-Spat. Inf. Sci., 20, 59-76. https://doi.org/10.1080/10095020.2017.1325594.

Sepulcre-Canto, G., Zarco-Tejada, P.J., Jimenez-Munoz, J.C., Sobrino, J.A., de Miguel, E., & Villalobos, F.J. (2006). Detection of water stress in an olive orchard with thermal remote sensing imagery. Agric. For. Meteorol., 136, 31-44. https://doi.org/10.1016/j.agrformet.2006.01.008.

Sepulcre-Canto, G., Zarco-Tejada, P.J., Jimenez-Munoz, J.C., Sobrino, J.A., Soriano, M.A., Fereres, E., Vega, V., & Pastor, M. (2007). Monitoring yield and fruit quality parameters in open-

canopy tree crops under water stress. Implications for ASTER. Remote Sens. Environ., 107, 455-470. https://doi.org/10.1016/j.rse.2006.09.014.

Serbin, S.P., Singh, A., Desai, A.R., Dubois, S.G., Jablonski, A.D., Kingdon, C.C., Kruger, E.L., & Townsend, P.A. (2015). Remotely estimating photosynthetic capacity, and its response to temperature, in vegetation canopies using imaging spectroscopy. Remote Sens. Environ., 167, 78-87. https://doi.org/10.1016/j.rse.2015.05.024.

Serbin, S.P., Singh, A., McNeil, B.E., Kingdon, C.C., & Townsend, P.A. (2016). Spectroscopic determination of leaf morphological and biochemical traits for northern temperate and boreal tree species. Ecol. Appl., 24, 1651-1669. https://doi.org/10.1890/13-2110.1.

Sgherri, C., Navari-Izzo, F., Pardossi, A., Soressi, G., & Izzo, R. (2007). The influence of diluted seawater and ripening stage on the content of antioxidants in fruits of different tomato genotypes. J. Agric. Food Chem., 55, 2452-2458. https://doi.org/10.1021/jf0634451.

Shinozaki, K., Uemura, M., Bailey-Serres, J., Bray, E., & Weretilnyk, E. (2015). Responses to abiotic stress. Wiley Blackwell. ISBN 9781118502198.

Shivers, S.W., Roberts, D.A., & McFadden, J.P. (2019). Using paired thermal and hyperspectral aerial imagery to quantify land surface temperature variability and assess crop stress within California orchards. Remote Sens. Environ., 222, 215-231. https://doi.org/10.1016/j.rse.2018.12.030.

Shrivastava, P., & Kumar, R. (2015). Soil salinity: A serious environmental issue and plant growth promoting bacteria as one of the tools for its alleviation. Saudi J. Biol. Sci., 22, 123-131. https://doi.org/10.1016/j.sjbs.2014.12.001.

Singh, A. (2021). Soil salinization management for sustainable development: A review. J. Environ. Manage., 277, 111383. https://doi.org/10.1016/j.jenvman.2020.111383.

Singh Parihar, J., Justice, C., Soares, J., Leo, O., Kosuth, P., Jarvis, I., Williams, D., Bingfang, W., Latham, J., & Becker-Reshef, I. (2012). GEO-GLAM: A GEOSS-G20 initiative on global agricultural monitoring. In, 39th COSPAR Scientific Assembly (p. 1451). India. https://ui.adsabs.harvard.edu/abs/2012cosp...39.1451S/abstract.

Smith, A.B. (2020). U.S. Billion-dollar Weather and Climate Disasters, 1980 - present (NCEI Accession 0209268). In N.N.C.f.E. Information (Ed.): NOAA National Centers for Environmental Information. https://doi.org/10.25921/stkw-7w73.

Smith, M.N., Stark, S.C., Taylor, T.C., Ferreira, M.L., de Oliveira, E., Restrepo-Coupe, N., Chen, S., Woodcock, T., dos Santos, D.B., & Alves, L.F. (2019). Seasonal and drought-related changes in leaf area profiles depend on height and light environment in an Amazon forest. New Phytol., 222, 1284-1297. https://doi.org/10.1111/nph.15726.

Song, C., White, B.L., & Heumann, B.W. (2011). Hyperspectral remote sensing of salinity stress on red (Rhizophora mangle) and white (Laguncularia racemosa) mangroves on Galapagos Islands. Remote Sens. Lett., 2, 221-230. https://doi.org/10.1080/01431161.2010.514305.

Souza, R., Machado, E., Silva, J., Lagôa, A., & Silveira, J. (2004). Photosynthetic gas exchange, chlorophyll fluorescence and some associated metabolic changes in cowpea (Vigna unguiculata) during water stress and recovery. Environ. Exp. Bot., 51, 45-56. https://doi.org/10.1016/S0098-8472(03)00059-5.

Stagakis, S., González-Dugo, V., Cid, P., Guillén-Climent, M.L., & Zarco-Tejada, P.J. (2012). Monitoring water stress and fruit quality in an orange orchard under regulated deficit irrigation using narrow-band structural and physiological remote sensing indices. ISPRS J. Photogramm. Remote Sens., 71, 47-61. https://doi.org/10.1016/j.isprsjprs.2012.05.003.

Stamatiadis, S., Tsadilas, C., & Schepers, J.S. (2010). Ground-based canopy sensing for detecting effects of water stress in cotton. Plant Soil, 331, 277-287. https://doi.org/10.1007/s11104-009-0252-2.

Steidle Neto, A.J., Lopes, D.d.C., Silva, T.G.F.d., Ferreira, S.O., & Grossi, J.A.S. (2017). Estimation of leaf water content in sunflower under drought conditions by means of spectral reflectance. Eng. Agric. Environ. Food, 10, 104-108. https://doi.org/10.1016/j.eaef.2016.11.006.

Stuyt, L.C.P.M., Blom-Zandstra, M., & Kselik, R. A. L. (2016). Inventarisatie en analyse zouttolerantie van landbouwgewassen op basis van bestaande gegevens. Wageningen Environmental Research rapport. https://doi.org/10.18174/391931.

Stylinski, C., Gamon, J., & Oechel, W. (2002). Seasonal patterns of reflectance indices, carotenoid pigments and photosynthesis of evergreen chaparral species. Oecologia, 131, 366-374. https://doi.org/10.1007/s00442-002-0905-9.

Su, B., Huang, J., Fischer, T., Wang, Y., Kundzewicz, Z.W., Zhai, J., Sun, H., Wang, A., Zeng, X., Wang, G., Tao, H., Gemmer, M., Li, X., & Jiang, T. (2018). Drought losses in China might double between the 1.5 degrees C and 2.0 degrees C warming. Proc. Natl. Acad. Sci. U. S. A., 115, 10600-10605. https://doi.org/10.1073/pnas.1802129115.

Suarez, D.L., Celis, N., Anderson, R.G., & Sandhu, D. (2019). Grape rootstock response to salinity, water and combined salinity and water stresses. Agronomy, 9, 321. https://doi.org/10.3390/agronomy9060321.

Suárez, L., Zarco-Tejada, P., González-Dugo, V., Berni, J., Sagardoy, R., Morales, F., & Fereres, E. (2010). Detecting water stress effects on fruit quality in orchards with time-series PRI airborne imagery. Remote Sens. Environ., 114, 286-298. https://doi.org/10.1016/j.rse.2009.09.006.

Suarez, L., Zarco-Tejada, P.J., Berni, J.A.J., Gonzalez-Dugo, V., & Fereres, E. (2009). Modelling PRI for water stress detection using radiative transfer models. Remote Sens. Environ., 113, 730-744. https://doi.org/10.1016/j.rse.2008.12.001.

Suarez, L., Zarco-Tejada, P.J., Sepulcre-Canto, G., Perez-Priego, O., Miller, J.R., Jimenez-Munoz, J.C., & Sobrino, J. (2008). Assessing canopy PRI for water stress detection with diurnal airborne imagery. Remote Sens. Environ., 112, 560-575. https://doi.org/10.1016/j.rse.2007.05.009.

Summy, Y., Payal, M., Akanksha, D., Akdasbanu, V., Disha, P., & Mohini, P. (2020). Effect of Abiotic Stress on Crops. In H. Mirza, F. Marcelo Carvalho Minhoto Teixeira, F. Masayuki, & N. Thiago Assis Rodrigues (Eds.), Sustainable Crop Production (p. Ch. 1). Rijeka: IntechOpen. https://doi.org/10.5772/intechopen.88434.

Sun, L., Gao, F., Anderson, M.C., Kustas, W.P., Alsina, M.M., Sanchez, L., Sams, B., McKee, L., Dulaney, W., White, W.A., Alfieri, J.G., Prueger, J.H., Melton, F., & Post, K. (2017). Daily mapping of 30 m LAI and NDVI for grape yield prediction in California vineyards. Remote Sens., 9. https://doi.org/10.3390/rs9040317.

Sun, P., Grignetti, A., Liu, S., Casacchia, R., Salvatori, R., Pietrini, F., Loreto, F., & Centritto, M. (2008). Associated changes in physiological parameters and spectral reflectance indices in olive (Olea europaea L.) leaves in response to different levels of water stress. Int. J. Remote Sens., 29, 1725-1743. https://doi.org/10.1080/01431160701373754.

Sytar, O., Brestic, M., Zivcak, M., Olsovska, K., Kovar, M., Shao, H., & He, X. (2017). Applying hyperspectral imaging to explore natural plant diversity towards improving salt stress tolerance. Sci. Total Environ., 578, 90-99. https://doi.org/10.1016/j.scitotenv.2016.08.014.

Tanirbergenov, S., Saljnikov, E., Suleimenov, B., Saparov, A., & Cakmak, D. (2020). Salt affected soils under cotton-based irrigation agriculture in southern Kazakhstan. Zemljiste i biljka, 69, 1-14. https://doi.org/10.5937/ZemBilj2002001T.

Tao, H., Borth, H., Fraedrich, K., Su, B., & Zhu, X. (2014). Drought and wetness variability in the Tarim River Basin and connection to large-scale atmospheric circulation. Int. J. Climatol., 34, 2678-2684. https://doi.org/10.1002/joc.3867.

Tedeschi, A., Lavini, A., Riccardi, M., Pulvento, C., & d'Andria, R. (2011). Melon crops (Cucumis melo L., cv. Tendral) grown in a mediterranean environment under saline-sodic conditions:

Part I. Yield and quality. Agric. Water Manag., 98, 1329-1338. https://doi.org/10.1016/j.agwat.2011.04.007.

Thenkabail, P.S., Biradar, C.M., Noojipady, P., Dheeravath, V., Li, Y., Velpuri, M., Gumma, M., Gangalakunta, O.R.P., Turral, H., Cai, X., Vithanage, J., Schull, M.A., & Dutta, R. (2009). Global irrigated area map (GIAM), derived from remote sensing, for the end of the last millennium. Int. J. Remote Sens., 30, 3679-3733. https://doi.org/10.1080/01431160802698919.

Thenot, F., Méthy, M., & Winkel, T. (2002). The Photochemical Reflectance Index (PRI) as a water-stress index. Int. J. Remote Sens., 23, 5135-5139. https://doi.org/10.1080/01431160210163100.

Tilley, D.R., Ahmed, M., Son, J.H., & Badrinarayanan, H. (2007). Hyperspectral reflectance response of freshwater macrophytes to salinity in a brackish subtropical marsh. J. Environ. Qual., 36, 780-789. https://doi.org/10.2134/jeq2005.0327.

Tilman, D., Balzer, C., Hill, J., & Befort, B.L. (2011). Global food demand and the sustainable intensification of agriculture. Proc. Natl. Acad. Sci. U.S.A., 108, 20260-20264. https://doi.org/10.1073/pnas.1116437108.

Timmermans, J., Verhoef, W., van der Tol, C., & Su, Z. (2009). Retrieval of canopy component temperatures through Bayesian inversion of directional thermal measurements. Hydrol. Earth Syst. Sci., 13, 1249-1260. https://doi.org/10.5194/hess-13-1249-2009.

Tokarz, B., Wójtowicz, T., Makowski, W., Jędrzejczyk, R.J., & Tokarz, K.M. (2020). What is the difference between the response of grass pea (Lathyrus sativus L.) to salinity and drought stress? A physiological study. Agronomy, 10, 833. https://doi.org/10.3390/agronomy10060833.

Toker, C., Gorham, J., & Cagirgan, M.I. (1999). Assessment of response to drought and salinity stresses of barley (Hordeum vulgare L.) mutants. Cereal Res. Commun., 27, 411-418. https://doi.org/10.1007/BF03543557.

Touch, S., Pipatpongsa, T., Takeda, T., & Takemura, J. (2015). The relationships between electrical conductivity of soil and reflectance of canopy, grain, and leaf of rice in northeastern Thailand. Int. J. Remote Sens., 36, 1136-1166. https://doi.org/10.1080/01431161.2015.1007254.

Trenberth, K.E., Dai, A., van der Schrier, G., Jones, P.D., Barichivich, J., Briffa, K.R., & Sheffield, J. (2013). Global warming and changes in drought. Nat. Clim. Chang., 4, 17-22. https://doi.org/10.1038/nclimate2067.

Tsegai, D., Medel, M., Augenstein, P., & Huang, Z. (2022). Drought in numbers 2022-restoration for readiness and resilience. In S. Alexander, & G. Lipton (Eds.). https://www.unccd.int/sites/default/files/2022-05/Drought%20in%20Numbers.pdf.

Tucker, C.J. (1979). Red and photographic infrared linear combinations for monitoring vegetation. Remote Sens. Environ., 8, 127-150. https://doi.org/10.1016/0034-4257(79)90013-0.

Turhan, A., Kuscu, H., Ozmen, N., Sitki Serbeci, M., & Osman Demir, A. (2014). Effect of different concentrations of diluted seawater on yield and quality of lettuce. Chil. J. Agric. Res., 74, 111-116. http://dx.doi.org/10.4067/S0718-58392014000100017

UN (2015). Transforming our world: the 2030 Agenda for Sustainable Development. United Nations: New York, NY, USA. https://sustainabledevelopment.un.org/content/documents/21252030%20Agenda%20for%20Sustainable%20Development%20web.pdf.

UN (2022). The Sustainable Development Goals: Report 2022. In: UN. https://unstats.un.org/sdgs/report/2022/The-Sustainable-Development-Goals-Report-2022.pdf.

van Dijk, M., Morley, T., Rau, M.L., & Saghai, Y. (2021). A meta-analysis of projected global food demand and population at risk of hunger for the period 2010-2050. Nat. Food, 2, 494-501. https://doi.org/10.1038/s43016-021-00322-9.

Van Eck, N.J., & Waltman, L. (2011). Text mining and visualization using VOSviewer. ISSI Newsletter, 7, 50-54. https://arxiv.org/ftp/arxiv/papers/1109/1109.2058.pdf.

Van Eck, N.J., & Waltman, L. (2014). Visualizing bibliometric networks. Measuring scholarly impact (pp. 285-320): Springer. https://doi.org/10.1007/978-3-319-10377-8_13.

van Straten, G., Bruning, B., de Vos, A.C., González, A.P., Rozema, J., & van Bodegom, P.M. (2021). Estimating cultivar-specific salt tolerance model parameters from multi-annual field tests for identification of salt tolerant potato cultivars. Agric. Water Manag., 252, 106902. https://doi.org/10.1016/j.agwat.2021.106902.

van Vliet, M.T.H., & Zwolsman, J.J.G. (2008). Impact of summer droughts on the water quality of the Meuse river. J. Hydrol., 353, 1-17. https://doi.org/10.1016/j.jhydrol.2008.01.001.

Vannoppen, A., Gobin, A., Kotova, L., Top, S., De Cruz, L., Vīksna, A., Aniskevich, S., Bobylev, L., Buntemeyer, L., Caluwaerts, S., De Troch, R., Gnatiuk, N., Hamdi, R., Reca Remedio, A., Sakalli, A., Van De Vyver, H., Van Schaeybroeck, B., & Termonia, P. (2020). Wheat yield estimation from NDVI and regional climate models in Latvia. Remote Sens., 12. https://doi.org/10.3390/rs12142206.

Vereecken, H., Weihermuller, L., Jonard, F., & Montzka, C. (2012). Characterization of crop canopies and water stress related phenomena using microwave remote sensing methods: a review. Vadose Zone J., 11, vzj2011.0138ra. https://doi.org/10.2136/vzj2011.0138ra.

Verhoef, W. (1984). Light scattering by leaf layers with application to canopy reflectance modeling: The SAIL model. Remote Sensing of Environment, 16, 125-141. https://doi.org/10.1016/0034-4257(84)90057-9.

Verrelst, J., Camps-Valls, G., Muñoz-Marí, J., Rivera, J.P., Veroustraete, F., Clevers, J.G.P.W., & Moreno, J. (2015). Optical remote sensing and the retrieval of terrestrial vegetation bio-geophysical properties – A review. ISPRS J. Photogramm. Remote Sens., 108, 273-290. https://doi.org/10.1016/j.isprsjprs.2015.05.005.

Verrelst, J., Malenovský, Z., Van der Tol, C., Camps-Valls, G., Gastellu-Etchegorry, J.-P., Lewis, P., North, P., & Moreno, J. (2019). Quantifying vegetation biophysical variables from imaging spectroscopy data: A review on retrieval methods. Surv. Geophys., 40, 589-629. https://doi.org/10.1007/s10712-018-9478-y.

Violle, C., Navas, M.-L., Vile, D., Kazakou, E., Fortunel, C., Hummel, I., & Garnier, E. (2007). Let the concept of trait be functional! Oikos, 116, 882-892. https://doi.org/10.1111/j.0030-1299.2007.15559.x.

Vogelmann, J.E., Rock, B.N., & Moss, D.M. (1993). Red edge spectral measurements from sugar maple leaves. Int. J. Remote Sens., 14, 1563-1575. https://doi.org/10.1080/01431169308953986.

Wagg, C., Hann, S., Kupriyanovich, Y., & Li, S. (2021). Timing of short period water stress determines potato plant growth, yield and tuber quality. Agric. Water Manag., 247, 106731. https://doi.org/10.1016/j.agwat.2020.106731.

Wallach, D., Makowski, D., Jones, J.W., & Brun, F. (2006). Working with dynamic crop models: evaluation, analysis, parameterization, and applications. Elsevier. ISBN: 9780080461939.

Walter, A., Studer, B., & Kölliker, R. (2012). Advanced phenotyping offers opportunities for improved breeding of forage and turf species. Ann. Bot., 110, 1271-1279. https://doi.org/10.1093/aob/mcs026.

Wang, D., Chen, Y., Jarin, M., & Xie, X. (2022). Increasingly frequent extreme weather events urge the development of point-of-use water treatment systems. npj Clean Water, 5, 36. https://doi.org/10.1038/s41545-022-00182-1.

Wang, D., Poss, J.A., Donovan, T.J., Shannon, M.C., & Lesch, S.M. (2002a). Biophysical properties and biomass production of elephant grass under saline conditions. J. Arid Environ., 52, 447-456. https://doi.org/10.1006/jare.2002.1016.

Wang, D., Wilson, C., & Shannon, M. (2002b). Interpretation of salinity and irrigation effects on soybean canopy reflectance in visible and near-infrared spectrum domain. Int. J. Remote Sens., 23, 811-824. https://doi.org/10.1080/01431160110070717.

Wang, J., Li, X., Lu, L., & Fang, F. (2013a). Estimating near future regional corn yields by integrating multi-source observations into a crop growth model. Eur. J. Agron., 49, 126-140. https://doi.org/10.1016/j.eja.2013.03.005.

Wang, J., Zhen, J., Hu, W., Chen, S., Lizaga, I., Zeraatpisheh, M., & Yang, X. (2023a). Remote sensing of soil degradation: Progress and perspective. Int. Soil Water Conserv. Res. https://doi.org/10.1016/j.iswcr.2023.03.002.

Wang, J.L., Huang, X.J., Zhong, T.Y., & Chen, Z.G. (2013b). Climate change impacts and adaptation for saline agriculture in north Jiangsu Province, China. Environ. Sci. Policy, 25, 83-93. https://doi.org/10.1016/j.envsci.2012.07.011.

Wang, X., Ji, M., Zhang, Y., Zhang, L., Akram, M.A., Dong, L., Hu, W., Xiong, J., Sun, Y., Li, H., Degen, A.A., Ran, J., & Deng, J. (2023b). Plant trait networks reveal adaptation strategies in the drylands of China. BMC Plant Biol., 23, 266. https://doi.org/10.1186/s12870-023-04273-0.

Wang, X.P., Zhao, C.Y., Guo, N., Li, Y.H., Jian, S.Q., & Yu, K. (2015). Determining the Canopy Water Stress for Spring Wheat Using Canopy Hyperspectral Reflectance Data in Loess Plateau Semiarid Regions. Spectrosc. Lett., 48, 492-498. https://doi.org/10.1080/00387010.2014.909495.

Wardlow, B.D., Tadesse, T., Brown, J.F., & Gu, Y. (2008). The Vegetation Drought Response Index (VegDRI): A New Drought Monitoring Approach for Vegetation. GIsci. Remote Sens., 45, 16-46. https://doi.org/10.2747/1548-1603.45.1.16.

Webber, H.A., Madramootoo, C.A., Bourgault, M., Horst, M.G., Stulina, G., & Smith, D.L. (2010). Adapting the CROPGRO model for saline soils: the case for a common bean crop. Irrig. Sci., 28, 317-329. https://doi.org/10.1007/s00271-009-0189-5.

Wei, Y., Jin, J., Jiang, S., Ning, S., & Liu, L. (2018). Quantitative response of soybean development and yield to drought stress during different growth stages in the huaibei plain, China. Agronomy, 8. https://doi.org/10.3390/agronomy8070097.

Weiss, M., Baret, F., & Jay, S. (2016). S2ToolBox Level 2 products LAI, FAPAR, FCOVER, Version 1.1. https://step.esa.int/docs/extra/ATBD_S2ToolBox_L2B_V1.1.pdf.

Weiss, M., Jacob, F., & Duveiller, G. (2020). Remote sensing for agricultural applications: a meta-review. Remote Sens. Environ., 236, 111402. https://doi.org/10.1016/j.rse.2019.111402.

Wengert, M., Piepho, H.P., Astor, T., Grass, R., Wijesingha, J., & Wachendorf, M. (2021). Assessing spatial variability of barley whole crop biomass yield and leaf area index in Silvoarable agroforestry systems using UAV-borne remote sensing. Remote Sens., 13, 2751. https://doi.org/10.3390/rs13142751.

West, H., Quinn, N., & Horswell, M. (2019). Remote sensing for drought monitoring & impact assessment: Progress, past challenges and future opportunities. Remote Sens. Environ., 232, 111291. https://doi.org/10.1016/j.rse.2019.111291.

Wheeler, T., & von Braun, J. (2013). Climate change impacts on global food security. Science, 341, 508-513. https://doi.org/10.1126/science.1239402.

Whitcraft, A.K., Becker-Reshef, I., Justice, C.O., Gifford, L., Kavvada, A., & Jarvis, I. (2019). No pixel left behind: Toward integrating earth observations for agriculture into the United Nations Sustainable Development Goals framework. Remote Sens. Environ., 235. https://doi.org/10.1016/j.rse.2019.111470.

Wilcox, K.R., Blumenthal, D.M., Kray, J.A., Mueller, K.E., Derner, J.D., Ocheltree, T., & Porensky, L.M. (2021). Plant traits related to precipitation sensitivity of species and communities in semiarid shortgrass prairie. New Phytol., 229, 2007-2019. https://doi.org/10.1111/nph.17000.

Williams, J.R., Jones, C.A., Kiniry, J.R., & Spanel, D.A. (1989). The EPIC crop growth model. Trans. ASABE, 32, 497-511. https://www.ars.usda.gov/ARSUserFiles/30980500/The%20EPIC%20Crop%20Growth%20Model.pdf.

Winkel, T., Méthy, M., & Thénot, F. (2002). Radiation use efficiency, chlorophyll fluorescence, and reflectance indices associated with ontogenic changes in water-limited Chenopodium quinoa leaves. Photosynthetica, 40, 227-232. https://doi.org/10.1023/A:1021345724248.

Wocher, M., Berger, K., Danner, M., Mauser, W., & Hank, T. (2020). RTM-based dynamic absorption integrals for the retrieval of biochemical vegetation traits. Int. J. Appl. Earth Obs. Geoinf., 93, 102219. https://doi.org/10.1016/j.jag.2020.102219.

Wright, I.J., Reich, P.B., & Westoby, M. (2003). Least-cost input mixtures of water and nitrogen for photosynthesis. Am. Nat., 161, 98-111. https://doi.org/10.1086/344920.

Wu, B., Gommes, R., Zhang, M., Zeng, H., Yan, N., Zou, W., Zheng, Y., Zhang, N., Chang, S., Xing, Q., & van Heijden, A. (2015). Global crop monitoring: A satellite-based hierarchical approach. Remote Sens., 7, 3907-3933. https://doi.org/10.3390/rs70403907.

Wu, B., Zhang, M., Zeng, H., Tian, F., Potgieter, A.B., Qin, X., Yan, N., Chang, S., Zhao, Y., Dong, Q., Boken, V., Plotnikov, D., Guo, H., Wu, F., Zhao, H., Deronde, B., Tits, L., & Loupian, E. (2023). Challenges and opportunities in remote sensing-based crop monitoring: a review. Natl. Sci. Rev., 10, nwac290. https://doi.org/10.1093/nsr/nwac290.

Xu, H., Tian, Z., He, X., Wang, J., Sun, L., Fischer, G., Fan, D., Zhong, H., Wu, W., Pope, E., Kent, C., & Liu, J. (2019). Future increases in irrigation water requirement challenge the water-food nexus in the northeast farming region of China. Agric. Water Manag., 213, 594-604. https://doi.org/10.1016/j.agwat.2018.10.045.

Yadav, J.S.P. (2003). Managing soil health for sustained high productivity. J. Indian Soc. Soil Sci., 51, 448-465. https://www.indianjournals.com/ijor.aspx?target=ijor:jisss&volume=51&issue=4&article=012.

Yang, L., Jia, K., Liang, S., Liu, M., Wei, X., Yao, Y., Zhang, X., & Liu, D. (2018). Spatio-temporal analysis and uncertainty of fractional vegetation cover change over northern China during 2001–2012 based on multiple vegetation data sets. Remote Sens., 10, 549. https://doi.org/10.3390/rs10040549.

Yang, X., Lu, M., Wang, Y., Wang, Y., Liu, Z., & Chen, S. (2021). Response mechanism of plants to drought stress. Horticulturae, 7, 50. https://doi.org/10.3390/horticulturae7030050.

Yeo, A. (1998). Molecular biology of salt tolerance in the context of whole-plant physiology. J. Exp. Bot., 49, 915-929. https://doi.org/10.1093/jexbot/49.323.915.

Yoshizumi, Y., Li, M.-s., & Akihiro, I. (2010). Assessment of photochemical reflectance index as a tool for evaluation of chlorophyll fluorescence parameters in cotton and peanut cultivars under water stress condition. Agric. Sci. China, 9, 662-670. https://doi.org/10.1016/S1671-2927(09)60141-3.

Zakharova, L., Meyer, K.M., & Seifan, M. (2019). Trait-based modelling in ecology: A review of two decades of research. Ecol. Model., 407, 108703. https://doi.org/10.1016/j.ecolmodel.2019.05.008.

Zarco-Tejada, P.J., Berni, J.A., Suárez, L., Sepulcre-Cantó, G., Morales, F., & Miller, J.R. (2009). Imaging chlorophyll fluorescence with an airborne narrow-band multispectral camera for vegetation stress detection. Remote Sens. Environ., 113, 1262-1275. https://doi.org/10.1016/j.rse.2009.02.016.

Zarco-Tejada, P.J., Camino, C., Beck, P.S.A., Calderon, R., Hornero, A., Hernández-Clemente, R., Kattenborn, T., Montes-Borrego, M., Susca, L., Morelli, M., Gonzalez-Dugo, V., North, P.R.J., Landa, B.B., Boscia, D., Saponari, M., & Navas-Cortes, J.A. (2018). Previsual symptoms of Xylella fastidiosa infection revealed in spectral plant-trait alterations. Nature Plants, 4, 432-439. https://doi.org/10.1038/s41477-018-0189-7.

Zarco-Tejada, P.J., Catalina, A., González, M., & Martín, P. (2013a). Relationships between net photosynthesis and steady-state chlorophyll fluorescence retrieved from airborne hyperspectral imagery. Remote Sens. Environ., 136, 247-258. https://doi.org/10.1016/j.rse.2013.05.011.

Zarco-Tejada, P.J., González-Dugo, V., & Berni, J.A.J. (2012). Fluorescence, temperature and narrow-band indices acquired from a UAV platform for water stress detection using a micro-hyperspectral imager and a thermal camera. Remote Sens. Environ., 117, 322-337. https://doi.org/10.1016/j.rse.2011.10.007.

Zarco-Tejada, P.J., González-Dugo, V., Williams, L.E., Suárez, L., Berni, J.A.J., Goldhamer, D., & Fereres, E. (2013b). A PRI-based water stress index combining structural and chlorophyll effects: Assessment using diurnal narrow-band airborne imagery and the CWSI thermal index. Remote Sens. Environ., 138, 38-50. https://doi.org/10.1016/j.rse.2013.07.024.

Zarco-Tejada, P.J., Miller, J.R., Harron, J., Hu, B., Noland, T.L., Goel, N., Mohammed, G.H., & Sampson, P. (2004). Needle chlorophyll content estimation through model inversion using hyperspectral data from boreal conifer forest canopies. Remote Sens. Environ., 89, 189-199. https://doi.org/10.1016/j.rse.2002.06.002.

Zarco-Tejada, P.J., Miller, J.R., Noland, T.L., Mohammed, G.H., & Sampson, P.H. (2001). Scaling-up and model inversion methods with narrowband optical indices for chlorophyll content estimation in closed forest canopies with hyperspectral data. IEEE Trans. Geosci. Remote Sens., 39, 1491-1507. https://doi.org/10.1109/36.934080.

Zargar, A., Sadiq, R., Naser, B., & Khan, F.I. (2011). A review of drought indices. Environ. Rev., 19, 333-349. https://doi.org/10.1139/a11-013.

Zhang, F., & Zhou, G. (2015). Estimation of canopy water content by means of hyperspectral indices based on drought stress gradient experiments of maize in the north plain China. Remote Sens., 7, 15203-15223. https://doi.org/10.3390/rs71115203.

Zhang, F., Zhou, G.S., & Nilsson, C. (2015). Remote estimation of the fraction of absorbed photosynthetically active radiation for a maize canopy in Northeast China. J. Plant Ecol., 8, 429-435. https://doi.org/10.1093/jpe/rtu027.

Zhang, H., Han, M., Comas, L.H., DeJonge, K.C., Gleason, S.M., Trout, T.J., & Ma, L. (2019). Response of maize yield components to growth stage-based deficit irrigation. Agron. J., 111, 3244-3252. https://doi.org/10.2134/agronj2019.03.0214.

Zhang, H., Xu, N., Wu, X., Wang, J., Ma, S., Li, X., & Sun, G. (2018). Effects of four types of sodium salt stress on plant growth and photosynthetic apparatus in sorghum leaves. J. Plant Interact., 13, 506-513. https://doi.org/10.1080/17429145.2018.1526978.

Zhang, J., Mu, Q., & Huang, J. (2016). Assessing the remotely sensed Drought Severity Index for agricultural drought monitoring and impact analysis in North China. Ecol. Indic., 63, 296-309. https://doi.org/10.1016/j.ecolind.2015.11.062.

Zhang, J., Zhang, Z., Chen, J., Chen, H., Jin, J., Han, J., Wang, X., Song, Z., & Wei, G. (2020). Estimating soil salinity with different fractional vegetation cover using remote sensing. Land Degrad. Dev., 32, 597-612. https://doi.org/10.1002/ldr.3737.

Zhang, L., Chen, B., Zhang, G., Li, J., Wang, Y., Meng, Y., & Zhou, Z. (2013). Effect of soil salinity, soil drought, and their combined action on the biochemical characteristics of cotton roots. Acta Physiol. Plant, 35, 3167-3179. https://doi.org/10.1007/s11738-013-1350-6.

Zhang, L., Zhou, Z., Zhang, G., Meng, Y., Chen, B., & Wang, Y. (2017). Monitoring cotton (Gossypium hirsutum L.) leaf ion content and leaf water content in saline soil with

hyperspectral reflectance. Eur. J. Remote Sens., 47, 593-610. https://doi.org/10.5721/EuJRS20144733.

Zhou, D., Ni, Y., Yu, X., Lin, K., Du, N., Liu, L., Guo, X., & Guo, W. (2021). Trait-based adaptability of Phragmites australis to the effects of soil water and salinity in the Yellow River Delta. Ecol. Evol., 11, 11352-11361. https://doi.org/10.1002/ece3.7925.

Zhou, J., Zhou, J., Ye, H., Ali, M.L., Nguyen, H.T., & Chen, P. (2020). Classification of soybean leaf wilting due to drought stress using UAV-based imagery. Comput. Electron. Agric., 175, 105576. https://doi.org/10.1016/j.compag.2020.105576.

Zhu, X., Wang, T.J., Skidmore, A.K., Darvishzadeh, R., Niemann, K.O., & Liu, J. (2017). Canopy leaf water content estimated using terrestrial LiDAR. Agric. For. Meteorol., 232, 152-162. https://doi.org/10.1016/j.agrformet.2016.08.016.

Zhu, Y., Qu, Y., Liu, S., & Chen, S. (2014). A reflectance spectra model for copper-stressed leaves: advances in the PROSPECT model through addition of the specific absorption coefficients of the copper ion. Int. J. Remote Sens., 35, 1356-1373. https://doi.org/10.1080/01431161.2013.876123.

Zinnert, J.C., Nelson, J.D., & Hoffman, A.M. (2012). Effects of salinity on physiological responses and the photochemical reflectance index in two co-occurring coastal shrubs. Plant Soil, 354, 45-55. https://doi.org/10.1007/s11104-011-0955-z.

Zscheischler, J., Westra, S., van den Hurk, B.J.J.M., Seneviratne, S.I., Ward, P.J., Pitman, A., AghaKouchak, A., Bresch, D.N., Leonard, M., Wahl, T., & Zhang, X. (2018). Future climate risk from compound events. Nat. Clim. Chang., 8, 469-477. https://doi.org/10.1038/s41558-018-0156-3.

Summary

Food security is challenged by a growing global population and by climate change. Already, agricultural crops encounter various environmental stresses, limiting productivity and decreasing food production. Of these stresses, drought and soil salinity are considered the most important ones that inhibit crop yield and distribution. Worryingly, climate change is predicted to increase not only their frequency and severity, but also their co-occurrence, exacerbating their impacts. This also leads to increases in events where both stresses co-occur. This co-occurrence results in substantially more yield losses than individual stressors. While detrimental effects of combined drought and salinity stress on crops have been highlighted in small-scale experiments (with only a limited number of crop varieties), large regional uncertainties remain for real-life agricultural settings. Assessing these large-scale impacts using traditional methods is, however, not feasible. In contrast, satellite observations offer a promising perspective for enhancing global food security by providing reliable information on arable land extent and food production. Remote sensing has already been used to monitor crop productivity at multiple spatial and temporal scales, though not for yet characterizing crop growth under co-occurring drought and salinity stress. This thesis aims to assess the impact of drought and salinity on agriculture and sustainable development goals using remote sensing technology.

In Chapter 2, a systematic review was conducted to evaluate the current ability of remote sensing to identify and assess the impacts of drought and salinity stress on agricultural crops through vegetation indices (VIs) and plant traits. The results indicate that challenges still persist in utilizing satellite monitoring of these stress impacts. Specifically, traditional VIs do not consistently estimate these impacts accurately. In addition, plant traits, although promising in linking directly to the biochemical and biophysical pathways of crop growth, are not widely used to reflect upon stress response mechanisms. Osmosis traits in particular have high potential for monitoring the pathways through which drought and salinity affect crops but cannot be directly measured by remote sensing. Other remotely sensed plant traits are highlighted to contain significant potential -to assess the combined impacts of drought and salinity effects on agricultural crops- but only in small-scale experimental studies. Consequently, large-scale studies are necessary to showcase the relevance of remote sensing for assessing combined impacts under real-life agricultural scenarios.

In Chapter 3, a novel approach was proposed that utilized satellite remote sensing observations to estimate the impacts of drought, salinity, and their combination on five crop traits, including leaf area index (LAI), leaf chlorophyll content (Cab), leaf water content (Cw), the fraction of absorbed photosynthetically active radiation

(FAPAR) and the fraction of vegetation cover (FVC) using remote sensing. The approach was first tested in the Netherlands, and results indicate that the exacerbating effects of co-occurring drought and salinity stress highly depended on the moment in the growing season. Moreover, LAI, FAPAR, and FVC were impacted most under severe drought conditions for maize and potato while Cab and Cw were generally more inhibited by combined drought and salinity stress. Thus, this approach facilitates simultaneous monitoring of the effect of drought and salinity on crops in large-scale agricultural applications.

The approach presented in Chapter 3 was adapted to suit the assessment of a larger spatial extent and multiple crops, by applying a pair-wise method of retrieving stressed and non-stressed crops (Chapter 4). Furthermore, multiple techniques were integrated to assess trait expressions concerning drought, salinity, and their combined impacts compared to control conditions, to allow evaluating stress impacts more precisely for a much larger range of crops and spatial conditions. The results across the United States indicate that stress impacts were highly time-dependent and that crops were more susceptible to combined drought and salinity than to individual stress. However, stress impacts also varied significantly between species. Most crops initially decrease primary production capability by reducing LAI before decreasing water or chlorophyll contents. In combination, a quantitative foundation was established for simultaneously assessing crop responses to the occurrence of stresses, both alone and collectively at large scale and under actual agricultural conditions, contributing in monitoring food security upon global climate change.

In Chapter 5, we explored how some of the findings related to large-scale salinity tolerance could be used to aid in achieving sustainable development goals (SDGs). Sustainable agriculture and food security are critical components of sustainable development goals, yet they are increasingly vulnerable to global climate change impacts. While salt-induced stress on crop growth and food production has been extensively studied, quantifying the potential contribution of saline farming on a global scale remains uncertain. In Chapter 5, the local and regional suitability areas for salt-tolerant potato cultivation in salt-affected soils were evaluated, thereby assessing the potential contribution of salt-tolerant potatoes to the current and future SDGs. The results reveal that Oceania (particularly Australia) has the greatest potential for enhancing food production through salt-tolerant potato cultivation in salt-affected soils. Moreover, other countries like Kazakhstan, the Russian Federation, and Australia can address food shortage challenges and achieve SDGs in the current state as well as in future scenarios. Furthermore, the suitability area for salt-tolerant potato is expected to expand even under future climatic and salinity conditions, potentially doubling food production in Kazakhstan and the Russian Federation. Consequently, salt-tolerant potato -as a

proxy for saline farming- can promote increased food production in salt-affected areas. Saline farming may thus enhance agricultural resilience and ensure food security.

This thesis emphasizes the potential of remote sensing-derived traits for evaluating crop growth under stress conditions. While it demonstrates the potential of remote sensing to detect stress responses through functional traits, its effectiveness varies across plant species and growth stages, indicating that several challenges are left open to be addressed in future studies. In particular, the identification and selection of representative traits need to be improved to more accurately reflect specific stress conditions at different moments during the growing season. Moreover, current remote sensing for agricultural applications faces challenges related to the increased demands for high spatial-temporal resolutions. We propose multi-platform data integration to improve the accuracy of observations and data fusion in future studies.

In conclusion, remote sensing offers a huge promise for effectively monitoring the attainment of SDGs and ensuring global food security, involving various stakeholders and policymakers. This thesis demonstrates how remote sensing techniques can be applied to detect stress responses and mitigate the impacts of those stresses on global crop production from review to application, offering valuable insights into the potential of remote sensing to enhance food security and address sustainable development goals.

Samenvatting

Onze voedselzekerheid staat onder druk door een groeiende wereldbevolking en door klimaatverandering. Momenteel hebben landbouwgewassen te maken met verschillende verstoringen, die de productiviteit beperken en de voedselproductie verminderen. Van de verschillende verstoringen worden droogte en bodemverzilting als de belangrijkste beschouwd, die de gewasopbrengst en -verspreiding belemmeren. Zorgwekkend is dat klimaatverandering naar verwachting beide verstoringen verder zal verergeren en de frequentie en ernst van beiden zal verhogen. Dit leidt ook tot een toename van gebeurtenissen waarin beide verstoringen samen voorkomen. Deze samenloop resulteert in aanzienlijk grotere opbrengstverliezen dan individuele stressfactoren. Hoewel de schadelijke effecten van de gecombineerde stress door droogte en verzilting op gewassen al zijn beschreven in kleinschalige experimenten (met slechts een beperkt aantal gewasvariëteiten), blijven er grote regionale onzekerheden bestaan voor landbouwsituaties in de praktijk. Het beoordelen van deze grootschalige gevolgen is echter niet haalbaar met behulp van traditionele methoden. In tegenstelling hiermee bieden satellietwaarnemingen een veelbelovend perspectief om de wereldwijde voedselzekerheid te verbeteren door betrouwbare informatie te verstrekken over de omvang van landbouwgronden en voedselproductie. Remote sensing wordt al gebruikt om de gewasproductiviteit op meerdere ruimtelijke en temporale schalen te monitoren, maar nog niet voor het karakteriseren van gewasgroei onder gelijktijdige droogte- en verziltingsstress. Dit proefschrift heeft tot doel de impact van droogte en verzilting op landbouw en de *Sustainable Development Goals* (SDGs) te beoordelen met behulp van remote sensing-technologie.

In Hoofdstuk 2 werd een systematische review uitgevoerd om de huidige mogelijkheden van remote sensing te evalueren om de impact van droogte- en verziltingsstress op landbouwgewassen te identificeren en te beoordelen via vegetatie-indices (VI's) en de eigenschappen van planten. De resultaten laten zien aan dat er nog steeds uitdagingen zijn bij het nauwkeurig monitoren van de impacts van stress met behulp van remote sensing via satellieten. De traditionele VI's laten niet toe deze impacts consistent en nauwkeurig te schatten. Daarentegen zijn planteigenschappen veelbelovend omdat ze rechtstreeks verbonden zijn met de biochemische en biologische processen van gewasgroei en stressresponsmechanismen weerspiegelen. Met name planteigenschappen gerelateerd aan osmose hebben een groot potentieel voor het monitoren van de manieren waarop droogte en verzilting gewassen beïnvloeden, maar kunnen niet rechtstreeks worden gemeten door remote sensing. Andere met remote sensing waargenomen planteigenschappen werden aangestipt als potentieel waardevol om de gecombineerde effecten van droogte- en verziltingseffecten op

landbouwgewassen te beoordelen, maar zijn alleen gebruikt in kleinschalige experimentele studies. Daarom zijn grootschalige studies noodzakelijk om de relevantie van remote sensing voor het beoordelen van gecombineerde effecten onder echte landbouwcondities te laten zien.

In Hoofdstuk 3 werd een nieuwe benadering voorgesteld die gebruikmaakte van satelliet remote sensing waarnemingen om de impact van droogte, verzilting en hun combinatie op vijf gewaseigenschappen te schatten, waaronder totale bladoppervlakte (Leaf Area Index; LAI), bladchlorofielgehalte (Cab), het watergehalte in bladeren (Cw), de fractie van geabsorbeerd fotosynthetisch actieve straling (FAPAR) en de fractie van vegetatiebedekking (FVC) met behulp van remote sensing. De benadering werd eerst getest in Nederland, en de resultaten geven aan dat de verergerende effecten van gelijktijdige droogte- en verziltingsstress sterk afhankelijk zijn van het moment in het groeiseizoen. Bovendien werden LAI, FAPAR en FVC het meest beïnvloed onder ernstige droogteomstandigheden voor maïs en aardappelen, terwijl Cab en Cw over het algemeen meer werden beïnvloed door gecombineerde droogte- en verziltingsstress. Deze benadering maakt dus gelijktijdige monitoring van het effect van droogte en verzilting op gewassen mogelijk in grootschalige landbouwtoepassingen.

In Hoofdstuk 4 werd de benadering van Hoofdstuk 3 aangepast om de beoordeling van een grotere ruimtelijke omvang en van meerdere gewassen mogelijk te maken, door paarsgewijs gestreste en niet-gestreste gewassen te vergelijken. Bovendien werden meerdere technieken geïntegreerd om planteigenschappen in relatie tot droogte, verzilting en hun gecombineerde effecten te vergelijken met die van controleomstandigheden. Zo kon het effect van stress nauwkeuriger geëvalueerd worden voor een veel groter scala aan gewassen en ruimtelijke omstandigheden. De resultaten voor de Verenigde Staten geven aan dat het effect van stress sterk afhankelijk was van de tijd in het groeiseizoen en dat gewassen gevoeliger waren voor de gecombineerde effecten van droogte en verzilting dan voor individuele stress. De stressimpact varieerde echter ook aanzienlijk tussen soorten. De meeste gewassen verminderden aanvankelijk hun primaire productiecapaciteit door de LAI te verlagen voordat ze water- of chlorofylgehalten verminderden. Door deze combinatie van methoden werd een kwantitatieve basis gelegd om tegelijktijdig de reacties van gewassen op stress te beoordelen, zowel afzonderlijk als in combinatie op grote schaal en onder werkelijke landbouwomstandigheden, zo bijdragend aan het monitoren van de voedselzekerheid bij wereldwijde klimaatverandering.

In Hoofdstuk 5, hebben we de resultaten - omtrent het verbouwen van zout-tolerante gewassen – gebruikt om te kijken hoe duurzame ontwikkelingsdoelen (SDG) bereikt kunnen worden. Duurzame landbouw en voedselzekerheid zijn cruciale componenten van de SDGs, maar ze zijn steeds kwetsbaarder voor de

gevolgen van wereldwijde klimaatverandering. Hoewel stress veroorzaakt door zout op gewasgroei en voedselproductie uitgebreid is bestudeerd, blijft de kwantificering van de mogelijke bijdrage van zouttolerante landbouw op wereldschaal onzeker. In Hoofdstuk 5 werden de lokaal en regionaal de geschikthe gebieden voor zouttolerante aardappelteelt op zoute bodems geëvalueerd, waarbij de mogelijke bijdrage van zouttolerante aardappelen aan de huidige en toekomstige SDGs werd beoordeeld. De resultaten tonen aan dat Oceanië (met name Australië) het grootste potentieel heeft om de voedselproductie te verbeteren door zouttolerante aardappelteelt op zoute bodems. Bovendien kunnen andere landen zoals Kazachstan, de Russische Federatie en Australië tekorten in het voedselaanbod aanpakken en SDGs bereiken zowel in de huidige omstandigheden als in scenario's van de toekomst. Bovendien wordt verwacht dat het gebied dat geschikt is voor zouttolerante aardappel onder toekomstige klimatologische en zoutgehalteomstandigheden zich zelfs zal uitbreiden, wat mogelijk de voedselproductie in Kazachstan en de Russische Federatie kan verdubbelen. Zo kan een zouttolerante aardappel - als een proxy voor zouttolerante landbouw - de voedselproductie in gebieden die aangetast zijn door zout bevorderen. Zouttolerante landbouw kan dus de veerkracht van de landbouw verbeteren en de voedselzekerheid waarborgen.

Dit proefschrift benadrukt het potentieel van met behulp van remote sensing afgeleide planteneigenschappen om de groei van gewassen onder stressvolle omstandigheden te evalueren. Hoewel het de mogelijkheden van remote sensing laat zien om stressreacties te detecteren via functionele planteneigenschappen, varieert de effectiviteit ervan tussen plantensoorten en groeistadia, wat aangeeft dat er nog enkele uitdagingen openstaan die in toekomstige studies moeten worden aangepakt. Met name de identificatie en selectie van eigenschappen moet worden verbeterd om specifieke stressomstandigheden tijdens verschillende momenten in het groeiseizoen nauwkeuriger te representeren. Bovendien heeft de huidige remote sensing te maken met beperkingen in de ruimtelijke en temporele resolutie voor landbouwtoepassingen. De integratie van gegevens van meerdere platforms kan helpen om de nauwkeurigheid van waarnemingen en de integratie van gegevens te verbeteren.

Concluderend biedt remote sensing een enorme belofte voor de effectieve monitoring van de realisatie van SDGs en het waarborgen van wereldwijde voedselzekerheid, voor de verschillende betrokken belanghebbenden en beleidsmakers. Dit proefschrift laat zien hoe remote sensing-technieken kunnen worden toegepast om stressreacties te detecteren en de impact van die stress op de wereldwijde gewasproductie te verminderen, en biedt waardevolle inzichten in het potentieel van remote sensing om de voedselzekerheid te verbeteren en de SDGs te realiseren.

List of Publications

Publications in peer-reviewed Journals (English):

1. **Wen, W.**, Timmermans, J., Chen, Q., and van Bodegom, P. M. (2023) Evaluating crop-specific responses to salinity and drought stress from remote sensing. International Journal of Applied Earth Observation and Geoinformation, 122, 103438. https://doi.org/10.1016/j.jag.2023.103438.
2. **Wen, W.**, Timmermans, J., Chen, Q., and van Bodegom, P. M. (2022) Monitoring the combined effects of drought and salinity stress on crops using remote sensing in the Netherlands. Hydrology and Earth System Sciences, 26, 4537-4552. https://doi.org/10.5194/hess-26-4537-2022.
3. **Wen, W.**, Li, Z., Shao, J., Tang, Y., Zhao, Z., Yang, J., Ding, M., Zhu, X., and Zhou, M. (2021) The distribution and sustainable utilization of buckwheat resources under climate change in China. Plants, 10. https://doi.org/10.3390/plants10102081.
4. **Wen, W.**, Timmermans, J., Chen, Q., and van Bodegom, P. M. (2020) A review of remote sensing challenges for food security with respect to salinity and drought threats. Remote Sensing, 13, 6. https://doi.org/10.3390/rs13010006.
5. **Wen, W.**, Zhao, H., Ma, J., Li, Z., Li, H., Zhu, X., Shao, J., Yang, Z., Yang, Y., He, F., and Liu, Y. (2018) Effects of mutual intercropping on Pb and Zn accumulation of accumulator plants *Rumex nepalensis*, *Lolium perenne* and *Trifolium repens*. Chemistry and Ecology, 34, 259-271. https://doi.org/10.1080/02757540.2018.1427229.
6. Chen, Q., Timmermans, J., **Wen, W.**, and van Bodegom, P. M. (2023) Ecosystems threatened by intensified drought with divergent vulnerability. Remote Sensing of Environment, 289, 113512. https://doi.org/10.1016/j.rse.2023.113512.
7. LI, W., Zhang, K., Tang, Y., Ding, M., **Wen, W.**, LI, B., and Zhou, M. (2023) Fagopyrum caudatum var. grandiflorum, a new variety from China. Phytotaxa, 587, 200-204. https://doi.org/10.11646/phytotaxa.587.2.9.
8. Chen, Q., Timmermans, J., **Wen, W.**, and van Bodegom, P. M. (2022) A multi-metric assessment of drought vulnerability across different vegetation types using high-resolution remote sensing. Science of The Total Environment, 832, 154970. https://doi.org/10.1016/j.scitotenv.2022.154970.
9. Ding, M., Zhang, K., Tang Y., Wang, J., Li, F., Yang, K., **Wen, W.**, & Zhou, M. (2021). Newly discovered tetraploid Fagopyrum homotropicum in Tibet, China. Phytotaxa, 528, 202-208. https://doi.org/10.11646/phytotaxa.528.3.4.
10. Li, Z., Li, Z., Huang, Y., Jiang, Y., Liu, Y., **Wen, W.**, Li, H., Shao, J., Wang, C., & Zhu, X. (2020). Antioxidant Capacity, Metal Contents, and Their Health Risk Assessment of Tartary Buckwheat Teas. ACS Omega, 5, 9724-9732.

https://pubs.acs.org/doi/10.1021/acsomega.9b04007.

11. Huang, Y., Li, Z., Wang, C., Zou, C., **Wen, W.**, Shao, J., & Zhu, X. (2019). psbE-psbL and ndhA Intron, the Promising Plastid DNA Barcode of Fagopyrum. International Journal of Molecular Sciences. https://doi.org/10.3390/ijms20143455.
12. **Wen, W.,** Timmermans, J., Chen, Q., & van Bodegom, P. M. Prospects of salt-tolerant potato to increase food productivity towards a zero hunger world. (In preparation)

Conference/Forum Abstracts:

1. **Wen, W.**, Timmermans, J., Chen, Q., and van Bodegom, P. M. Diverse responses of multiple crops to drought and salinity stress. EGU General Assembly. 2023, Vienna, Austria. (Oral presentation)
2. **Wen, W.**, Timmermans, J., Chen, Q., and van Bodegom, P. M. Evaluating crop-specific responses to salinity and drought stress from remote sensing. International Workshop on Geography and Sustainability. 2023, Beijing, China. (Best Presentation Award)
3. **Wen, W.**, Timmermans, J., Chen, Q., and van Bodegom, P. M. Monitoring the combined effects of drought and salinity stress on crops using remote sensing. 2nd WASAG International Forum on Water Scarcity in Agriculture–Making Agriculture Resilient to Climate Change. 2023, FAO. (Poster presentation)
4. **Wen, W.**, Timmermans, J., Chen, Q., and van Bodegom, P. M. Evaluating crop-specific responses to drought and salinity stress from remote sensing. 2nd Meeting of the International Network on Salt-affected Soils INSAS. 2023, FAO. (Poster presentation)

Acknowledgments

To begin with, I extend my deep appreciation to my promoter and supervisors, Prof. Peter van Bodegom and Dr. Joris Timmermans. Their consistent guidance and unwavering support were crucial to the successful culmination of both this doctoral thesis and my overall doctoral journey. I wish to convey my deep appreciation to Prof. Peter van Bodegom for his diligent supervision during the past four years. He not only epitomizes professionalism in doing research but also illuminates my academic journey. He has adeptly demonstrated the process of transforming intriguing research questions into meticulously structured studies. He consistently urged me to contemplate the significance of each research step and encouraged me to analyze, interpret, and disseminate our findings within the scientific community. I am profoundly thankful to him for being both a beacon and a benchmark in my scientific research journey, providing invaluable guidance through the highs and lows of these four years.

I also would like to express my heartfelt appreciation for Dr. Joris Timmermans, another vital pillar in my Ph.D. study. His authenticity and strong sense of responsibility convinced me to come to the Netherlands and study in Leiden University. His unceasing passion for scientific questions and continuous curiosity have consistently inspired me to sustain my enthusiasm for scientific exploration. His ability to approach challenges from a student's perspective and provide practical assistance has been invaluable, extending beyond scientific research into broader aspects of life. I am profoundly grateful to him for steering me toward the field of remote sensing and for the persistent support and guidance he has provided throughout this incredible journey.

I would like to express sincere gratitude to my office mates Amie Corbin, Eefje de Goede, and Jennifer Anderson. Thank you for your assistance and all the enjoyable conversations, which have enriched this journey with many interesting stories. I also want to thank every member of the remote sensing group, including Qi Chen, Nuno De Mesquita César de Sá, Leon Hauser, Anne Uilhoorn, Dirk-Jan Kok, Olivier Burggraaff, and Rosaleen March. Thank you all for your friendliness and warmth, which made me feel welcomed and integrated from the very beginning. A special thanks to Qi Chen for our fruitful exchanges and discussions. My gratitude also extends to the supporting staff at CML for their invaluable assistance.

I also would like to extend thanks to my Chinese colleagues in CML, including Weilin Huang, Chengguang Gao, Kaixuan Pan, Jianhong Zhou, Beilun Zhao, Juan Wu, Yingji Pan, Lingxing Xu, and others. Thank you for your companionship and assistance. I want to give special thanks to Yanan Liang and Zhenyang Chen. Over these four years, we have embarked on journeys together to explore the world, and each adventure has been filled with joy and cherished memories. In every moment

of happiness and challenges, we have stood by each other, providing mutual support. Your presence has made the entire four-year journey much easier. Thank you for being the most special and wonderful part of my doctoral experience.

I wish to express my gratitude to my longstanding friends Xia Wu, Xue Wan, Zhongjie Lu, and Ruiqi Zeng. I extend special thanks to Zhongjie Lu for your assistance and guidance in coding. I appreciate your warm greetings and the sharing of diverse perspectives.

Last but not least, I would like to express my heartfelt appreciation to my parents and family for their unwavering support and care.

Curriculum Vitae

Wen Wen was born in Shehong, China in July 1993. She obtained her bachelor's degree in Land Resource Management from the College of Resources and Environmental Sciences at Sichuan Agricultural University in 2016. During her undergraduate studies, she conducted geospatial analysis to investigate the spatial distribution patterns of economic coefficients related to agricultural land across diverse topographic zones in Sichuan Province. Upon graduation, she received a recommendation to pursue a master's degree at the College of Environmental Sciences at Sichuan Agricultural University. Wen completed her MSc thesis entitled “Phylogenetic Evolution of Buckwheat and Response of Its Distribution to Climate Change” under the supervision of Prof. Xuemei Zhu. During her master study, she joined the research group of Buckwheat Gene Germplasms as an exchange student at the Institute of Crop Sciences, Chinese Academy of Agricultural Sciences in 2018. In September 2019, she was awarded a scholarship for her PhD study funded by the CSC-Leiden University joint program to study at the Institute of Environmental Sciences (CML), Leiden University, the Netherlands. Her research focuses on monitoring the response of crops to simultaneous drought and salt stress from remote sensing for a sustainable future supervised by Prof. Peter van Bodegom and Dr. Joris Timmermans. After completing her Ph.D., Wen intends to further her research in sustainable agricultural systems in the context of climate change.